A Sweet Regulatory Landscape Of The Glycome

by

Thu Chu

A thesis submitted in partial fulfillment of the requirements for the degree of

Doctor of Philosophy

Department of Chemistry

University of Alberta

ABSTRACT

Events happening in cellular systems are regulated in an orchestrated and coordinated manner. To truly understand the cellular processes, it requires a precise knowledge of their components (DNA, RNA, proteins, carbohydrates, lipids, and metabolites) and their dynamic interactions. With the rapid development of technology, the template-encoded natural molecules (DNA, RNA and proteins) are more efficient and accessible to study. However, carbohydrates and lipids are generally understudied and underrepresented despite their crucial and significant biological roles mainly due to their non-template encoded nature, structural complexity and heterogeneity. Carbohydrates, known as glycans or oligosaccharides, are the products of multiple glycosyltransferases and glycosidases to synthesize structures appended to proteins and/or lipids. Glycans are one of the most abundant and diverse biomolecules on cells. The glycome is the complete pattern of glycan modifications in a cellular system. This pattern is generated by the synchronised and coordinated action of various glycosylation enzymes. These enzymes, including glycosyltransferases and glycosidases, work coordinately to create a highly sophisticated and dynamic network which is adaptive to environmental variations and changes. Aberrant glycosylation plays a fundamental role in key pathological steps of cancer, host-pathogen interactions, tumour cell development and progression, metastasis and immune modulation. However, it remains technically challenging to detect, characterize and quantify glycans. Previous work has identified miRNAs as key regulators of glycosylation, thus, we could utilize miRNAs as proxy to study glycosylation, which is termed "miRNA proxy approach". The lack of complete understanding of how miR interacts with mRNA under crowded cellular environment and inducing the down biological impacts postpones our capacity to use this powerful hypothesis. Furthermore, we predominantly relied on prediction algorithms to identify miR-target interactomes. However,

the low accuracy and sensitivity of miR target prediction tools hindered our ability to create reliable miR-target networks. The algorithms became worse for low abundance genes including glycosylation enzymes and protein membranes. The current high-throughput identification of miR-target interactions are not reliable and high-throughput enough for identifying miR-glycogene interactomes. There is a need to develop a better high-throughput experimental method for the creation of an accurate miR-target database with validated interactions. Herein, we created a high-throughput experimental platform, miRFluR, for mapping miR target.

With the development of this high-throughput miRFluR platform, we were able to obtain a comprehensive dataset of miRNA regulatory networks for glycosylation enzymes including B3GLCT, OGT and OGA. In the work of miR-B3GLCT interaction network, we successfully utilized downregulatory miR network to predict B3GLCT biological functions as supporting evidence for our miRNA proxy hypothesis. In addition, we not only identified miR impacting in the 3' untranslated region (3'UTR) but also expanding our platform to the 5'UTR. In summary, this work contributed to decipher the glycosylation code and understanding biological functions of certain regulatory networks

Preface

Sections of Chapter 1 of this thesis have been published as **Thu, C.T**., and Mahal, L.K. Sweet Control: MicroRNA Regulation of the Glycome. Biochemistry. *Biochemistry,* **2020**, 59, 34, 3098–3110.

The majority of Chapter 3 were published as **Thu, C.T**., Chung, J. Y., Dhawan, D., Vaiana, C. A., and Mahal, L. K. High-Throughput miRFluR Platform Identifies miRNA Regulating B3GLCT That Predict Peters' Plus Syndrome Phenotype, Supporting the miRNA Proxy Hypothesis. *ACS Chemical Biology,* **2021**, *16*, 1900-1907**.** Most of experiments and data analyses were performed by myself. The aliquoting of human miRNA mimic library and collecting 1 out of 27 384 well plates was performed by 2 technicians, Jonathan and Deepika.

Chapter 2 and 4 remain unpublished and some work is still ongoing. The research on Chapter 2 was conducted by myself with the initial testing of miRfect system was done by David Christian. I performed the majority of the work in Chapter 4 with the assistance of Dr. MacDonald on aliquoting the human miRNA mimic library.

DEDICATION

This dissertation is dedicated to my family for all your love and support along the way.

ACKNOWLEDGMENTS

First of all, I would like to express my great gratitude to my teacher, advisor and mentor, Prof. Lara K. Mahal, for her guidance and support during my time in graduate school. I still remember vividly the first day I met her in the Molecular Biology class and the day I decided to join her lab. She always patiently explained and answered my questions which was always encouraging and inspiring. I am very grateful to her empathy with my emotional intensity. I know it's not so easy. I also would like to acknowledge my committee members (Prof. Christopher W. Cairo, Prof. Matthew S. Macauley, Prof. Sheref Mansy and Prof. Yael David) for their valuable time, help, suggestions and comments on my work. I'm very grateful to Prof. Daniela Buccella and Prof. James Canary for all the guidance, assistance and collaborative work.

Secondly, I would like to thank all my beloved family and friends who were always there for me. My mom, my dad and 4 siblings (Vinh, Thuy, Huong, Hanh) mean the world to me. They just unconditionally love me for who I am, not what I do for them or anything. They just want me to be happy but little do they know, I love and value them so much and would sacrifice anything for their lives and well-beings. Linh, Jocelyn, Chris, Cherry, Tigist, Amaani, Helia, Fatema, and Guanmin showed me that not only we can talk passionately about science but also I don't have to be afraid opening up myself or be vulnerable with them. I hope you all know that I would always treasure our time together. I also remember how fun it was to play board games and puzzles with whom I not only considered as my colleagues but now and forever my friends (Jocelyn, Tigist, Helia, Amaani, Fatema, and Ric). I also appreciate all my friends and classmates (Shiyu, Chris, Johannes, Martin, Jocelyn, Jimmy, Shuhui, Nynkes, Julius, Tommy, Belinda, Jonathan, Deepika, James, and Mirat) to whom I really enjoyed their company and missed our science and research

conversations together. There are many more people who helped me along the way, I hope you know that I always remember and be grateful for you.

I also would like to acknowledge the path that I was walking and all experiences it brought me, both positive and negative. Sometimes, I realized that in order to gain something, it might also takes away something important. That was the feeling of losing part of myself in the process. It was painful, yes, but it helped me to grow and explore a different side of me that I never experienced before. So I wanted to acknowledge both the darkness and light that I went through:

What make a person who they are?
What is the meaning of it all?
When I am just a parasite for feeling
Relying on something so unstable to ever survive
And when it collapses
My whole belief system crashes
"Did I ever actually happy?"
Or am I just a borrower
And when it turned to dust
I left with a void of feeling
……
I made you my muse
My reason to survive
Just to realize
We don't share the same languages

We don't have similar frequencies

We just live in two different worlds

In my world

Everything covers in darkness

Now I'm learning to let go of things

That I once treasured

(I always imagined if I hold something so closely and tightly, I would be sure of its exact position.

Just to realize that, I can't be certain of its exact movement.)

….

Surely you live just to feel the pain

But what is life without that feeling

I went around the globe

Just to realize that

Convenient life doesn't guarantee happiness

I don't want to live like a soulless object

Striving for success just to fill my emptiness inside

……

Or to be evolved

As I understand myself

My purpose and existence in life

Seeking the truth

Amongst millions of lies that

They told me

It wasn't easy

Shedding away my tears,

My blood

My heart broken into millions of pieces

….

Or should I just live

to feel

The light falls into my eyes

And the gravitational field that keeps me here

Or just to appreciate all the force fields

that connect all the living systems

and make them flourish

I appreciate the science

Which used to be the reason

For keeping myself alive

It opened my eyes to see the whole universe

And how the sun sustains

lives here on Earth

and how it all governed by law of physics

entropy and enthalpy

Stochastically but orderly

…..

Sometimes I asked

Why do I feel everything so intensely?

Like a chain reaction

It amplifies and creates

A roller coaster

Where the ride is not very pleasant

Maybe if I feel less

My life would be better?

Or is it nothing more than just another path?

.....

But I learn to accept myself

With all the flaws, scars and imperfections

Plus the intrinsically disordered domain

That I let entropy

Get the best of me

Although I work on

Making it folded and structured

Or learn to make it useful one day

....

But relying on it for happiness

Only leads to detrimental consequences

To undercover

The fragile validation system

For my existence

Looking at it now

Maybe I should just be content

To just be a part of the life cycle

…

I should have known that the finished line is not the goal but the presence. Albert Einstein once said “Science is a wonderful thing if one does not have to earn one's living at it”. Sometimes, I thought it probably is applicable to myself and thought…

-Sometimes, I just want to evaporate into thin air with no trace of existence-

-Maybe being air particles would be fun-

-Are particles conscious?-

...

The complexities of life and questions draw me in and to became parts of me. My eyes sparkled just to imagine how proteins fold and how tiny molecules can do so much. I was always enthralled by all the questions science brought me. In the end, maybe I am just a loner on my imaginary path. Sometimes, I found a sparkling or interesting object, and I was so intrigued… Here I am... Here I found you and you found me.

a walking paradox. If you can read this, congrats, you have a useless skill. LOL, just kidding)

(an INTP 5w4

TABLE OF CONTENTS

LIST OF TABLES

LIST OF FIGURES

LIST OF ABBREVIATIONS

ATP	Adenosine triphosphate
B3GLCT	Beta 3-glucosyltransferase
CLIP	Cross-linking and immunoprecipitation
CMV	Cytomegalovirus
CSMA	Cell spot microarray
DMEM	Dulbecco's modified Eagle's medium
DNA	Deoxyribonucleic Acid
EMT	Epithelial to mesenchymal transition
ER	Endoplasmic reticulum
FBS	Fetal bovine serum
GALNT	N-Acetylgalactosaminyltransferases
GFP	Green fluorescent protein
GPI	Glycosylphosphatidylinositol
GWAS	Genome-Wide Association Studies
HBP	Hexosamine biosynthetic pathway
HBSS	Hanks' balanced salt solution
HGNC	HUGO Gene Nomenclature Committee

miR/miRNA	microRNA
NTC	Non-targeting control
OGA	O-GlcNAcase
O-GlcNAc	N-Acetylglucosamine
OGT	O-GlcNAc transferase
Opti-MEM	Opti-modified Eagle's medium
ORF	Open reading frame
OSER	Organized smooth endoplasmic reticulum
PCR	Polymerase chain reaction
PCT	Probability of conserved targeting
PPS	Peters plus syndrome
RISC	RNA-induced silencing complex
RNA	Ribonucleic acid
RT-qPCR	Real-time quantitative polymerase chain reaction
SNFG	Symbol Nomenclature for Glycans
TDMD	Target RNA-Directed MicroRNA Degradation
TSR	Thrombospondin type-1 repeat
UDP	Uridine diphosphate

UTR	Untranslated region
UV	Ultra-violet

CHAPTER 1

ROLES OF GLYCOSYLATION AND REGULATION

This chapter contains content published in **Thu, C.T**., and Mahal, L.K. Sweet Control: MicroRNA Regulation of the Glycome. Biochemistry. *Biochemistry,* **2020**, 59, 34, 3098–3110.

1.1 SIGNIFICANCE OF GLYCOSYLATION

The central dogma is a simplified explanation for the flow of genetic information coded in DNA. The transfer of information described by the central dogma, from DNA transcribed to RNA translated to protein, fails to account for properties inherent to biological systems on a cellular level.[1] The missing regulatory features, epigenetics, protein splicing or the mismatch between RNA and DNA, and RNA and protein, call the validity of the central dogma into question and challenge our current understanding of the big picture of how genes work together to produce living cells and organisms.

Carbohydrates and lipids underlie many essential biological functions, yet remain an understudied area of biology when compared to DNA, RNA and proteins. Indeed, both glycans and lipids have been shown to be key regulators of cellular activity and signal transduction that control nearly all aspects of cellular function[2, 3]. Despite the significance and prevalence of glycans, their study has been less accessible and is underrepresented compared to central dogmatic biomolecules mainly due to their non-template encoded nature, structural complexity and heterogeneity. Glycans remain neglected and poorly understood in the context of biology. This dissertation aims to address the current issues and challenges in glycosylation field by developing a new platform for researching the regulatory landscape and underlying biological functions of glycan biosynthetic networks.

1.2 AN OVERVIEW OF GLYCAN FUNCTIONS AND REGULATION

Carbohydrates, also known as glycans or oligosaccharides, are the products of multiple glycosyltransferases and glycosidases working in a coordinated and integrated manner to synthesize structures appended to proteins and/or lipids. Glycans are one of the most abundant and diverse biomolecules on cells (**Figure 1.1**). Given the dense coating of glycans on the cell surface, they are crucial in facilitating host-pathogen interactions and the host response [4]. They are also known to participate in various key biological functions and processes including protein homeostasis, immunity, cell adhesion, endocytosis, exocytosis, molecular trafficking and signal transduction[5, 6]. Glycosylation occurs in mainly in the endoplasmic reticulum (ER) and Golgi, with the exception of O-GlcNAcylation which takes place in the nucleus and cytoplasm. The covalent linkage of glycans to the polypeptide, lipid or other molecular backbones, determines its classification (**Figure 1.1** and **Figure 1.2**). These classifications include O-linked (a bond via the hydroxyl group of serine, threonine or collagen hydroxylysine[7]), N-linked (a bond via the amide group of asparagine), or, less commonly, C-linked (to tryptophan). Canonical N-linked glycoproteins tend to be more complex and highly branched structures. N-linked glycans bear a common branched core of the glycan, initiating with N-acetylglucosamine (GlcNAc) attached to asparagine residue by the anomeric carbon, followed by the second GlcNAc and the tri-mannose structure. Glycosylation gene defects, defined as congenital disorders of glycosylation, are often lethal, indicating vital roles of glycans. Dysfunctions of glycosylation also lead to development of diseases, cancer and pathogenesis of infectious diseases.

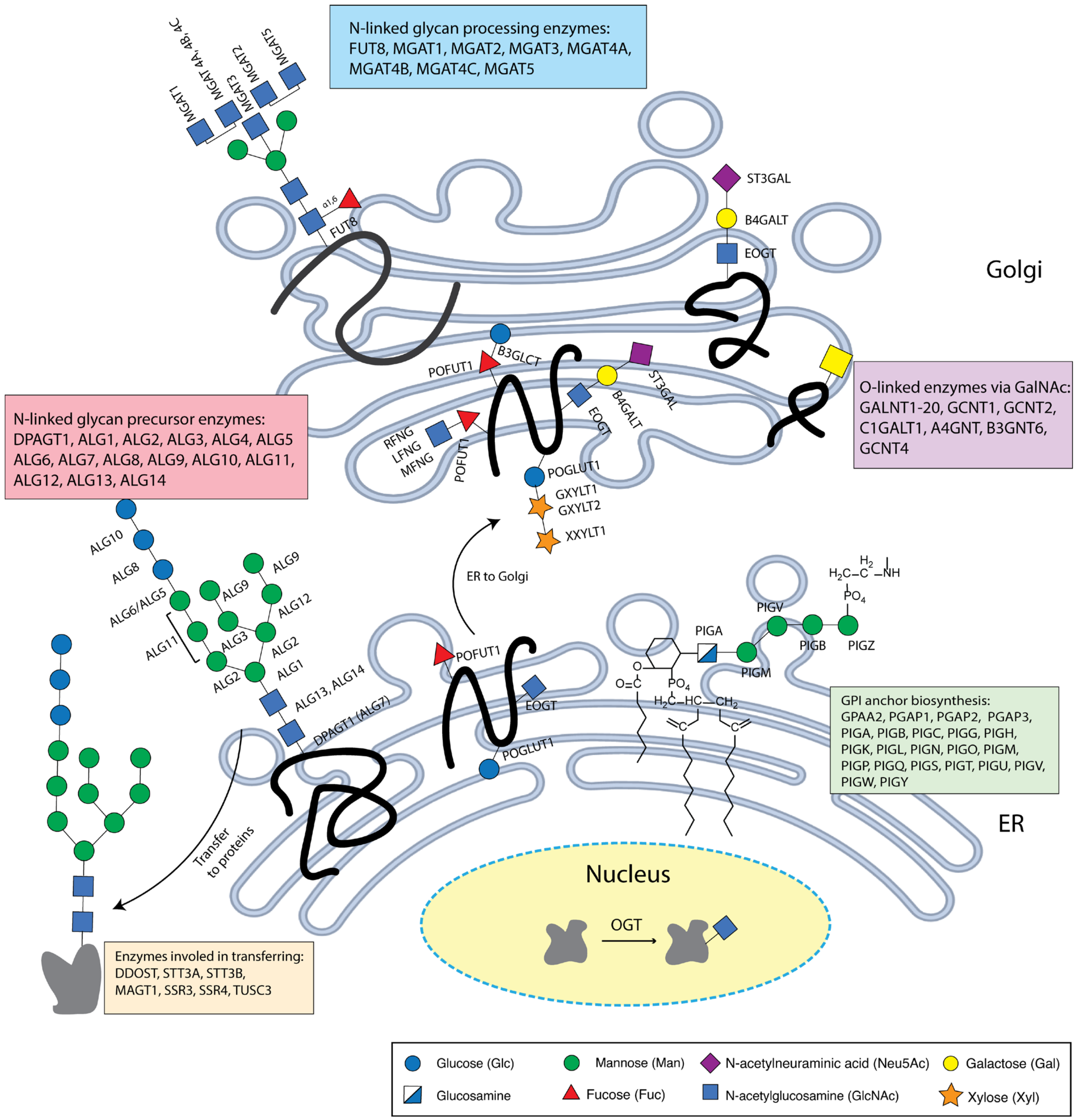

Figure 1.1. Glycan diversity on different cellular compartments: N-linked, O-linked, or GPI anchor processing enzymes.

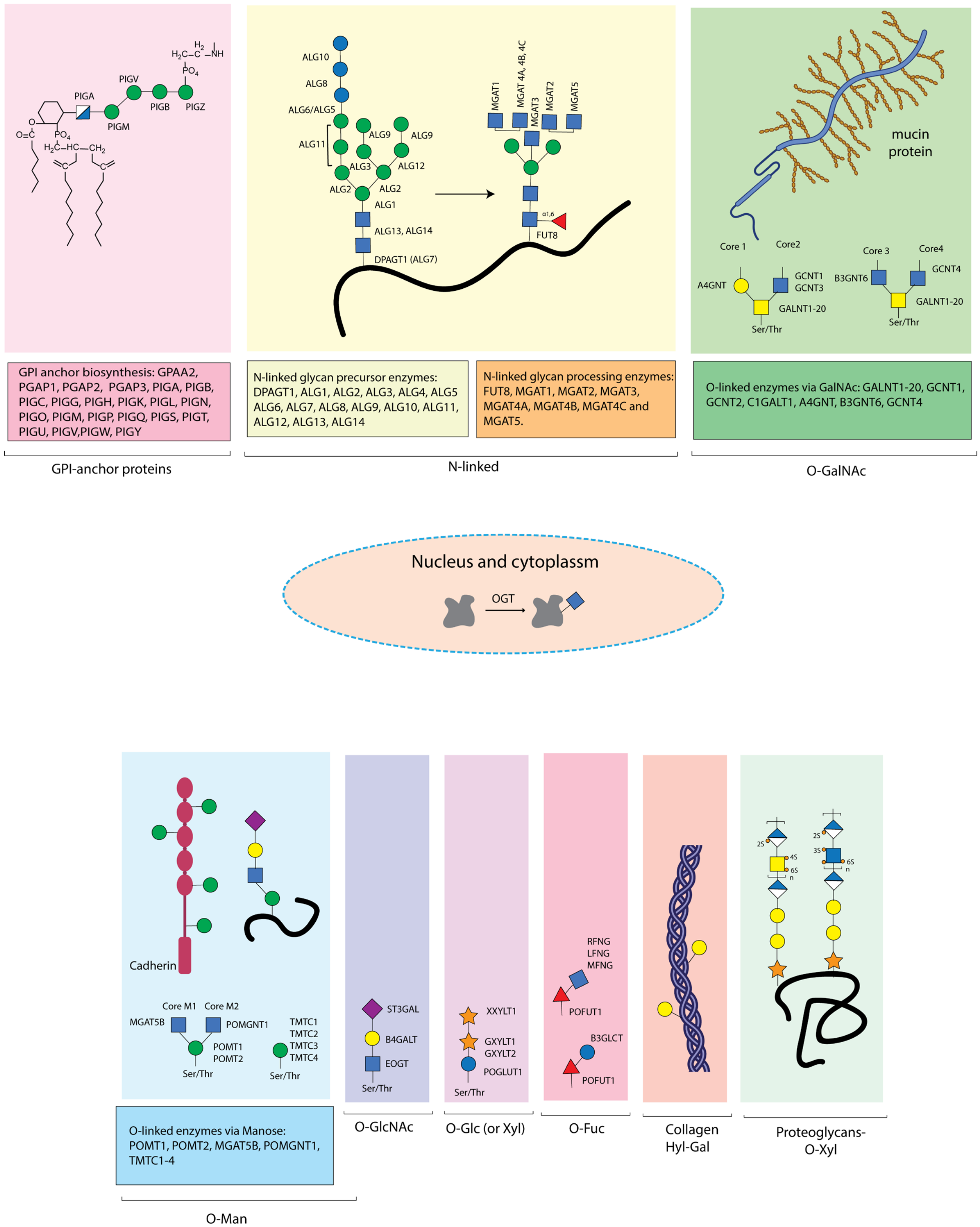

PIGA
PIGV
PIGB
PIGZ
PIGM
ALG10
ALG8
ALG6/ALG5
ALG11
ALG9
ALG9
ALG3
ALG12
ALG2
ALG2
ALG1
ALG13, ALG14
DPAGT1 (ALG7)
MGAT1
MGAT 4A, 4B, 4C
MGAT3
MGAT2
MGAT5
FUT8
mucin protein
Core 1
Core2
Core 3
Core4
A4GNT
GCNT1
GCNT3
B3GNT6
GCNT4
GALNT1-20
GALNT1-20
Ser/Thr
Ser/Thr
GPI anchor biosynthesis: GPAA2, PGAP1, PGAP2, PGAP3, PIGA, PIGB, PIGC, PIGG, PIGH, PIGK, PIGL, PIGN, PIGO, PIGM, PIGP, PIGQ, PIGS, PIGT, PIGU, PIGV,PIGW, PIGY
N-linked glycan precursor enzymes: DPAGT1, ALG1, ALG2, ALG3, ALG4, ALG5 ALG6, ALG7, ALG8, ALG9, ALG10, ALG11, ALG12, ALG13, ALG14
N-linked glycan processing enzymes: FUT8, MGAT1, MGAT2, MGAT3, MGAT4A, MGAT4B, MGAT4C and MGAT5.
O-linked enzymes via GalNAc: GALNT1-20, GCNT1, GCNT2, C1GALT1, A4GNT, B3GNT6, GCNT4
GPI-anchor proteins
N-linked
O-GalNAc
Nucleus and cytoplassm
OGT
Cadherin
Core M1
Core M2
MGAT5B
POMGNT1
POMT1
POMT2
TMTC1
TMTC2
TMTC3
TMTC4
Ser/Thr
Ser/Thr
ST3GAL
B4GALT
EOGT
Ser/Thr
XXYLT1
GXYLT1
GXYLT2
POGLUT1
Ser/Thr
RFNG
LFNG
MFNG
POFUT1
B3GLCT
POFUT1
O-linked enzymes via Manose: POMT1, POMT2, MGAT5B, POMGNT1, TMTC1-4
O-GlcNAc
O-Glc (or Xyl)
O-Fuc
Collagen Hyl-Gal
Proteoglycans-O-Xyl
O-Man

Figure 1.2. Diversity and classification of glycosylation. Illustration of the critical components of the cellular glycome, highlighting different types of glycosylation that are specific to protein classes or domains. The glycans represent examples of glycan structures that can be synthesized by the different types of glycosylation pathways. While N-glycans and most O-GalNAc types are commonly found on most trafficking proteins in cellular secretory pathway, the occurrence of domain-specific glycans is limited to specific protein domains. Glycan symbols are drawn according to the Symbol Nomenclature for Glycans (SNFG) format.

The importance of glycosylation is perhaps most apparent from the ever increasing number of genetic disorders and genome-wide association studies (GWAS) that point to glycosylation enzymes as causative agents of disease. In recent work, Joshi *et al* found that glycosylation enzymes implicated in complex diseases by GWAS are highly regulated, arguing that precise control over specific glycans is necessary[8]. The regulation of glycoprotein is complex and under multiple regulatory levels [9]. It not only involves regulation of the protein scaffold, but also glycan biosynthesis which is driven by around 500 glycosylation enzymes including glycosyltransferases, glycosydases and enzymes involved in metabolism, sulfation and transport. These scaffolds and enzymes are, in turn, regulated at transcriptional, translational and post-translational levels. At the transcriptional regulation, all glycosylation enzymes are controlled not only by transcription factors, but also by other epigenetic factors (ATP-dependent remodelers, histone modifying complexes, DNA methylation, etc…). Although transcriptional regulation is important in controlling the glycogene transcripts, the change in glycan structures are not quite well correlated with measurable glycogene transcript levels [10] [11] [12]. This could partially due to the less accurate measurement of low abundance glycogene mRNA levels. Since glycan structure patterns and levels are not correlated with the measurable glycogene transcripts, study of post-transcriptional regulation may play an important role in regulatory mechanisms of carbohydrate structure.

1.3 INTRODUCTION TO MIRNA AND THEIR REGULATION OF GLYCOSYLATION

1.3.1 miRNAs and their functions

MicroRNAs have emerged as critical regulators of the glycome over the last decade[13-15]. microRNAs (miRNAs, miRs) are small, non-coding RNAs that bind to messenger RNAs (mRNAs) and regulate mRNA translation into proteins. miRs possess distinctive and diverse expression patterns which impact various cellular processes and developmental pathways. They are known to target networks of numerous genes that regulate specific biological processes, tightening their expression window and dampening noisy expression [16, 17]. Most miRNA genes are transcribed into long primary transcripts, termed pri-miRNAs with typical hairpin structures (**Figure 1.2**). The pri-miRs are then processed by a microprocessor, consisting of protein DiGeorge Syndrome Critical Region 8 (DGCR8) and an RNase III enzyme, DROSHA, to produce ~70 nt stem-loop precursor miRs, termed pre-miRs. pre-miRs exit the nucleus as hairpin structures with a 2 nt 3' overhang, which are then exported to the cytoplasm by an exportin 5 (XPO5)/RanGTP complex. In the cytoplasm, pre-miRs are cut to remove the terminal loops in form mature miR duplex including the 5p miR (which comes from the 5' end, miR-5p) and the 3p miR (which is derived from the 3' end, miR-3p) (**Figure 1.2** and **Figure 1.3**). This process is catalyzed by another RNase III, DICER. The human immunodeficiency virus transactivating response RNA-binding protein (TRBP), then recruits the Dicer containing complex to the Argonaute protein to form RNA-induced silencing complex (RISC).[18] One miR strand is selected to become the mature miR and one strand is the passenger strand which is then degraded or stored for further usage.[19]. The mature strand is selected partially based on thermodynamic stability at the 5' ends of miR duplex or a 5'

U at the nucleotide position 1.[20] The RISC complex is loaded with a mRNA which is then inhibited or degraded.

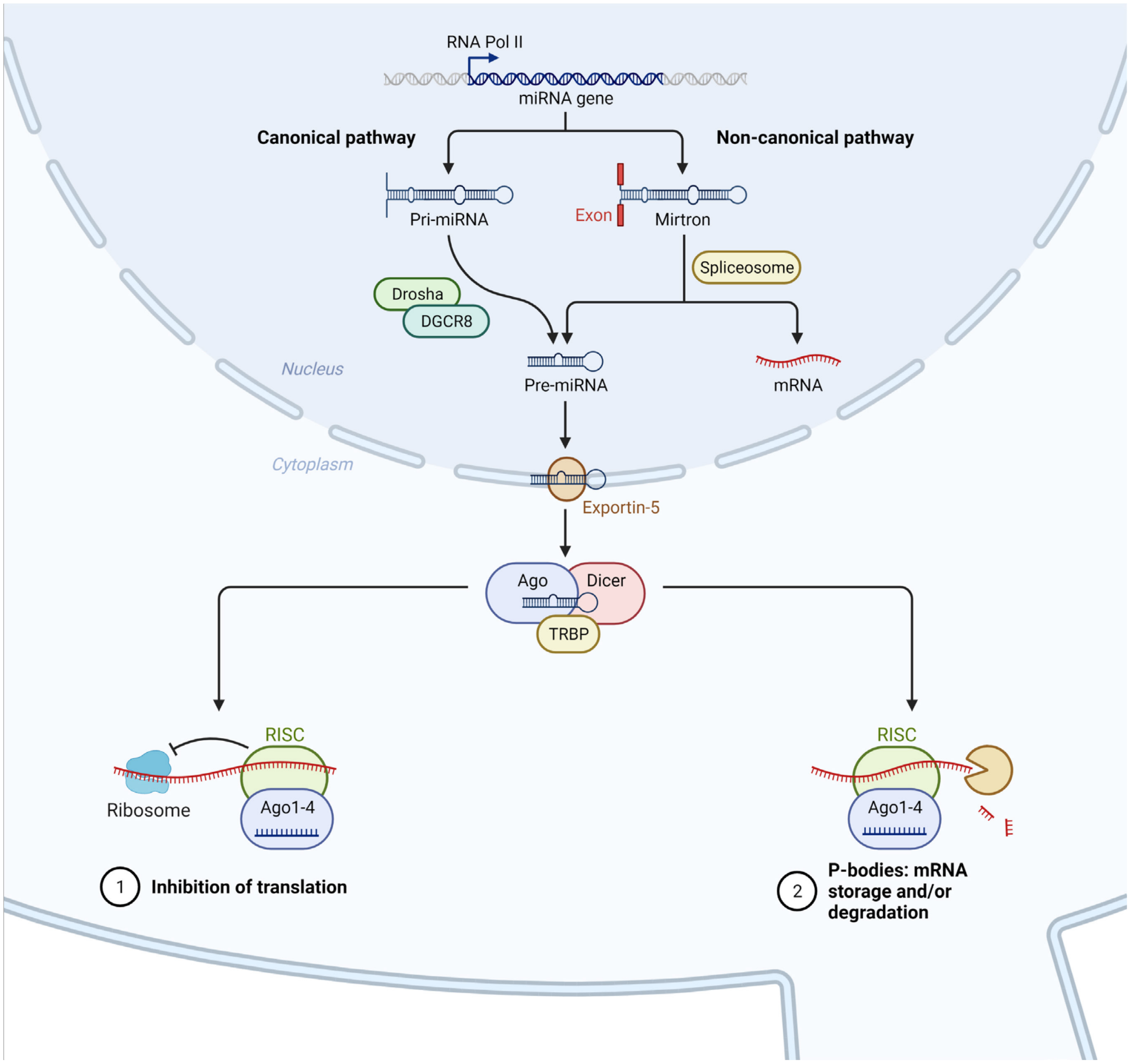

Figure 1.3. miR biogenesis and their functions (adopted from BioRender).

A single miR can have hundreds of targets. If a glycosylation enzyme or other glycan related protein (e.g. transporters, metabolic enzymes, etc.; with glycosylation enzymes, collectively known as glycogenes) is regulated by a miR, a loss of the associated glycan epitope is then observed (**Figure 1.3**). The function of miRs is not to turn a gene on or off but rather to tune protein expression, unlike transcriptional regulators [16]. Thus, miRs provide a mechanism to maintain tight regulation of protein levels within a specific window[16]. This control is dependent on the precise and specific mRNA transcript. Many genes have multiple transcripts that differ only in their 3'-UTRs but get translated into identical proteins.

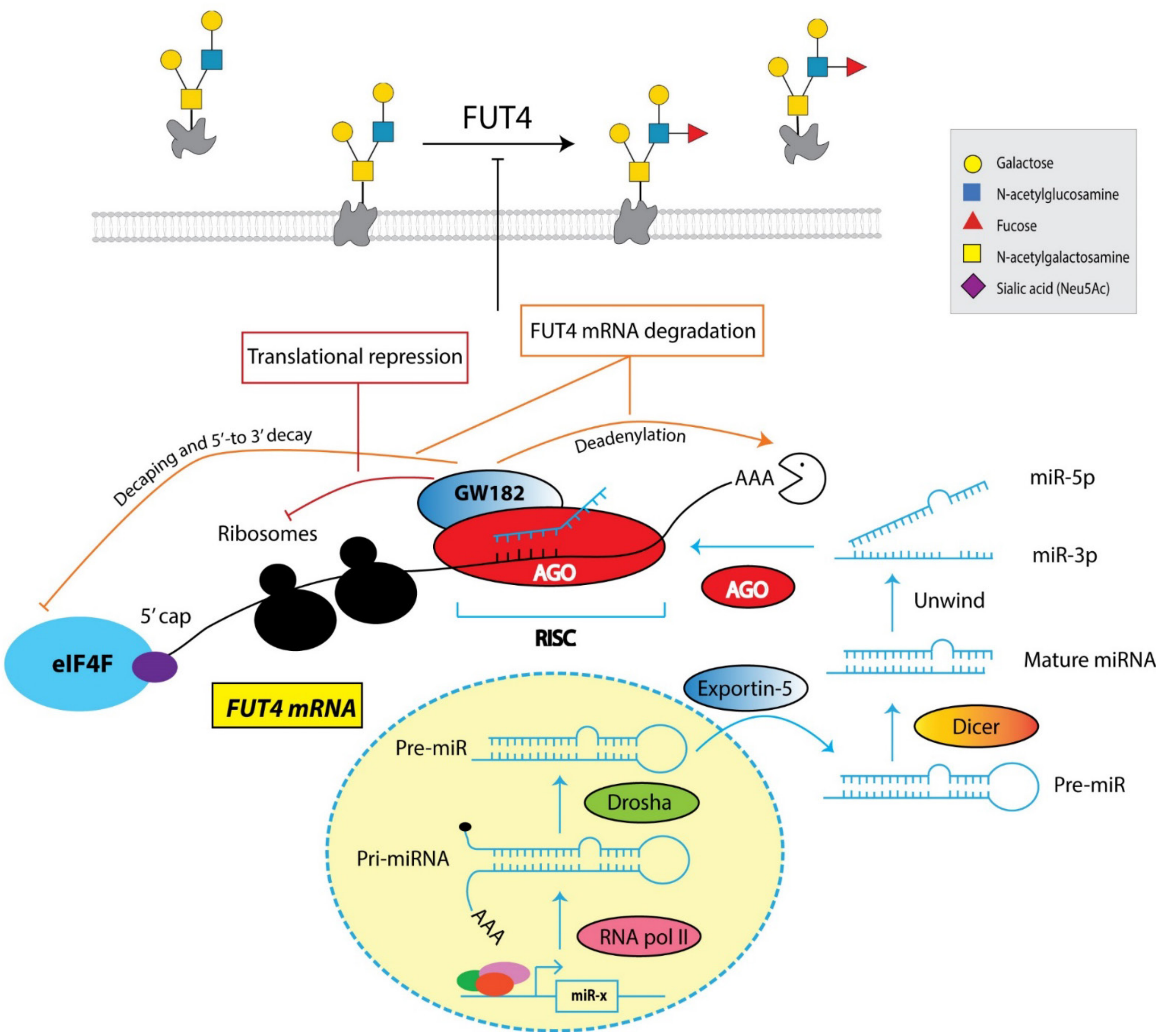

Figure 1.4. miRs are loaded into RISC complexes and inhibit protein expression through translational repression or mRNA degradation. This impacts glycosylation through repression of glycogenes such as FUT4. Lowered expression of the biosynthetic enzyme would shift the expression of the corresponding glycan epitope, as shown above.

Because networks of miRs act in concert, the biosynthesis of a glycan epitope may be regulated by multiple miRs, which simultaneously govern the expression of multiple glycogenes (**Figure 1.4**). The predicted glycogene targets of miRs are unevenly distributed. An analysis of miR:mRNA interactions predicted by the miRANDA algorithm identified some glycogene transcripts as highly-regulated, with multiple miR target sites, while others had few predicted sites[15]. Several glycogenes known to be involved in complex diseases (e.g. FUT8[21-23], GALNT7[24-33], and GALNT1[34-36]) were predicted to have highly-regulated transcripts, implying that miRs may play a direct role in dysregulation of these enzymes[15]. Enzymes previously believed to be "functionally redundant" such as the 20-member GALNT family, show large differences in potential miR regulation, suggesting that they control different biology. This argument against "redundancy" from the regulatory perspective, is borne out by new work showing that the GALNTs do indeed have distinct functions [37, 38].

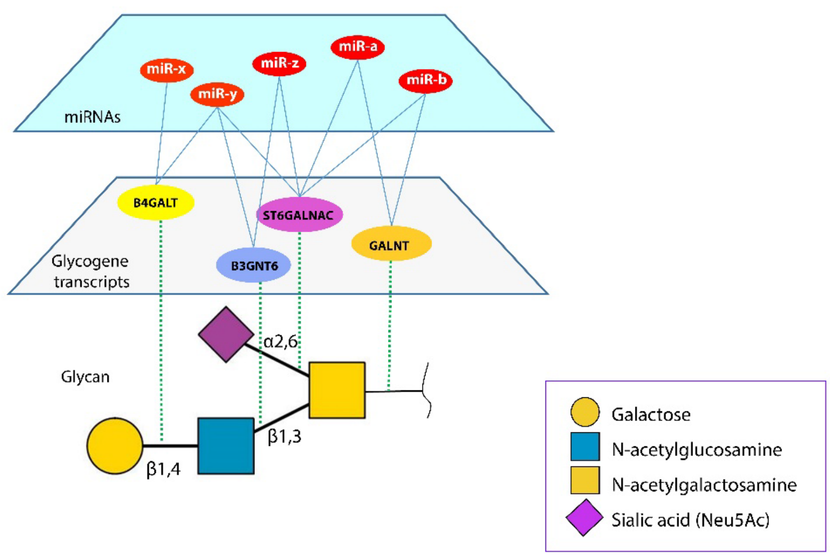

Figure 1.5. miRs can regulate multiple glycogenes in a network, modulating glycan structures.

1.3.2 MicroRNAs Are Critical Regulators Of The Glycome

A study in *Caenorhabditis elegans (C. elegans)* by Han and coworkers in 2009 was one of the earliest to show glycosylation as a major target of miRs[39]. In this work, they characterized the miRs found in RISC complexes during worm development. They found that miR targets were enriched in signaling proteins, while housekeeping genes were underrepresented. In addition, gene transcripts involved in glycosylation pathways were highly enriched in the pool of strong miR targets. They demonstrated that appending the 3'-UTR of one of the enriched glycogenes, *sqv-3*, was enough to repress expression of GFP in larval stages where this transcript was observed in the RISC complexes. To our knowledge, this work was the first example of glycogene regulation by a miR and supported a major role for miRs in the regulation of glycan biosynthesis.

In 2014, work from our laboratory directly demonstrated a critical role for miRs in the regulation of glycosylation in human cells[14]. Using bioinformatic methods we integrated miR profiles of the NCI-60, a 59 human cancer cell line panel, with glycomic analysis obtained using our lectin microarray approach[40, 41]. We identified multiple miRs that correlated with specific glycosylation patterns. These miRs directly targeted the transcripts of glycogenes underlying the observed glycans and were able to alter the glycosylation of cells. Our work underscored the important role of miRs in controlling the glycome. At the time of this publication in 2014, only 10 glycogenes were known targets of miRs. In the past 5 years, there has been an explosion of interest in miR regulation of glycogenes and over 80 glycogenes are currently known miR targets (**Table 1.1**).

1.4 MICRORNA PROXY HYPOTHESIS AND APPLICATION TO GLYCOSYLATION

In one of the earliest examples of glycan regulation by miRs, Hernando and coworkers identified the GALNT7 as a target for miR-30d, a microRNA that promoted melanoma metastasis in patients and mouse models. Downregulation of GALNT7 was found to phenocopy miR-30d, increasing metastasis as a result of inhibiting O-glycosylation[24]. This showcases a common theme in miR biology, namely that downregulation of the targets of a miR phenocopies the effects of miR expression. This observation led us to propose the microRNA proxy hypothesis. Our hypothesis states that the regulation of protein expression by changes in the expression levels of miRs identifies proteins holding a privileged position in driving the underlying biology. In other words, if a miR drives a specific biological phenotype, such as migration or metastasis, the targets of that miR will drive the same biological phenotype. Thus, miRs can be used to identify (by proxy) the biological functions of specific glycosylation enzymes (or other proteins). We first formulated and tested this powerful hypothesis in a publication in 2015[13]. In that work, we examined the targets of miR-200b-3p, a miR that controls epithelial to mesenchymal transition (EMT). This miR is high in epithelial cells and low in mesenchymal cells. We identified 5 targets of miR-200b-3p and tested 3 of them to see whether inhibiting the expression of these enzymes would phenocopy overexpression of the miR. In all 3 cases (B3GLCT, ST3GAL5 and ST6GALNAC5), mesenchymal cells reverted to an epithelial state upon repression of these glycosylation enzymes. This phenotype was not transduced by repression of the transcription factor ZEB1, another target of miR-200b-3p commonly thought to be responsible for the EMT phenotype. Instead knockdown of all 3 glycogenes caused increases in ZEB1 levels, arguing that inhibiting glycosylation can alter EMT independent of the transcription factor. This provided evidence that miRs target key hubs driving the biological phenotypes that they regulate, in line with our hypothesis. Further evidence was in a later on MGAT4A regulation which identified a role for this gene in cell-cycle regulation.

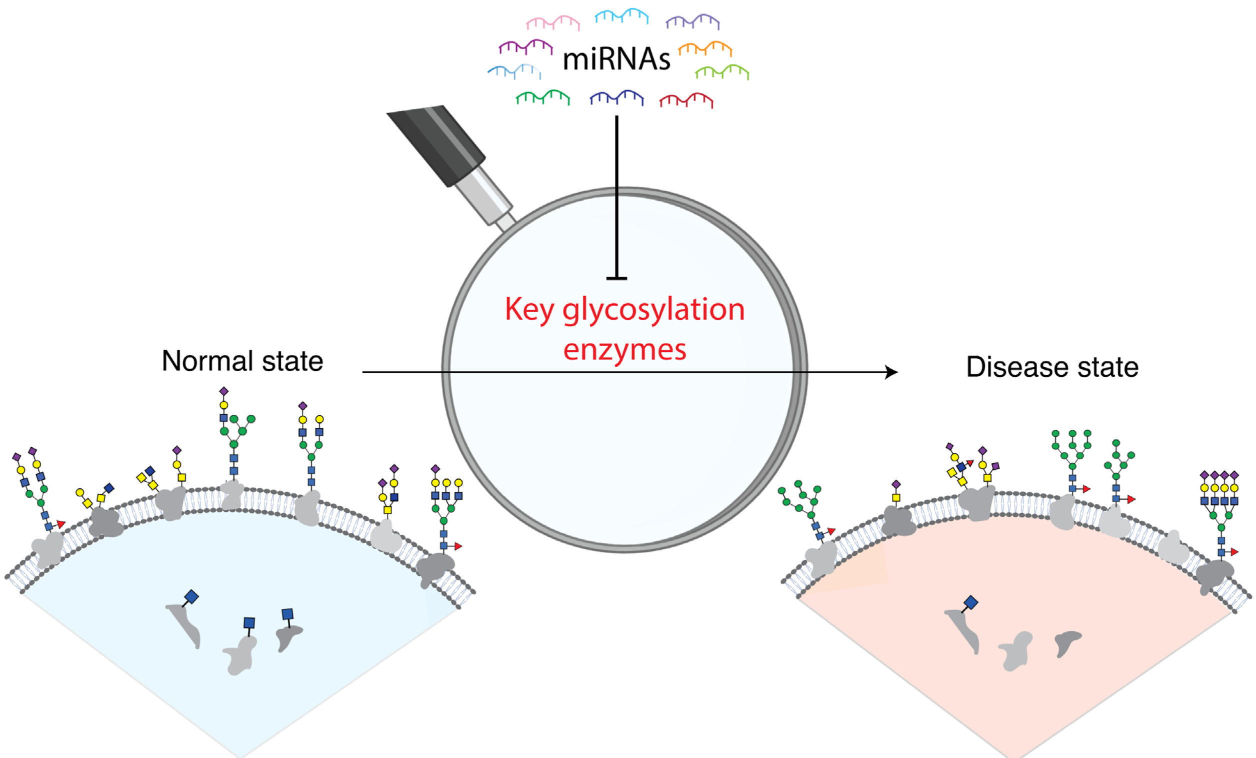

Figure 1.6. miRNA proxy approach: the regulation of protein expression by changes in the expression levels of miRs identifies proteins holding a privileged position in driving the underlying biology.

1.5 MIRNA TARGET PREDICTION ALGORITHMS FAILED TO ACCURATELY IDENTIFY MIRNA TARGETS

Currently, our understanding of miRNA-targets relies mainly on prediction algorithms to identify interactions. Predicted target are then experimentally validated. To date, only 0.01% of predictions have been validated[42]. The accuracy and sensitivity of the prediction tools are also highly questionable (20-60% accuracy[43-45]) with high false negatives and positives even for canonical miR-target interactions with conserved seed regions[46]. Canonically, miRNAs target mRNA in metazoans via interaction between the 5′-end bases position from 2 to 7 of the miRNA, designated the miRNA "seed region," and the 3′ untranslated region (3′-UTR) of the target mRNA. Recently, the 3' half of miR has gained more attention in directing miR target specificity and regulation. Additional sites in the 3' of miRs compensate for "seed" mismatches and, although more rarely, the "centered" miRNA sites can also participated in base-pairing between miRs and mRNAs. In addition, the pairing to the miR 3' end can impact the stability of miR, termed target-directed miRNA degradation (TDMD), in which the mRNA promotes the degradation of its miRNA binding partner via specific complementary binding patterns in both miR 3' and 5' end [47] [48] [49] [50]. Those findings highlight the significance of miR sequences beyond the seed region in modulating the existence and functions of miRs and also enhancing the regulatory complexity in mammalian cells[51]. Therefore, relying solely on seed regions in miR target prediction tools is detrimental to the accuracy and sensitivity of the algorithms. Other features beside the seed regions are utilized in miR target bioinformatics tools including free energy of miR-mRNA pairing, accessibility of the binding sites, AU rich elements in mRNA and the evolutionary conservation of sequences amongst species.

Despite continuous effort, experimental evidence still indicates high false positive and negative rates for prediction tools. This failure to accurately identify miR targets *in silico* is likely attributable to the simplified rules used to predict interactions and functions. Furthermore, the interior of the cells is a densely crowded environment which alters the binding properties and macromolecular interactions. Thus, the underlying biological mechanisms driving biologically relevant actions and functions of miRs remain largely enigmatic.

The prediction accuracy and sensitivity is exacerbated for low abundance gene including most of glycosylation enzymes and membrane receptor proteins. The current high-throughput experimental methods of identifying miRNA targets (transcriptomic analysis and crosslinking assay) failed to pinpoint the real miRNA targets for low abundance gene and the actual biological impacts of miRNAs on protein levels. It has also been shown that mRNA and protein level are not highly correlated and in many cases, miRs have of completely different impacts on the mRNA and protein levels[44, 52]. An analysis of the agreement between protein expression and mRNA expression levels using data from the Human Proteome Map and Genotype-Tissue expression project found strong concordance in the expression levels for only 6.1% of genes[53]. Other studies indicated that mRNA and protein level correlation largely varies between 20-40% depending on genes and biological systems studied [54] [55] [56] [57]. For low abundance proteins, such as glycogenes, it is known that transcription levels are not accurate to protein abundance [58]. All miR interactions impact translation, and at best only ~80% of interactions impact the transcriptome[59]. This may be lower for low abundance genes, where transcriptional data is inherently more noisy. Thus, reliance on the transcriptome may bias current algorithms.

1.6 CONTEMPORARY KNOWLEDGE ON MIRNA MECHANISMS OF ACTION

miRs can have distinct and diverse mRNA targets within the cell. The binding is often, but not exclusively, to the 3'-untranslated region (3'-UTR) and leads to translational repression[60, 61]. There are currently three currently known mechanisms of miRNA-mediated repression (**Figure 1.7**). The first mechanism involves inhibition of the translation initiation complexes (eIF4F complexes). The second one is blocking translation via polysome elongation, leading to ribosomal stalling. The third mechanism is miRNA-mediated deadenylation and decapping via the CAF1/CCR4 deadenylase complex and Dcp1/2 decapping complex. In this case, mRNA degradation also occurs. We have yet to understand the miR-mRNA binding rules that corresponds to each mechanism and when cells utilized each mechanism and which factors are important in regulating them. More research is needed to clarify how miRNAs function and their relevant impacts.

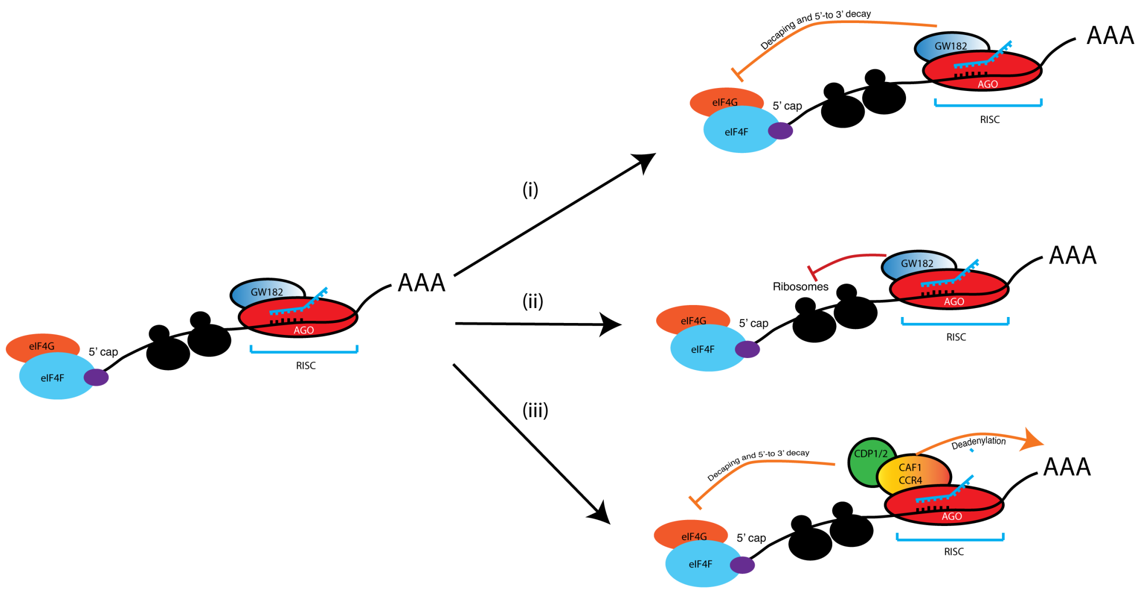

Figure 1.7. Three currently known mechanisms of miRNA-mediated repression.

1.7 THE SCOPE OF THIS DISSERTATION

Glycosylation enzymes that are more tightly regulated appear to be more prevalent in controlling underlying complex disease states. Study of carbohydrates requires developing and utilizing novel chemical biological tools to decipher the language of the "glycocode" or "sugar code" [62]- the concept that the specific glycan structure conveys biological information to cells. Dysregulation of glycosylation may underlie some of the most complex and common diseases of the modern era. MicroRNA is an emerging regulator of glycosylation, tuning low abundance glycan biosynthetic enzymes. Given the emerging importance of miRs in disease and their potential to identify genes that underlie specific biological function, it is clear that more attention should be paid to miR:glycogene interactions and further technological advancements are needed to study miR regulation of glycosylation.

Our current view relies mainly on prediction algorithms to identify miR:target interactions. Predicted target are then experimentally validated. However, to date, only 0.01% of predictions were validated[42]. The accuracy and sensitivity of the prediction tools are also highly questionable (20-60% accuracy[43-45]) with high false negatives and positives. This could stem our lack of understanding of the mechanisms and rules of miR interactions with mRNA targets and their relevant impacts. At present, studies into accurate miR:mRNA interactions requires that each interaction be experimentally validated by luciferase assay. If one were to study multiple miRs that co-regulate a biological phenotype, this would then require tens to hundreds of luciferase assays to validate interactions and identify a common target set. However, luciferase assays require the lysis of cells, expensive reagents and only in moderate throughput. My thesis focuses on the development of a high-throughput experimental platform to map miR-target interactions and application of this technology to understand regulatory networks and functions of genes particularly glycosylation enzymes.

TABLE 1.1. List of known miR regulators for human glycogenes organized by pathway. The HUGO Genome Nomenclature Committee (HGNC) symbol is given for each gene along with the nomenclature used in the accompanying literature cited. For the miRs, Designations for -5p and-3p are noted where specified in reference.

Pathway	Gene Symbol (HGNC)	Alternative symbols used in literature	miRNAs
O-GlcNAc	OGT	O-GLCNAC, HRNT1, MGC22921, FLJ23071, OGT1	hsa-miR-485-5p[63, 64], hsa-miR-101[65], hsa-miR-483[66], hsa-miR-200a/200b-3p[67], hsa-miR-24-1[68], hsa-miR-424[69], hsa-miR-423-5p[70], hsa-miR-7[71]
	OGA	MGEA5, MEA5, NCOAT	hsa-miR-539[72]

N-linked pathway			
Glycosyltransferases	RPN2	SWP1, RPNII, RIBIIR, RPN-II	hsa-miR-128[73], hsa-miR-378[74]
	ALG3	NOT56L, Not56, CDGS4, D16Ertd36e	hsa-miR-342[75]
	ALG12	ECM39, CDG1G	hsa-miR-147a[76]
	ALG13	GLT28D1, CXorf45, CDG1S	hsa-miR-34a[77]
	FUT8		hsa-miR-122[23], hsa-miR-34a[23], hsa-miR-26a[78], has-miR-26b[78], hsa-miR-146a[22], hsa-miR-198 [79]
	MGAT3	GNT-III	hsa-miR-23a [80]
	MGAT4A	GnT-Iva, GnT-4a	hsa-miR-424[69], hsa-let-7c[81]
Glycosidases	EDEM1	KIAA0212, EDEM	hsa-miR-211 [82], hsa-miR-581 [83, 84], hsa-miR-204 [83, 84]
	MAN1A2	MAN1B	hsa-miR-30c, hsa-miR-361[14]
	MAN1B1		hsa-miR-125b[85, 86]
	MANEA	FLJ12838	hsa-miR-1202[87]
O-linked pathway			
Initiation	GALNT1	GalNAc-T1	hsa-miR-216b[35], hsa-miR-30b/30d[24], hsa-miR-10a[88], hsa-miR-129[34]
	GALNT2	GalNAc-T2	hsa-let-7b[89]
	GALNT3	GalNAc-T3, HHS, HFTC	hsa-miR-26a[90], hsa-miR-17-3p and hsa-miR-221[91]
	GALNT4	GalNAc-T4	hsa-miR-4262[92], hsa-miR-9[93], hsa-miR-365[94]
	GALNT5	GalNAc-T5	hsa-miR-196b-5p[95]
	GALNT7	GalNAc-T7	hsa-miR-154[32], hsa-miR-214[25, 31], hsa-miR-30a-5p[30], hsa-miR-494[28, 29], hsa-miR-34a/c[27], hsa-miR-17-3p/5p[26], hsa-miR-214[25, 31],hsa-miR-30b/30d[24], hsa-miR-378 [24-33]
	GALNT10	GalNAc-T10	hsa-miR-122[96]
	GALNT13	GalNAc-T13, KIAA1918	hsa-miR-424[69]

	GALNT14	GalNAc-T14, FLJ12691	hsa-miR-125a[97]
	TMTC2	DKFZp762A217	hsa-miR-142[98]
	POGLUT1	KDELCL1, MDS010, MDS010, MGC32995, 9630046K23Rik, MDSRP, hCLP46, Rumi	hsa-miR-134[99], hsa-miR-142[99, 100]
Elongation and Branching	B3GAT3	GlcAT-I	hsa-miR-23b[101]
	B3GLCT	B3GALTL	hsa-miR-200b, hsa-miR-200c, hsa-miR-429[13]
	B3GNT5	B3GN-T5, beta3Gn-T5	hsa-miR-203[102]
	C1GALT1	C1GALT, T-synthase	hsa-miR-148b[103]
	C1GALT1C1	COSMC, C1GALT2	hsa-miR-320[104], hsa-miR-155[105], hsa-miR-374b[106]
	GCNT2	NACGT1, II, GCNT5, CCAT, IGNT, NAGCT1, bA421M1.1, bA360O19.2, ULG3	hsa-miR-199a/b-5p [107]
	GCNT3	C2GnT-M, C2/4GnT, C2GnT2	hsa-miR-302b-3p [108], hsa-miR-15b [109]
	LFNG	SCDO3	hsa-miR-200f [110], hsa-miR-125a-5p [111, 112], hsa-miR-146a [113]
Capping			
PolyLacNAc	B3GALT5	beta3Gal-T5, B3GalT-V, GLCT5, B3T5	hsa-miR-203[114]
	B4GALT1	GGTB2	hsa-miR-124-3p[115]
Sialylation	ST3GAL3	ST3Gal III, SIAT6, MRT12	hsa-miR-200a[116]
	ST3GAL4	STZ, SAT3, FLJ11867, CGS23, SIAT4, NANTA3, SIAT4C	hsa-miR-200a[116], hsa-miR-370[113]
	ST3GAL5	SIAT9, ST3GalV, SIATGM3S	hsa-miR-26a[117], hsa-miR-548l[117], hsa-miR-34a[117], hsa-miR-200b[13], hsa-miR-200c[13], hsa-miR-429[13]
	ST3GAL6	SIAT10, ST3GALVI	hsa-miR-26a[118, 119]
	ST6GAL1	SIAT1, ST6Gal I	hsa-miR-9[120]
	ST6GALNAC1	SIAT7A, ST6GalNAcI	hsa-miR-30d-5p[121]

	ST6GALNAC2	SIAT7, SIAT7B, SIATL1	hsa-miR-182[122, 123], hsa-miR-135b[122, 123]
	ST6GALNAC4	SIAT7D, ST6GALNACIV, SIAT3C	hsa-miR-4299[124]
	ST6GALNAC5	SIAT7E, MGC3184, ST6GalNAcV	hsa-miR-200b, hsa-miR-200c, hsa-miR-429[13]
	ST8SIA1	SIAT8, SIAT8A	hsa-miR-33a,hsa- let-7e[125]
	ST8SIA2	SIAT8B, STX, ST8SIA-II, HsT19690	hsa-miR-3099[126]
	ST8SIA4	SIAT8D, ST8Sia IV	hsa-miR-26a/26b[127], hsa-miR-146a/146b[128], hsa-miR-181c[128]
Fucosylation	FUT1	H, HSC	hsa-miR-140-5p[129], hsa-miR-149 [129], hsa-miR-34a [130]
	FUT2	SE, sej, Se2, SEC2	hsa-miR-15b [131]
	FUT4	CD15, FUC-TIV, FCT3A, ELFT	hsa-miR-125a-5p [129], hsa-miR-26a/26b [78, 132], hsa-miR-200c [133], hsa-miR-200b [133], hsa-miR-493-5p [134], hsa-miR-224-3p [135]
	FUT5	FUC-TV	hsa-miR-125a-3p [136]
	FUT6	FT1A, FCT3A, FucT-VI, FLJ40754	hsa-miR-326 [137], hsa-miR-125a-3p [136], hsa-miR-106b [137]
	FUT8*	See above in *N*-linked pathway	
GAG related enzymes			
Chondroitin Sulfate Synthetases	CHSY1	KIAA0990, CSS1	has-miR-194, hsa-miR-515[138]
	CHPF	CSS2, CHSY2	has-miR-194, hsa-miR-515[138]
	CHSY3	CSS3, CHSY-2	has-miR-194, hsa-miR-515[138]
Glucuronyl acid epimerase	GLCE	KIAA0836, HSEPI	hsa-miR-218[139]
Sulfotransferases/sulfatases	CHST3	C6ST, C6ST1	hsa-miR-513a-5p [140]
	HS3ST2	3OST2	hsa-miR-100 [141]
	HS6ST2		hsa-miR-141-3p, hsa-miR-145-5p [142]
	NDST1	HSST, NST1	hsa-miR-149[143], hsa-miR-24[143], hsa-miR-191[143]
	SULF1	KIAA1077, SULF-1, hSulf-1	hsa-miR-21[144]

Hyaluronan synthetases	HAS1	HAS	hsa-miR-125a[145], hsa-miR-214[145]
	HAS2		hsa-miR-410 (up-regulating) [146], hsa-miR-7[147], hsa-miR-26b[148], hsa-miR-378[148], hsa-miR-23a-3p [149], hsa-miR-424/424*[150], hsa-miR-23[151], hsa-miR-574[151], hsa-miR-101-3p[152]
	HAS3		hsa-miR-26a-5p[153], hsa-miR-29a-3p[154]
Others			
Glycosidases	FUCA2	MGC1314, dJ20N2.5	hsa-miR-145[155], hsa-miR-200b, hsa-miR-200c, hsa-miR-429 [14]
	GALC		hsa-miR-140-5p[156]
	GBA	GLUC, GBA1	hsa-miR-22-3p[157]
	NEU1	NEU	hsa-miR-125b[158]
	HEXB		hsa-miR-207, hsa-miR-352 [159]
Nucleotide Sugar Metabolism	PMM2	CDG1, CDGS, CDG1a, PMI, PMI1	hsa-miR-451a[160, 161]
	TSTA3	FX, P35B, SDR4E1	hsa-miR-125a-5p, hsa-miR-125b[162]
	CMAHP	CMAH	hsa-miR-155-5p, hsa-miR-425-5p, hsa-miR-15a-5p, hsa-miR-503-5p, hsa-miR-16-5p, hsa-miR-29a-3p, and hsa-miR-29b-3p[163]
	UAP1	SPAG2, AGX1, AgX	hsa-miR-224-5p [164]
Nucleotide sugar transporters	SLC35B2	PAPST1, UGTrel4	hsa-miR-22[165]
	SLC35B4	FLJ14697, YEA4	hsa-miR-1764, hsa-miR-1700[166]
	SLC35F5	FLJ22004	hsa-miR-369-3p [167]
UDP-Glucuronyltransferases (involved in Drug Metabolism)	UGT2B15	UGT2B8	hsa-miR-331-5p[168, 169], hsa-miR-376c [170], hsa-miR-770-5p [169], hsa-miR-103b [169], hsa-miR-3924 [169], hsa-miR-376b-3p [169], hsa-miR-455-5p, [169] hsa-miR-605 [169], hsa-miR-624-3p [169], hsa-miR-4712-5p [169], hsa-miR-3675-3p [169], hsa-miR-6500-5p [169], hsa-miR-548as-3p [169], hsa-miR-4292 [169]
	UGT2B17		hsa-miR-376c [170]
	UGT2B7	UGT2B9	hsa-miR-1293, hsa-miR-3664-3p, hsa-miR-4317, hsa-miR-513c-3p, hsa-miR-4483, and hsa-miR-142-3p [168, 171]
	COG6	COD2, KIAA1134	hsa-miR-1 [172]

Other Glycosylation Related Proteins	KL (Klotho)		hsa-miR-34a[173], hsa-miR-199b-5p[174, 175], hsa-miR-504[176], hsa-miR-339[176], hsa-miR-556[177]
	SPOCK1	TIC1, SPOCK, testican-1	hsa-miR-150-3p/5p [178, 179], hsa-miR-129-5p [178], hsa-miR-585 [179]
	SPOCK3	testican-3	hsa-miR-145[180]

1.7 REFERENCES

1. Piras, V.; Tomita, M.; Selvarajoo, K., Is central dogma a global property of cellular information flow? *Front Physiol* **2012,** *3*, 439.
2. Wymann, M. P.; Schneiter, R., Lipid signalling in disease. *Nat Rev Mol Cell Biol* **2008,** *9* (2), 162-76.
3. Sasisekharan, R.; Shriver, Z.; Venkataraman, G.; Narayanasami, U., Roles of heparan-sulphate glycosaminoglycans in cancer. *Nat Rev Cancer* **2002,** *2* (7), 521-8.
4. Heindel, D. W.; Koppolu, S.; Zhang, Y.; Kasper, B.; Meche, L.; Vaiana, C. A.; Bissel, S. J.; Carter, C. E.; Kelvin, A. A.; Elaish, M.; Lopez-Orozco, J.; Zhang, B.; Zhou, B.; Chou, T. W.; Lashua, L.; Hobman, T. C.; Ross, T. M.; Ghedin, E.; Mahal, L. K., Glycomic analysis of host response reveals high mannose as a key mediator of influenza severity. *Proc Natl Acad Sci U S A* **2020,** *117* (43), 26926-26935.
5. Amon, R.; Reuven, E. M.; Leviatan Ben-Arye, S.; Padler-Karavani, V., Glycans in immune recognition and response. *Carbohydr Res* **2014,** *389*, 115-22.
6. van den Berg, T. K.; Honing, H.; Franke, N.; van Remoortere, A.; Schiphorst, W. E.; Liu, F. T.; Deelder, A. M.; Cummings, R. D.; Hokke, C. H.; van Die, I., LacdiNAc-glycans constitute a parasite pattern for galectin-3-mediated immune recognition. *J Immunol* **2004,** *173* (3), 1902-7.
7. De Giorgi, F.; Fumagalli, M.; Scietti, L.; Forneris, F., Collagen hydroxylysine glycosylation: non-conventional substrates for atypical glycosyltransferase enzymes. *Biochem Soc Trans* **2021,** *49* (2), 855-866.
8. Joshi, H. J.; Hansen, L.; Narimatsu, Y.; Freeze, H. H.; Henrissat, B.; Bennett, E.; Wandall, H. H.; Clausen, H.; Schjoldager, K. T., Glycosyltransferase genes that cause monogenic congenital disorders of glycosylation are distinct from glycosyltransferase genes associated with complex diseases. *Glycobiology* **2018,** *28* (5), 284-294.
9. Neelamegham, S.; Mahal, L. K., Multi-level regulation of cellular glycosylation: from genes to transcript to enzyme to structure. *Curr Opin Struct Biol* **2016,** *40*, 145-152.
10. Anugraham, M.; Jacob, F.; Nixdorf, S.; Everest-Dass, A. V.; Heinzelmann-Schwarz, V.; Packer, N. H., Specific glycosylation of membrane proteins in epithelial ovarian cancer cell lines: glycan structures reflect gene expression and DNA methylation status. *Mol Cell Proteomics* **2014,** *13* (9), 2213-32.
11. Nairn, A. V.; York, W. S.; Harris, K.; Hall, E. M.; Pierce, J. M.; Moremen, K. W., Regulation of glycan structures in animal tissues: transcript profiling of glycan-related genes. *J Biol Chem* **2008,** *283* (25), 17298-313.

12. Liu, G.; Marathe, D. D.; Matta, K. L.; Neelamegham, S., Systems-level modeling of cellular glycosylation reaction networks: O-linked glycan formation on natural selectin ligands. *Bioinformatics* **2008,** *24* (23), 2740-7.
13. Kurcon, T.; Liu, Z.; Paradkar, A. V.; Vaiana, C. A.; Koppolu, S.; Agrawal, P.; Mahal, L. K., miRNA proxy approach reveals hidden functions of glycosylation. *Proc Natl Acad Sci U S A* **2015,** *112* (23), 7327-32.
14. Agrawal, P.; Kurcon, T.; Pilobello, K. T.; Rakus, J. F.; Koppolu, S.; Liu, Z.; Batista, B. S.; Eng, W. S.; Hsu, K. L.; Liang, Y.; Mahal, L. K., Mapping posttranscriptional regulation of the human glycome uncovers microRNA defining the glycocode. *Proc Natl Acad Sci U S A* **2014,** *111* (11), 4338-43.
15. Kasper, B. T.; Koppolu, S.; Mahal, L. K., Insights into miRNA regulation of the human glycome. *Biochem Biophys Res Commun* **2014,** *445* (4), 774-9.
16. Schmiedel, J. M.; Klemm, S. L.; Zheng, Y.; Sahay, A.; Bluthgen, N.; Marks, D. S.; van Oudenaarden, A., Gene expression. MicroRNA control of protein expression noise. *Science* **2015,** *348* (6230), 128-32.
17. Liu, B.; Li, J.; Cairns, M. J., Identifying miRNAs, targets and functions. *Brief Bioinform* **2014,** *15* (1), 1-19.
18. Chendrimada, T. P.; Gregory, R. I.; Kumaraswamy, E.; Norman, J.; Cooch, N.; Nishikura, K.; Shiekhattar, R., TRBP recruits the Dicer complex to Ago2 for microRNA processing and gene silencing. *Nature* **2005,** *436* (7051), 740-4.
19. Michlewski, G.; Caceres, J. F., Post-transcriptional control of miRNA biogenesis. *RNA* **2019,** *25* (1), 1-16.
20. Khvorova, A.; Reynolds, A.; Jayasena, S. D., Functional siRNAs and miRNAs exhibit strand bias. *Cell* **2003,** *115* (2), 209-16.
21. Agrawal, P.; Fontanals-Cirera, B.; Sokolova, E.; Jacob, S.; Vaiana, C. A.; Argibay, D.; Davalos, V.; McDermott, M.; Nayak, S.; Darvishian, F.; Castillo, M.; Ueberheide, B.; Osman, I.; Fenyo, D.; Mahal, L. K.; Hernando, E., A Systems Biology Approach Identifies FUT8 as a Driver of Melanoma Metastasis. *Cancer Cell* **2017,** *31* (6), 804-819 e7.
22. Cheng, L.; Gao, S.; Song, X.; Dong, W.; Zhou, H.; Zhao, L.; Jia, L., Comprehensive N-glycan profiles of hepatocellular carcinoma reveal association of fucosylation with tumor progression and regulation of FUT8 by microRNAs. *Oncotarget* **2016,** *7* (38), 61199-61214.
23. Bernardi, C.; Soffientini, U.; Piacente, F.; Tonetti, M. G., Effects of microRNAs on fucosyltransferase 8 (FUT8) expression in hepatocarcinoma cells. *PLoS One* **2013,** *8* (10), e76540.
24. Gaziel-Sovran, A.; Segura, M. F.; Di Micco, R.; Collins, M. K.; Hanniford, D.; Vega-Saenz de Miera, E.; Rakus, J. F.; Dankert, J. F.; Shang, S.; Kerbel, R. S.; Bhardwaj, N.; Shao, Y.; Darvishian, F.; Zavadil, J.; Erlebacher, A.; Mahal, L. K.; Osman, I.; Hernando, E., miR-30b/30d regulation of GalNAc transferases enhances invasion and immunosuppression during metastasis. *Cancer Cell* **2011,** *20* (1), 104-18.
25. Peng, R. Q.; Wan, H. Y.; Li, H. F.; Liu, M.; Li, X.; Tang, H., MicroRNA-214 suppresses growth and invasiveness of cervical cancer cells by targeting UDP-N-acetyl-alpha-D-galactosamine:polypeptide N-acetylgalactosaminyltransferase 7. *J Biol Chem* **2012,** *287* (17), 14301-9.
26. Shan, S. W.; Fang, L.; Shatseva, T.; Rutnam, Z. J.; Yang, X.; Du, W.; Lu, W. Y.; Xuan, J. W.; Deng, Z.; Yang, B. B., Mature miR-17-5p and passenger miR-17-3p induce hepatocellular carcinoma by targeting PTEN, GalNT7 and vimentin in different signal pathways. *J Cell Sci* **2013,** *126* (Pt 6), 1517-30.

27. Li, W.; Ma, H.; Sun, J., MicroRNA34a/c function as tumor suppressors in Hep2 laryngeal carcinoma cells and may reduce GALNT7 expression. *Mol Med Rep* **2014,** *9* (4), 1293-8.
28. Duan, H. F.; Li, X. Q.; Hu, H. Y.; Li, Y. C.; Cai, Z.; Mei, X. S.; Yu, P.; Nie, L. P.; Zhang, W.; Yu, Z. D.; Nie, G. H., Functional elucidation of miR-494 in the tumorigenesis of nasopharyngeal carcinoma. *Tumour Biol* **2015,** *36* (9), 6679-89.
29. Nie, G. H.; Luo, L.; Duan, H. F.; Li, X. Q.; Yin, M. J.; Li, Z.; Zhang, W., GALNT7, a target of miR-494, participates in the oncogenesis of nasopharyngeal carcinoma. *Tumour Biol* **2016,** *37* (4), 4559-67.
30. Li, Y.; Li, Y.; Chen, D.; Jin, L.; Su, Z.; Liu, J.; Duan, H.; Li, X.; Qi, Z.; Shi, M.; Ni, L.; Yang, S.; Gui, Y.; Mao, X.; Chen, Y.; Lai, Y., miR30a5p in the tumorigenesis of renal cell carcinoma: A tumor suppressive microRNA. *Mol Med Rep* **2016,** *13* (5), 4085-94.
31. Lu, Q.; Xu, L.; Li, C.; Yuan, Y.; Huang, S.; Chen, H., miR-214 inhibits invasion and migration via downregulating GALNT7 in esophageal squamous cell cancer. *Tumour Biol* **2016,** *37* (11), 14605-14614.
32. Niu, J. T.; Zhang, L. J.; Huang, Y. W.; Li, C.; Jiang, N.; Niu, Y. J., MiR-154 inhibits the growth of laryngeal squamous cell carcinoma by targeting GALNT7. *Biochem Cell Biol* **2018,** *96* (6), 752-760.
33. Kahai, S.; Lee, S. C.; Lee, D. Y.; Yang, J.; Li, M.; Wang, C. H.; Jiang, Z.; Zhang, Y.; Peng, C.; Yang, B. B., MicroRNA miR-378 regulates nephronectin expression modulating osteoblast differentiation by targeting GalNT-7. *PLoS One* **2009,** *4* (10), e7535.
34. Dyrskjot, L.; Ostenfeld, M. S.; Bramsen, J. B.; Silahtaroglu, A. N.; Lamy, P.; Ramanathan, R.; Fristrup, N.; Jensen, J. L.; Andersen, C. L.; Zieger, K.; Kauppinen, S.; Ulhoi, B. P.; Kjems, J.; Borre, M.; Orntoft, T. F., Genomic profiling of microRNAs in bladder cancer: miR-129 is associated with poor outcome and promotes cell death in vitro. *Cancer Res* **2009,** *69* (11), 4851-60.
35. Shan, Y.; Ma, J.; Pan, Y.; Hu, J.; Liu, B.; Jia, L., LncRNA SNHG7 sponges miR-216b to promote proliferation and liver metastasis of colorectal cancer through upregulating GALNT1. *Cell Death Dis* **2018,** *9* (7), 722.
36. Nakagawa, Y.; Nishikimi, T.; Kuwahara, K.; Fujishima, A.; Oka, S.; Tsutamoto, T.; Kinoshita, H.; Nakao, K.; Cho, K.; Inazumi, H.; Okamoto, H.; Nishida, M.; Kato, T.; Fukushima, H.; Yamashita, J. K.; Wijnen, W. J.; Creemers, E. E.; Kangawa, K.; Minamino, N.; Nakao, K.; Kimura, T., MiR30-GALNT1/2 Axis-Mediated Glycosylation Contributes to the Increased Secretion of Inactive Human Prohormone for Brain Natriuretic Peptide (proBNP) From Failing Hearts. *J Am Heart Assoc* **2017,** *6* (2).
37. Schjoldager, K. T.; Joshi, H. J.; Kong, Y.; Goth, C. K.; King, S. L.; Wandall, H. H.; Bennett, E. P.; Vakhrushev, S. Y.; Clausen, H., Deconstruction of O-glycosylation--GalNAc-T isoforms direct distinct subsets of the O-glycoproteome. *EMBO Rep* **2015,** *16* (12), 1713-22.
38. Hintze, J.; Ye, Z.; Narimatsu, Y.; Madsen, T. D.; Joshi, H. J.; Goth, C. K.; Linstedt, A.; Bachert, C.; Mandel, U.; Bennett, E. P.; Vakhrushev, S. Y.; Schjoldager, K. T., Probing the contribution of individual polypeptide GalNAc-transferase isoforms to the O-glycoproteome by inducible expression in isogenic cell lines. *J Biol Chem* **2018,** *293* (49), 19064-19077.
39. Zhang, L.; Hammell, M.; Kudlow, B. A.; Ambros, V.; Han, M., Systematic analysis of dynamic miRNA-target interactions during C. elegans development. *Development* **2009,** *136* (18), 3043-55.
40. Pilobello, K. T.; Krishnamoorthy, L.; Slawek, D.; Mahal, L. K., Development of a lectin microarray for the rapid analysis of protein glycopatterns. *Chembiochem* **2005,** *6* (6), 985-9.

41. Pilobello, K. T.; Slawek, D. E.; Mahal, L. K., A ratiometric lectin microarray approach to analysis of the dynamic mammalian glycome. *Proc Natl Acad Sci U S A* **2007,** *104* (28), 11534-9.
42. Hsu, S. D.; Lin, F. M.; Wu, W. Y.; Liang, C.; Huang, W. C.; Chan, W. L.; Tsai, W. T.; Chen, G. Z.; Lee, C. J.; Chiu, C. M.; Chien, C. H.; Wu, M. C.; Huang, C. Y.; Tsou, A. P.; Huang, H. D., miRTarBase: a database curates experimentally validated microRNA-target interactions. *Nucleic Acids Res* **2011,** *39* (Database issue), D163-9.
43. Lee, T.; Wang, N.; Houel, S.; Couts, K.; Old, W.; Ahn, N., Dosage and temporal thresholds in microRNA proteomics. *Mol Cell Proteomics* **2015,** *14* (2), 289-302.
44. Wolter, J. M.; Kotagama, K.; Pierre-Bez, A. C.; Firago, M.; Mangone, M., 3'LIFE: a functional assay to detect miRNA targets in high-throughput. *Nucleic Acids Res* **2014,** *42* (17), e132.
45. Zhou, P.; Xu, W.; Peng, X.; Luo, Z.; Xing, Q.; Chen, X.; Hou, C.; Liang, W.; Zhou, J.; Wu, X.; Songyang, Z.; Jiang, S., Large-scale screens of miRNA-mRNA interactions unveiled that the 3'UTR of a gene is targeted by multiple miRNAs. *PLoS One* **2013,** *8* (7), e68204.
46. Liu, W.; Wang, X., Prediction of functional microRNA targets by integrative modeling of microRNA binding and target expression data. *Genome Biol* **2019,** *20* (1), 18.
47. Ameres, S. L.; Horwich, M. D.; Hung, J. H.; Xu, J.; Ghildiyal, M.; Weng, Z.; Zamore, P. D., Target RNA-directed trimming and tailing of small silencing RNAs. *Science* **2010,** *328* (5985), 1534-9.
48. Ameres, S. L.; Hung, J. H.; Xu, J.; Weng, Z.; Zamore, P. D., Target RNA-directed tailing and trimming purifies the sorting of endo-siRNAs between the two Drosophila Argonaute proteins. *RNA* **2011,** *17* (1), 54-63.
49. Cazalla, D.; Yario, T.; Steitz, J. A., Down-regulation of a host microRNA by a Herpesvirus saimiri noncoding RNA. *Science* **2010,** *328* (5985), 1563-6.
50. Baccarini, A.; Chauhan, H.; Gardner, T. J.; Jayaprakash, A. D.; Sachidanandam, R.; Brown, B. D., Kinetic analysis reveals the fate of a microRNA following target regulation in mammalian cells. *Curr Biol* **2011,** *21* (5), 369-76.
51. Chipman, L. B.; Pasquinelli, A. E., miRNA Targeting: Growing beyond the Seed. *Trends Genet* **2019,** *35* (3), 215-222.
52. Vogel, C.; Marcotte, E. M., Insights into the regulation of protein abundance from proteomic and transcriptomic analyses. *Nat Rev Genet* **2012,** *13* (4), 227-32.
53. Kosti, I.; Jain, N.; Aran, D.; Butte, A. J.; Sirota, M., Cross-tissue Analysis of Gene and Protein Expression in Normal and Cancer Tissues. *Sci. Rep.* **2016,** *6*, 24799.
54. Buccitelli, C.; Selbach, M., mRNAs, proteins and the emerging principles of gene expression control. *Nat Rev Genet* **2020,** *21* (10), 630-644.
55. Pascal, L. E.; True, L. D.; Campbell, D. S.; Deutsch, E. W.; Risk, M.; Coleman, I. M.; Eichner, L. J.; Nelson, P. S.; Liu, A. Y., Correlation of mRNA and protein levels: cell type-specific gene expression of cluster designation antigens in the prostate. *BMC Genomics* **2008,** *9*, 246.
56. Maier, T.; Guell, M.; Serrano, L., Correlation of mRNA and protein in complex biological samples. *FEBS Lett* **2009,** *583* (24), 3966-73.
57. Koussounadis, A.; Langdon, S. P.; Um, I. H.; Harrison, D. J.; Smith, V. A., Relationship between differentially expressed mRNA and mRNA-protein correlations in a xenograft model system. *Sci Rep* **2015,** *5*, 10775.
58. Ostlund, G.; Sonnhammer, E. L., Quality criteria for finding genes with high mRNA-protein expression correlation and coexpression correlation. *Gene* **2012,** *497* (2), 228-36.

59. Eichhorn, S. W.; Guo, H.; McGeary, S. E.; Rodriguez-Mias, R. A.; Shin, C.; Baek, D.; Hsu, S. H.; Ghoshal, K.; Villen, J.; Bartel, D. P., mRNA destabilization is the dominant effect of mammalian microRNAs by the time substantial repression ensues. *Mol Cell* **2014,** *56* (1), 104-15.
60. Zhang, X.; Zuo, X.; Yang, B.; Li, Z.; Xue, Y.; Zhou, Y.; Huang, J.; Zhao, X.; Zhou, J.; Yan, Y.; Zhang, H.; Guo, P.; Sun, H.; Guo, L.; Zhang, Y.; Fu, X. D., MicroRNA directly enhances mitochondrial translation during muscle differentiation. *Cell* **2014,** *158* (3), 607-19.
61. Panda, A. C.; Sahu, I.; Kulkarni, S. D.; Martindale, J. L.; Abdelmohsen, K.; Vindu, A.; Joseph, J.; Gorospe, M.; Seshadri, V., miR-196b-mediated translation regulation of mouse insulin2 via the 5'UTR. *PLoS One* **2014,** *9* (7), e101084.
62. Gabius, H. J.; Andre, S.; Jimenez-Barbero, J.; Romero, A.; Solis, D., From lectin structure to functional glycomics: principles of the sugar code. *Trends Biochem Sci* **2011,** *36* (6), 298-313.
63. Chai, Y.; Du, Y.; Zhang, S.; Xiao, J.; Luo, Z.; He, F.; Huang, K., MicroRNA-485-5p reduces O-GlcNAcylation of Bmi-1 and inhibits colorectal cancer proliferation. *Exp Cell Res* **2018,** *368* (1), 111-118.
64. Han, D. L.; Wang, L. L.; Zhang, G. F.; Yang, W. F.; Chai, J.; Lin, H. M.; Fu, Z.; Yu, J. M., MiRNA-485-5p, inhibits esophageal cancer cells proliferation and invasion by down-regulating O-linked N-acetylglucosamine transferase. *Eur Rev Med Pharmacol Sci* **2019,** *23* (7), 2809-2816.
65. Jiang, M.; Xu, B.; Li, X.; Shang, Y.; Chu, Y.; Wang, W.; Chen, D.; Wu, N.; Hu, S.; Zhang, S.; Li, M.; Wu, K.; Yang, X.; Liang, J.; Nie, Y.; Fan, D., O-GlcNAcylation promotes colorectal cancer metastasis via the miR-101-O-GlcNAc/EZH2 regulatory feedback circuit. *Oncogene* **2019,** *38* (3), 301-316.
66. Yu, F. Y.; Zhou, C. Y.; Liu, Y. B.; Wang, B.; Mao, L.; Li, Y., miR-483 is down-regulated in gastric cancer and suppresses cell proliferation, invasion and protein O-GlcNAcylation by targeting OGT. *Neoplasma* **2018,** *65* (3), 406-414.
67. Lo, W. Y.; Yang, W. K.; Peng, C. T.; Pai, W. Y.; Wang, H. J., MicroRNA-200a/200b Modulate High Glucose-Induced Endothelial Inflammation by Targeting O-linked N-Acetylglucosamine Transferase Expression. *Front Physiol* **2018,** *9*, 355.
68. Liu, Y.; Huang, H.; Liu, M.; Wu, Q.; Li, W.; Zhang, J., MicroRNA-24-1 suppresses mouse hepatoma cell invasion and metastasis via directly targeting O-GlcNAc transferase. *Biomed Pharmacother* **2017,** *91*, 731-738.
69. Vaiana, C. A.; Kurcon, T.; Mahal, L. K., MicroRNA-424 Predicts a Role for beta-1,4 Branched Glycosylation in Cell Cycle Progression. *J Biol Chem* **2016,** *291* (3), 1529-37.
70. Luo, P.; He, T.; Jiang, R.; Li, G., MicroRNA-423-5p targets O-GlcNAc transferase to induce apoptosis in cardiomyocytes. *Mol Med Rep* **2015,** *12* (1), 1163-8.
71. Babae, N.; Bourajjaj, M.; Liu, Y.; Van Beijnum, J. R.; Cerisoli, F.; Scaria, P. V.; Verheul, M.; Van Berkel, M. P.; Pieters, E. H.; Van Haastert, R. J.; Yousefi, A.; Mastrobattista, E.; Storm, G.; Berezikov, E.; Cuppen, E.; Woodle, M.; Schaapveld, R. Q.; Prevost, G. P.; Griffioen, A. W.; Van Noort, P. I.; Schiffelers, R. M., Systemic miRNA-7 delivery inhibits tumor angiogenesis and growth in murine xenograft glioblastoma. *Oncotarget* **2014,** *5* (16), 6687-700.
72. Muthusamy, S.; DeMartino, A. M.; Watson, L. J.; Brittian, K. R.; Zafir, A.; Dassanayaka, S.; Hong, K. U.; Jones, S. P., MicroRNA-539 is up-regulated in failing heart, and suppresses O-GlcNAcase expression. *J Biol Chem* **2014,** *289* (43), 29665-76.
73. Ghahramani Seno, M. M.; Gwadry, F. G.; Hu, P.; Scherer, S. W., Neuregulin 1-alpha regulates phosphorylation, acetylation, and alternative splicing in lymphoblastoid cells. *Genome* **2013,** *56* (10), 619-25.

74. Chan, J. K.; Kiet, T. K.; Blansit, K.; Ramasubbaiah, R.; Hilton, J. F.; Kapp, D. S.; Matei, D., MiR-378 as a biomarker for response to anti-angiogenic treatment in ovarian cancer. *Gynecol Oncol* **2014,** *133* (3), 568-74.
75. Liu, B.; Ma, X.; Liu, Q.; Xiao, Y.; Pan, S.; Jia, L., Aberrant mannosylation profile and FTX/miR-342/ALG3-axis contribute to development of drug resistance in acute myeloid leukemia. *Cell Death Dis* **2018,** *9* (6), 688.
76. Tatura, R.; Buchholz, M.; Dickson, D. W.; van Swieten, J.; McLean, C.; Hoglinger, G.; Muller, U., microRNA profiling: increased expression of miR-147a and miR-518e in progressive supranuclear palsy (PSP). *Neurogenetics* **2016,** *17* (3), 165-71.
77. De Antonellis, P.; Carotenuto, M.; Vandenbussche, J.; De Vita, G.; Ferrucci, V.; Medaglia, C.; Boffa, I.; Galiero, A.; Di Somma, S.; Magliulo, D.; Aiese, N.; Alonzi, A.; Spano, D.; Liguori, L.; Chiarolla, C.; Verrico, A.; Schulte, J. H.; Mestdagh, P.; Vandesompele, J.; Gevaert, K.; Zollo, M., Early targets of miR-34a in neuroblastoma. *Mol Cell Proteomics* **2014,** *13* (8), 2114-31.
78. Li, Y.; Sun, Z.; Liu, B.; Shan, Y.; Zhao, L.; Jia, L., Tumor-suppressive miR-26a and miR-26b inhibit cell aggressiveness by regulating FUT4 in colorectal cancer. *Cell Death Dis* **2017,** *8* (6), e2892.
79. Wang, M.; Wang, J.; Kong, X.; Chen, H.; Wang, Y.; Qin, M.; Lin, Y.; Chen, H.; Xu, J.; Hong, J.; Chen, Y. X.; Zou, W.; Fang, J. Y., MiR-198 represses tumor growth and metastasis in colorectal cancer by targeting fucosyl transferase 8. *Sci Rep* **2014,** *4*, 6145.
80. Huang, H.; Liu, Y.; Yu, P.; Qu, J.; Guo, Y.; Li, W.; Wang, S.; Zhang, J., MiR-23a transcriptional activated by Runx2 increases metastatic potential of mouse hepatoma cell via directly targeting Mgat3. *Sci Rep* **2018,** *8* (1), 7366.
81. Guo, Y.; Li, S.; Qu, J.; Ye, L.; Wang, S.; Fan, J.; Wang, Q.; Zhang, J., Let-7c inhibits metastatic ability of mouse hepatocarcinoma cells via targeting mannoside acetylglucosaminyltransferase 4 isoenzyme A. *Int J Biochem Cell Biol* **2014,** *53*, 1-8.
82. Wang, Y. Q.; Ren, Y. F.; Song, Y. J.; Xue, Y. F.; Zhang, X. J.; Cao, S. T.; Deng, Z. J.; Wu, J.; Chen, L.; Li, G.; Shi, K. Q.; Chen, Y. P.; Ren, H.; Huang, A. L.; Tang, K. F., MicroRNA-581 promotes hepatitis B virus surface antigen expression by targeting Dicer and EDEM1. *Carcinogenesis* **2014,** *35* (9), 2127-33.
83. Li, G.; Luna, C.; Qiu, J.; Epstein, D. L.; Gonzalez, P., Role of miR-204 in the regulation of apoptosis, endoplasmic reticulum stress response, and inflammation in human trabecular meshwork cells. *Invest Ophthalmol Vis Sci* **2011,** *52* (6), 2999-3007.
84. Vitiello, M.; Tuccoli, A.; D'Aurizio, R.; Sarti, S.; Giannecchini, L.; Lubrano, S.; Marranci, A.; Evangelista, M.; Peppicelli, S.; Ippolito, C.; Barravecchia, I.; Guzzolino, E.; Montagnani, V.; Gowen, M.; Mercoledi, E.; Mercatanti, A.; Comelli, L.; Gurrieri, S.; Wu, L. W.; Ope, O.; Flaherty, K.; Boland, G. M.; Hammond, M. R.; Kwong, L.; Chiariello, M.; Stecca, B.; Zhang, G.; Salvetti, A.; Angeloni, D.; Pitto, L.; Calorini, L.; Chiorino, G.; Pellegrini, M.; Herlyn, M.; Osman, I.; Poliseno, L., Context-dependent miR-204 and miR-211 affect the biological properties of amelanotic and melanotic melanoma cells. *Oncotarget* **2017,** *8* (15), 25395-25417.
85. Lim, S. M.; Park, S. H.; Lee, J. H.; Kim, S. H.; Kim, J. Y.; Min, J. K.; Lee, G. M.; Kim, Y. G., Differential expression of microRNAs in recombinant Chinese hamster ovary cells treated with sodium butyrate using digital RNA counting. *J Biotechnol* **2018,** *283*, 37-42.

86. Pan, S.; Cheng, X.; Chen, H.; Castro, P. D.; Ittmann, M. M.; Hutson, A. W.; Zapata, S. K.; Sifers, R. N., ERManI is a target of miR-125b and promotes transformation phenotypes in hepatocellular carcinoma (HCC). *PLoS One* **2013,** *8* (8), e72829.
87. Adhikari, S.; Mandal, P., Integrated analysis of global gene and microRNA expression profiling associated with aplastic anaemia. *Life Sci* **2019,** *228*, 47-52.
88. Bhise, N. S.; Chauhan, L.; Shin, M.; Cao, X.; Pounds, S.; Lamba, V.; Lamba, J. K., MicroRNA-mRNA Pairs Associated with Outcome in AML: From In Vitro Cell-Based Studies to AML Patients. *Front Pharmacol* **2015,** *6*, 324.
89. Serino, G.; Sallustio, F.; Curci, C.; Cox, S. N.; Pesce, F.; De Palma, G.; Schena, F. P., Role of let-7b in the regulation of N-acetylgalactosaminyltransferase 2 in IgA nephropathy. *Nephrol Dial Transplant* **2015,** *30* (7), 1132-9.
90. Liu, B.; Pan, S.; Xiao, Y.; Liu, Q.; Xu, J.; Jia, L., LINC01296/miR-26a/GALNT3 axis contributes to colorectal cancer progression by regulating O-glycosylated MUC1 via PI3K/AKT pathway. *J Exp Clin Cancer Res* **2018,** *37* (1), 316.
91. Nakamura, S.; Horie, M.; Daidoji, T.; Honda, T.; Yasugi, M.; Kuno, A.; Komori, T.; Okuzaki, D.; Narimatsu, H.; Nakaya, T.; Tomonaga, K., Influenza A Virus-Induced Expression of a GalNAc Transferase, GALNT3, via MicroRNAs Is Required for Enhanced Viral Replication. *J Virol* **2016,** *90* (4), 1788-801.
92. Qu, J. J.; Qu, X. Y.; Zhou, D. Z., miR4262 inhibits colon cancer cell proliferation via targeting of GALNT4. *Mol Med Rep* **2017,** *16* (4), 3731-3736.
93. Liu, Y.; Liu, H.; Yang, L.; Wu, Q.; Liu, W.; Fu, Q.; Zhang, W.; Zhang, H.; Xu, J.; Gu, J., Loss of N-Acetylgalactosaminyltransferase-4 Orchestrates Oncogenic MicroRNA-9 in Hepatocellular Carcinoma. *J Biol Chem* **2017,** *292* (8), 3186-3200.
94. Zhang, J.; Zhang, Z.; Wang, Q.; Xing, X. J.; Zhao, Y., Overexpression of microRNA-365 inhibits breast cancer cell growth and chemo-resistance through GALNT4. *Eur Rev Med Pharmacol Sci* **2016,** *20* (22), 4710-4718.
95. Stiegelbauer, V.; Vychytilova-Faltejskova, P.; Karbiener, M.; Pehserl, A. M.; Reicher, A.; Resel, M.; Heitzer, E.; Ivan, C.; Bullock, M.; Ling, H.; Deutsch, A.; Wulf-Goldenberg, A.; Adiprasito, J. B.; Stoeger, H.; Haybaeck, J.; Svoboda, M.; Stotz, M.; Hoefler, G.; Slaby, O.; Calin, G. A.; Gerger, A.; Pichler, M., miR-196b-5p Regulates Colorectal Cancer Cell Migration and Metastases through Interaction with HOXB7 and GALNT5. *Clin Cancer Res* **2017,** *23* (17), 5255-5266.
96. Wu, Q.; Liu, H. O.; Liu, Y. D.; Liu, W. S.; Pan, D.; Zhang, W. J.; Yang, L.; Fu, Q.; Xu, J. J.; Gu, J. X., Decreased expression of hepatocyte nuclear factor 4alpha (Hnf4alpha)/microRNA-122 (miR-122) axis in hepatitis B virus-associated hepatocellular carcinoma enhances potential oncogenic GALNT10 protein activity. *J Biol Chem* **2015,** *290* (2), 1170-85.
97. Yang, J.; Li, G.; Zhang, K., MiR-125a regulates ovarian cancer proliferation and invasion by repressing GALNT14 expression. *Biomed Pharmacother* **2016,** *80*, 381-387.
98. Liu, X.; Chen, J.; Guan, T.; Yao, H.; Zhang, W.; Guan, Z.; Wang, Y., miRNAs and target genes in the blood as biomarkers for the early diagnosis of Parkinson's disease. *BMC Syst Biol* **2019,** *13* (1), 10.
99. Gao, Y.; Liu, T.; Huang, Y., MicroRNA-134 suppresses endometrial cancer stem cells by targeting POGLUT1 and Notch pathway proteins. *FEBS Lett* **2015,** *589* (2), 207-14.
100. Thapa, I.; Fox, H. S.; Bastola, D., Coexpression Network Analysis of miRNA-142 Overexpression in Neuronal Cells. *Biomed Res Int* **2015,** *2015*, 921517.

101. Metzler-Guillemain, C.; Victorero, G.; Lepoivre, C.; Bergon, A.; Yammine, M.; Perrin, J.; Sari-Minodier, I.; Boulanger, N.; Rihet, P.; Nguyen, C., Sperm mRNAs and microRNAs as candidate markers for the impact of toxicants on human spermatogenesis: an application to tobacco smoking. *Syst Biol Reprod Med* **2015,** *61* (3), 139-49.
102. Wang, R.; Fang, J.; Ma, H.; Feng, L.; Lian, M.; Yang, F.; Wang, H.; Wang, Q.; Chen, X., Effect of microRNA-203 on tumor growth in human hypopharyngeal squamous cell carcinoma. *Mol Cell Biochem* **2015,** *405* (1-2), 97-104.
103. Serino, G.; Sallustio, F.; Cox, S. N.; Pesce, F.; Schena, F. P., Abnormal miR-148b expression promotes aberrant glycosylation of IgA1 in IgA nephropathy. *J Am Soc Nephrol* **2012,** *23* (5), 814-24.
104. Li, C.; Shi, J.; Zhao, Y., MiR-320 promotes B cell proliferation and the production of aberrant glycosylated IgA1 in IgA nephropathy. *J Cell Biochem* **2018,** *119* (6), 4607-4614.
105. Yang, L.; Zhang, X.; Peng, W.; Wei, M.; Qin, W., MicroRNA-155-induced T lymphocyte subgroup drifting in IgA nephropathy. *Int Urol Nephrol* **2017,** *49* (2), 353-361.
106. Hu, S.; Bao, H.; Xu, X.; Zhou, X.; Qin, W.; Zeng, C.; Liu, Z., Increased miR-374b promotes cell proliferation and the production of aberrant glycosylated IgA1 in B cells of IgA nephropathy. *FEBS Lett* **2015,** *589* (24 Pt B), 4019-25.
107. Chao, C. C.; Wu, P. H.; Huang, H. C.; Chung, H. Y.; Chou, Y. C.; Cai, B. H.; Kannagi, R., Downregulation of miR-199a/b-5p is associated with GCNT2 induction upon epithelial-mesenchymal transition in colon cancer. *FEBS Lett* **2017,** *591* (13), 1902-1917.
108. Li, Q.; Ran, P.; Zhang, X.; Guo, X.; Yuan, Y.; Dong, T.; Zhu, B.; Zheng, S.; Xiao, C., Downregulation of N-Acetylglucosaminyltransferase GCNT3 by miR-302b-3p Decreases Non-Small Cell Lung Cancer (NSCLC) Cell Proliferation, Migration and Invasion. *Cell Physiol Biochem* **2018,** *50* (3), 987-1004.
109. Gonzalez-Vallinas, M.; Molina, S.; Vicente, G.; Zarza, V.; Martin-Hernandez, R.; Garcia-Risco, M. R.; Fornari, T.; Reglero, G.; Ramirez de Molina, A., Expression of microRNA-15b and the glycosyltransferase GCNT3 correlates with antitumor efficacy of Rosemary diterpenes in colon and pancreatic cancer. *PLoS One* **2014,** *9* (6), e98556.
110. He, X. J.; Xiao, Y.; Zhang, Q.; Ma, L. P.; Li, N.; Yang, J., Detection and functional annotation of misregulated microRNAs in the brain of the Ts65Dn mouse model of Down syndrome. *Chin Med J (Engl)* **2013,** *126* (1), 108-13.
111. Riley, M. F.; Bochter, M. S.; Wahi, K.; Nuovo, G. J.; Cole, S. E., Mir-125a-5p-mediated regulation of Lfng is essential for the avian segmentation clock. *Dev Cell* **2013,** *24* (5), 554-61.
112. Wahi, K.; Friesen, S.; Coppola, V.; Cole, S. E., Putative binding sites for mir-125 family miRNAs in the mouse Lfng 3'UTR affect transcript expression in the segmentation clock, but mir-125a-5p is dispensable for normal somitogenesis. *Dev Dyn* **2017,** *246* (10), 740-748.
113. Raimo, M.; Orso, F.; Grassi, E.; Cimino, D.; Penna, E.; De Pitta, C.; Stadler, M. B.; Primo, L.; Calautti, E.; Quaglino, P.; Provero, P.; Taverna, D., miR-146a Exerts Differential Effects on Melanoma Growth and Metastatization. *Mol Cancer Res* **2016,** *14* (6), 548-62.
114. Wang, L.; Wei, Z.; Wu, K.; Dai, W.; Zhang, C.; Peng, J.; He, Y., Long noncoding RNA B3GALT5-AS1 suppresses colon cancer liver metastasis via repressing microRNA-203. *Aging (Albany NY)* **2018,** *10* (12), 3662-3682.
115. Liu, Y. X.; Wang, L.; Liu, W. J.; Zhang, H. T.; Xue, J. H.; Zhang, Z. W.; Gao, C. J., MiR-124-3p/B4GALT1 axis plays an important role in SOCS3-regulated growth and chemo-sensitivity of CML. *J Hematol Oncol* **2016,** *9* (1), 69.

116. Teruel, R.; Martinez-Martinez, I.; Guerrero, J. A.; Gonzalez-Conejero, R.; de la Morena-Barrio, M. E.; Salloum-Asfar, S.; Arroyo, A. B.; Aguila, S.; Garcia-Barbera, N.; Minano, A.; Vicente, V.; Corral, J.; Martinez, C., Control of post-translational modifications in antithrombin during murine post-natal development by miR-200a. *J Biomed Sci* **2013,** *20*, 29.
117. Cai, H.; Zhou, H.; Miao, Y.; Li, N.; Zhao, L.; Jia, L., MiRNA expression profiles reveal the involvement of miR-26a, miR-548l and miR-34a in hepatocellular carcinoma progression through regulation of ST3GAL5. *Lab Invest* **2017,** *97* (5), 530-542.
118. Tonevitsky, A. G.; Maltseva, D. V.; Abbasi, A.; Samatov, T. R.; Sakharov, D. A.; Shkurnikov, M. U.; Lebedev, A. E.; Galatenko, V. V.; Grigoriev, A. I.; Northoff, H., Dynamically regulated miRNA-mRNA networks revealed by exercise. *BMC Physiol* **2013,** *13*, 9.
119. Sun, M.; Zhao, X.; Liang, L.; Pan, X.; Lv, H.; Zhao, Y., Sialyltransferase ST3GAL6 mediates the effect of microRNA-26a on cell growth, migration, and invasion in hepatocellular carcinoma through the protein kinase B/mammalian target of rapamycin pathway. *Cancer Sci* **2017,** *108* (2), 267-276.
120. Han, Y.; Liu, Y.; Fu, X.; Zhang, Q.; Huang, H.; Zhang, C.; Li, W.; Zhang, J., miR-9 inhibits the metastatic ability of hepatocellular carcinoma via targeting beta galactoside alpha-2,6-sialyltransferase 1. *J Physiol Biochem* **2018,** *74* (3), 491-501.
121. Gao, L.; He, R. Q.; Wu, H. Y.; Zhang, T. T.; Liang, H. W.; Ye, Z. H.; Li, Z. Y.; Xie, T. T.; Shi, Q.; Ma, J.; Hu, X. H.; Chen, G., Expression Signature and Role of miR-30d-5p in Non-Small Cell Lung Cancer: a Comprehensive Study Based on in Silico Analysis of Public Databases and in Vitro Experiments. *Cell Physiol Biochem* **2018,** *50* (5), 1964-1987.
122. Liu, B.; Liu, Y.; Zhao, L.; Pan, Y.; Shan, Y.; Li, Y.; Jia, L., Upregulation of microRNA-135b and microRNA-182 promotes chemoresistance of colorectal cancer by targeting ST6GALNAC2 via PI3K/AKT pathway. *Mol Carcinog* **2017,** *56* (12), 2669-2680.
123. Jia, L.; Luo, S.; Ren, X.; Li, Y.; Hu, J.; Liu, B.; Zhao, L.; Shan, Y.; Zhou, H., miR-182 and miR-135b Mediate the Tumorigenesis and Invasiveness of Colorectal Cancer Cells via Targeting ST6GALNAC2 and PI3K/AKT Pathway. *Dig Dis Sci* **2017,** *62* (12), 3447-3459.
124. Miao, X.; Jia, L.; Zhou, H.; Song, X.; Zhou, M.; Xu, J.; Zhao, L.; Feng, X.; Zhao, Y., miR-4299 mediates the invasive properties and tumorigenicity of human follicular thyroid carcinoma by targeting ST6GALNAC4. *IUBMB Life* **2016,** *68* (2), 136-44.
125. Shan, Y.; Liu, Y.; Zhao, L.; Liu, B.; Li, Y.; Jia, L., MicroRNA-33a and let-7e inhibit human colorectal cancer progression by targeting ST8SIA1. *Int J Biochem Cell Biol* **2017,** *90*, 48-58.
126. Liu, Q. Y.; Miao, Y.; Wang, X. H.; Wang, P.; Cheng, Z. C.; Qian, T. M., Increased levels of miR-3099 induced by peripheral nerve injury promote Schwann cell proliferation and migration. *Neural Regen Res* **2019,** *14* (3), 525-531.
127. Ma, X.; Dong, W.; Su, Z.; Zhao, L.; Miao, Y.; Li, N.; Zhou, H.; Jia, L., Functional roles of sialylation in breast cancer progression through miR-26a/26b targeting ST8SIA4. *Cell Death Dis* **2016,** *7* (12), e2561.
128. Zhao, L.; Li, Y.; Song, X.; Zhou, H.; Li, N.; Miao, Y.; Jia, L., Upregulation of miR-181c inhibits chemoresistance by targeting ST8SIA4 in chronic myelocytic leukemia. *Oncotarget* **2016,** *7* (37), 60074-60086.
129. Wang, Z.; Hu, J.; Pan, Y.; Shan, Y.; Jiang, L.; Qi, X.; Jia, L., miR-140-5p/miR-149 Affects Chondrocyte Proliferation, Apoptosis, and Autophagy by Targeting FUT1 in Osteoarthritis. *Inflammation* **2018,** *41* (3), 959-971.

130. Wang, Y.; Chen, J.; Chen, X.; Jiang, F.; Sun, Y.; Pan, Y.; Zhang, W.; Zhang, J., MiR-34a suppresses HNSCC growth through modulating cell cycle arrest and senescence. *Neoplasma* **2017,** *64* (4), 543-553.
131. Wu, C. S.; Yen, C. J.; Chou, R. H.; Chen, J. N.; Huang, W. C.; Wu, C. Y.; Yu, Y. L., Downregulation of microRNA-15b by hepatitis B virus X enhances hepatocellular carcinoma proliferation via fucosyltransferase 2-induced Globo H expression. *Int J Cancer* **2014,** *134* (7), 1638-47.
132. Hu, J.; Wang, Z.; Pan, Y.; Ma, J.; Miao, X.; Qi, X.; Zhou, H.; Jia, L., MiR-26a and miR-26b mediate osteoarthritis progression by targeting FUT4 via NF-kappaB signaling pathway. *Int J Biochem Cell Biol* **2018,** *94*, 79-88.
133. Zheng, Q.; Zhang, D.; Yang, Y. U.; Cui, X.; Sun, J.; Liang, C.; Qin, H.; Yang, X.; Liu, S.; Yan, Q., MicroRNA-200c impairs uterine receptivity formation by targeting FUT4 and alpha1,3-fucosylation. *Cell Death Differ* **2017,** *24* (12), 2161-2172.
134. Zhao, L.; Feng, X.; Song, X.; Zhou, H.; Zhao, Y.; Cheng, L.; Jia, L., miR-493-5p attenuates the invasiveness and tumorigenicity in human breast cancer by targeting FUT4. *Oncol Rep* **2016,** *36* (2), 1007-15.
135. Feng, X.; Zhao, L.; Gao, S.; Song, X.; Dong, W.; Zhao, Y.; Zhou, H.; Cheng, L.; Miao, X.; Jia, L., Increased fucosylation has a pivotal role in multidrug resistance of breast cancer cells through miR-224-3p targeting FUT4. *Gene* **2016,** *578* (2), 232-41.
136. Liang, L.; Gao, C.; Li, Y.; Sun, M.; Xu, J.; Li, H.; Jia, L.; Zhao, Y., miR-125a-3p/FUT5-FUT6 axis mediates colorectal cancer cell proliferation, migration, invasion and pathological angiogenesis via PI3K-Akt pathway. *Cell Death Dis* **2017,** *8* (8), e2968.
137. Li, N.; Liu, Y.; Miao, Y.; Zhao, L.; Zhou, H.; Jia, L., MicroRNA-106b targets FUT6 to promote cell migration, invasion, and proliferation in human breast cancer. *IUBMB Life* **2016,** *68* (9), 764-75.
138. Hu, B.; Xu, C.; Tian, Y.; Shi, C.; Zhang, Y.; Deng, L.; Zhou, H.; Cao, P.; Chen, H.; Yuan, W., Inflammatory microRNA-194 and -515 attenuate the biosynthesis of chondroitin sulfate during human intervertebral disc degeneration. *Oncotarget* **2017,** *8* (30), 49303-49317.
139. Prudnikova, T. Y.; Mostovich, L. A.; Kashuba, V. I.; Ernberg, I.; Zabarovsky, E. R.; Grigorieva, E. V., miRNA-218 contributes to the regulation of D-glucuronyl C5-epimerase expression in normal and tumor breast tissues. *Epigenetics* **2012,** *7* (10), 1109-14.
140. Song, Y. Q.; Karasugi, T.; Cheung, K. M.; Chiba, K.; Ho, D. W.; Miyake, A.; Kao, P. Y.; Sze, K. L.; Yee, A.; Takahashi, A.; Kawaguchi, Y.; Mikami, Y.; Matsumoto, M.; Togawa, D.; Kanayama, M.; Shi, D.; Dai, J.; Jiang, Q.; Wu, C.; Tian, W.; Wang, N.; Leong, J. C.; Luk, K. D.; Yip, S. P.; Cherny, S. S.; Wang, J.; Mundlos, S.; Kelempisioti, A.; Eskola, P. J.; Mannikko, M.; Makela, P.; Karppinen, J.; Jarvelin, M. R.; O'Reilly, P. F.; Kubo, M.; Kimura, T.; Kubo, T.; Toyama, Y.; Mizuta, H.; Cheah, K. S.; Tsunoda, T.; Sham, P. C.; Ikegawa, S.; Chan, D., Lumbar disc degeneration is linked to a carbohydrate sulfotransferase 3 variant. *J Clin Invest* **2013,** *123* (11), 4909-17.
141. Yang, G.; Gong, Y.; Wang, Q.; Wang, Y.; Zhang, X., The role of miR-100-mediated Notch pathway in apoptosis of gastric tumor cells. *Cell Signal* **2015,** *27* (6), 1087-101.
142. Liep, J.; Kilic, E.; Meyer, H. A.; Busch, J.; Jung, K.; Rabien, A., Cooperative Effect of miR-141-3p and miR-145-5p in the Regulation of Targets in Clear Cell Renal Cell Carcinoma. *PLoS One* **2016,** *11* (6), e0157801.

143. Shi, X.; Su, S.; Long, J.; Mei, B.; Chen, Y., MicroRNA-191 targets N-deacetylase/N-sulfotransferase 1 and promotes cell growth in human gastric carcinoma cell line MGC803. *Acta Biochim Biophys Sin (Shanghai)* **2011,** *43* (11), 849-56.
144. Bao, L.; Yan, Y.; Xu, C.; Ji, W.; Shen, S.; Xu, G.; Zeng, Y.; Sun, B.; Qian, H.; Chen, L.; Wu, M.; Su, C.; Chen, J., MicroRNA-21 suppresses PTEN and hSulf-1 expression and promotes hepatocellular carcinoma progression through AKT/ERK pathways. *Cancer Lett* **2013,** *337* (2), 226-36.
145. Yang, L.; Zhang, S.; Guo, K.; Huang, H.; Qi, S.; Yao, J.; Zhang, Z., miR-125a restrains cell migration and invasion by targeting STAT3 in gastric cancer cells. *Onco Targets Ther* **2019,** *12*, 205-215.
146. Wang, G.; Zhao, W.; Gao, X.; Zhang, D.; Li, Y.; Zhang, Y.; Li, W., HNF1AAS1 promotes growth and metastasis of esophageal squamous cell carcinoma by sponging miR214 to upregulate the expression of SOX-4. *Int J Oncol* **2017,** *51* (2), 657-667.
147. Midgley, A. C.; Morris, G.; Phillips, A. O.; Steadman, R., 17beta-estradiol ameliorates age-associated loss of fibroblast function by attenuating IFN-gamma/STAT1-dependent miR-7 upregulation. *Aging Cell* **2016,** *15* (3), 531-41.
148. Pan, B.; Toms, D.; Shen, W.; Li, J., MicroRNA-378 regulates oocyte maturation via the suppression of aromatase in porcine cumulus cells. *Am J Physiol Endocrinol Metab* **2015,** *308* (6), E525-34.
149. Rock, K.; Tigges, J.; Sass, S.; Schutze, A.; Florea, A. M.; Fender, A. C.; Theis, F. J.; Krutmann, J.; Boege, F.; Fritsche, E.; Reifenberger, G.; Fischer, J. W., miR-23a-3p causes cellular senescence by targeting hyaluronan synthase 2: possible implication for skin aging. *J Invest Dermatol* **2015,** *135* (2), 369-377.
150. Zhang, J.; Chang, J. J.; Xu, F.; Ma, X. J.; Wu, Y.; Li, W. C.; Wang, H. J.; Huang, G. Y.; Ma, D., MicroRNA deregulation in right ventricular outflow tract myocardium in nonsyndromic tetralogy of fallot. *Can J Cardiol* **2013,** *29* (12), 1695-703.
151. Lagendijk, A. K.; Goumans, M. J.; Burkhard, S. B.; Bakkers, J., MicroRNA-23 restricts cardiac valve formation by inhibiting Has2 and extracellular hyaluronic acid production. *Circ Res* **2011,** *109* (6), 649-57.
152. Pan, B.; Toms, D.; Li, J., MicroRNA-574 suppresses oocyte maturation via targeting hyaluronan synthase 2 in porcine cumulus cells. *Am J Physiol Cell Physiol* **2018,** *314* (3), C268-C277.
153. Li, H. M.; Xiao, Y. J.; Min, Z. S.; Tan, C., Identification and interaction analysis of key genes and microRNAs in atopic dermatitis by bioinformatics analysis. *Clin Exp Dermatol* **2019,** *44* (3), 257-264.
154. Bai, F.; Jiu, M.; You, Y.; Feng, Y.; Xin, R.; Liu, X.; Mo, L.; Nie, Y., miR29a3p represses proliferation and metastasis of gastric cancer cells via attenuating HAS3 levels. *Mol Med Rep* **2018,** *17* (6), 8145-8152.
155. Pashaei, E.; Guzel, E.; Ozgurses, M. E.; Demirel, G.; Aydin, N.; Ozen, M., A Meta-Analysis: Identification of Common Mir-145 Target Genes that have Similar Behavior in Different GEO Datasets. *PLoS One* **2016,** *11* (9), e0161491.
156. Barter, M. J.; Tselepi, M.; Gomez, R.; Woods, S.; Hui, W.; Smith, G. R.; Shanley, D. P.; Clark, I. M.; Young, D. A., Genome-Wide MicroRNA and Gene Analysis of Mesenchymal Stem Cell Chondrogenesis Identifies an Essential Role and Multiple Targets for miR-140-5p. *Stem Cells* **2015,** *33* (11), 3266-80.

157. Straniero, L.; Rimoldi, V.; Samarani, M.; Goldwurm, S.; Di Fonzo, A.; Kruger, R.; Deleidi, M.; Aureli, M.; Solda, G.; Duga, S.; Asselta, R., The GBAP1 pseudogene acts as a ceRNA for the glucocerebrosidase gene GBA by sponging miR-22-3p. *Sci Rep* **2017,** *7* (1), 12702.
158. Chang, S.; He, S.; Qiu, G.; Lu, J.; Wang, J.; Liu, J.; Fan, L.; Zhao, W.; Che, X., MicroRNA-125b promotes invasion and metastasis of gastric cancer by targeting STARD13 and NEU1. *Tumour Biol* **2016,** *37* (9), 12141-12151.
159. Tao, J.; Liu, W.; Shang, G.; Zheng, Y.; Huang, J.; Lin, R.; Chen, L., MiR-207/352 regulate lysosomal-associated membrane proteins and enzymes following ischemic stroke. *Neuroscience* **2015,** *305*, 1-14.
160. Yang, C.; Ren, J.; Li, B.; Zhang, D.; Ma, C.; Cheng, C.; Sun, Y.; Fu, L.; Shi, X., Identification of clinical tumor stages related mRNAs and miRNAs in cervical squamous cell carcinoma. *Pathol Res Pract* **2018,** *214* (10), 1638-1647.
161. Yamada, Y.; Arai, T.; Sugawara, S.; Okato, A.; Kato, M.; Kojima, S.; Yamazaki, K.; Naya, Y.; Ichikawa, T.; Seki, N., Impact of novel oncogenic pathways regulated by antitumor miR-451a in renal cell carcinoma. *Cancer Sci* **2018,** *109* (4), 1239-1253.
162. Sun, Y.; Liu, X.; Zhang, Q.; Mao, X.; Feng, L.; Su, P.; Chen, H.; Guo, Y.; Jin, F., Oncogenic potential of TSTA3 in breast cancer and its regulation by the tumor suppressors miR-125a-5p and miR-125b. *Tumour Biol* **2016,** *37* (4), 4963-72.
163. Kwon, D. N.; Chang, B. S.; Kim, J. H., MicroRNA dysregulation in liver and pancreas of CMP-Neu5Ac hydroxylase null mice disrupts insulin/PI3K-AKT signaling. *Biomed Res Int* **2014,** *2014*, 236385.
164. Gan, B. L.; Zhang, L. J.; Gao, L.; Ma, F. C.; He, R. Q.; Chen, G.; Ma, J.; Zhong, J. C.; Hu, X. H., Downregulation of miR2245p in prostate cancer and its relevant molecular mechanism via TCGA, GEO database and in silico analyses. *Oncol Rep* **2018,** *40* (6), 3171-3188.
165. Xu, Q. F.; Pan, Y. W.; Li, L. C.; Zhou, Z.; Huang, Q. L.; Pang, J. C.; Zhu, X. P.; Ren, Y.; Yang, H.; Ohgaki, H.; Lv, S. Q., MiR-22 is frequently downregulated in medulloblastomas and inhibits cell proliferation via the novel target PAPST1. *Brain Pathol* **2014,** *24* (6), 568-83.
166. Lim, C. H.; Jeong, W.; Lim, W.; Kim, J.; Song, G.; Bazer, F. W., Differential expression of select members of the SLC family of genes and regulation of expression by microRNAs in the chicken oviduct. *Biol Reprod* **2012,** *87* (6), 145.
167. Hao, G. J.; Ding, Y. H.; Wen, H.; Li, X. F.; Zhang, W.; Su, H. Y.; Liu, D. M.; Xie, N. L., Attenuation of deregulated miR-369-3p expression sensitizes non-small cell lung cancer cells to cisplatin via modulation of the nucleotide sugar transporter SLC35F5. *Biochem Biophys Res Commun* **2017,** *488* (3), 501-508.
168. Wijayakumara, D. D.; Mackenzie, P. I.; McKinnon, R. A.; Hu, D. G.; Meech, R., Regulation of UDP-Glucuronosyltransferase 2B15 by miR-331-5p in Prostate Cancer Cells Involves Canonical and Noncanonical Target Sites. *J Pharmacol Exp Ther* **2018,** *365* (1), 48-59.
169. Margaillan, G.; Levesque, E.; Guillemette, C., Epigenetic regulation of steroid inactivating UDP-glucuronosyltransferases by microRNAs in prostate cancer. *J Steroid Biochem Mol Biol* **2016,** *155* (Pt A), 85-93.
170. Wijayakumara, D. D.; Hu, D. G.; Meech, R.; McKinnon, R. A.; Mackenzie, P. I., Regulation of Human UGT2B15 and UGT2B17 by miR-376c in Prostate Cancer Cell Lines. *J Pharmacol Exp Ther* **2015,** *354* (3), 417-25.
171. Papageorgiou, I.; Court, M. H., Identification and validation of the microRNA response elements in the 3'-untranslated region of the UDP glucuronosyltransferase (UGT) 2B7 and 2B15 genes by a functional genomics approach. *Biochem Pharmacol* **2017,** *146*, 199-213.

172. Zhang, J. J.; Wang, L. N.; Feng, Y.; Zhi, H.; Ma, G. S.; Ye, X. Z.; Qian, S. S.; Wang, B., [Association study on the microRNA-1 target gene polymorphism and the risk of premature coronary artery disease]. *Zhonghua Xin Xue Guan Bing Za Zhi* **2012,** *40* (5), 386-91.
173. Fu, T.; Kemper, J. K., MicroRNA-34a and Impaired FGF19/21 Signaling in Obesity. *Vitam Horm* **2016,** *101*, 175-96.
174. Kang, W. L.; Xu, G. S., Atrasentan increased the expression of klotho by mediating miR-199b-5p and prevented renal tubular injury in diabetic nephropathy. *Sci Rep* **2016,** *6*, 19979.
175. He, X. J.; Ma, Y. Y.; Yu, S.; Jiang, X. T.; Lu, Y. D.; Tao, L.; Wang, H. P.; Hu, Z. M.; Tao, H. Q., Up-regulated miR-199a-5p in gastric cancer functions as an oncogene and targets klotho. *BMC Cancer* **2014,** *14*, 218.
176. Jiang, B.; Gu, Y.; Chen, Y., Identification of novel predictive markers for the prognosis of pancreatic ductal adenocarcinoma. *Cancer Invest* **2014,** *32* (6), 218-25.
177. Mehi, S. J.; Maltare, A.; Abraham, C. R.; King, G. D., MicroRNA-339 and microRNA-556 regulate Klotho expression in vitro. *Age (Dordr)* **2014,** *36* (1), 141-9.
178. Koshizuka, K.; Hanazawa, T.; Kikkawa, N.; Katada, K.; Okato, A.; Arai, T.; Idichi, T.; Osako, Y.; Okamoto, Y.; Seki, N., Antitumor miR-150-5p and miR-150-3p inhibit cancer cell aggressiveness by targeting SPOCK1 in head and neck squamous cell carcinoma. *Auris Nasus Larynx* **2018,** *45* (4), 854-865.
179. Osako, Y.; Seki, N.; Koshizuka, K.; Okato, A.; Idichi, T.; Arai, T.; Omoto, I.; Sasaki, K.; Uchikado, Y.; Kita, Y.; Kurahara, H.; Maemura, K.; Natsugoe, S., Regulation of SPOCK1 by dual strands of pre-miR-150 inhibit cancer cell migration and invasion in esophageal squamous cell carcinoma. *J Hum Genet* **2017,** *62* (11), 935-944.
180. Lee, S. J.; Kim, S. J.; Seo, H. H.; Shin, S. P.; Kim, D.; Park, C. S.; Kim, K. T.; Kim, Y. H.; Jeong, J. S.; Kim, I. H., Over-expression of miR-145 enhances the effectiveness of HSVtk gene therapy for malignant glioma. *Cancer Lett* **2012,** *320* (1), 72-80.

CHAPTER 2

DEVELOPMENT OF HIGH-THROUGHPUT TECHNOLOGY FOR MAPPING MIRNA-GENE INTERACTOME NETWORK

2.1 ABSTRACT

MicroRNAs are a class of small endogenous non-coding RNAs that act as rheostats and coordinately fine-tune gene expression, dampening translational noise by targeting a vast number of messenger RNA (mRNA). miRs are primarily known to interact with the 3'-unstranslated region (3'UTR) of mRNA targets to impact protein translational expression. As mentioned in the previous chapter, miR target prediction algorithms fail to accurately identify miR targets. The work in this chapter describes the initial development of a high-throughput experimental platform to analyze miR:mRNA interaction to identify miR target space.

2.2 INTRODUCTION

MiRNAs (miRs) perform their biological function by guiding the RNAi-induced silencing complex (RISC) to modulate gene expression via partial complementary interactions with the 5'UTR, coding region, gene promoter or predominately, the 3'UTR of mRNAs[1, 2]. Within the RISC complex, miRNAs bind to mRNAs through imperfect Watson-Crick base pairing, ultimately leading to repression of gene expression primarily by mRNA decay and, to a lesser extent, translational repression[3, 4]. Deciphering the roles of individual miR depends upon identifying their targets and downstream effects to reveal the mechanistic context of their cellular functions.

Contemporary identification of miR:target interactomes is hindered by three issues. First, the low accuracy and sensitivity of prediction (17-66%) which was discussed in detail in chapter 1 [5]. Second, the low expression of subset of genes, such as glycogenes, resulting in technical challenges including complications in transcriptomic analysis and RISC complex pulldown [6, 7]. Third, the suboptimal throughput of more direct miR:mRNA validations (e.g. luciferase assay) and the inappropriate use of transcriptomic profiling to understand the protein regulatory network of miRNAs.

All commonly used target prediction algorithms were improved using high-throughput profiling data. Most use transcriptomic profiling data to map miRNA and mRNA interactions [8, 9] which fails to take into account the disconnect between the mRNA and protein levels, especially for low abundance genes including glycosylation enzymes and membrane proteins [10]. It is known that the measurable transcriptome levels do not accurately reflect the proteome levels[11]. This low correlation could stem from the detection methods or the underlying biological mechanisms. More recently, crosslinking and immunoprecipitation (CLIP) sequencing data was utilized to identify transcript targets associated with the functional miRNA-RNA-induced silencing complex (RISC) complex[12-14 15, 16]. This method, which mostly focuses on a specific miR and is cell-type dependent, is also less accurate when considering low abundance genes like glycogenes or receptor genes [6, 7]. The gold-standard experimental analyses of miR-mRNA interactions have focused on the use of either luciferase assays [5]. However, even in 96 well format, luciferase assays require the lysis of cells, expensive reagents, and longer processing time thus lowering throughput.

We wanted to create a platform that would enable collection of a high-throughput dataset equivalent to the gold-standard luciferase assay to address these issues and limitations of current technology. A high-throughput cell spot microarray system, miRfect, is described in this chapter as the initial step for the development of a platform to accurately pinpoint miR-target interaction network.

2.4 DEVELOPMENT OF HIGH-THROUGHPUT MIRFLUR PLATFORM FOR IDENTIFICATIONS OF THE MIR-GENE INTERACTOME

2.4.1 Current high-throughput methods of validating miR-target interactions and their limitations

Current high-throughput mapping of miR-target interactions rely on three methods. The first method is high-throughput transcriptomic profiling upon miR perturbation to identify mRNA targets [17]. This method assumes that the biological effect of miR on mRNA is the same as on the protein expression level. Previous studies shown that mRNA and protein levels are not highly correlated and in many cases, miRs have different impacts on the mRNA and protein levels[5]. Furthermore, low abundance transcripts are often missed in many of the transcriptomic-based profiling methods to determine miRNA targets. In addition, transcriptomic profiling upon miR perturbation does not differentiate direct from indirect effects of the miR. Thus, transcriptomic analysis displays an incomplete picture of actual miR biological impacts and failed to accurately identify impacts on low abundance transcripts like glycogenes. The second method is the cross-linking and immunoprecipitation (CLIP) assay. Covalent cross-linking is performed by using formaldehyde or UV light, and followed by partial RNA digestion to create RNA fragments which are subjected to high-throughput sequencing. CLIP reads reflect short-lived interactions and do not separate functional and non-functional biological impacts. For glycogenes, the low abundance of transcripts significantly reduces the accuracy of this method. Comparison of published data for HIT-CLIP analysis of the interactions of miR-200b with its targets in *MDA-MB-231* cells failed to observe any of the three glycogenes previously identified as targets of miR-200b-3p in the same cell line (B3GLCT, ST6GALNAC5, ST3GAL5) [7]. B3GLCT catalyzes for the, ST6GALNAC5 predominantly catalyzes the transfer of sialyl group (N-acetyl-alpha-neuraminyl or NeuAc) from

CMP-NeuAc to the GalNAc residue on specific glycans, and ST3GAL5 catalyzes the formation of GM3 using lactosylceramide as the substrate. The biological impact and interaction of miR-200b-3p with the 3 genes above were validated using multiple methods following the standards of the field including transcriptomics and Western blot analysis of the glycosylation enzymes upon miR transfection however CLIP assay failed to identify this interaction. Transcriptomic validation usually uses quantitative real-time polymerase chain reaction (RT-qPCR), which enables the detection and measurement of mRNA levels through reverse transcription to cDNA and qPCR reaction. In the Western blot validation method, protein levels are detected and quantified upon miR transfection. The third "high-throughput" method of mapping miR:target interactions is luciferase-based assays which is currently the gold-standard assay to identify direct functional miR-target interactions. This method utilizes a luciferase plasmid reporter with the 3'UTR of a gene of interest co-tranfected with miR to determine their interactions. The limitation of this method is the requirement for cell lysis and expensive reagents. Additionally, it is only considered as moderate throughput due to the inherent time requirements.

In summary, none of the three available methods were optimal for the high-throughput identifications of miR-glycogene interactomes. Thus, there was a need to develop a better high-throughput experimental assay and create an accurate miR-target database based on validated interactions.

2.4.2 Design of first generation high-throughput miRfect system

Our ideal high-throughput assay would be simple, not require extra lysis steps and reagents but still follow the principles of the gold-standard of luciferase assay to identify more direct binders. Previous work had shown fluorescent protein-based probes could substitute for luciferase in standard assays. While both single and dual-color genetically encoded fluorescent reporters have been used to study miRs in live cells, their use has been limited to examining single miR:mRNA interactions by microscopy or flow cytometry [18, 19]. In preliminary work, Chris Vaiana in our lab had created a sensor for miR analysis used Cerulean and mCherry fluorescent probes. To adapt this to a high-throughput format, we initially envisioned using a microarray approach, as our lab specialized in this field.

The general idea of the assay was to have a whole human miR library printed on a slide (miR chip), which would then be incubated with cells to induce transfection with miRs within specific spots (miRfect slide, **Figure 2.1**). Transfection of the dual-color genetically encoded fluorescent reporter into cells on miRfect slide provides the fluorescence readout which indicates the extent of miR-target regulation.

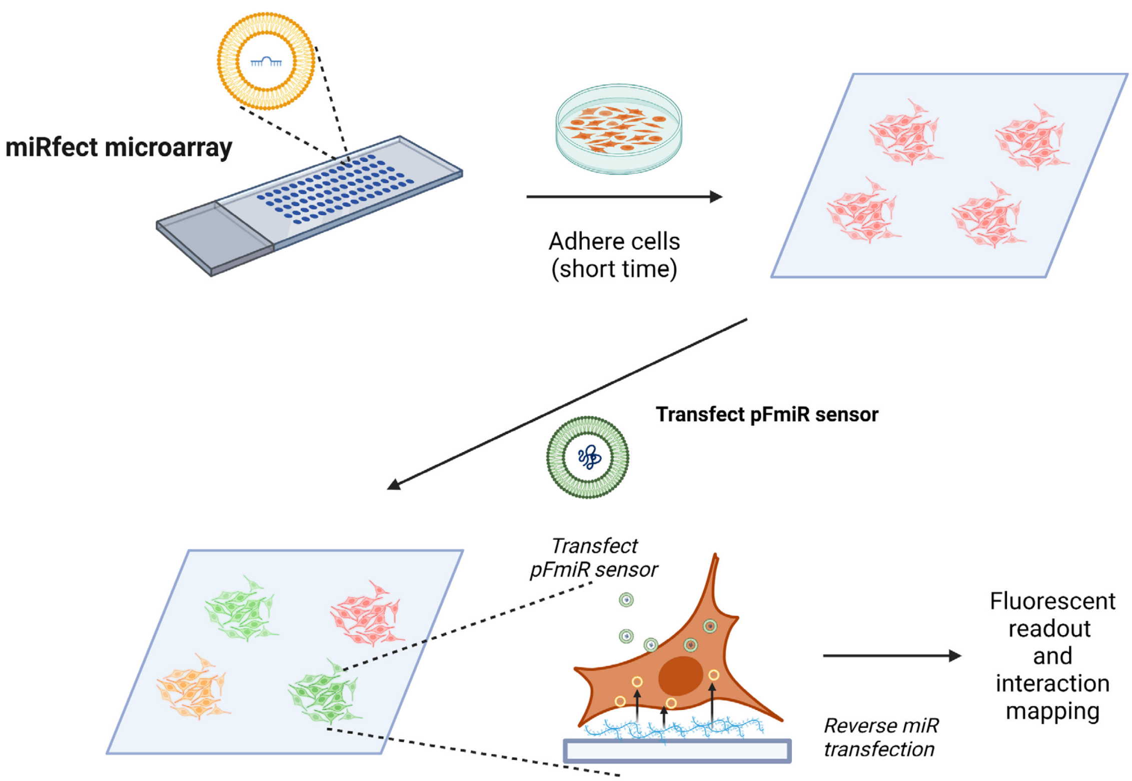

Figure 2.1. General scheme of miRfect high-throughput assay. miRNA mimic library and matrices are printed on a polystyrene slide. Cells are then adhered to specific miRNA spots and non-adherent cells are washed and removed. This specific cell spot microarray are then co-transfected with a pFmiR sensor to identify the miR-mRNA interaction network.

2.4.3 General scheme of how dual-color genetically encoded fluorescent reporter in miRfect system

In the fluorescent reporter, the 3'UTR of a gene of interest is cloned downstream of a fluorescent protein (**Figure 2.2**, Fluorophore 2, F1), our reporter protein. A second fluorescent protein (**Figure 2.2**, Fluorophore 1, F1), is incorporated into the same plasmid, to control for transfection efficiency and any non-specific effects of the miR on the transfected cells, thus making possible quantitative analysis. When reporter and miR mimics are co-transfected into mammalian cells, the readout of ratio of F2/F1 fluorescence in miR transfected cells, is normalized to the data from a non-targeting control (NTC), reflects the extent of miR-target regulation (**Figure 2.2**). For miRs that repress protein expression via binding to the 3'UTR in the sensor, a loss of F2 fluorescence is expected, with a concomitant reduction in the normalized fluorescence ratio. Our ratiometric fluorescent-based reporter system is highly compatible with high-throughput downstream applications for mapping miR-target interactions.

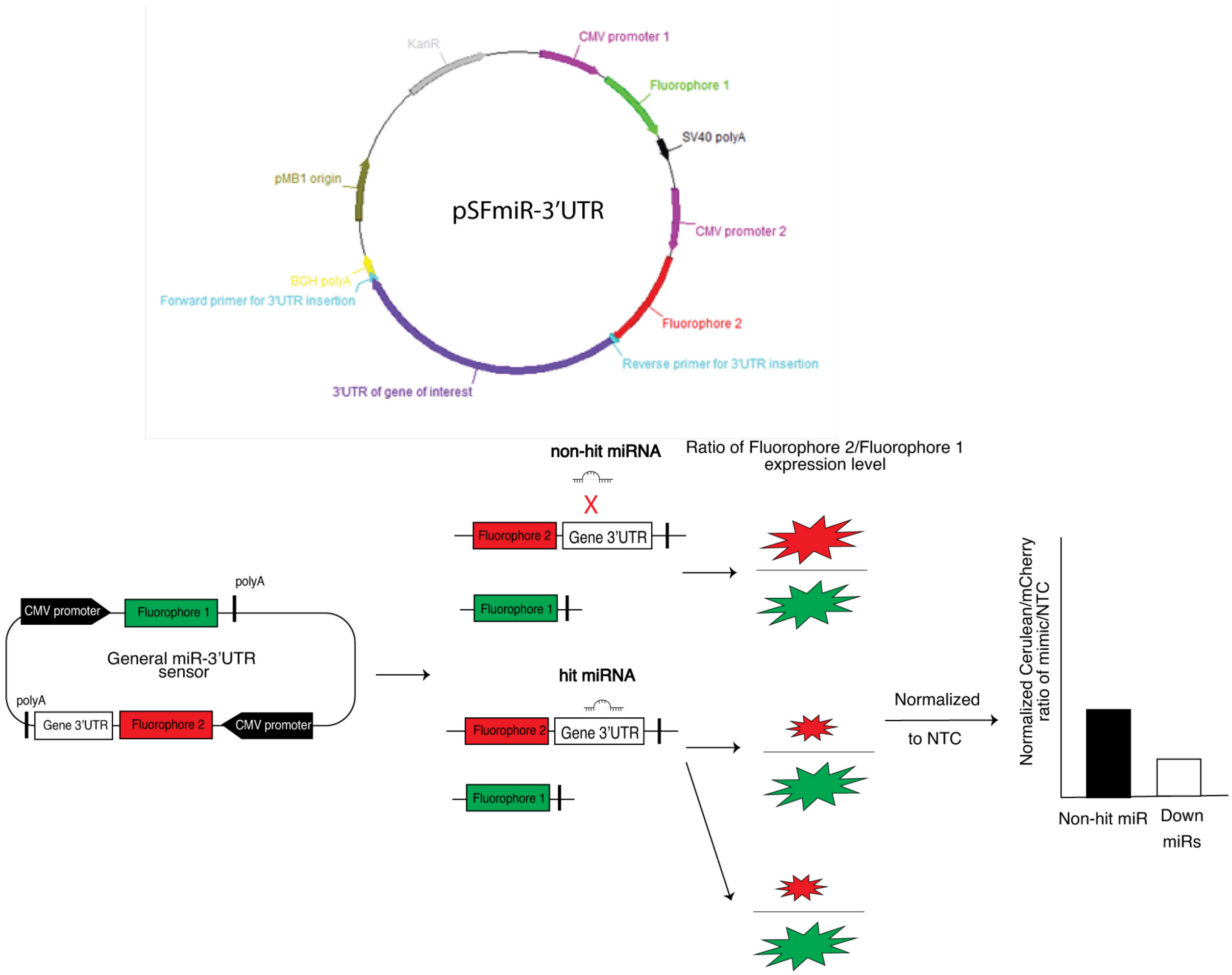

Figure 2.2. Schematic representation of high-throughput assay of miR-target interactomes. The ratio of Fluorophore 1/Fluorophore 2 fluorescence signal in miR transfected cells is normalized to the data from a non-targeting control (NTC) and reflects the extent of miR-target regulation. For miRs that repress protein expression via gene 3'UTR, a loss of fluorophore 2 expression is expected, with a corresponding reduction in the normalized fluorescence ratio.

2.4.3 Background on cell spot microarray (CSMA) method and advantages

Reverse transfection cell microarrays are a high-throughput system used to explore the role of DNA or siRNAs for functional analysis in mammalian cells (**Figure 2.3**) [20-28]. The first report of this technology was initiated in the Sabatini lab using the lipid-DNA method [20]. In reverse-transfection cell microarrays, genetic materials (i.e. DNA, siRNA, miR mimics) are arrayed with transfection reagents and a matrix printed on a solid support. The slide is then briefly incubated with mammalian cells to facilitate the cell adhesion specifically on the spots containing the matrix. The choice of matrix are based on the surface properties (i.e. functional group modifications), hydrophobicity, hydrophilicity of the solid support material and the choice of mammalian cells. The most commonly used matrices are fibronectin, matrigel (laminin, collagen, entactin and heparin sulfate proteoglycan perlecan), poly-L-lysine (PLL) and gelatin. The cell spot microarray is then transfected with the reagent. The output readout is dependent on the experimental designs to investigate phenotypic changes or activation of cellular pathways post-transfection using a fluorescence-based assay. This method is highly advantageous for reduced screening time, rapid readout, and visualisation of cell phenotypes and morphology.

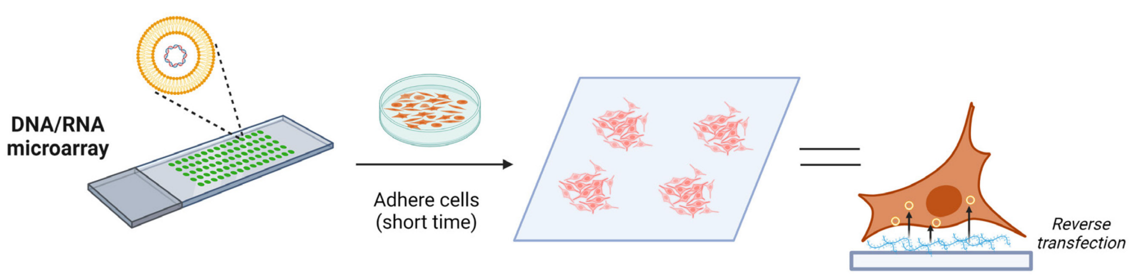

Figure 2.3. General scheme of cell spot microarray (CSMA) method and reverse transfection. In current literature, DNA or siRNA are printed on slide to produce specific cell microarray. Adherent cells in specific spots were reverse-transfected to generate stable cell lines.

2.4.4 Testing the miRfect system

In previous work, miR-200b-3p was identified as a regulator of this enzyme and demonstrated a role for B3GLCT in epithelial to mesenchymal transition (EMT) [7]. Bioinformatics analysis of miRNA predictions identified this glycogene as a highly regulated target [7]. Thus, we anticipated that a large number of miRs would downregulate this enzyme, making it a good choice for assay development. The miRfect system was initially tested by David Christian, a technician in the lab, using pMIR-B3GLCT with Cerulean and mCherry fluorescent reporters. Cells were adhered to the miRfect specific spots containing NTC and miR-200b-3p. They were then transfected with pMIR-B3GLCT. miRfect spots were imaged and analyzed 48h post-transfection. Well and clear defined spots were observed with high transfection efficiency. We found 17% inhibition was observed for Cer/mCherry in miR-200b in normalization to NTC (**Figure 2.4**). Whereas, 40% inhibition was observed with the luciferase assay. These results indicated further improvement of the assay was needed.

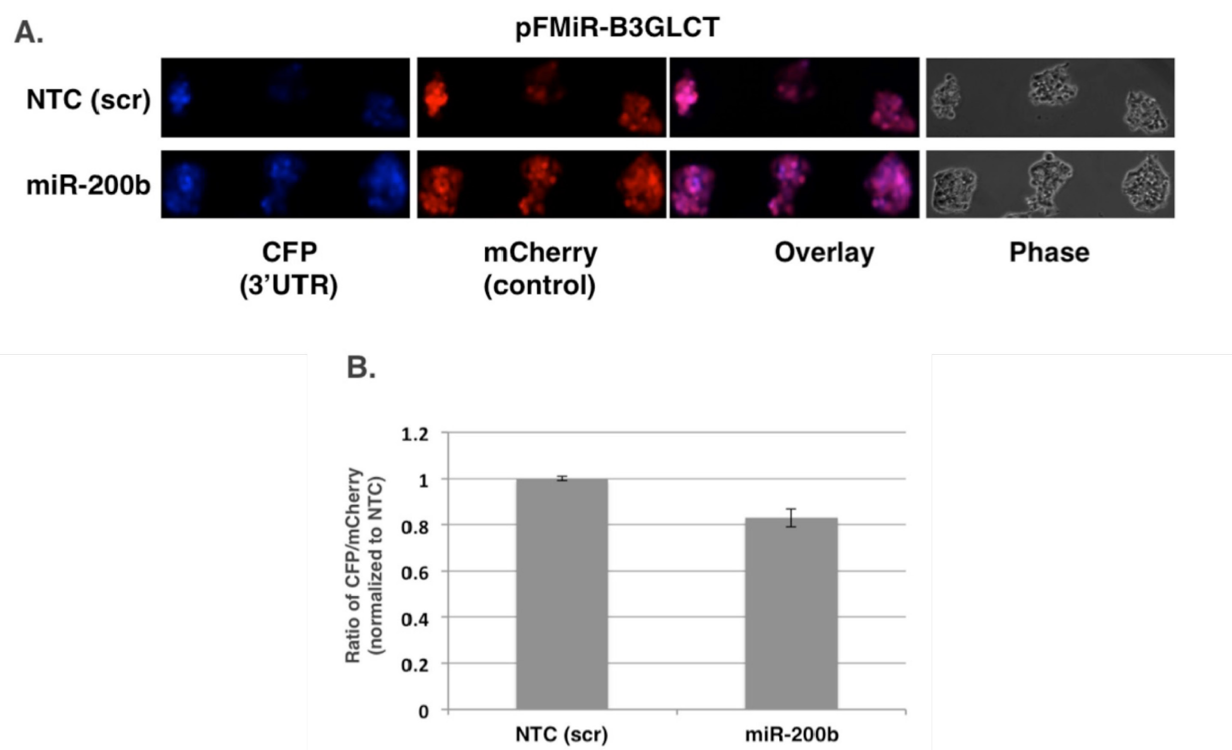

Figure 2.4. (A) Microscopic imaging of miRfect microarray printed with NTC (non targeting control or scramble) or miR-200b-3p mimics with *HEK293T* attachment, followed by transfection with pFMiR-B3GLCT. (B) Quantitation of data from A presented as ratio of Cerulean/mCherry normalized to NTC.

2.4.5 Creating compatible pFmiR sensors for the Genepix Pro microarray system

Our lab specializes in microarray technology and the Genepix microarray system that we currently use is designed for high-throughput fluorescent-based applications. However, it has only 4 built-in lasers (488nm, 532nm, 594nm, 635nm) and corresponding emission filters (blue: 513-555nm, green: 562-596nm, yellow: 619-641nm, red: 661-690nm) (**Figure 2.5**). The fluorophores of the sensors must be chosen to match the instrument for better quantitative analysis and higher sensitivity.

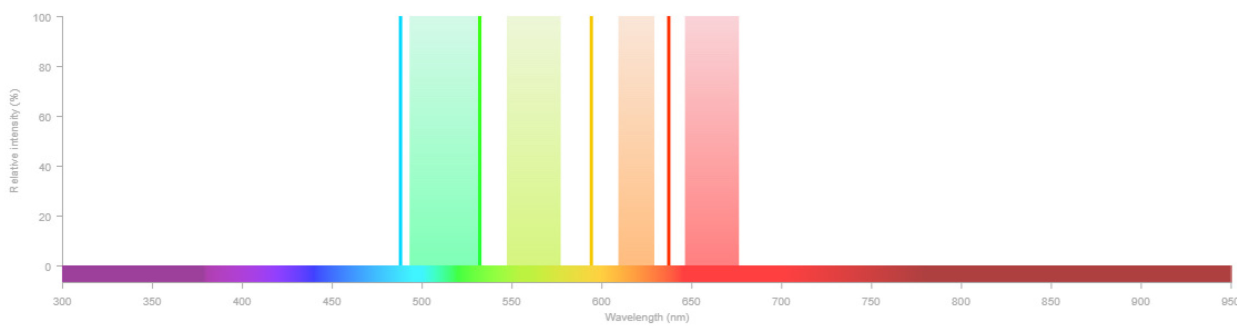

Figure 2.5. Laser settings and corresponding emission filters on our scanner. 4 built-in lasers (488nm, 532nm, 594nm, 635nm) and corresponding emission filters (blue: 513-555nm, green: 562-596nm, yellow: 619-641nm, red: 661-690nm).

The original pSFmiR sensor with used the fluorescent proteins Cerulean and mCherry as fluorophores, created by Chris Vaiana, was not compatible with our scanner due to the far excitation of cerulean in comparison to the Alexa488 laser. Thus, we created different versions of the sensors for testing. Version 2 used the mClover3-mRuby3 pair (pSFmiR-mClover3-mRuby3). These fluorophores could be observed with our Genepix and had improved brightness and photostability [29]. However, we observed bleed-through between the mClover3 and mRuby3 channels. We then replaced mRuby3 with mCherry but the fluorescence crossover was still observable. Thus, we generated the fourth generation of our sensor (pSFmiR) which utilises mClover3 as the control fluorophore and miRFP670 as the reporter. miRFP670 is a near IR fluorescent protein with excitation/emission of 642/670 which is matched with the red laser and filter in the scanner.

2.4.6 Creating a library of genetically encoded fluorescent sensors (pSFmiR-glycogene 3'UTR) for high-throughput mapping of miR:glycogene interactions.

With the use of Gibson assembly, we constructed a library of around 100 glycogene 3'UTR inserted downstream of the miRFP670 stop codon in pSFmiR sensor (**Figure 2.6**). Briefly, pSFmiR-empty plasmid is amplified and served as a linear vector fragment using appropriate primer set and the polymerase chain reaction (PCR). This universal backbone is used to construct the whole library of pSFmiR-3'UTR. The 3'UTR of glycosylation enzymes is amplified from genomic DNA with overlapping regions to pSFmiR linearized fragment and then assembled with the backbone. With the high efficiency of this method, to date, around 100 pSFmiR-3'UTR were created (see **Table 2** and **Methods**).

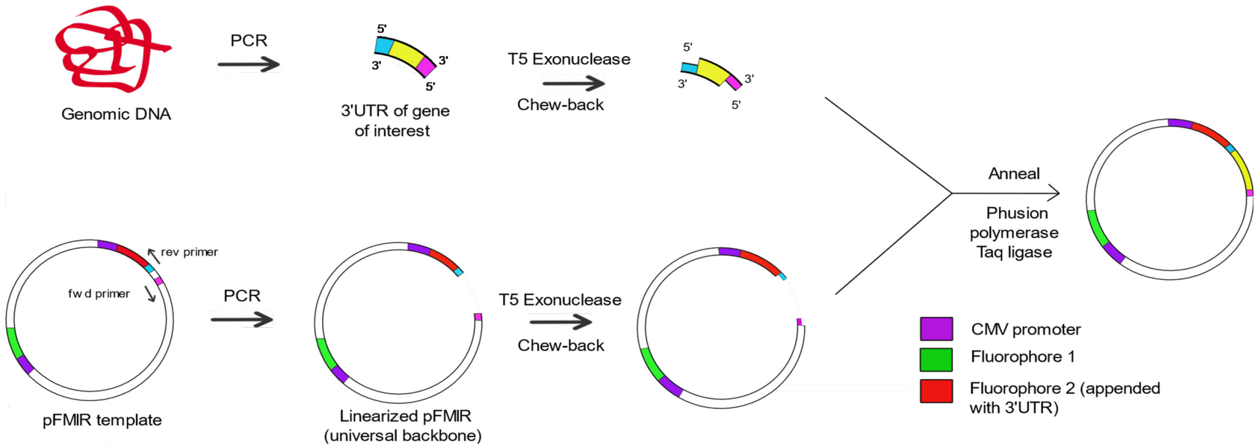

Figure 2.6. Schematic of Gibson Assembly procedure for construction of pFMiR2-glycogene library. The universal pFmiR backbone vector was amplified by PCR. Genomic DNAs were extracted from various cell lines (*MCF7*, *HEK293T* and *A549*). Specific primers were designed to amplify a specific 3'UTR of gene of interest with the overlapping region with the backbone. This 3'UTR was then inserted into the linearized backbone vector through Gibson Assembly. Gibson Assembly utilized the T5 Exonuclease to create sticky end and Phusion polymerase Taq ligase for ligation of the 3'UTR insert and backbone.

2.4.7 Optimization of reagents in miRfect System.

The miRfect system utilizes a highly efficient miRNA reverse-transfection cell microarray in tandem with a transiently transfected reporter (pSFmiR-3'UTR) to provide comprehensive information on the miR-target interactions. Although cell microarray technology has been developed for a while, its applications were not widely spread and often used to mainly study functional cellular impacts including cell morphology, migration or proliferation. To date there have been no studies that use this technique to directly study the miR-protein interactome. Thus, we designed and developed the miRfect system to optimize gathering large datasets to identify miR-target networks (**Figure 2.7**). miRfect is produced by growing cells on small (~200 mm diameter) spots on a untreated polystyrene slide with each spot carrying a miR with transfection reagent, sucrose and fibronectin as a cell adherence aiding matrix proteins. The untreated polystyrene slide is hydrophobic with a non-treated surface (not presenting hydrophilic functional groups) therefore preventing the non-specific cell adherence in other area in the slide besides the spots. The addition of sucrose to the matrix is to maintain the integrity and transfectibility of miR transfected complexes for long-term storage. Fibronectin was used as the supporting matrix instead of gelatin or matrigel to aid cell adhesion because of its hydrophobic and hydrophilic properties and ability to adsorb to a hydrophobic surface (untreated polystyrene slide). Gelatin has abundant hydrophilic properties so it is usually used with glass surfaces. Matrigel forms different networks depending heavily on the surface properties [30]. Specifically, it forms globular network on hydrophobic surfaces or fibrillar network on hydrophilic surfaces. It was also shown that cells attach and grow poorly on Matrigel adsorbed onto polystyrene. Thus, fibronectin matrix was used. For transfection reagents, we used lipofectamine 2000 for co-transfection of miRs from the bottom and plasmid reporter on top.

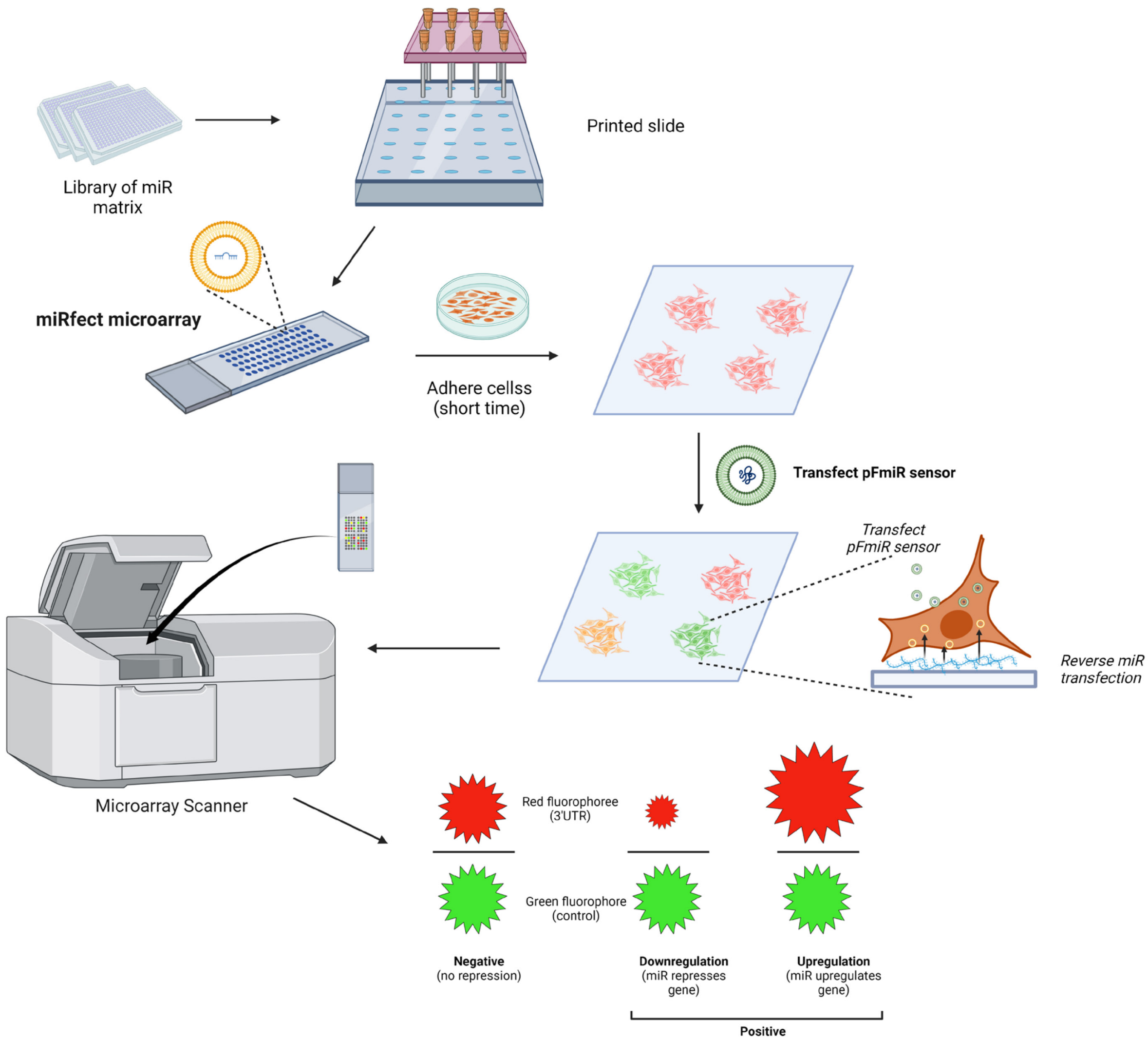

Figure 2.7. miRfect system: Hydrophobic slides are printed with human miRNA library, fibronectin matrix and transfection reagent (miRfect slides). They are then incubated briefly with mammalian cells, washed and cells are transfected with pFMiR-glycogene sensors. After 48h, slides are rinsed with buffer, cells are fixed and imaged using a microarray scanner and the fluorescence analyzed. If a miR targets a glycogene through its 3'-UTR, it will repress the red fluorescent signal (with 3'UTR inserted downstream) in comparison to the green fluorescent signal (as control).

The visualization of the cell spot microarray is shown in **Figure 2.8**.

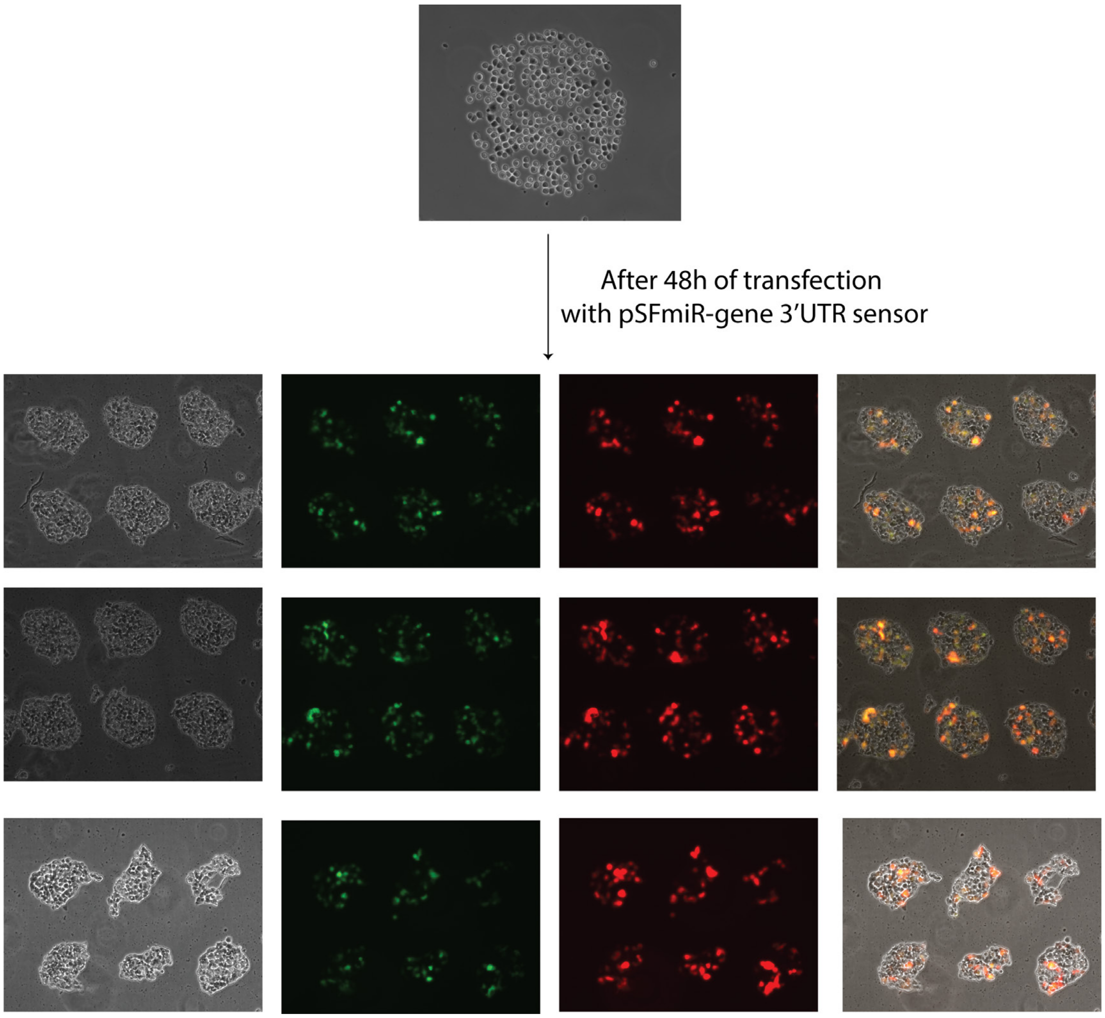

Figure 2.8. Spot morphology after cell adhesion on the slide.

2.4.8 Optimization of the miRfect system.

To optimize the miRfect system, various concentrations of miR, pFSmiR-B3GLCT and lipofectamine 2000 were using and the optimized protocol was established (see Method section). To test that our miRfect worked as expected, we compared the miRFP670/mClover3 fluorescence ratios upon co-transfection of pSFmiR-B3GLCT 3'UTR with either NTC, the positive control miR-200b-3p or the known negative control miR-200a-3p in the replicate of spot format (**Figure. 2.9**). We observed well defined cell spots and a good transfection efficiency represented by the mClover3 control channel. We also saw a clear loss (~50%) of miRFP670 signal in comparison to mClover3 in the hsa-miR-200b-3p spots when normalized to the NTC which is not seen in hsa-miR-200a-3p. This result indicates the validity of miRfect system to experimentally identify miR hits for B3GLCT.

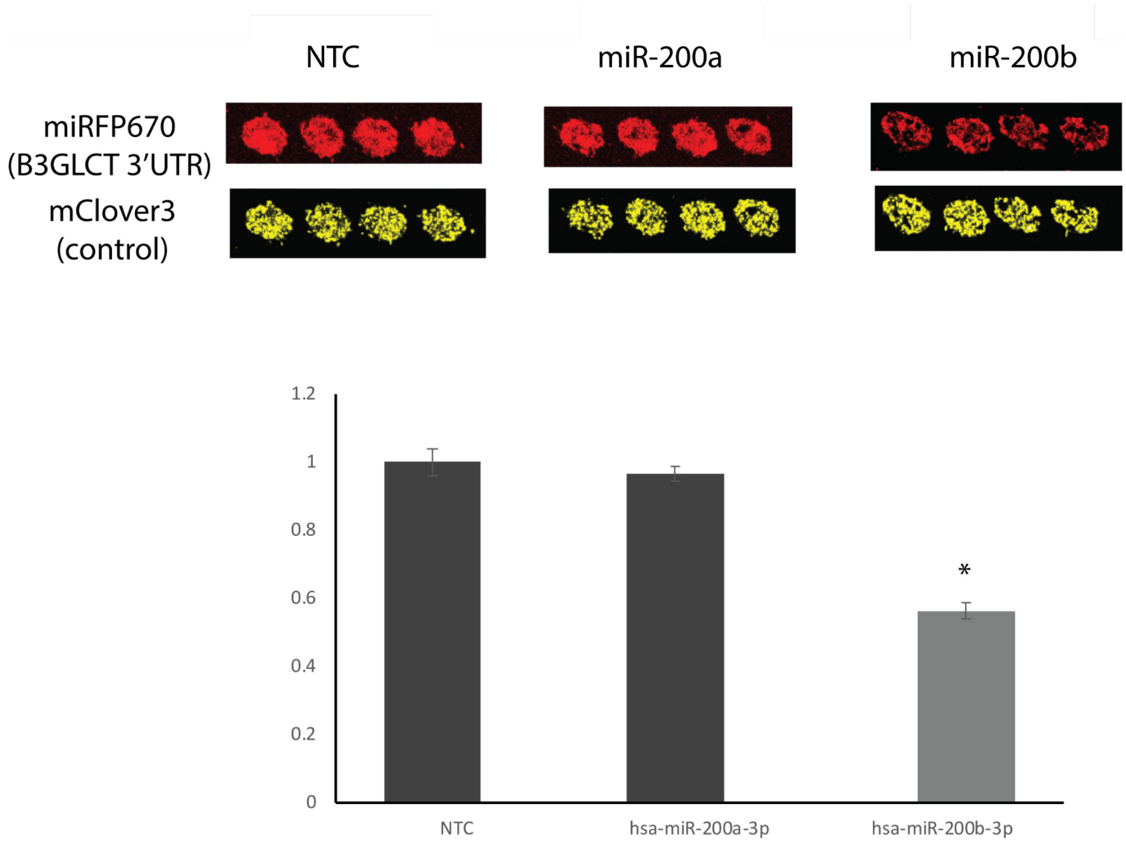

Figure 2.9. Hsa-miR-200b-3p downregulates B3GLCT in comparison to negative control (NTC) and another negative control, hsa-miR-200a-3p in miRfect assay. Hydrophobic slides are printed with different miRs (NTC, miR-200a, miR-200b with the concentration of 1.5 µM), fibronectin matrix and lipofectamine-2000 reagent (miRfect slides). They are then incubated briefly with *HEK293T* cells, washed and cells are transfected with pSFMiR-glycogene sensors. After 48h,

slides are rinsed with buffer, cells are fixed and imaged using a microarray scanner and the fluorescence analyzed. Error bars represent standard deviations. P-values were calculated using the two-tailed unpaired Student's t-test with equal variances for comparison to scramble control, *P < 0.05.

We next performed a larger scale microarray with around 1/8 of the MISSION miR mimic library and analyzed data for B3GLCT (**Figure 2.10**). We identified 30 downregulatory miRs for B3GLCT (**Table 2.1**). This was not a comprehensive dataset of miR-B3GLCT interactomes due to problems with slide manufacture. Thus, we wanted to gather a complete interaction network for the whole human miRome and B3GLCT before validating smaller subset of miRs regulating B3GLCT in protein and mRNA levels using Western Blot and RT-PCR respectively.

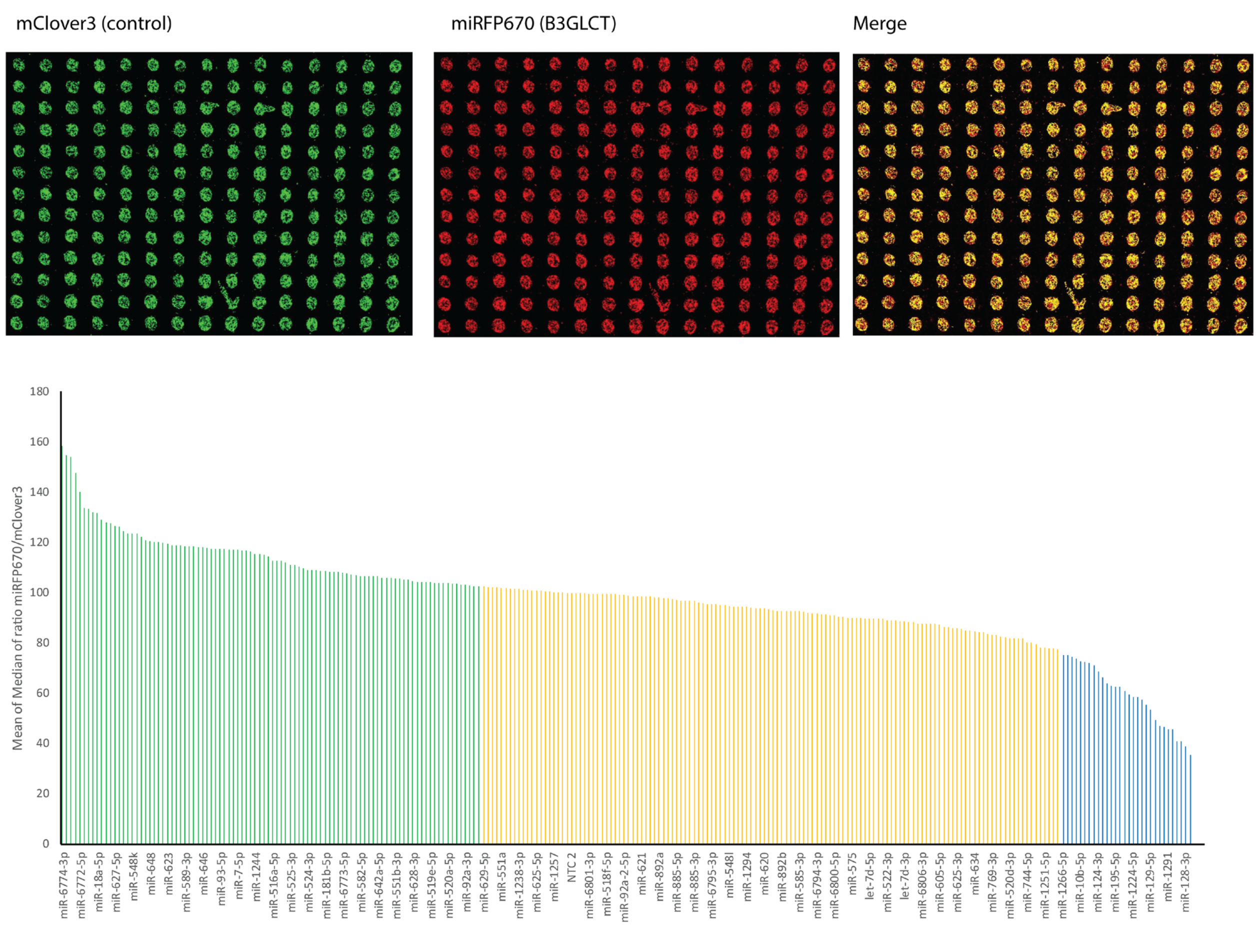

Figure 2.10. Identification and validation of hits for B3GLCT. Spot morphology and bar graph of ratiometric data for miRs.

Table 2.1 List of miR hits for B3GLCT

miRNA	%NTC
miR-1266-5p	75.1749714
miR-6780a-5p	75.0801662
miR-1272	74.4128117
miR-1908-5p	73.8551339
miR-10b-5p	72.5724749
miR-526a	72.2504097
miR-1301-3p	71.9613529
miR-1293	71.1708446
miR-124-3p	68.6111034
miR-151a-3p	66.4361598
miR-6796-3p	63.9019114
miR-182-5p	62.8363494
miR-195-5p	62.5017427
miR-146b-5p	62.4180911
miR-181a-5p	60.7868834
miR-193b-3p	59.4540334
miR-1224-5p	58.584056
miR-15b-3p	58.5561721
miR-6776-5p	57.5314391
miR-6761-5p	55.4238816
miR-129-5p	53.3140005
miR-6782-3p	49.319633
miR-6783-5p	46.8821162
miR-1226-3p	46.5884059
miR-1291	45.7714079
miR-194-5p	45.4897806
miR-146a-3p	41.0520592
miR-6782-5p	40.9544656
miR-128-3p**	38.8608501
miR-130a-3p	35.4218368

Although our initial system appeared successful, we were unable to use it due to the manufacture of untreated polystyrene slides. The company (EMS) changed the slide properties and surface treatment of the slides which induces heterogeneity of surface functional groups. As a result, more non-specific adherence and varying spot morphologies were observed across the slide (**Figure 2.11**).

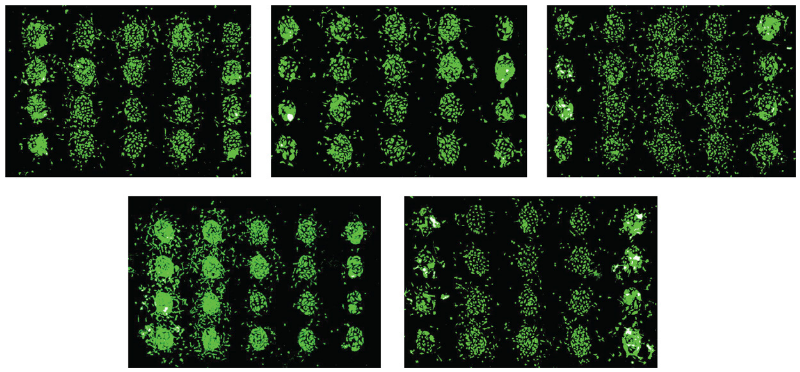

Figure 2.11. Highly variable spot morphologies were observed after cell adhesion on the new polystyrene slide. miRfect slide is represented using mClover3 channels.

Since the defined cell spots depend on multiple factors including the surface properties (i.e. functional group modifications), hydrophobicity, hydrophilicity of the solid support material and the choice of mammalian cells. We tried other cell lines and different transfection reagents to attempt to re-optimize the system and transfection efficiency with the new slide material and surface properties. This is important since the transfection efficiency on top (with plasmid sensor) and on bottom (with miRs) impacts the population of cells with both plasmid sensor and miR for accurately identifying interactions. We want to increase population of cells with both plasmid sensor and miR as much as possible. Thus, optimising high transfection efficiency is necessary. I first examined the use of *HeLa* cells (**Figure 2.12**) and found Xfect transfection reagent (0.0375%) to perform best in term of cell health and transfection efficiency.

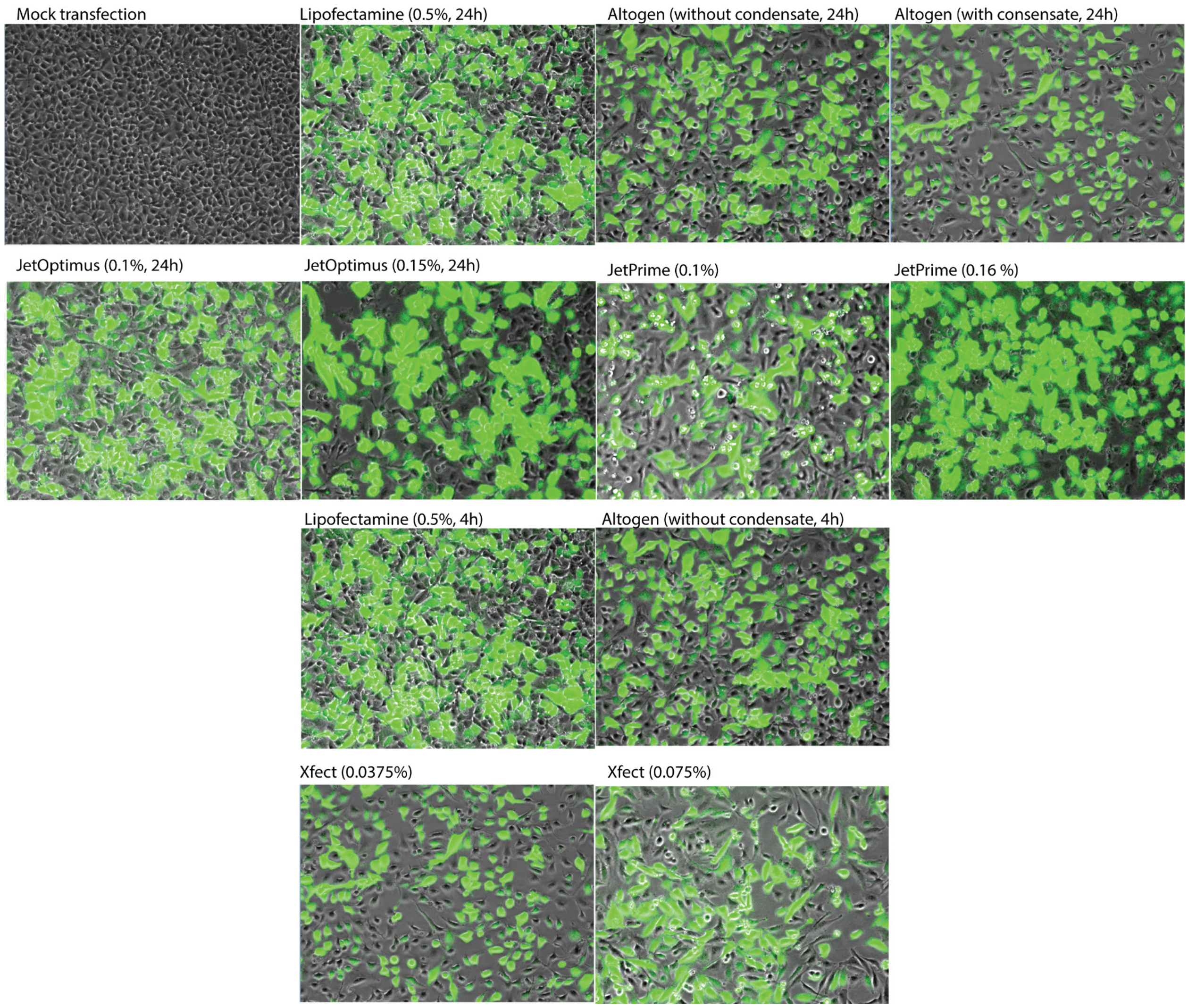

Figure 2.12. Optimizing transfection reagents for pSFmiR-B3GLCT 3UTR sensor transfection on *HeLa*. *HeLa* cells were transfected with pSFmiR-B3GLCT 3'UTR sensor (time indicates the hours of transfection before changing the transfection media into fresh media)

MiRfect was then performed using *HeLa* cells and Xfect transfection reagent. Unfortunately, the obtained spot morphologies from the microarray were not so well defined and miR-200b-3p did not inhibit the sensor as expected (**Figure 2.13**). This result is due to the non-specific adherence of *HeLa* cells to other areas of a specific spot (smear morphology) or poor transfection of Xfect to *HeLa* within the slide format. In addition, *HeLa* cells adhere to the spot fibronectin matrix and the reverse miRNA transfection from the bottom which can impact the transfection efficiency of pSFmiR- B3GLCT 3'UTR on top.

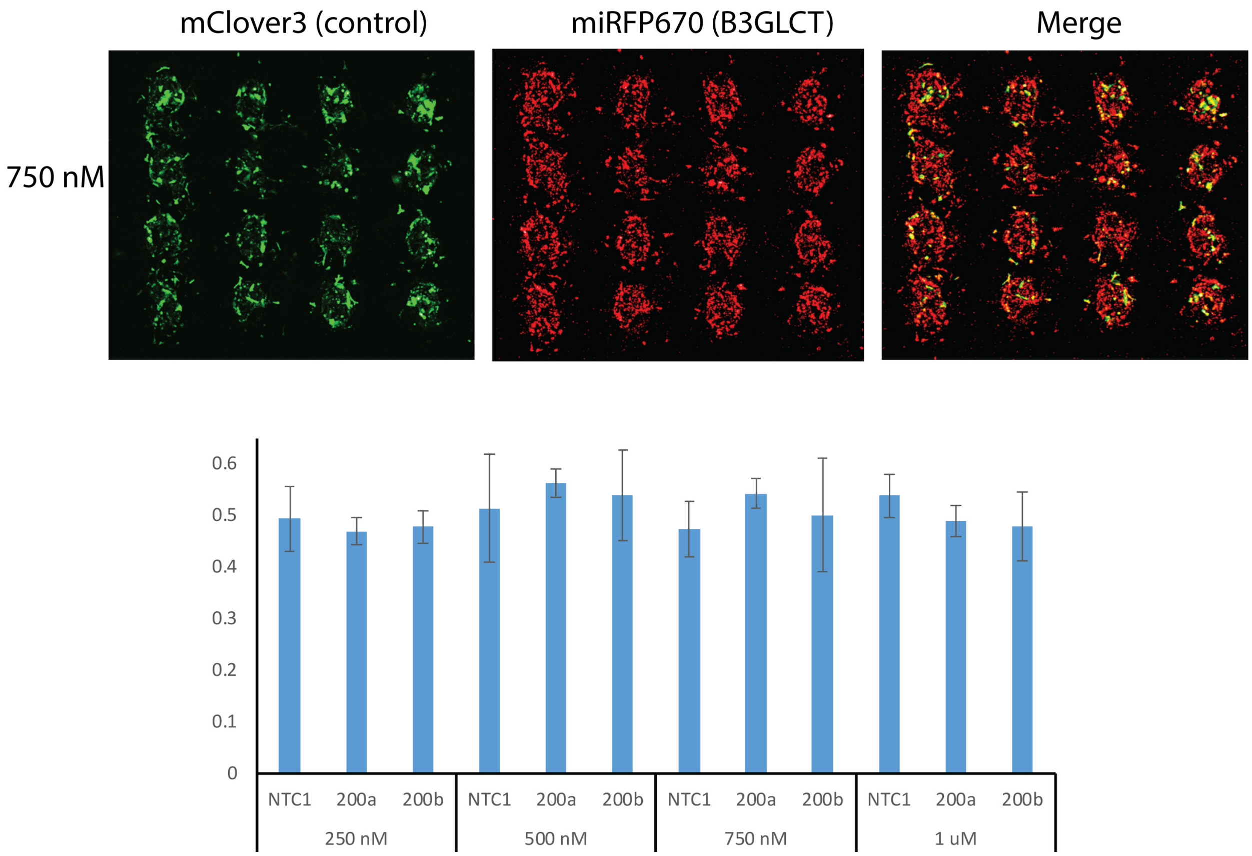

Figure 2.13. MiRfect system using *HeLa* cells. Hydrophobic slides were printed with different miRs (NTC, miR-200a, miR-200b with various concentrations), fibronectin matrix and lipofectamine-2000 reagent (miRfect slides). They are then incubated briefly with *HeLa* cells, washed and cells are transfected with pSFMiR-B3GLCT sensors. After 48h, slides are rinsed with buffer, cells are fixed and imaged using a microarray scanner and the fluorescence analyzed. Error bars represent standard deviations.

After testing few other cell lines, *LNCap* cells produced the best spot morphologies and transfection efficiency using viromer blue (**Figure 2.14**). The transfection condition and inhibition optimization were also conducted (optimized miR concentration is 1 µl). However, we were unable to stabilize the transfection complexes on the slide and it was impractical to print prior to each experiment. Thus, we had to rethink our strategy for further development of a platform for high-throughput experimental identifications of miR-target interactions.

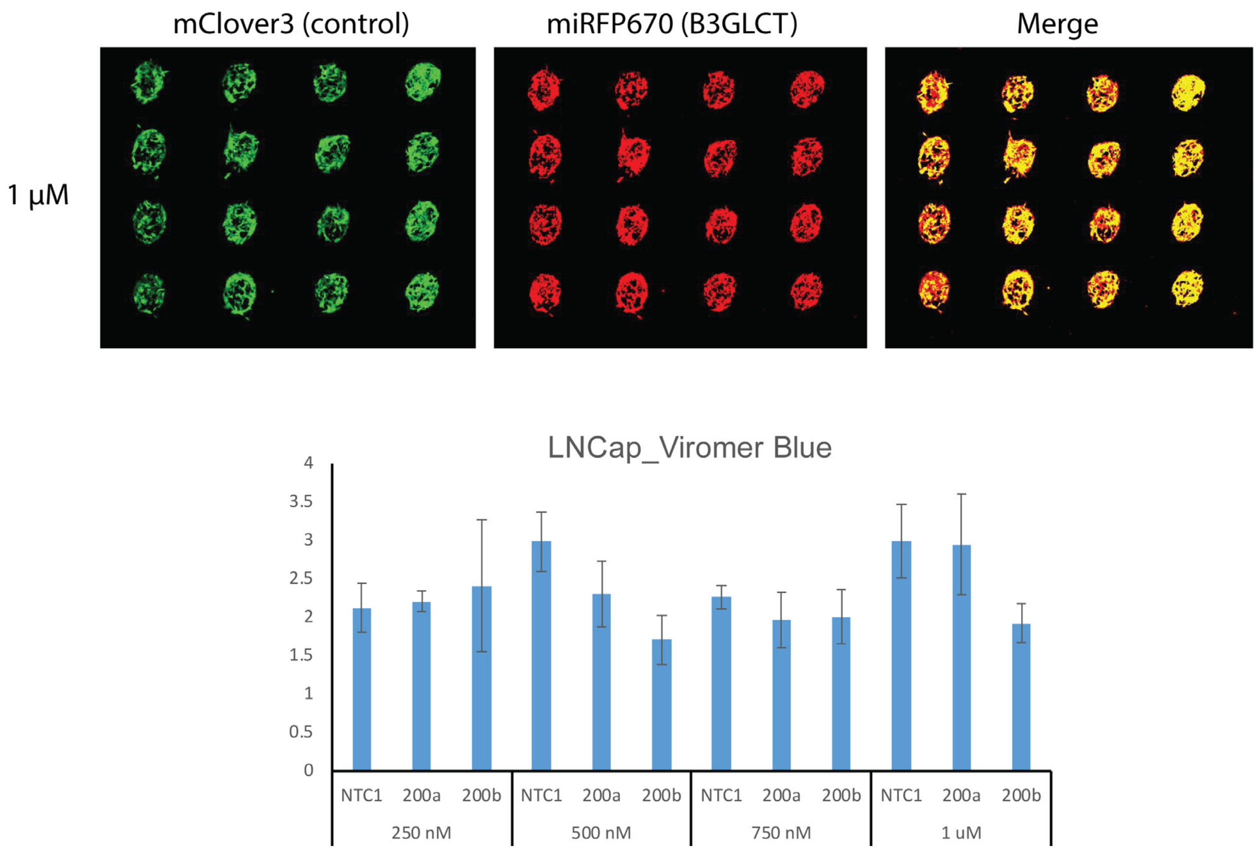

Figure 2.14. MiRfect system using *LNCap* cells. Hydrophobic slides were printed with different miRs (NTC, miR-200a, miR-200b with various concentrations), fibronectin matrix and lipofectamine-2000 reagent (miRfect slides). They are then incubated briefly with *LNCap* cells, washed and cells are transfected with pSFMiR-B3GLCT sensors. After 48h, slides are rinsed with buffer, cells are fixed and imaged using a microarray scanner and the fluorescence analyzed. Error bars represent standard deviations.

2.5 COMPARISON B3GLCT DATA FROM MIRFECT SYSTEM TO MIRFLUR PLATFORM

The details of miRFluR platform, our alternative system for high-throughput analysis, will be discussed in chapter 3. However, we were interested to compare our miRfect result for B3GLCT to our miRFluR result for B3GLCT (**Table 2.2**). I did the comparison and found that their results did not match. The reasons for this misalignment will be discussed further in chapter 3, but are most likely due to normalization issues.

Table 2.2 Comparison of the results for B3GLCT from miRfect system and miRFluR platform

miRNA	miRFluR_normalization	miRfect_normalization
miR-130a-3p	0.99	0.35
miR-6782-5p	0.87	0.41
miR-146a-3p	0.91	0.41
miR-194-5p	0.95	0.45
miR-194-5p	0.93	0.45
miR-6783-5p	0.88	0.47
miR-6782-3p	0.83	0.49
miR-6761-5p	0.86	0.55
miR-6776-5p	0.87	0.58
miR-15b-3p	0.96	0.59
miR-146b-5p	0.87	0.62
miR-195-5p	0.94	0.63
miR-182-5p	0.93	0.63
miR-6796-3p	0.93	0.64
miR-151a-3p	1.02	0.66
miR-526a	0.90	0.72
miR-1908-5p	1.25	0.74
miR-6780a-5p	0.92	0.75

2.6 CONCLUSION

miRNAs have been shown to be key regulators of glycosylation and the utilization of miRNAs could be the open door to understand complexity of glycosylation and functions. Our understanding relies mainly on prediction algorithms to identify miR:target interactions which is prone to high false positive and negative rates. This failure to accurately identify miR targets *in silico* is likely attributable to the oversimplified rules used to predict interactions and functions which could be biologically irrelevant and variable in different biological systems. Thus, the underlying biological mechanisms driving biologically relevant actions and functions of miRs remain largely enigmatic. The current methods to identify miR-target interactions (transcriptomic profiling and cross-linking assay) failed to pinpoint the real miRNA targets for low abundance gene and the actual biological impacts of miRNAs on protein levels and luciferase assay exhibits only moderate through-put in term of identifying miRNA targets.

In our effort to address these issues and limitations of current technology, we developed the miRfect system which utilizes a highly efficient miRNA reverse-transfection cell microarray in tandem with a transiently transfected reporter (pSFmiR-3'UTR) to provide comprehensive information on the miR-target interactions. Although miRfect cell spot microarray is a potential application for mapping miR-target interaction network experimentally, there are different factors that could impact the reproducibility and reliability of the miRfect system including non-specific cell adherence, spreading phenomenon in microarray since miRNAs and matrix are not covalently linked to the slide surface, slide material and surface alteration, stability of transfection, etc. Although our miRfect system was ultimately not usable, it provided the initial step for the development of a high-throughput miRFluR platform (as discussed in chapter 3).

2.7 MATERIALS AND EXPERIMENTAL METHODS

2.7.1 Cloning of pSFmiR-empty and a library of genetically-encoded fluorescent sensors for high-throughput mapping of miR-target interactions

The mClover3 fragment was amplified from pKanCMV-mClover3-mRuby3 (Addgene, plasmid #74252) by the PCR using primers mClover3_fwd and mClover3_rev with HindIII and NheI restriction sites. It was then subcloned to the commercially available plasmid (pSF-CMV-CMV-Sblf, Oxford Genetics) with the sites of HinIII and NheI to make pSF-mClover3.

mClover3_fwd: CGTCTCGTCGACCTAGCGCTACCGGTCGC

mClover3_rev: GGTACAACTAGTGCCTTTGCTCACCATCGGATC

The miRFP670 fragment was amplified from pmiRFP670-N1 (Addgene, plasmid #79987) by the PCR using primers miRFP670_fwd and miRFP670_rev with AcII and SpeI restriction sites. It was then inserted to the pSF-mClover3 with the restriction sites of AcII and SpeI to create pSFmiR-empty sensor.

miRFP670_fwd: CGTCTAACGTTATGGTAGCAGGTCATGC

miRFP670_rev: GGTACACTAGTTTAGCTCTCAAGCGCG

The pSFmiR linearized backbone fragment was amplified by PCR using pSFmiR_fwd and pSFmiR_rev below. Library of glycogene 3'UTR was cloned from cDNA using primers in the **Table. 2** using standard PCR conditions with the 5' overhangs compatible with the pSFmiR backbone. The DNA fragment of gene 3'UTR was cloned into our pSFmiR-empty backbone using the forward and reverse primers downstream of miRFP670 utilizing a standard Gibson assembly protocol. Plasmid maps and sequences for pSFmiR and gene 3'UTR can be found in **Plasmid maps and sequences.**

pSFmiR_fwd: AGCCTGTGCCTTCTAGTTG

pSFmiR_rev: CTAGTTTAGCTCTCAAGCG

And 5' overhangs for gene 3'UTR primers

Forward overhang: CGCTTGAGAGCTAAACTAG

Reverse overhang: CAACTAGAAGGCACAGGCT

2.7.2 miRfect high-throughput system.

The human MISSION miRNA mimics (Sigma, for small scale) and the miR mimic library (MISSION, Sigma) were resuspended in nuclease-free water and aliquoted into 384-well plate with the concentration of miRNA varying for optimization (1.5 µM, 2 µM, 2.5 µM and 3 µM) including controls (NTC and others for different sensors). Preparing the Opti-MEM (Gibco) with sucrose to obtain the final concentration of 100mM (OMEM-S media).

To each well in the plate was added 2 µl lipofectamine 2000 (Invitrogen) and OMEM-S media. The solution was allowed to incubate at room temperature for 25 min. Then, 4 µl of fibronectin (Sigma Aldrich, 1 µg/ml) was added to each well and mixed by pipetting gently. This miRNA transfection mixture was printed on hydrophobic polystyrene slides (Electron Microscopic Science, EMS using a piezoelectric tip and a nanoplotter II (GeSim, with set voltage is 75-90V and aspiration volume was set to 1.5 µl) at 4 °C and 55–60% relative humidity to prevent the evaporation of samples. Printed spots were 150–250 µm in diameter (around 0.1-0.2 nl of sample pipetted) with a 700 µm spot-to-spot interval. The prepared miRfect slides were allowed to dry in the printing chamber for around 1h, and then stored at -80 °C in an air-free sealer bag until further use.

Acquiring miRfect slide and cell-defined attachment and miRNA reverse transfection were induced as following: *HEK293T* cells were trypsinized, counted and diluted to 5.6×10^5 cells/mL in 7.7 mL DMEM w/ 10% FBS and 3.3 mL OMEM. 5.5 mL of this mixture were added to the miRfect slide in a well of Nunc 4-well rectangular chamber (Thermofisher). Cell adhesion was facilitated by incubating the slide incubated at 37°C, 5% CO_2 for 15-20 minutes (depending on the cell lines). After that, wells were aspirated and washed with 6 ml of HBSS (Corning) 2-3 times to obtain miRfect cell-defined pattern slides.

Preparing the plasmid transfection mixture for top-layer transfection simultaneously with the above procedure as follows: 16.5 µl of lipofectamine 2000 was added to 2.5 ml of Opti-MEM and incubated for 5 minutes. pSF-B3GLCT 3'UTR (15 µg) were diluted to 2.5 ml of Opti-MEM, then added to the lipofectamine 2000 mixture for 25 minutes. After 25 minutes, 5.5 µl penicillin-streptomycin (Sigma, 100x) was added. This plasmid transfection mixture was then loaded to the Nunc rectangular well containing miRfect cell-defined pattern slides. This transfection media was then removed after 24 hours and replaced by normal media (DMEM with 10%FBS).

After 48h post-transfection, cells are fixed at room temperature using 4% paraformaldehyde solution (diluted with HBSS from 20% paraformaldehyde solution (EMS)) for 30 minutes. The paraformaldehyde was aspirated and slides were washed with HBSS. Slides were imaged with the Genepix 4300A scanner in the miRFP670 (3'UTR, 635 nm) and mClover (control, 488 nm) channels. The mClover3 channel was used to determine spot morphology and features were extracted.

2.7.3 Data Processing

The median of ratios for miRFP670/mClover3 signal (mR/mC) was extracted for each spot. The median is considered more accurate for microarray analysis, as the mean is more sensitive to spot morphology and distribution of signals. The mR/mC for each spot was normalized to the average mR/mC for non-targeting control spots (NTC) to give a ratiometric signal (Rs=

(mR/mC)mir ÷ (mR/mC)NTC-ave) to eliminate both pSFmiR-3'UTR and miR effects on general protein translation/cell health. The average ratiometric signal for 4-replicate spots (AR) is calculated for each miR-target interaction, those for which the AR is <80% of the mean AR across the array (i.e. ~20% repression) and that are statistically significant (Student's t-test, $p<0.05$, compared to NTC) will be defined as positive hits. Data analysis was automated using Genepix Pro analysis software and the R statistical environment.

List of primers for 114 glycogene 3'UTR

Adding 5' overhangs for gene 3'UTR primers in **Table 2.3**

Forward overhang: CGCTTGAGAGCTAAACTAG

Reverse overhang: CAACTAGAAGGCACAGGCT

For example:

PIGA_fwd: CGCTTGAGAGCTAAACTAGAAGGAAGCCTAGATTGTAAGAT

PIGA_rev: CAACTAGAAGGCACAGGCTGAAAATTATCAAAATGTCATTCTGGTC

Table 2.3 List of primers for 114 glycogene 3'UTR (without the overhangs).

Category	**RefSeq**	**Gene**	**Forward Primer (5'-3')**	**Reverse Primer (5'-3')**
GPI Anchor Biosynthesis	NM_002641	PIGA	AAGGAAGCCTAGATTGTAAGAT	GAAAATTATCAAAATGTCATTCTGGTC
GPI Anchor Biosynthesis	NM_145167	PIGM	CCTGACAGAGAGAATCAAATATG	TTGAAGGTGTTATTAAAGGATTAAAAAG
GPI Anchor Biosynthesis	NM_005482	PIGK	GACTTGATGATGAATGAAGAATG	TTCCATGTTTGGAGTAAATAAATTTTTAATAAC

GPI Anchor Biosynthesis	NM_012327	PIGN	GTATGTTCCACACCCTCTG	TAAAATTTGAAGGTGTTATTAAAGGATTAAAAAG
Galactosyltransferases	AK294438	UGT8	CAACAGCCCAGGTGATA	CTATTTTAAATCATGTTTATTATTTAAGTTTTTATC
Galactosyltransferases	NM_004776	B4GALT5	GAGTACTGAGAGGAGAGAATG	TTTGGTTCTTGAATATGTATTTTTTACTG
Galactosyltransferases	NM_004775	B4GALT6	CAGAGTTAGCTCCAATCGAAG	TAATTTGCATTTGCAATGTATTTGTTAATC
N-Acetylgalactosaminyltransferases	NM_033169	B3GALNT1	CATGCTAAGGAACACCACAT	TTATAAAAAGTAAATACACAAACCGGTG
N-Acetylglucosaminyltransferases	NM_032047	B3GNT5	CTTGTAGGGCTGCGTTTATC	TCATGATAATTTTTCAGTTGTTTATTGG
N-Glycan Precursor Biosynthesis, en-bloc Transfer and Processing	NM_019109	ALG1	CCTTTGGTTATGGACACATAAC	TCATGGGAAGAATTTTTATATGGG
N-Glycan Precursor Biosynthesis, en-bloc Transfer and Processing	NM_033087	ALG2	CGATATGTTACCAAACTGCTG	TTTATGATAAACACCTTTTATTATATCTCAG
N-Glycan Precursor Biosynthesis, en-	AK297701	ALG3	CAACACAGCAAGAAAGCC	TTGAGTGAATTCTTTATCTGCTC

bloc Transfer and Processing				
Transferase Donor Substrate Biosynthesis and Related Reactions	NM_013338	ALG5	GCTTGAGCAAACTCGGAAA	AAAAGGCAGACAATGACAAG
N-Glycan Precursor Biosynthesis, en-bloc Transfer and Processing	CR618543	ALG6	GCTTGAACTTCCTGTTCTTC	TCAGGTGCATTTCATTTTAC
N-Glycan Precursor Biosynthesis, en-bloc Transfer and Processing	AK298811	ALG9	CAGGAAGAAAAGTGGAGG	ACTAGCCCAGAGCACC
N-Glycan Precursor Biosynthesis, en-bloc Transfer and Processing	NM_032834	ALG10	CAGTGGCCAAATAGTCAG	TTTGAGGTGATGGATAGATTAGC
N-Glycan Precursor Biosynthesis, en-bloc Transfer and Processing	NM_001004127	ALG11	GTGACATTCCTATCATCTGTG	TTTTCAATTTTTTCCATTTCTTCCAG
N-Glycan Precursor	NM_024105	ALG12	GTGTGAGTCTGAACCTGAC	CAATTTTTTCCATTTCTTCCAGTG

Biosynthesis, en-bloc Transfer and Processing				
N-Glycan Precursor Biosynthesis, en-bloc Transfer and Processing	NM_018466	ALG13	CCAGCTTCTCATTATGTACC	TTTTGGCAATTTTAAATGCTAATTTTTATT
N-Glycan Precursor Biosynthesis, en-bloc Transfer and Processing	NM_144988	ALG14	CGAATTGTTTGACAAATGGC	CTGTTTAAATGCTCAAGTTTATTAGAG
Oligosacharyltransferase	NM_152713	STT3A	GCTTGTCAAGGACATAAATGTC	TTTTTTGAGACAGTCTTGCTCTG
Oligosacharyltransferase	CR620015	STT3B	GAAGAGCAGAGAGCTTACTAA	TTAACACAAAATTTGAATTAACTTTATTTCC
N-Acetylglucosaminyltransferases	NM_002406	MGAT1	GCTATGATCCTAGCTGGAATTAG	ATGTATGAATTTTATTTTCCTTTTATTTTTC
Fucosyltransferases	BC142958	FUT8	GAGCTCAGATGGAAGAGATAAA	TTTGTTTCAAATGACTTTTATTTGTACC
N-Acetylglucosaminyltransferases	NM_002408	MGAT2	GTTTACTGTGGTAGCCATTTC	TGCATTGTCATAAGCTGG

N-Acetylglucosaminyltransferases	NM_001098270	MGAT3	CCAAGTACCTGCTGAAGAAC	CAGACTTTGTAGCTGTTTTTATTATTAATAT
N-Acetylglucosaminyltransferases	NM_001160154	MGAT4A	CACCAACTGATCATCTGAGAAAC	GTTTCACCTATTTTTATTAGAAGGAATC
N-Acetylglucosaminyltransferases	NM_014275	MGAT4B	GCTCTTCCAGATCTTCCTG	TTTGAGGCACACACTTCATTAAC
N-Acetylglucosaminyltransferases	NM_013244	MGAT4C	GCAAACAAAGGAGACAATGTTC	TCACCTACACAAAAAATTATGTAAAGAC
N-Acetylglucosaminyltransferases	NA	MGAT5	CCTATAGCAGCTACCTGC	TCACACAAGAAAAGTTTATTGAAAAAT
N-Acetylgalactosaminyltransferase	NM_020474	GALNT1	CAGCATTAGAGACTGCAATGG	TATTCAGGAATATTTTGTATTTTCAAAG
N-Acetylgalactosaminyltransferase	AK304029	GALNT2	GAAGTTCACGCTCAACCT	TATCTAGAAAGTATCTTCTCTTTATTTAAG
N-Acetylgalactosaminyltransferase	NM_004482	GALNT3	AGTGTTCCTTAAAATTAAGTTGA	GATGCTTAAGGAACTTTATCAG
N-Acetylgalactosaminyltransferase	NM_003774	GALNT4	GGAGTTTTGAGAAATAGAGCAC	AAAACATCATTCAGAAGAGATTAATCTGAA

N-Acetylgalactosaminyltransferase	BC144211	GALNT5	GAAGCCTGAAGTGTAACTGA	GTAAAGGCAATGACCTAAGCTAAT
N-Acetylgalactosaminyltransferase	NM_007210	GALNT6	GTGGCTCTTTGTCTAGGAC	GAGACAGAGTCTTACCTGTTG
N-Acetylgalactosaminyltransferase	NM_017423	GALNT7	CATCCATAGTGTTTAGAGAGAA	TGAATTAAAATACAATATTTATTTTTGTCA
N-Acetylgalactosaminyltransferase	NM_017417	GALNT8	CCTCAGATGGTGCTGGAT	CCACCTGAAGTCGCCATA
N-Acetylgalactosaminyltransferase	NM_001122636	GALNT9	CTGGATCAAACACGCACG	GCTGCCTAATCCTCTCTTTATTTG
N-Acetylgalactosaminyltransferase	NM_198321	GALNT10	CAGTCTTGGAAAAATTCAATAGG	TTTAGAGAAAGTCTGGAGGTTTAC
N-Acetylgalactosaminyltransferase	AK128545	GALNT11	GTGGACCTTTGGGAAAAAC	CAAAAGGATTCTTTATTATGTAGATTG
N-Acetylgalactosaminyltransferase	NM_024642	GALNT12	AGCCTCGTGTATCAAGGAG	CAAAATCTCAGGGTTGGTCTG
N-Acetylgalactosaminyltransferase	NM_052917	GALNT13	AGATCATGTCCTCCAAGC	CACTTAGCAACTTTAACACAC

N-Acetylgalactosaminyltransferase	NM_024572	GALNT14	GAGGACAGAGGAAAACATCAC	CCAGAGACAACTTCTAAGTTTC
Galactosyltransferases	NM_020156	C1GALT1	GTGAAGTTAGGAAATCCTTGAAAG	ATATTGGTTAAAAATAATCAGATGAAACAAC
N-Acetylglucosaminyltransferases	NM_001097633	GCNT1	CCATTACGGGCAATTTTATGAAC	GGTTTCTGAATGGATGATTTTAATGG
N-Acetylglucosaminyltransferases	NM_004751	GCNT3	GACACACTATGAGAGCGTTG	CTTTGAATCAGGAGCTATTTATTTTTAAG
N-Acetylglucosaminyltransferases	NM_138706	B3GNT6	CTACGAGATGCTGCTCATG	TTTTTTGAGATGCAGTCTTGCTC
Glucosyltransferases	NA	B3GLCT	CTAGCATCAGGGTGACCTG	GATCCTTTTCATTACATAATAAAG
N-Acetylglucosaminyltransferases	NM_144677	MGAT5B	GGCTGTCTGTGAATCCG	CACATCCCAATAAAATATTTATTATTTCAAG
N-Acetylgalactosaminyltransferases	NM_152490	B3GALNT2	CGATGTCAAGCAAGATAACAG	TCAGGATTTAGAAATATTTTTCTTTTATAAA
Glucosyltransferases	NA	POGLUT1	GGAGAACCTCTTGAGTGAAT	TTTGTGTTATGCAAGTATCCC
Xylosyltransferase	NM_173601	GXYLT1	GATCGTTATGCCAGATCAC	TTTGAGGAAATAAAACGTTTATTGAG

Galactosyltransferases	NM_007255	B4GALT7	GCACTGTCCTCAACATCATG	TTTTGTCTGGCCTGCCATAC
Galactosyltransferases	NM_080605	B3GALT6	GAGGACATGCTGGAGAAG	TTTGTTCTGATATGAAATTTAATGTCTTAGG
GAG Polymerase and Related Enzymes	NM_018371	CSGALNACT1	CATGAACTCCCAGAGAAG	TCATATCCACAAATCATATTTTATTAGC
GAG Polymerase and Related Enzymes	NM_018590	CSGALNACT2	CATACAGGACAAACAGTGAAG	CATTTAACTTTTGGTAATAAAATACTTTATTGG
GAG Polymerase and Related Enzymes	NM_014918	CHSY1	GCAATAATAATGGCTCAGTGAG	TGAATCGTGTTTAAGTTTTTTACTCTC
N-Acetylglucosaminyltransferases	NM_181672	OGT	CACATGATTAAGCCTGTTGAAGTCAC	GATCCCCGTATTAAAGGGAAATCATTC
Galactosyltransferases	NM_003783	B3GALT2	GCCACCGTAAACTACATTAG	TAAAGTTTTTTGTTTTCCTTTATTTTTAAAAAC
Galactosyltransferases	NM_003782	B3GALT4	GCTTCAGAGCTGAGAGTG	GAAGTGGAGACAAGTTTATTGGAG
N-Acetylglucosaminyltransferases	NM_006577	B3GNT2	GCAGAGTGCTCATTTAAAATG	TTAAAAATACAGTGGCTTTATTTCC
N-Acetylglucosaminyltransferases	NM_014256	B3GNT3	GCAATCAGACACAGATCTAC	TCCAAGTCTTCACAAAATTTTATATTC

N-Acetylglucosaminyltransferases	NM_145236	B3GNT7	GATCGACGACGTCTTTCTG	TTAAAGAAGGAAGAGGTTTTTATTCG
N-Acetylglucosaminyltransferases	NM_033309	B3GNT9	GTGAGCTGGTTGTAGTGC	AATTTTATCCCATTTTTAATATTTTGGTCTAGC
Galactosyltransferases	NM_001497	B4GALT1	GAGCTAGCGTTTTGGTACAC	TGCAGTTACAAAGATAGGGTC
Galactosyltransferases	NM_001005417	B4GALT2	GCTGACACTAATGGACAGAG	GCTCCATTCACGTTTTTACTAAAG
Galactosyltransferases	NM_003779	B4GALT3	CTCTATCTACTGCCAACCAC	GCGAGACAAAGTCCTTTATTAG
Galactosyltransferases	NM_003778	B4GALT4	CAACATCACAGTGGATTTCTG	GCTTTTTCACATTTTACTACAGAGG
N-Acetylglucosaminyltransferases	AL832714	GCNT2	GCTATTCATGAGCTACTCATGAC	TGGAAAACAATATATTAATTTATTCCCAAG
N-Acetylglucosaminyltransferases	NM_004751	GCNT3	GACACACTATGAGAGCGTTG	CTTTGAATCAGGAGCTATTTATTTTTAAG
Sialyltransferases	NM_173344	ST3GAL1	GCAGACTTTGAGTCTAACG	AACAATAAAATAGCTCTTTGTTTATTCAC
Sialyltransferases	NM_005668	ST8SIA4	GACAACAGGAAAGTGTGTAAAG	TCACTTGTGAAATACTTTATTCCC
Fucosyltransferases	NM_000148	FUT1	GTCTCCACTCTGGACATTG	GTGCTGTAGACTTTTAATTCATACC

Fucosyltransferases	NM_000511	FUT2	CCTTTCCTCAAAATCTTTAAGC	CCATCCGCAAAGTCATAATTG
Fucosyltransferases	NM_001097641	FUT3	GCTACCTGAGCTACTTTCG	CTGGCCGGCCTATTATTTTTTAT
Fucosyltransferases	NM_002033	FUT4	CCAAGAGCATACGGAACTTG	CATTTTCCATCTCATTATTTTAATCATTTTGTC
Fucosyltransferases	NM_002034	FUT5	GCAGGAATCTAGGTACCAG	TGAAAATGTTAACAGCATTATCTG
Fucosyltransferases	NM_004479	FUT7	GAAGTCTATGAGGACCTTGAG	TCACTGCTCAGATGTTTATTGT
N-Acetylglucosaminyltransferases	NM_020469	ABO	CTGAGGAAGCTGAGGTTCA	GTGTCTTTCTGTGTGTGTCTG
N-Acetylglucosaminyltransferases	NM_016161	A4GNT	CTGTGATTAGAGGAAGCAAC	CTCAGTTAATATTTATTGACTGAATGC
GAG Polymerase and Related Enzymes	NM_005328	HAS2	TCTTCCATGTTTTGACGTTTG	CTTATCAAAAATATTTTATTTACAAAAAATTAATTATAC
GAG Polymerase and Related Enzymes	NM_005329	HAS3	CAGTACAGCTTGGCTTTTG	TTCGAGATAACCGGCATATG
Sulfotransferases	NM_005715	UST	GTGATGTGACTGTGTTGC	TCAAACACAGATTGCTTTTATTTTAGC
Sulfotransferases	NM_012262	HS2ST1	CGAACTGAGTATAAGGTGTG	GGAATGTATGATCTTTATTAATTTTTAATCC

Sulfotransferases	NM_005114	HS3ST1	GCAATAAGCTAAGCTCAGAAA	TTAGTTCTAAGTGGAATATTTATCAAAC
Sulfotransferases	NM_153612	HS3ST5	GCTACCAGAGGGTTTTACT	GAGGGGAAAGGGCTATTTATTTAG
Sulfotransferases	NM_004784	NDST3	GCACTGAGAGAAAACTTGAG	CCAGGTCCAAACTCTTCAT
N-Glycan Precursor Biosynthesis, en-bloc Transfer and Processing	AK095122	DPAGT1	GCTCGTTCGACTCTTCTATG	TAAACAATAAGAAAAAGACAACACTTTATTG
N-Glycan Precursor Biosynthesis, en-bloc Transfer and Processing	AK304655	MOGS	GCTACAATGTCTTCTGGAC	TGTTTTTTCCAATTTATTTAGAAAAATAGACTC
N-Glycan Precursor Biosynthesis, en-bloc Transfer and Processing	NM_198335	GANAB	GCATCAATGTGGCATCTG	TGATTTCTCCATCTTAAGTGC
N-Glycan Precursor Biosynthesis, en-bloc Transfer and Processing	NM_002743	PRKCSH	GGAAAGAGACCATGGTGAC	CGAGTCACCAAGGTGG

N-Glycan Precursor Biosynthesis, en-bloc Transfer and Processing	NM_006699	MAN1A2	GCTAGCTTCAGGTAATCCTG	CTCGAGAAATGTGCAACC
N-Glycan Precursor Biosynthesis, en-bloc Transfer and Processing	AK315797	MAN1B1	GATGCCTACGTGTTCAACA	GCGGTTAGAGCAAATCAAC
Nucleotide Sugar Transporter	NM_001042498	SLC35A2	CAAAGTCAGTGCTGGTGA	CAAGATACACAACACATTTTATTTGC
Nucleotide Sugar Transporter	BC005136	SLC35A3	GAGCCATCCTTGTAATAACAG	TTGTATAGAGTTCTTTATGAAAATAATCTATTTC
Nucleotide Sugar Transporter	NM_080670	SLC35A4	GTCCCTGACAACTTCCAC	TGGCTGTGGTTGTAGGAA
Nucleotide Sugar Transporter	NM_015139	SLC35D1	CAGAGGATTGCTTCATCTG	TCTGGATTAGTCTCTGTATGC
Nucleotide Sugar Transporter	NM_001008783	SLC35D3	GAAGGAGGTGCATGTAC	TTTAATAGTTAGACTCATACTTTATTTTGAC
Nucleotide Sugar Transporter	BX640761	SLC35F1	GAACCCTCAGTCACCTAC	TTCGGTGCTTTCATAAAGCAT
Nucleotide Sugar Transporter	AL833969	SLC35F2	CCACTCTGCTGTCTTGTAG	TGTATTTCCATGAATTCAAAGCC
Nucleotide Sugar Transporter	NM_173508	SLC35F3	CACCACTCCTCTAGAACTC	AACGCTTCTTTTCAAATATTTTATTAATC

Nucleotide Sugar Transporter	NM_025181	SLC35F5	GCTGTCTGTTGTCTGTAGG	GATATCAGAAATTTCTATTTGTTTTTAGATTC
Nucleotide Sugar Transporter	CR597058	SLC35D2	CTGTTTGGATTTGAAGAGC	TACATAGAAATGATTTTTATTTACTTTGA
Transferase Donor Substrate Biosynthesis and Related Reactions	NM_003359	UGDH	GAAACCTAAAGTGTAGAGATTGC	TAGTTGTTGATGGAGAATGTTTTATTTATG
Transferase Donor Substrate Biosynthesis and Related Reactions	NM_001128227	GNE	CCTCCAGGAACAGACATG	TTTCAACAAGGAAATGTATTTATTTTTTC
Transferase Donor Substrate Biosynthesis and Related Reactions	NM_003838	FPGT	GCAGTTTGATGTAGAGATATTTTAA	TAACAAAAAAAGCAGTGTCATG
Mannosidase	NM_014674	EDEM1	CAGATGGTTGGTTTGATTTG	GAAATCTTTTAATAAAAATTACTCATAAAAATCC
Mannosidase	NM_025191	EDEM3	GCTATGACTTGCTAAACAATCTG	CATAATTTATACACAATTCTAGAGTTTTATTCAC
Glucosidase	NM_000642	AGL	GCTACTATTCTTGAGACACTTTA	GACCTTTAGAAAATATTTTTATTTTCTTAACAC
Hyaluronidase	NM_012215	MGEA5	CTGTGACATTTGTTGACACTG	ACAAGCATTCACTTCAAGTTTTATTTTG
Glucosaminidase	NM_000027	AGA	TCCATCTTTACTGTCAACATC	AAAGTTTGAATATCGTACATGTAC

Arylsulfatase	NM_000046	ARSB	GATTTCAGGGAGGCTAGAA	GTAAAAATTTAGAACTAAAAAAA
N-Acetylglucosaminyltransferases	NM_001009905	B3GNTL1	GACTTCCTTCACTTCAGCT	GGTTGGAATAAAATATTTAAATCTCGTAAAAA

Appendix 2A. Plasmid maps and sequences

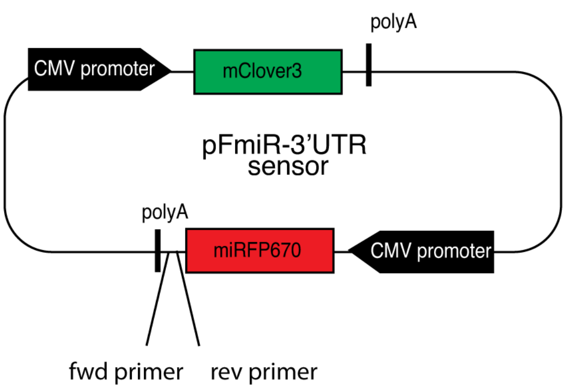

List of features:

mClover3 (896..1600)
CMV promoter 1 (238..810)
CMV promoter 2 (2139..2711)
miRFP670 (2779..3716)
SV40 polyA (1660..1851)
BGH polyA (3737..3961)

Sequence 1_pSFmiR-empty:

GCGATCGCGGCTCCCGACATCTTGGACCATTAGCTCCACAGGTATCTTCTTCCCTCTAGTGGTCATAACAGCAGCTTCAGCTACCT
CTCAATTCAAAAAACCCCTCAAGACCCGTTTAGAGGCCCCAAGGGGTTATGCTATCAATCGTTGCGTTACACACACAAAAAACCA
ACACACATCCATCTTCGATGGATAGCGATTTTATTATCTAACTGCTGATCGAGTGTAGCCAGATCTAGTAATCAATTACGGGGTCA
TTAGTTCATAGCCCATATATGGAGTTCCGCGTTACATAACTTACGGTAAATGGCCCGCCTGGCTGACCGCCCAACGACCCCCGCCC
ATTGACGTCAATAATGACGTATGTTCCCATAGTAACGCCAATAGGGACTTTCCATTGACGTCAATGGGTGGAGTATTTACGGTAAA
CTGCCCACTTGGCAGTACATCAAGTGTATCATATGCCAAGTACGCCCCCTATTGACGTCAATGACGGTAAATGGCCCGCCTGGCAT
TATGCCCAGTACATGACCTTATGGGACTTTCCTACTTGGCAGTACATCTACGTATTAGTCATCGCTATTACCATGCTGATGCGGTTT
TGGCAGTACATCAATGGGCGTGGATAGCGGTTTGACTCACGGGGATTTCCAAGTCTCCACCCCATTGACGTCAATGGGAGTTTGTT
TTGGCACCAAAATCAACGGGACTTTCCAAAATGTCGTAACAACTCCGCCCCATTGACGCAAATGGGCGGTAGGCGTGTACGGTGG
GAGGTCTATATAAGCAGAGCTGGTTTAGTGAACCGTCAGATCAGATCTTTGTCGATCCTACCATCCACTCGACACACCCGCCAGC
GGCCGCTGCCAAGCTTCTAGCGCTACCGGTCGCCACCATGCATCATCACCATCACCACGTGAGCAAGGGCGAGGAGCTGTTCACC
GGGGTGGTGCCCATCCTGGTCGAGCTGGACGGCGACGTAAACGGCCACAAGTTCAGCGTCCGCGGCGAGGGCGAGGGCGATGCC
ACCAACGGCAAGCTGACCCTGAAGTTCATCTGCACCACCGGCAAGCTGCCCGTGCCCTGGCCCACCCTCGTGACCACCTTCGGCT
ACGGCGTGGCCTGCTTCAGCCGCTACCCCGACCACATGAAGCAGCACGACTTCTTCAAGTCCGCCATGCCCGAAGGCTACGTCCA
GGAGCGCACCATCTCTTTCAAGGACGACGGTACCTACAAGACCCGCGCCGAGGTGAAGTTCGAGGGCGACACCCTGGTGAACCG

CATCGAGCTGAAGGGCATCGACTTCAAGGAGGACGGCAACATCCTGGGGCACAAGCTGGAGTACAACTTCAACAGCCACTACGT
CTATATCACGGCCGACAAGCAGAAGAACTGCATCAAGGCTAACTTCAAGATCCGCCACAACGTTGAGGACGGCAGCGTGCAGCT
CGCCGACCACTACCAGCAGAACACCCCCATCGGCGACGGCCCCGTGCTGCTGCCCGACAACCACTACCTGAGCCATCAGTCCAAG
CTGAGCAAAGACCCCAACGAGAAGCGCGATCACATGGTCCTGCTGGAGTTCGTGACCGCCGCCTAATCTAGAGCTCGCTGATCAG
GCTAGCTTGACTGACTGAGATACAGCGTACCTTCAGCTCACAGACATGATAAGATACATTGATGAGTTTGGACAAACCACAACTA
GAATGCAGTGAAAAAAATGCTTTATTTGTGAAATTTGTGATGCTATTGCTTTATTTGTAACCATTATAAGCTGCAATAAACAAGTT
AACAACAACAATTGCATTCATTTTATGTTTCAGGTTCAGGGGGAGGTGTGGGAGGTTTTTTAAAGCAAGTAAAACCTCTACAAAT
GTGGTATTGGCCCATCTCTATCGGTATCGTAGCATAACCCCTTGGGGCCTCTAAACGGGTCTTGAGGGGTTTTTTGTGCCCCTCGG
GCCGGATTGCTATCTACCGGCATTGGCGCAGAAAAAAATGCCTGATGCGACGCTGCGCGTCTTATACTCCCACATATGCCAGATT
CAGCAACGGATACGGCTTCCCCAACTTGCCCACTTCCATACGTGTCCTCCTTACCAGAAATTTATCCTTAAGGTCGTCAGCTATCC
TGCAGGAGTAATCAATTACGGGGTCATTAGTTCATAGCCCATATATGGAGTTCCGCGTTACATAACTTACGGTAAATGGCCCGCCT
GGCTGACCGCCCAACGACCCCCGCCCATTGACGTCAATAATGACGTATGTTCCCATAGTAACGCCAATAGGGACTTTCCATTGAC
GTCAATGGGTGGAGTATTTACGGTAAACTGCCCACTTGGCAGTACATCAAGTGTATCATATGCCAAGTACGCCCCCTATTGACGTC
AATGACGGTAAATGGCCCGCCTGGCATTATGCCCAGTACATGACCTTATGGGACTTTCCTACTTGGCAGTACATCTACGTATTAGT
CATCGCTATTACCATGCTGATGCGGTTTTGGCAGTACATCAATGGGCGTGGATAGCGGTTTGACTCACGGGGATTTCCAAGTCTCC
ACCCCATTGACGTCAATGGGAGTTTGTTTTGGCACCAAAATCAACGGGACTTTCCAAAATGTCGTAACAACTCCGCCCCATTGACG
CAAATGGGCGGTAGGCGTGTACGGTGGGAGGTCTATATAAGCAGAGCTGGTTTAGTGAACCGTCATTCGACCAACCTTCCTTCGA
CACGGGGCCCAAAGTACTAAAGTCGACGCCAACATGTAATAACGTTATGGTAGCAGGTCATGCCTCTGGCAGCCCCGCATTCGGG
ACCGCCTCTCATTCGAATTGCGAACATGAAGAGATCCACCTCGCCGGCTCGATCCAGCCGCATGGCGCGCTTCTGGTCGTCAGCG
AACATGATCATCGCGTCATCCAGGCCAGCGCCAACGCCGCGGAATTTCTGAATCTCGGAAGCGTACTCGGCGTTCCGCTCGCCGA
GATCGACGGCGATCTGTTGATCAAGATCCTGCCGCATCTCGATCCCACCGCCGAAGGCATGCCGGTCGCGGTGCGCTGCCGGATC
GGCAATCCCTCTACGGAGTACTGCGGTCTGATGCATCGGCCTCCGGAAGGCGGGCTGATCATCGAACTCGAACGTGCCGGCCCGT
CGATCGATCTGTCAGGCACGCTGGCGCCGGCGCTGGAGCGGATCCGCACGGCGGGTTCACTGCGCGCGCTGTGCGATGACACCGT
GCTGCTGTTTCAGCAGTGCACCGGCTACGACCGGGTGATGGTGTATCGTTTCGATGAGCAAGGCCACGGCCTGGTATTCTCCGAGT
GCCATGTGCCTGGGCTCGAATCCTATTTCGGCAACCGCTATCCGTCGTCGACTGTCCCGCAGATGGCGCGGCAGCTGTACGTGCGG
CAGCGCGTCCGCGTGCTGGTCGACGTCACCTATCAGCCGGTGCCGCTGGAGCCGCGGCTGTCGCCGCTGACCGGGCGCGATCTCG
ACATGTCGGGCTGCTTCCTGCGCTCGATGTCGCCGTGCCATCTGCAGTTCCTGAAGGACATGGGCGTGCGCGCCACCCTGGCGGTG
TCGCTGGTGGTCGGCGGCAAGCTGTGGGGCCTGGTTGTCTGTCACCATTATCTGCCGCGCTTCATCCGTTTCGAGCTGCGGGCGAT
CTGCAAACGGCTCGCCGAAAGGATCGCGACGCGGATCACCGCGCTTGAGAGCTAAACTAGTTAGCCTGTGCCTTCTAGTTGCCAG
CCATCTGTTGTTTGCCCCTCCCCCGTGCCTTCCTTGACCCTGGAAGGTGCCACTCCCACTGTCCTTTCCTAATAAAATGAGGAAATT
GCATCGCATTGTCTGAGTAGGTGTCATTCTATTCTGGGGGGTGGGGTGGGGCAGGACAGCAAGGGGGAGGATTGGGAAGACAAT
AGCAGGCATGCTGGGGATGCGGTGGGCTCTATGGCCTGCAGGCGATCTCTCGATTTCGATCAAGACATTCCTTTAATGGTCTTTTC
TGGACACCACTAGGGGTCAGAAGTAGTTCATCAAACTTTCTTCCCTCCCTAATCTCATTGGTTACCTTGGGCTATCGAAACTTAATT
AACCAGTCAAGTCAGCTACTTGGCGAGATCGACTTGTCTGGGTTTCGACTACGCTCAGAATTGCGTCAGTCAAGTTCGATCTGGTC
CTTGCTATTGCACCCGTTCTCCGATTACGAGTTTCATTTAAATCATGTGAGCAAAAGGCCAGCAAAAGGCCAGGAACCGTAAAAA
GGCCGCGTTGCTGGCGTTTTTCCATAGGCTCCGCCCCCCTGACGAGCATCACAAAAATCGACGCTCAAGTCAGAGGTGGCGAAAC
CCGACAGGACTATAAAGATACCAGGCGTTTCCCCCTGGAAGCTCCCTCGTGCGCTCTCCTGTTCCGACCCTGCCGCTTACCGGATA
CCTGTCCGCCTTTCTCCCTTCGGGAAGCGTGGCGCTTTCTCATAGCTCACGCTGTAGGTATCTCAGTTCGGTGTAGGTCGTTCGCTC
CAAGCTGGGCTGTGTGCACGAACCCCCCGTTCAGCCCGACCGCTGCGCCTTATCCGGTAACTATCGTCTTGAGTCCAACCCGGTAA
GACACGACTTATCGCCACTGGCAGCAGCCACTGGTAACAGGATTAGCAGAGCGAGGTATGTAGGCGGTGCTACAGAGTTCTTGAA
GTGGTGGCCTAACTACGGCTACACTAGAAGAACAGTATTTGGTATCTGCGCTCTGCTGAAGCCAGTTACCTTCGGAAAAAGAGTT
GGTAGCTCTTGATCCGGCAAACAAACCACCGCTGGTAGCGGTGGTTTTTTTGTTTGCAAGCAGCAGATTACGCGCAGAAAAAAAG
GATCTCAAGAAGATCCTTTGATCTTTTCTACGGGGTCTGACGCTCAGTGGAACGAAAACTCACGTTAAGGGATTTTGGTCATGAGA
TTATCAAAAAGGATCTTCACCTAGATCCTTTTAAATTAAAAATGAAGTTTTAAATCAATCTAAAGTATATATGAGTAAACTTGGTC
TGACAGTTACCAATGCTTAATCAGTGAGGCACCTATCTCAGCGATCTGTCTATTTCGTTCATCCATAGTTGCATTTAAATTTCCGAA
CTCTCCAAGGCCCTCGTCGGAAAATCTTCAAACCTTTCGTCCGATCCATCTTGCAGGCTACCTCTCGAACGAACTATCGCAAGTCT
CTTGGCCGGCCTTGCGCCTTGGCTATTGCTTGGCAGCGCCTATCGCCAGGTATTACTCCAATCCCGAATATCCGAGATCGGGATCA
CCCGAGAGAAGTTCAACCTACATCCTCAATCCCGATCTATCCGAGATCCGAGGAATATCGAAATCGGGGCGCGCCTGGTGTACCG
AGAACGATCCTCTCAGTGCGAGTCTCGACGATCCATATCGTTGCTTGGCAGTCAGCCAGTCGGAATCCAGCTTGGGACCCAGGAA
GTCCAATCGTCAGATATTGTACTCAAGCCTGGTCACGGCAGCGTACCGATCTGTTTAAACCTAGATATTGATAGTCTGATCGGTCA
ACGTATAATCGAGTCCTAGCTTTTGCAAACATCTATCAAGAGACAGGATCAGCAGGAGGCTTTCGCATGATTGAACAAGATGGAT
TGCACGCAGGTTCTCCGGCGGCTTGGGTGGAGAGGCTATTCGGCTATGACTGGGCACAACAGACAATCGGCTGCTCTGATGCCGC
CGTGTTCCGGCTGTCAGCGCAGGGGCGTCCGGTTCTTTTTGTCAAGACCGACCTGTCCGGTGCCCTGAATGAACTGCAAGACGAG
GCAGCGCGGCTATCGTGGCTGGCGACGACGGGCGTTCCTTGCGCGGCTGTGCTCGACGTTGTCACTGAAGCGGGAAGGGACTGGC
TGCTATTGGGCGAAGTGCCGGGGCAGGATCTCCTGTCATCTCACCTTGCTCCTGCCGAGAAAGTATCCATCATGGCTGATGCAATG
CGGCGGCTGCATACGCTTGATCCGGCTACCTGCCCATTCGACCACCAAGCGAAACATCGCATCGAGCGAGCACGTACTCGGATGG
AAGCCGGTCTTGTCGATCAGGATGATCTGGACGAAGAGCATCAGGGGCTCGCGCCAGCCGAACTGTTCGCCAGGCTCAAGGCGTC
TATGCCCGACGGCGAGGATCTCGTCGTGACCCACGGCGATGCCTGCTTGCCGAATATCATGGTGGAAAATGGCCGCTTTTCTGGAT
TCATCGACTGTGGCCGTCTGGGTGTGGCGGACCGCTATCAGGACATAGCGTTGGCTACCCGTGATATTGCTGAAGAGCTTGGCGG
CGAATGGGCTGACCGCTTCCTTGTGCTTTACGGTATCGCCGCGCCCGATTCGCAGCGCATCGCCTTCTATCGCCTTCTTGACGAGTT
CTTCTGACCGATTCTAGGTGCATTGGCGCAGAAAAAAATGCCTGATGCGACGCTGCGCGTCTTATACTCCCACATATGCCAGATTC
AGCAACGGATACGGCTTCCCCAACTTGCCCACTTCCATACGTGTCCTCCTTACCAGAAATTTATCCTTAAGGTCGTTTAAACTCGA
CTCTGGCTCTATCGAATCTCCGTCGTTTCGAGCTTACGCGAACAGCCGTGGCGCTCATTTGCTCGTCGGGCATCGAATCTCGTCAG
CTATCGTCAGCTTACCTTTTTGGCA

With the insertion into downstream of miRFP670

. cgcggatcaccgcgcttgagagctaaACTAGTTAGCCTGTGCCTTCTAGTTGCCAGCCATCTGTTGTTT

miRFP670 ***forward primer*** ***reverse primer*** ***polyA***

GCCCCTCCCCCGTGCCTT….

Sequence 1. Plasmid Map of pFmiR-empty and sequence.

Appendix 2B. pSFmiR-gene-3'UTR plasmid map and gene 3'UTR sequences

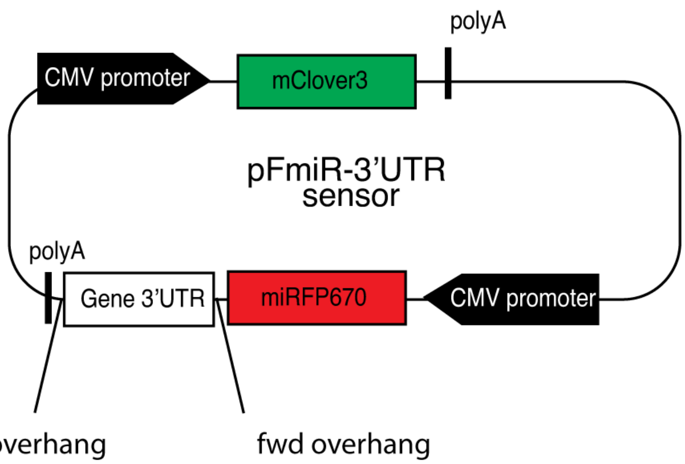

B3GLCT 3'UTR sequence:

GCTAGCATCAGGGTGACCTGTGCGCCTAGCCTGCTCAGGGAGTGAACTGGAGACTGTGGCCTCATCCCACTGTGCTGTGCTCACA
ACACTTGTGTCTGCCACATGGCATTGGGTGCTTCCTGACTTTAGGGGGAGATTTTATGTATGGTATTTTTTGACAGAGGAAGAAAA
GGGGTCACAGGAGAAACATTTTTTTTTCTGGGAAAAATCACTTGCTTTTGACTTATGCAGTTGTTTTAACACTTAGTGATGACTGTG
TATTCTCCAAGCTGTGATACAGCAGTTTTTTTTTATTGTCACAGGGAAATAAATGGTACCAGAAGTCCCTTTCCTGTTCTGTCTCTT
CATTGTAATGGAAGTTTCAGTTGGGCATGAGCCTGGAGAGATGTGACTGTCTACAGTTCTATTTGTATATATAAAAAGAAGACTG
AAAGTCTTTTGACATGGATATTGTGAATGGTATGAACTTTTAAACCATATTATTGATGATGAAAATTATTTCCTGGGAACTCAGTA
GGAATAATACCGTATTAAGGAATAATACTGTACATAAAACATCATGAAACCCTAGATATGAAATCCCCTGAAGTCTGTAATCATG
GTGGTTATGTTTGTCTATTCTTTTGCTGTTTGTGCCTCATAAAAAGAGAATGAGGTCTTCTGCTAGAGCTTCGTATTGCTTTGGAA
GTTCATCTGTGTTTTATTTCTCCCTGAAGCCCTATCTTTATGGCTTACTTGTAACATGAAAGTAGTAGATGCTGCCAGAAAATAGTG
TCCTCAATATTTAAAACAATGTTGACATGTTTTGTTCAAGTCAGCAAGCTCTATGTGAGTCTCAGGAAGTGAATTAAATTTGGAC
CTTATGTTTTACTCTTGTTTTTTTTTTTTTTTTAAATGTTACTTAATGACTCTCTCCTGACTCAGGAGAGAAACCCCTTGTGGAAGGA
CAGCATGGTGATCAGGCAATTTCTCTGGGTTCCCAAAGAATGACATTTGAACACAGTATTTTGAAACAGCTCTAGTTTTCAAATTA
TATCTTTAATATATAGTAATGTAACATATTCAGTATTAATGTATAAAAAGCACTCTAATTATATAATTCAGTTTTTGTAAAGGTATT
TGCATAAAATTTAATATGTCTTAAACTAATTTTGGTAAATTACTTCTTTTTTTTCTTTTTAATAAAAACTGTTACTCATTAACTTTGC
TTATAATGCTTTTTATAGCCCAGCACAGAATTTAAAGCCATACCACCAAAAGTACCTGTGTGTGTTAATATGTTTTTCTTGTAGCAT
AGATTGACTATTTGCAATAGTATTAGTATTTACCATTTTTCCAAATTAGCAACTACCAGACCTCACGTGTTGCAGTGATAACACAA
TGCATTGGATTCAGTTTTGTGAAAATGGATTCTGTGGCCATCCAAGGGATGTATCAGGGATGATCAGCTGATGAGAGGCTCCAGA
AGGATTTCTAGATCGCTTCAAGCCTATACTGATGGCCTTAGCTTTGTTCAGTCATTGTAACTGGGATTGTTGTCATTGCTACCGTGG
TAGTCACCTTCATGTCATCTATAATAGTACTCCTGGAGAGCCCTGGCTGCCTACACCAGTGGAAAAGAGTCTCCAGTTCTGCTCTG
GCCTACTAACTGTTACCACTGAGAGAACAACATGTTCATTTGACATGATTGAAGCTGGCATCCGTATATGAAGATCCTTGTCAAGC
TTTCTTCTGTGGTCTGATTAGTGCCTTCTACTGATACCGGGGCACCTCCTCTGGTACTTTTAAGTGTTTTGTTAATTATATTTACTTT
TTGGAATGGTGTAAGCCTAACCACAAGTAAAAGATCTTTGCCTAAGTTTTTGATTTCTCAAATATTGTGTTCATTAGTCTAGACTG
GGAATGGGGAGGGGAAATGGGGAAAATGAATGAATGAAATCAGAAAAAAGTCAGCGGCTCAGTAAATACAGTTTAAAGAGAGA

ATAATTACTTCAGAGCTACCCTTTTAAGAGAAAACCATCAGAAATTGATAATGTTTATATAAAGTTTATAAAGCCATTGTGTTTTG
TTATATAACAAATCAGAGATGTTATTTTAGAATCGATTCCCATCTAAAGAACTCAATTTTGAGTCTGACATTTCCAGGACCAGATA
TTGTCTTACTCACATTTCCTTTGCTTTGAAATAGGGCTTTCCTTCCAAATGGCTATTTTTAGGCTAGGGATGTTAACATCAGGGATT
TGTGTGTGGAATAACTGGAATGTCATTTTTGCTTTTAAGCCATTTCTGATGATATAGCCAAAGCAGGTTGTCTGACTATGTAGGAT
TTTTACATCTTGAAACTAAATCAGAAATCCAGACATGAAAATAACCTTTCTAGAATGCCTAGGAGCAGAAAACAATAATAGCATG
CTAAATCACAAATGATGCTATGTATGGGTATGTAAATATCAGTGCTGTCTGCATTTCTGGGTTTATTGAAGACCTCTTGTTGTATAT
ATCCTCAAAAATTAATGTAATTGACATCTTCAAGAATGTTTCTATTGTCTTCCATTCATAATCAGAGATGTAATTTGTATGGACTAA
ATAAAAACTTTATTATGTAATGAAAAG

OGT 3’UTR sequence:

CACATGATTAAGCCTGTTGAAGTCACTGAGTCAGCATAAATAAAGACTGCACAGGAGAATTACCCCTATACCTGAGCCTCAACCT
TCTGGGGGAAAGGGAACTAGATAACATACTTCTTACTTGTCTGTACAGTACCTTGTTGCAGATGGGTGATATATAATGGTAATAGA
ATAGCACAGCCAGACTTGCTTCCTGCATGGTAGGGAGAGACACAAAAGATGGGAAACTGCTTTTCCACAAGGAATCTCCGTAGAA
TTTTGCGGCGACCAGATGGTGCATAGGTCTGGAAGGTCTGATCTCCCTTGGTCTTCCATGGGATGGTTAGTGTGGAGGGGAGATAT
AGATTGTCCGGCCGCTTTGTGATTCCATGGATTGATTCAGTCTTCTGGATTTTTTTTTCTTTATATTTTGGGTACTGGAGCTTTTAAA
AATGTTTGGTTTCAGGTATTTTTATTCATGTGAAGTGTATATGATTCTCTTGAGATAAGGTTTTAAGCTAAAATGTTACTCCCTGTT
TTAGTTTCTGAACTCTGACAGATTGACAGGGACTTTGCTGGTGTAGTCTTTTTATAGGTTTTATAAACCACTTGAGCCTATATCAGT
CGTTTTAGTGTCTGACCTAATATTTGGAGCTATCAGTGCTTTGTTGATTTAGATGATGACTCAAGATTTTTTCTGGTCCATTTCCCAT
TTCCTTTTCTTCCCTGACCCCCATACCCTCACCCTTAAAATTCTCCTGTAACTCAACTAACAAAATCAAGCCTGATTCAAAACATCC
TAGGGTGTTTTAAACACACCATCTGGTGCCAAATGAAGATTTTTAGGAGTGATTACTAATTATCAAGGGCACAGTTGTGGTACTGT
CATTGATAATAATATAGTTTTTTTTTTTTTCCTAATTTTGACCTGTTTCACCAGTGTTTTACCCTTGACTGCCCCTTCTATGCTGCTTC
CAAAAGTGATAGTGTGTGTAAGATTTTTACCTTCCTTTCTAAAGTTTTTTTTTTTTTTTTTTAAGTGAGTCCTGTTCTTCCTATTTCTT
TCAGCAGAAATGAAATCCCAGGTAAGTATAAGTATTCAAGTATTTGATCAGTAAGTCACAGTTATCTCCAGTGCATTAAATAACCT
TCATCAAGAAATAGGTTATAGGTAAAATCTCTGAAGGATCATCTATGTATTCAAGTAATTATTTTTTAGATAATAACTGTCTTCTG
GACTTGGTCTTGAAGTCTGTACAGATTCAGCCTCAGTAGTAGCGAACTGCACTGCTGTTTGGTTTGGAGTACAAATTAGACTTATA
GTCCTCCTGGAACTTGAGTTATTAAAATCATAGGAATAAAATTATGGGATCTCAACAAAGGGTCGAGGGTTTGAGGCTTAAACAA
GCCAACATATGAATATATGTTTTGTCTCGCTATACTGCACTTACGCTATCCAGTTGCAGGTAATTTTTTGTCTGCTAGTAGTGTTCT
AGATTATGTCTTTCCAAAGCGCTGAGGCTGTGCACCTATTCTGTAGTTGCAGCTGATGCCTGAATGTATCCTAGCTGACAAATTAT
TGATTAATAAGAACTTGAATTTCTGGAAGATTCTTACTGTTAACCAAATTTTGAGCAAGGAGTCTCAAAGGTAATTCTGAACCAGA
ATTACATGTTAATGAACAGTGTACCTTTTAACAGTGTAAATCACGGAATATCCGTGAAGGGATTTCTTAATTTATTTTTTACCGGTT
GATTGAAATATCAGTTAAAGGTTGCCAGCATGGTTGCAGATAAACTGATGTTTGAAATTCGCTGAAATACTTAATGTGGAATAGG
ATAATATACTTCCAATGCCCTCAAGGCTGTGACCTTACAGCCATTTTACATAGCACATCATTCCTCCTATAGGGATGAACTTTTTCC
TGGCACGAAAAGTAGCCGCTCTGGTTGAAGCTTTGCTTATTGTAACAGGCTTTTATTTCCAGGTAATATGTCTTGGAAGACTTAAT
TCTGATTAGAGATATAGATATTACTGGAAACTAATTGTTTTTTTTCTATTGTACTCTGCTTTATCAAAGAAGTAAAACATTTAAATC
GTACTACAGAAATTAAGATGTTGTCTTGCGATCCTTAATAAATGAATGATTTCCCTTTAATACGGGGATC

OGA 3’UTR sequence:

CTGTGACATTTGTTGACACTGTGAACTGTCCAAAAGTCTCTTAACTGCACCTTGTGAATGGTAGTTGAGGTCTTCATACAGTTCAG
CCTCTAGAATGGTAACAAATCAGCCAATTGGATTCGAAACAAAGAAGACTATGTAAAACTCACCCATCACACTTTGAGACTACTC
ACTGGTTGGAAGAATATAGTATTGCAGCAAATCCTGTATGAAAGAGAGATGTGGGCTTCCTTTTTGAGTCTTGTGTTAGGTGCTGA
GACCTTTTACATGGGCTTATACAGGGAGAGAGTCTTCAATAAATGTAGTCAGCACTATTTTCTGCATCCAGTGTGGTTGCGTTTCT
CACCTGAGAGTAATCAAGATAACATCTGTCATCTTCCTTGGTTTATTGAGTGAAATGCCTCTCAGTCTTAGGGGACATGGCAGAGA
TGAAAGAAAGAAAGAGTGGGTTTCAGAAGTGTCAGGGTGGAGTGATTCCAAGTGGGATGGTTGTGGCATTAGTTTAAGCTGAATA
AATAATTTCAATTTGGGGCAGTTATTCTGCTTTTTGTAAAGCCGTGGCCAATTGTCTCCTGTAATGACTGTTGGTTCAGGCATGTTG
TACTTTGTAGGGACAAATGTGCATTTGTTTGTGGCAAAAGCCTACAATTGACAAACTTGTAAATTTCTTTGTATATAAACTAGCTG
TAACCTGACTATCCTTTGTGTTTACTGTTTTTGTAAATTTTTTTCCTCTATAAATGAAAGGGTGTTGGTTCAGAATGGCACTTTGAA
TAATGTAAACCAGTGAAAAGTGGATTTTCTTTACTTTTGTCTTTGGGTTTGGGGTTGTTTTTGTTCTTTTTGAAGTTTTATTATTTTT
AAAGTGCCTCCCACCTAGGCGTAGGCCATGACCATTTGGGGTACGAGAGCCTAATTTTGTAGGACTTAATCTGTTGAAAAGTGCA
GTTACTTCTGGAAATTAACCTCAATATTAGGTCAGCATGTGAAATGTTGGATTTGACATGTCAGGTAGGGTTCAGGGACTGATTGG
TCCCATTTGCCCTCAGGTCAGTTGTTTAATCTCAAGACCTGTTACTACTGATTTTATTAAATCAGAGTCTTTAATTCTTGCATGTTTG
TATCTAATTTCTGAATGAATGAGCACACTTTAACCAGTTATTTACAGTTACCTTTTTCCTTTAACCGGATTGTGAAAGCTTCATGTA
TTTTAATTTAGATTCTGTGTTTTTAAGGGTTCTGAGCATGAAGCTGGCAGATAGTCGGCAGGACTCATTTTTTCATCATGGCTGGCT
GATTTCTCCATAGATTGATAACAGTATTTTGTTATCTTGCTTCTCTGTAGTTTTGCATCAGCTGTTTAACTTTGAGCTGAGTGAGGG
GAGAGGGGTAAAGAGAAAGAAACTTAAGTTTTCTTTCACAGAACTCCACCATTGTGGGCTTTGAGAGAGCCCTAAAGCATTGTAC
CTAGTGGTACCTAGTGACTTCCAACCAAAGCCTTTGAGTATGCACTAAATAGGTGAGAAGAAAGGAGAGAAGGTTTTTAGGTTAG
AAACCTTTAACCGATAGAAGGATATGGTATGTTGTAAAGCTGGAACCAAGTTTGCATTTTTGAGGGCTTGAGATGAAGGGAAGAC
TCTTACCAGATAGTAAGACAGCTGAGTTTTCCTCAGTTTTCTCGTCTTAACACTAGTGGACAATTCTAGCATTTTGTTTGGAGGATT
TCAGAGTTAACCTCATGGAATTCAGGATTTTTTAGCAAGTTTGCTTTTGGTTTTATCTTGGCTTTTAGTAATCATGTTGGCTGGTCT
GGTCACAGGTGACTGTGAAACAGATGCCCTGGTCTTGCTTTCATCACTCTAGGATCATGAAGTGCTATGCTATTTCCTGGTTATGA

ATATTAAGGTTGGAATTACATTTTTATTGATTGTTTGGATCAGAGCTCAGTTCCTGTAGAAAACGAACTGTAAAAGACCATGCAAG
AGGCAAAATAAAACTTGAAGTGAATGCTTGT

FUT1 3’UTR sequence:

GAGCCAGGGAGACTTTCTGAAGTAGCCTGATCTTTCTAGAGCCAGCAGTACGTGGCTTCAGAGGCCTGGCATCTTCTGGAGAAGC
TTGTGGTGTTCCTGAAGCAAATGGGTGCCCGTATCCAGAGTGATTCTAGTTGGGAGAGTTGGAGAGAAGGGGGACGTTTCTGGAA
CTGTCTGAATATTCTAGAACTAGCAAAACATCTTTTCCTGATGGCTGGCAGGCAGTTCTAGAAGCCACAGTGCCCACCTGCTCTTC
CCAGCCCATATCTACAGTACTTCCAGATGGCTGCCCCCAGGAATGGGGAACTCTCCCTCTGGTCTACTCTAGAAGAGGGGTTACTT
CTCCCCTGGGTCCTCCAAAGACTGAAGGAGCATATGATTGCTCCAGAGCAAGCATTCACCAAGTCCCCTTCTGTGTTTCTGGAGTG
ATTCTAGAGGGAGACTTGTTCTAGAGAGGACCAGGTTTGATGCCTGTGAAGAACCCTGCAGGGCCCTTATGGACAGGATGGGGTT
CTGGAAATCCAGATAACTAAGGTGAAGAATCTTTTTAGTTTTTTTTTTTTTTTTTTGGAGACAGGGTCTCGCTCTGTTGCCCAGGCT
GGAGTGCAGTGGCGTGATCTTGGCTCACTGCAACTTCCGCCTCCTGTGTTCAAGCGATTCTCCTGTCTCAGCCTCCTGAGTAGATG
GGACTACAGGCACAGGCCATTATGCCTGGCTAATTTTTGTATTTTTAGTAGAGACAGGGTTTCACCATGTTGGCCAGGATGGTCTC
GATCTCCTGACCTTGTCATCCACCTGTCTTGGCCTCCCAAAGTGCTGGGATTACTGGCATGAGCCACTGTGCCCAGCCCGGATATT
TTTTTTTTAATTATTTATTTATTTATTTATTTATTGAGACGGAGTCTTGCTCTGTAGCCCAGGCCAGAGTGCAGTGGCGCGATCTCA
GCTCACTGCAAGCTCTGCCTCCCGGGTTCATGCCATTCTGCCTCAGCCTCCTGAGTAGCTGGGACTACAGGCGCCCGCCACCACGC
CCGGCTAATTTTTTTTGTATTTTTAGTAGAGACGGGGTTTCATCGTGTTAACCAGGATGGTCTCGATCTCCTGACCTCGTGATCTGC
CCACCTCGGCCTCCCACAGTGCTGGGATTACCGGCGTGAGCCACCATGCCTGGCCCGGATAATTTTTTTTAATTTTTGTAGAGACG
AGGTCTTGTGATATTGCCCAGGCTGTTCTTCAACTCCTGGGCTCAAGCAGTCCTCCCACCTTGGCCTCCCAGAATGCTGGGTTTATA
GATGTGAGCCAGCACACCGGGCCAAGTGAAGAATCTAATGAATGTGCAACCTAATTGTAGCATCTAATGAATGTTCCACCATTGC
TGGAAAAATTGAGATGGAAAACAAACCATCTCTAGTTGGCCAGCGTCTTGCTCTGTTCACAGTCTCTGGAAAAGCTGGGGTAGTT
GGTGAGCAGAGCGGGACTCTGTCCAACAAGCCCCACAGCCCCTCAAAGACTTTTTTTTGTTTGTTTTGAGCAGACAGGCTAAAATG
TGAACGTGGGGTGAGGGATCACTGCCAAAATGGTACAGCTTCTGGAGCAGAACTTTCCAGGGATCCAGGGACACTTTTTTTTAAA
GCTCATAAACTGCCAAGAGCTCCATATATTGGGTGTGAGTTCAGGTTGCCTCTCACAATGAAGGAAGTTGGTCTTTGTCTGCAGGT
GGGCTGCTGAGGGTCTGGGATCTGTTTTCTGGAAGTGTGCAGGTATAAACACACCCTCTGTGCTTGTGACAAACTGGCAGGTACC
GTGCTCATTGCTAACCACTGTCTGTCCCTGAACTCCCAGAACCACTACATCTGGCTTTGGGCAGGTCTGAGATAAAACGATCTAAA
GGTAGGCAGACCCTGGACCCAGCCTCAGATCCAGGCAGGAGCACGAGGTCTGGCCAAGGTGGACGGGGTTGTCGAGATCTCAGG
AGCCCCTTGCTGTTTTTGGAGGGTGAAAGAAGAAACCTTAAACATAGTCAGCTCTGATCACATCCCCTGTCTACTCATCCAGACC
CCATGCCTGTAGGCTTATCAGGGAGTTACAGTTACAATTGTTACAGTACTGTTCCCAACTCAGCTGCCACGGGTGAGAGAGCAGG
AGGTATGAATTAAAAGTCTACAGCAC

FUT2 3’UTR sequence:

TGCTGGCCCATTCTTTGAGACCTTTTCTCCTTCTCTGCCTCCCTCAAGATGAGTGCCCGGGCATGAGAAGCACATGGTTCCATGAG
CAGGACCCATCTCTCTTCTGTGAAGATGCGTTGGGCTGCAAGTAACAGAAATCTCAGTGAACAGTGGCCTGGCGTGGTGGCTCAT
GCCTGTAATGCTCGCACTTTGTGAGGCCAGGGTGGGTGGATCACTTGAGGTCAGGAGTTCAAGACTAGCCTGGCCAACATGGTGA
AACCCCATCTCGACTAAAAATACAAAAATTAGCCAGGCGTGGTGGTGCACACCTGTAATCCCAGCTACTCGGGAGGCTGAGGCAA
GAGAATCACTTGAACCCAGGAGGCGGAGGTTGCAGTGAGCCAAGATGGTGCCGCTGCACTCCAGTCTGGGTGACACAGCAAGAC
TCCATCTCAAAAAAAAAAAAAAAAAAAAAGAAAAGAAAAAGAAATGAATGGGTTCAAAGACCATAATCATGCATATCACATAAG
ACCAGAAGTGGCCCAGGTCCAGGGTCAGTTAATTTAGCGGCTCCACAAAGTCATCAGTCACCTGAGCTCCATCCATCTTCACATG
CTGTGCTACCATTTCTTAGCTGTATCATCCCATGGTCCCAAAAGGGCTGCTACACATCCAGCCATCACATGCAGATAATTCCTTTC
AAAAACAGCAGAAAGAGGCTCGTTCTTGTCTTGGTCCCTTTTGAAGAATGAATGAAACCTTCCTAAGCCTTCCAGCAATTTCCCCC
CAACTCCGATGGGTAGGAATTGTCACATACCCATGTGACCCGATAGGAGGCAAAAGAAATGAGACTTCTGGGATTAGTTTAGCCT
CAGATTCTGCAGCTGAGAAGTTGATCAGCCACCTCTGAAGGACATGCAGCTTGCAGAAAATTAGGGTGGTGTTACCAAGGTGAAA
AGGGGAAATGGCTTTAGAGTAGACAACAGAGATGCCCTGAGGGGTTGTGTAGGTTGTTCACTGCAGGAAGTCCCCTGGTTAAGAA
GGCAAGTGGGGTTTAAACAGACCCACAGTCTACTCATCAAACCAGGTGTCCTTGGCATTGTGTCCACCCAGAGAGCTCACTGTTTT
CTTTTCTTTTTCTTTTCTTTTTTTTTTTTTTTTTTGAGATGGAGTCTTGCTGCATCCCCCAGGCTGGAGTGCAGTGGCATGATCTTGGCT
CACTGCAGCCTCCGCCTCCCAGGTTCAAGCGATTCTCCTGCCTCAGCCTCCCGAGTAGCTAGGATTACAGGTGCGTGCCACCACGC
CCAGCTAATTTTTATATGTTTAGTGGAAATGGAGTTTCACCATGTTGGTCAGGCTGGTCTCAAACTCCTGACCTCATGATCCGCCTT
CCTCGGCCTCCCAAAGTGCTGGGATTACAGGTGTTAGCCACTGCGCCCGGCCCTAGAGCTCACTGTTTTCTAGTTAGTCCATCTGG
AAGTGGAGCCTTTTTCCAGTTTGCACAAATGTGCCATATTGGCTTGTAGCTGGCATGCATCCAAGTCCATAGGTCCTGCCTCTTCA
ATCCTGGCTTTCTAGGGCCTGGGATGATCATTGCTAGAACTGAGAGACCAGCCTGGCTCAGTGAACTTCAGGGCGTTCCGTTCATT
CTTTCAGTAAATGTTTGCAGCACATGTGTTACATGTCAGGCAGTGAAACCCCCCACAGCAGCCTTCCCTCTCAGAGGATACATTTG
TAACCATTACACAGTCATCAAAGGAATAATTTTTTTTAATCACCAGTGTGCATACAGTCATGGAGTTGGGTATTCCCAGCTACCAG
GGAGGCTGAGGTGGGAGGATTGCTTGATGCCAGGAGTTAGGGAATATAGTGCACCGTGATTGGACTTGCGAATAGCCACTGCACT
GCGGCCTGGACGACGTAGTGATACCCTGACTCTTATAAATAAATAAATGAATAAACACAATTATGACTTTGCGGATGG

FUT3 3’UTR sequence:

GAGGCCGGCATGGTGCCTGGGCTGCCGGGAACCTCATCTGCCTGGGGCCTCACCTGCTGGAGTCCTTTGTGGCCAACCCTCTCTCT
TACCTGGGACCTCACACGCTGGGCTTCACGGCTGCCAGGAGCCTCTCCCCTCCAGAAGACTTGCCTGCTAGGGACCTCGCCTGCTG
GGGACCTCGCCTGTTGGGGACCTCACCTGCTGGGGACCTCACCTGCTGGGGACCTTGGCTGCTGGAGGCTGCACCTACTGAGGAT
GTCGGCGGTCGGGGACTTTACCTGCTGGGACCTGCTCCCAGAGACCTTGCCACACTGAATCTCACCTGCTGGGGACCTCACCCTGG
AGGGCCCTGGGCCCTGGGGAACTGGCTTACTTGGGGCCCCACCCGGGAGTGATGGTTCTGGCTGATTTGTTTGTGATGTTGTTAGC
CGCCTGTGAGGGGTGCAGAGAGATCATCACGGCACGGTTTCCAGATGTAATACTGCAAGGAAAAATGATGACGTGTCTCCTCACT
CTAGAGGGGTTGGTCCCATGGGTTAAGAGCTCACCCCAGGTTCTCACCTCAGGGGTTAAGAGCTCAGAGTTCAGACAGGTCCAAG
TTCAAGCCCAGGACCACCACTTATAGGGTACAGGTGGGATCGACTGTAAATGAGGACTTCTGGAACATTCCAAATATTCTGGGGT
TGAGGGAAATTGCTGCTGTCTACAAAATGCCAAGGGTGGACAGGCGCTGTGGCTCACGCCTGTAATCCCAGCACTTTGGGAGGCT
GAGGTAGGAGGATTGATTGAGGCCAAGAGTTAAAGACCAGCCTGGTCAATATAGCAAGACCACGTCTCTAAATAAAAAATAATA
GGCCGGCCAG

FUT4 3’UTR sequence:

CCAAGAGCATACGGAACTTGGCCAGCTGGTTCGAGCGGTGAAGCCGCGCTCCCCTGGAAGCGACCCAGGGGAGGCCAAGTTGTC
AGCTTTTTGATCCTCTACTGTGCATCTCCTTGACTGCCGCATCATGGGAGTAAGTTCTTCAAACACCCATTTTTGCTCTATGGGAAA
AAAACGATTTACCAATTAATATTACTCAGCACAGAGATGGGGGCCCGGTTTCCATATTTTTTGCACAGCTAGCAATTGGGCTCCCT
TTGCTGCTGATGGGCATCATTGTTTAGGGGTGAAGGAGGGGGTTCTTCCTCACCTTGTAACCAGTGCAGAAATGAAATAGCTTAGC
GGCAAGAAGCCGTTGAGGCGGTTTCCTGAATTTCCCCATCTGCCACAGGCCATATTTGTGGCCCGTGCAGCTTCCAAATCTCATAC
ACAACTGTTCCCGATTCACGTTTTTCTGGACCAAGGTGAAGCAAATTTGTGGTTGTAGAAGGAGCCTTGTTGGTGGAGAGTGGAA
GGACTGTGGCTGCAGGTGGGACTTTGTTGTTTGGATTCCTCACAGCCTTGGCTCCTGAGAAAGGTGAGGAGGGCAGTCCAAGAGG
GGCCGCTGACTTCTTTCACAAGTACTATCTGTTCCCCTGTCCTGTGAATGGAAGCAAAGTGCTGGATTGTCCTTGGAGGAAACTTA
AGATGAATACATGCGTGTACCTCACTTTACATAAGAAATGTATTCCTGAAAAGCTGCATTTAAATCAAGTCCCAAATTCATTGACT
TAGGGGAGTTCAGTATTTAATGAAACCCTATGGAGAATTTATCCCTTTACAATGTGAATAGTCATCTCCTAATTTGTTTCTTCTGTC
TTTATGTTTTTCTATAACCTGGATTTTTTAAATCATATTAAAATTACAGATGTGAAAATAAAGCAGAAGCAACCTTTTTCCCTCTTC
CCAGAAAACCAGTCTGTGTTTACAGACAGAAGAGAAGGAAGCCATAGTGTCACTTCCACACAATTATTTATTTCATGTCTTTACTG
GACCTGAAATTTAAACTGCAATGCCAGTCCTGCAGGAGTGCTGGCATTACCCTCTGCAGAACAGTGAAAGGTATTGCACTACATT
ATGGAATCATGCAAAAGGAAAAAAAGTTTCATGATATCTGTTGTTGGCAGTTTTTGTTTATCTCTGACAGTTTTTAGTTAAATGTTT
AGATCCTCAGAACTACATTAGTGCCTACTATTAACTTACTCTGTCTCTTGTTAAAGGCTAAATCTGCGCTTCTCCCTGGTGCCAGCA
GGTTCCCCTCACAGTCAATGCAGTGGTATAGCATATCCTCACATTTCTAGTGCCCTTGAGACTGTGCTATGGAACCAATCTTGAAC
ATACATGCATTGACTTGACAAGTTACTGAGTAAGCAGCATATTCAGCAGGTGCCACTACATGCCTACTCTGCCAGACACTGAGCTT
GGGGCCCTAGGGAAGATAGAGAATTATACAAGGCAAAGTCCTTCTCTTTAGGGCTCTTACAATCTATCACTTCCAAAAAGTAAAT
GGTGACTGATAAAACAATTGGCAGAACCTGTTTGATTACTGTGACAGTCTTAATGATACCATAAATCAATATTAGAAAGCTAGTT
GACTTAAAGCCTGAAATAATGGGAGTTTTCTCCTCCACTTATTAGAATAAGGACCCTCAGTGACTAATTATTGTGGGTAGGGTCAA
GATTAACTAGTTTTATACAGAGTTCTGCTGTAAATAGTCATTTTGCATTTGATTAGTGCAGTTCTCTGAATCATAAAGCAAGTTTTA
CCTCTCTGTACATGTTTTTGCAGACATACTTGAAAAGCTCACTTAAATCTAGGTGCTTCAATTCACTTTCTTGAGAGGACAAATGA
AAAGCTGTGGAGAAAATGTCCTCATTAAAGTATTAAAGTGTGGGCAGAATTACAATTACAAAGTGCCAGCCACCGAATAAAGAT
AAAAGTTCAGTTCTTAAAATGAGTTTTTATGAGATAACAGTCAGTGATCTTGGTGTTACCGGGATTCCACATGGGGCAGTGGGAA
AGAGTTCAGGTTTTGAAGGTAACCTAGTTTAGATTTGAATTCCAGCTATGTGACATTGGGTAAATTAGTAGTAGTCCTGAGCCTCA
GCGTCCTCATCTATAAAATGACTGGCGAAAATACTTCACAAGCTCATTTTGAGCACTTTAGGAAGTAAGTGAAAGTACCTAAAAT
AGCAGGCACCCAATTGATGATTTTATATCTTCCTTCTTTGCTTGCAGTGATTTCAGGATGTCCTCATATCTATTTATAGGTCTAAAA
TTATATCTTAAGGTATGTTGTAGAATAAATTAAAAGGATAATCTAAATCACCATTTAGATTAAGCTTGACTTGCAAACTAGGAAGA
AGCACCTAGGCTTTCTTTGAAAATATTTTTTTGGTTCGTTTTGGTAAAGCTCTATAAATTGGTATCTATTATTTTACCAATTTTTTTT
TAGTATTAAGTCCATTTAGAACTAACCATATTATTTATGGAATAATTAGCATGAGGAAGGTATAATTGCATTTTTTTTTTTTTGAGA
CGGAGTCTTGCACTGTAGCCCCAGCTGGACTGCAGTGGCGTGATCTTGGCTCACTGCAACCTCCGCCTCCCAGGTTCAAGCGATTC
TCCTGCCTCAGCCTCCCGAGCAGCTGAGACTACAGGCGCCTGCCACCACGCCTGGCCAATTTTTTGTATTTTTAGTAGAGACTGCG
TTTCACCATGTTGGGCAGGCTGGTCTTGAACTCCTGACCTTGTGATCCACCTGCCTCGGCCTCTCAGAGAGCTGGGATTACAGGTG
TGAGCCGCCGTGCCCAGCCATTGCATTTTTATTCACATACACATTGTTAATGTGGAACAATTTAACACTAATCTCATCAGAGAGCG
AGATGAATGTGGCAATTGCTCATTTTATTTTGCATATATTAAATTGAGTAGGTTCAGCTCTAACATACCTTAAGAAAAATGCATAT
CGGTGCACTGTATGTATTTCAAAATGCCTTTCCTATGATTGTCATGTCCTCCTTTAAGGCTTTTCCCTCAAATTTATTACAAATTTAG
TATTTTTAGTACTTGATGACTCTAATTACATGAATGCACCTGGAATGACATTTGTAACAGAAGACGGTCTGACTTGCTTTCAGTATT
CACAAGTTCTTTCCAGTTTCCAAGTCTTTTCCTAGCAGTAATTTAGGGGAGACAGAGGAGTTTCATGTAAAGAGCATGCAGTTTGG
AGTCAGAACCTGGGTATGACTCTGTGGCCTTGATGAAGCAAGTTACTTAAACTCTTGAGTTTTAGCTTTCTCCTTTACAATGCATG
AATGCCTATCCCCCTACAAAACAAAGATTAAATGTGATGATGTATGCCAAGGTGCTTTGTATATTGTAAAGTGCTATATAATTATA
AGATGTTCTAAATTTTCAAGGATCTAAACCAGGGATTGGCAAACGTTTTTCCAGGGAGTAAATATTTTACGCTTTGCATATATAAT
TTATGGAGGTGTTGAGAGGATAGATTAGACACTTGAAGTACTCAGGATAGTGCCTGGCATGTAGGAAGCACCTGGAAAATATTCG
CTGTGATTACCATCAGTCCATTTACCGAGGAAGGAGCCAAGGTCCAGGCCCACTGAAGGACTTGCATAACATTACAATAGCAGT
GGCAGAACCAGCCATGCTTCTGCAAATCACAACCTCTTTGAGCCTCTGTCACCTGAACTGCAAAATGAGTGGGTTAGACAAAATC
ATCTGTTGGGACCTCCTAGTTCCACGTGCTATCATTCTACTAACTGGCACCCTAAGGTTGAAAGTGCTTATCTGCTTTCCAATGTGG

CTTCCTTACAGTCTGGAACTGACAATATGCAGGAGCAGTAAACTGGCAGAAAACCAGGAATCAGAGAAAGAAAATATAATTTAA
CTTTAAAGATGTAAATTATATATATAGTATATTATATATATTTTTAAAGCTTTATATGCCTCAAATATCAGGGAAAGGAGCCAAGT
CCTTGGTATTTAGTTTGGTGAATACTTGCATTGAATACATGTCAAGATGTCAAGTCATTTTTGAATGTGTCTCAGGGATTTCTATGC
TACACATTCTTTTAACAAATCAAGTATTTATGTACACATGTTCAGATTTTTTGACAAAATGATTAAAATAATGAGATGGAAAATGA

FUT5 3'UTR sequence:

GCAGGAATCTAGGTACCAGACGGTGCGCAGCATAGCGGCTTGGTTCACCTGAGAGGCCGGCATGGGGCCTGGGCTGCCGGGACC
TCACTTTCCCAGGGCCTCACCTACCTAGGGTCTCACTAGTCGGGGGATTTACCTACCTGGGGCCTCGGCTGCCTGGGGCCTCGGCT
GCCTGGGGTCTCACCTGCCTGGGGCCTCACCTGCTGGAGTCTTTGGTGGCCAGGCATGTGACTTACCTGGGATTTCACTTGCCGGG
CTTCACTGCCAGGAGCCTCCCCTGCTGGGGACCTTGCCAGCTGGGGCTGGGGATGGTGCCTACTGGGGACCTTGCTTTCTGGAGGC
TGCACCTACTGAGGATCTCGGCTGTTGGGGACTTTACCTGCTGGGACCTGCTCCCAGAGACCTTGCCACACTGAATGTCACCTGCT
AGGAGCCTCACCCGCTGGGAGGCACAGGGCCCAAGGGAGCTGGATGTGTTGCCCAAGGTGTGCAGGGCAGGTCAGGGAAGGGCA
GGGTCCCCTAAGGAGGAGGGCGAAGGGTATGTGTGTGACCATCAGCAGTGGTGTGCACATGGCTGGGGGACACTCGGTTTGACC
GCCAGCGGATGGGTGTCACAAATGCATCACTATGGGTGTGACCTCGGCGTGACTCTGATAGTGCCTGTGGATGTGTTGCGATGCCT
CACCCTGGAGGGCACTGGGCCCTGAGAACGGGTGCCCTTGAGGCCCTGCCCCCGGGCGATGGTGCAGGCTGGTTTGCTTGTGGTT
TTATTGCTGTTGTTAACCACCCATGAGGGGTGCAAACAGATAATGCTGTTAACATTTTCA

FUT7 3'UTR sequence:

GATCCGCTGGCCGGGGGAGGTGGGTGTGGGTGGAAGGGCTGGGTGTCGAAATCAAACCACCAGGCATCCGGCCCTTACCGGCAA
GCAGCGGGCTAACGGGAGGCTGGGCACAGAGGTCAGGAAGCAGGGGTGGGGGGTGCAGGTGGGCACTGGAGCATGCAGAGGAG
GTGAGAGTGGGAGGGAGGTAACGGGTGCCTGCTGCGGCAGACGGGAGGGGAAAGGCTGCCGAGGACCCTCCCCACCCTGAACA
AATCTTGGGTGGGTGAAGGCCTGGCTGGAAGAGGGTGAAAGGCAGGGCCCTTGGGGCTGGGGGGCACCCCAGCCTGAAGTTTGT
GGGGGCCAAACCTGGGACCCCGAGCTTCCTCGGTAGCAGAGGCCCTGTGGTCCCCGAGACACAGGCACGGGTCCCTGCCACGTCC
ATAGTTCTGAGGTCCCTGTGTGTAGGCTGGGGCGGGGCCCAGGAGACCACGGGGAGCAAACCAGCTTGTTCTGGGCTCAGGGAG
GGAGGGCGGTGGACAATAAACATCTGAGCAGTG

FUT8 3'UTR sequence:

AGCTCAGATGGAAGAGATAAACGACCAAACTCAGTTCGACCAAACTCAGTTCAAACCATTTCAGCCAAACTGTAGATGAAGAGG
GCTCTGATCTAACAAAATAAGGTTATATGAGTAGATACTCTCAGCACCAAGAGCAGCTGGGAACTGACATAGGCTTCAATTGGTG
GAATTCCTCTTTAACAAGGGCTGCAATGCCCTCATACCCATGCACAGTACAATAATGTACTCACATATAACATGCAAACAGGTTGT
TTTCTACTTTGCCCCTTTCAGTATGTCCCCATAAGACAAACACTGCCATATTGTGTAATTTAAGTGACACAGACATTTTGTGTGAGA
CTTAAAACATGGTGCCTATATCTGAGAGACCTGTGTGAACTATTGAGAAGATCGGAACAGCTCCTTACTCTGAGGAAGTTGATTCT
TATTTGATGGTGGTATTGTGACCACTGAATTCACTCCAGTCAACAGATTCAGAATGAGAATGGACGTTTGGTTTTTTTTTGTTTTTG
TTTTTGTTTTTTCCTTTATAAGGTTGTCTGTTTTTTTTTTTTTTAAATAATTGCATCAGTTCATTGACCTCATCATTAATAAGTGAAGA
ATACATCAGAAAATAAAATATTCACTCTCCATTAGAAAATTTTGTAAAACAATGCCATGAACAAATTCTTTAGTACTCAATGTTTC
TGGACATTCTCTTTGATAACAAAAAATAAATTTTAAAAAGGAATTTTGTAAAGTTTCTAGAATTTTATATCATTGGATGATATGTT
GATCAGCCTTATGTGGAAGAACTGTGATAAAAAGAGGAGCTTTTTAGTTTTTCAGCTTATTTACTTTGTTTTTTTTCCTGTTTCTGAT
ATAGTAACTAATTCTTAACTCAGAGACATTGGTCCATTTTAATACTGAAAACCAATTTTCATTGGTACACATTACAAAATTGCTAA
GAACACTGTTTGGGAGCTTTCATTCTCATATTTTGGACATTGTTTTAATTGAGTGAAATAATCATAACTCCTTGCTCCCAGAGAAGC
TATCACCTCCATTTCTAAAACCATTTCAGGTTTGTTTGGTAGTCTTTCTTAATGTATTTATTATCGCTTTTTGTGAGTAGGGTCCTGT
TTTATCCAGGAACCAATTTCTGCCCTAGCCTATCATGCCCTGCTTTTGAGAGTACCAGGTATCTTTGGGATTGGGAAGCTGGCTGTT
TCAGAAGTATATGTCTCATAGTGTGCAGAACTTGGTGACCAAGTGAGAAGCGGGACCAATGGGAGACTCACAATGGACTGAGTCT
TGGGATTATCTTTTCCAAATTCTTCCATGTTAGAATCACTTCAGAAAATAAGACTTTGATGCTTTGTCTCTGAGCATCATTTTTCTC
CTCATAAAAACACTTCCTTATTGTATGTAGCCTGCCTCCTACAGAGGCCTGGTAGGTGTTACTGCATTCTAAAAGAAAAATGTCAT
CTCTGTAGGAGCGACTATCAGGCCTAGTGTGAAATATTAGGGATCCTAGGCAGAAGAGCTATTAGTCCTGGCCTTCATATCTTCAC
CAAATGAAAATACTGTATATAAAATTTCACCACCAAACTTAACTAAATTCTTTTTCTCAAGTCAAGCCTCCCAAAGAAAAAAGAA
ATTAACTTCCTACAGTGTCAGCAAGCAATTTTCCATTTAGTTTTGGTACAAATAAAAGTCATTTGAAACAA

FUT10 3'UTR sequence:

CTGGTTGATAGGAATCAAAACTTTTCATCTCAAGAGTTTTGGGGCCTAGTATTCAAGGACTGATTTCAAAAATGATCAGAATGAA
ACAGACTAGAGCCTTCTTGAGGTTTATTTTCTAGGTTGCCTTAATATTTGAACATAATAGCTATTCTGTTGACTATCCATCAGGATA
ATAATTAGTTGCTGCAGTACTCATAATGAGCCCTTTCAAGGAATAGATGTAAATTACCCTTAGGGGTAGCCACTATATTTTTTATA
CTAAAAAAGGAAATATTTCTTATGGACACTGGTTATCTTCCATGTCCGTGTCTGTGGACCCACATACTTACTGCCTTTTGTGGAAAT
TCACCTAGAGTGAGTACTTTCCTTGTGCAATGGAGGGAGACGATCTAGCTATAGATTCTTGATACTCACCTCACTCTCAACAGCTT
ATTGGTATTTGGCAAACCTGGTATCCTGCAGCCGAGCATGAACATGAAATACATTAGAACTTGGCAATGAGAGATCCCATCTGTT

GGTTTCCAGGGATGTAAGTGAGTAATAAAAGCTGTTTCAAGTTTATCCACTATCCACTCTTCAAGTGAAAAGAACTTATGTGTGTC
TACCTTCTTCTCCATACCCTGAGCCACCTCTCTCACTTTCTTTAGTTGTGCCTTGCCCTATCGCCTCCCATTTTCCCTTCAAAGTAGA
ATGTCTTGTAAAGACACAGTAACTCCTGTGTGTTTTGATTAGTGAGATGTTACCACTTACCCCTTCTGCTGCGCAGAATAATATTA
AGAATTGCTATGCTTATGATTCAGGCTGGACAGCCTGGACATTTTGAGCAGCGCGAGAGTAGAAGTGAATACCCCCAGGAACTCC
AATTGTGCTGAAGCTGATTTGTCTGTTCGTAGGATGATGTGCAGCCTGTCACAGTGGCAGCCACAGGCATTCAGTTTGTGGGCATT
TCCTGTCATTTCGGATCCTGCTATAGGGAAGGTTCAGCTCTCCTGTCTGGGGCATCTACTGGAGCACCTCAGAAGACAAGGAGGA
AAACACTGGCTCATGTTTTCTTTCCATGTGAGGGAGGGGAGGTTTCTAGATGATACTAAAAGCCTGTTGCCACTGTTGTGTCATGA
TTTCCATTCTTCATCATGGAAAGCCACAAGCCTCAGAAGGCAGCCAGAGGACAGGAAGAGTCTGTGATGCTCATGTCTGTGTCAT
GGCATGAGGGGGAATTGACGAGTGCTTGCTTAGCATCAGCTCTCATTGTATTGAAGGCTGTGCCCTTGGTGTGCTTAGCAGTGAGC
AGCGTCTTCATTAGGTAGCTCTGGCTGGGCTTTGTCAGCCAGCGTGTGAGAAAGGAGAACCAAAACCAATACCTCCTTATAGAAG
CCAGAAGGATCACATTGGATGAGAGAAGGTGTCTATAACTGGGTTCTTCCCAATCCCAGCTCTTTCATTAACTAAATATGATCTTG
GACATATCTCTTAACCTCCATCGGCCTTAGTTTTTGCATCCAAAAAGAAGTGATTGGGCTGGTCTTGGAAGGTTTTTTTCTTTTTTT
TCCCCTGTGTAACATTCTTCATTGTTCATCAACATTTAAGAAATTTAATTTTGTAGATGTTTTTACTAAAGAGGGTAACAAACTATT
TTGGAACTGCTGTATGTTATTCAAGGGAAGCACGCTGTTTGGAGGAAGGAGCATACTTAATGGGTAGTATTGAGGATGAAAGGGA
ATTTCTCTCTCTGCCATTTTATTTGATAATATTAAAGAAATAAAGACTGGAAAGGGGGATTCCTTGTTAAAGGTCAGATTTTAAAT
TGCATATAAAA

GALNT1 3’UTR sequence:

AGCATTAGAGACTGCAATGGAAGTCGGTCCCAGCAGTGGCTTCTTCGAAACGTCACCCTGCCAGAAATATTCTGAGACCAAATTT
ACAAAAAAACGAAAAAAATAAGGATTGACTGGGCTACCTCAGCATACATTTCTGCCACATTCTTAAGTAGCAAAAAAGGAAAAG
TGCTTTCCTCCTCTGCAGGATGTAAGGTTTATCAGCCATTAAAACTTAGACTTCTCTAGCTTTTCACTAGCTGTGAACCAGCCTTCC
TGTCCATGGACGTGAAACTGCATAGTAATGAGACTGTGCACACTGATGTTTACAAGATTGAAAGAGTCTTTCTCCGAAAATCATG
GTAAAGAATACTGAGACAATGAAAAAAAATCAACAAAATATGCTTTCTGGAGAACTGTACCTTTTATGGTTTGCTTGCACATCAG
TAGTTTCTGCTGAACGTGCTGTCATAATGAAGAGATTTCCAAGATTTTTTTTCCTGATTAGAACTGGTAGCCAGTATATTAAATATT
GATATAAAAATAAAAGAACTGGAACCAGATTCAGAATCATGAAAACAACATTTTTACAACAACAAAAAAACTATATTAAACAGG
GTTTAAAGGAAATTAAAACAGAACTATGAGAAGTACAATTTGTTATAGTATAGTATCAAATTTCTATATAGATTTTATACCTCAGT
GGGGAAAAATAACTGATTCCAATGACATTCATTTTGTTTTCATCTGTGATAGTCATGGATGCTTTTATTTTCCTTGGGGTGCTGAAA
TTGAGCTGAAAAAAAAAAGGCTCTTTGAATATAGTTTTAATTTCTCTCTACAGTTTTTTTTGTTTGGTTTGTGGGCTGTTGGAATTGT
AATTTTTAATTGCCTTCTAAAAAATGGAAATTTAACAATGTCTGATCTCAGCTGAACAAATTAGATGTTTCAGTTGCTCTTGGGTC
AACTGGCTTACAGATTTACATGTGCACACACACACAAATTTCTTATCACATTTTCGACTTCTTCACTTGACCTAACTGATTATGCGA
AATACCCAAGATTCATGCTACTGTACCACAGATTTGTTTTCACAGCAATAAATCTTCAGTTCTTTGTTTATGATTCCACTTAACAAA
AGGCCTGCAGAAGTGATTTATTATTTGGGTATTTGGAGATAATACATTTGATGGTTTTTTGGAAAACCTTTTTCACTCCATACTCAG
ATATGCTTCATTGTCAAATGCATATTTAGATTAGATTATTGAATTGTAATGTTTATCTGCTGCTTTTTTTAAATAAAATTTGACTGA
AAATGTTTAATTGGCATTTTTTAATGACTTAGCCAAAGAAGTGCAGCTATTATTCCATATTAATAGGCTTGCATTTCTTTTCCTAAA
TCTTATTTAGGCTAAATCAGTTTTATTTTTCTCTGATTTTTTTTAATACCACAGAATCACCTGAGTGTCAATTGAAAGTTGTCAATTA
AAAGGTAACCTTTTAATCTCGTAGGAGGAATCTCATTAAGACATTTTTCCTGATATGTAGAGCAGTCTGTTGGCAAAAATGCATAT
ATTTTCTTTCATATTTGTAAAATTATATTTAATGGAATTCTTTTCTTTGATTATCAAGGACTTTCACTGCAGGCAGTGCTATTTCTTG
TGCCTAAGAATGTTTCCAAAAGTCGCATCGCTAATGATATTTGCCAAGTTGAGTGTACACAAAGTTTCTCATATCCTGTTCAAGTT
AATCAACATCAAGCACATGGGGATGCTTTAGGGTGAGTCTATAGTACAAAATGCATAAACCATGTCCCCAGGAAATTTGAAAGGA
AGCAGGTGCTGAATGGAATTTTTTTCCTTTTCCATGAGCTGTGTTAATTCTATCTCCAGTAGGCCTAATGCTTGAATAAGCAAGAT
GTCTAATCAATAAATTATTTTCATGCTCAGAATTTCAGGTTTTTGTACTCCAGCATAGCTTGGTCTTATTTCTTACTGTATGAAAGC
TTAACAGCAATGTGATTTAAGGTTTTGTTTTAAATGGGAGATGTAAGTGATTTAATTCATGGGTACTTTTAGAACCTGATAGATAA
TCCCATTGCCTTTATTTTTCTAATTAAAGAATTCCTAAATACTTTGAAAATACAAAATATTCCTGAATA

GALNT3 3’UTR sequence:

AGTGTTCCTTAAAATTAAGTTGAAAAAGGAAATATTCTTTCTCATAAAACTGTGACTAGGCATACACTGTAGTTTTTGAAAATTAT
GCAAAAGCAGCTAAATGTAACTTATTCCAAGTGCATTTTTCTTATTTATATCTTTATGTAGCACTACTACAGAAATTCTGCAAGTTT
CTGTTTCAAAGCACAATAACTAGTAATACCAAAGACTATTTCAAAATGTCCAGATGTAGGGGAAGAGATGTTTACAGTATGATGA
AAATAATTTTCCAAGTAAAGTGATGTTTGTGTGTTTTGTACACTTAGGGATATATATATATATAGCTACATTCACACACTCACAATTTA
AAATATTTCCCCTAGTTTTTTGGGGGGATAGGAAGAAAGATTTGTTACTGTATTTTTTTAACTACATAAAAATAGATCAATAAATG
TCAGCATTGGCCTCTGTGTACAAACCAAGAGCTTTTACAGATCCAGAATTTATTAGTTTAAAATGCAGGTGAACTTTTTTTTGCGTT
TGGTTTACTTGTCTGTCAAATGTTTCCTTAAACATGAAACTGAATAAGGAGAAGAGTATTTTTAACACTTAAATTTCTTGGCAAAT
TTTAAAACATTTTTTAGTCTGTAATACACTCCACTTGAAGCACTTAAGTCTTCCTTAAATGACTTTTCTTAAGTAATGATACTGTGT
GTTTTCCCAAAGCACTTTTAAAAAAATTTTTATAAATTACTATCTGTTGAAAAGGTGTCCTTTTCCTTTCTTCTAGTATTTTTTTCTT
ACCAAAATTCACTAATCTTGAATGTTTGTGATATTAAATTTCAAATGCAGAATACTTGACTCATTTAAAGCTAAATTTTGTTACTGA
TTCAATTATAATTGTAATGGATTTTTGACTTTGTAATGGATTCTTTTCATCAAAAAGCCTTATTTTTTTATCTATGTGGAAAACACA
ATAAAAAATCCTCAACACTATTGTAATCATTTGGTTAAGTTTTTTTCCTCTTTTGGGTAAAATCTGTAATTGATAATAGGTGGGGGA
AAATGAATTTTGTATGCTGAATTTCTAAGCGCCTATTGTTTGTAAAACCATCAGATATTTCTTATGGCACAAAAAAATGAGGAATAG
CAAAATTCCTGTGTTCAATATTTAGAAAATTTTGTATTAATTTCTGATAAAGTTCCTTAAGCATC

GALNT7 3’UTR sequence:

AGAGAAAAAAATAAACCAATAACCTACCTACTGACAAGTAAATTTATACAGGACTGAAAACCGCCTGAAACCTGCTGCAACTATT
GTTATTAACTCTGTATAGCTCCAAACCTGGAACCTCCTGATCAGTTTGAAGGACATTGATAAACTGTGATTTTACAATAACATTAT
CATCTGCAGTTACTGTTTACAAGACTGCTTTTACCTTAAACTTTGTAGATGTTTACATCTTTTTGTTGTGTTTTAAGATGATGTTGGT
AATTTGTGCCTTTAGCTCTGTTTTATTAGACAGAGTTAAAGCATGTTGTCTTCTTTGGGATTACACTCAGGGGTCTGAAAGGCAGTT
TGATTTTTATTTTTAACACACTTGAAAAAAGGTTGGAGTAGCCAGACTTTCATATATAACTTGGTGATTATCAACCTGTTGTGTCTT
TATTTAATTTTACATCTTTTTGAAGCACTGCCACAGGTTATTAGCCAAGGTGGCCTTCCTTCACAGTCATGCTGCTTTTTTGAAAGG
TGAATTTCAACACATTTAGTGCCTCTTTCATTTCTCAGTATATATTTCAAGAGCTTGTGATGAAATCTATAGGATGGTAATGATGGA
CTTGTCACCTGTATGGGGAATACTTTTACTACTCAGAAATGAATTTATGTGCTGCCATTTGCTATAAAGTTGAACTTTGTATGGCTT
GAAAAAGAAATGACAATATGGAACATCCCAAGGCTGTCCCATAGGGTTGGAAGTTGTGTAGCATTCACTCCCTTACCTACTGGCA
TTCCCAGTGCCCTCTGTCCATACCTACTTCTAGGATTGCAAAGGAGTCTTCCAACTAGAGAAAAATTGTCCACTGACATTTGGGAT
TTACTTTTCTCCAATACCTGCCAATACAGAAAACTATTATCAGTTGTTATTGTTATCCCTTGAAAGCGAGGGTGACAAAAACAACA
AAACACCGTTATAAACACATCAAAGGTTCATTCTGACTGAGGTAAGACTTTCCAAGCCCTTGTTAGATTAGGCCTTATAAAACTTG
TGTGCATTATAACCTAAGCTGTGCAACCTGTGAAGCCAAGAGTGAACTGATGTTTCATTTATATTTTCATCCAAATGACATTATCT
GCACGTTTTTAAAATTTAAAAACAAAGGACTATTTAAAAATACAGTTTATTAACAAACGTGAACTACTTTCTGTTACATTAGGTGT
TCCCTAGTGTTTCTTAATTTCTTTTTAGAAAGTGTATTTTTATTAGTATTTTTCCGGTGAACAGAAGATTTGTTTGGATTTAAACATT
TACTAAGACAGTACCTATTAGGAAAACCAAATATTGCAAATGGTCAATTCGATTTTAATTTCTCAAAAGATACTCTGTTATCCAGA
AGATTAAAATGCCTACATTGAGTGCTTAAAAAAAAAAAAAACAACTGTGATGATGTGAGCAGAATGGCAAGTAAGTTAAGCATTTT
TGATCCTGTAATCATGGTATCATTACAATGAAAGGAATTCACAAACTACTGCCAGAGGAAGTTTGTTTTTTAATTTAAGAGGGAAA
TATAACCTATAAATTTGTTTCTTCCAAGCTTAGCTCTTAAATTTGGAGACTCAAAGTTAAACATCCTCAACAGAGTTTTATTTATAA
TTTTGAATTGTCAATTTGTATTTTGCTACTGATCTGTGATCAACCATTTTAACTTTCATCTCTAGGGATGTTTAACATTTATAATTGC
AAAATAAACCAACTATAAAAAAAGAAACTAAGAGAGAATTGGTACTTTAATTACTTGTGTGTTTGCAAATAGGCTCCATTTTCCA
TGTTGAGTAGATTATAACCTTATTAACTATGCATAGGCCTAAGAAAGGTGGCAATGAACTGTGCATGTAAATTTTAAATGGGTACT
TTGTGCAATTCGTTAAAAGAAGATACTCTATGAATATGATTCTATATATTGAAATCAGAAAACCTACCAAACAAAAACATCAGAA
GCTGCTGCCATAATGACTATTTTCTACTGTAGGCTGCTTTGGAAATAATTCCCATATCCTTGCTTTGTAAGTTGGTAATATCACTAT
GCATTTCTACACATTTTATAAATTTGATTTATGCAGATTTTGATACACTGTATGTTTCTGTAGAAATTGTATAAATATTCAAAATTT
TATTAGGATAAATTTGAGAAACTTACGTATATCTTAATTCTGGGTTGCTTGTTTTTTAGGTGACAAAAATAAAATATTGTATTTTAA
TTCA

MGAT1 3’UTR sequence:

GCTATGATCCTAGCTGGAATTAGCACCTGCCTGTCCTTCCTGGGCCCCTCCTTGCCACATCATGAGCTGAGGTGGGACCACAGTCC
CCAGGCTGCATCGGCCTGCCTGTGTTTCCCTCTTAGGTGCATTTATCTTTTTGATTTTTCCGAGTGGCATTTAAGTGCACAAATGAT
AACAAGAGGATTATTCTCCCGTTCTCAAGGGAGTCAGATCAGGGGAACTATTCTAGGGTATGTTGCGGGGTATTAAGCAGGAAAC
CACTGTGTGGTGGGGGGCACTGGGCTTGTTGGGGCCAGAAATGTCCACGTCCTGAGCTTTCTCCTGGAGCATGTGCAGAGAGTTT
GGCAACGTTCGCTCTCTTGACCAGACCCCTTCTCCCTGACCTGGCTCTTCCAGCCAGGGCACGAGCCCTCCTTCTATACCTGCTCCC
CTTCCCCCAGTGGGGACTGAGTTATGGGAGAAGGGGACATATTTGTGGCCAAAATGATACTAACCAAAGGGGCTTCCTTGTCAGG
GCCTGGTGGAGTTGGTGGGTCATCGGGGCTCACTGCCTCCTGCCCTTCTCTCCTGTCTGACCCCCACTTAGCCCTTCTCTCCTTGCA
GCCTAGCAGTTTATAGTTCTGAGATGGAAAGTTGAAGGGGGCAAGCAAGACCTCTCCTCAGCCCATGCCCAGCTGTCAGGAGAGA
GGTGCAGGGAGGAAGGCCTTGTGCTGGGACAACCTCTCTCTTGCCTTACCTCAGAGAGGGACTATGCCCTGACCCCTCCTTTCTGA
AAATCAGTGCCCTCCCTGTTGCTCTAGGAGGCTCCTGCTGGCTTGGTAGAAGACAGAATTCGATCTGCCTGTCCCTTTTTCCCCTGG
GGTTTGACACACAGGCTCCTCTCAGCATGAGGTGGAGCAGTGACCAGGTGGAGCAGTGACCAGGACGCCTCTGGCCCAGTGCTGC
CCAGCCTCCCCGCCCGCTCCCAGGCGCCCCATGTCCTCACAGGCCAGGACGCCATGGCAGGATGGAGAGGACTTGGTGGATTTTT
GTTTCTTGCCTGACCTCAGTTTCATGAAAGAAAGTGGAAGCTACAGAATTATTTTCTAAAATAAAGGCTGAATTGTCTGAAAAATA
TTTATGTGTGTGTGTCCTGGAAAAGGAGGTGGCAGGCAGGGAAAGAAAGGAAAAGGGAGAATGAAGAGTTAAGGAGAGGGCTA
GACGGGTGGGAGGAAGCAAAGTTGAGGAAAGAAAGCAGATGAGTGGGAGGGAAGAGCCAGGGACAGCCCAGGGGATGGGGGC
CAGGTGGGAAAGGAAGTCCAGGCCACAAGGTGGAGAGGAGCCCCGGACTGTGCTCCTGCTGATCGTCCTGTAGAGCCAGGAGGC
CGCAGCAGGAAAGCTGGTGAGTGTCTCCTGCTTCTGCCTCCTGCTGGCTGGGCAGGCCTGGTCTGGGGAAGAACCAGGTCCTCTG
ATCAGGGTGGTCCCTGAGTGGTGCTTTGTGCCCGGTGCCCTCTGCTGGCCCAGGCAGTGCTTATTGAGTGCCCTTTATGACGTGCC
GGGGAGCCTCAGGGTACACAGCTGATACCAGGGTTGGCCTCACAGTGGCGCTTGGACTCCCAAACGCAACCCCAGTGAGAGTGC
CTGTTTTGCTAATACCCAGAACACAGACAGACTGTTACCTCTGCATATCACGTGCAACATTCTGAGAGTTTCTGTTCTCCACTAATT
CATTTAAAAGAACAAAACGCGGCCGGGCGCAGTGGCTTACACATGTAATCCCAGCACTTTGGGAGGCTGAGGCGGACGGATCAC
GAAGTCAGGAGTTCGGGACCATCCTGGCCAACATGGTGAAACCTAAAAATACTCTACTAAAAATACAAAAACTTGCTGGGCATGG
TGGCACACACCTGTAATCCCAGCTACTCAGGAAGCTGAGGCTGGAGAATCACTTGAACCCGGGAGGCAGAGGTTGCAGTAATCC
AAGATCATACCACTGCACTCCAGCCTGGGCGACAGAGCAAGACTCTGTCTCGGAAAAACAAAACGCTTTTTGTGACTCACGAACT
TGATTTCATGAGTGGGTTTGAAAACCCTGGGCTAGTCCAGGCGCGGTGGCTCACGCCTGTAATCCCAGTACTTTGGGAGGCTGAG
GCGGGTGGATCACTTCAGGAGTTTGAGACCAGCCTGGCTAACATGGTGAAACCCCATCTCTACTAAAAATACAAAAATTAGCTGG
GTGTGGTGGCACATGCCTGTAATTCCAGCTACTTGGGAGGCTGAGGCAGGAGAATTGCTTGAACCCGGGACGGGGTGGTTGCAGT
GACCTGAGATCGCACCACTGCACTCCAGCCTGGGCGGTAAGAGCGAAACTGCGTCTCAAAACAAAACAAACCAAAAACCCTGGG
CTAGGCAACTTTCTTGGCAGAAACTACTTTGGAGCTCGACACCAGATGGTGGCAGAGTTGTCTGGGGAGCTGTGTCGAGGGCCGT
GGCCTTGGGAGCAGCTCCAACCTCCCATCTGGGCTCAGAAACCAGTGTCAGACATTGGTTTTATTTTAACCTTTGAGATTTGTGTG
GAGCGGGTTTTGCCTTCCCCTGTTGCTTAGATGGATTATTTAGCCATATTTTTTGTTAAATAAGGGGAGGTGGTCATTATCCGTGAT
TTCAGACGTGGAATCGGCCCGGCGATAGCTGCATTGTGCCCTTTCCGGTGGAGCCAGGAGGAGTTTGGCCGCCACGCTCCATGCG
CATAGCATGTCATGCAGCTAGCCAAGTGCATTGTTCTGAGTGCTCCAGGATAAGTACCAACTTACTTAGTGCTCCAGGATAAGTAC
CAACTTAGTGCTCCAGGATAAGTACCAACTTACTTAGTGCTCCAGGATAAGTACCAACTTACTTAGTGCTCCAGGATAAGTACCAA
CTTACTTAGTGCTCCAGGATAAGTACCAACTTACTTAGTGCTCCAGGATAAGTACCAACTTACTTAGTGCTCCAGGATAAGTACCA

ACTTACTTAGTGCTCCAGGATAAGTACCAACTTACTTGATCCTCAGAGCAAGCCTAGGCGGTGGGTACTGTTTTGCTCCTGTTTTA
CCAGTGAGGAAGCAGGCACACAGAGGTGAAGTTGCCCAAGGTCACACAGATGGTTGAGGGAGAGCCGGATTGGAATGAACTCTG
TGCTGTTAGCCACTGTGTGAGGCTGGACTGTTCCATTCCAGCCTTTACGGCCTCTTCCAGGCCATTCCCCAGCTGCACTTGGATTCT
CAGGCCAGGCACCGGCGGTCTCCTGTGAGGGTGGAGAGGAAGAGGGGGCTGCGTGGCTCGGGGAGGTCCAGGAGAGATGGCGG
GAGGAGTAGAGTTTGGGGCCTGCGGTGCCAGAGGACCCCCTTACAAGACGAAAGACTGGGTTCTCAGGCTCCTGAAGCAAGGAG
CACCTTCAGGGGTCTCCTGGTATTCACCCATCAAGGCTTGCTCAGGTGGCATGCGTGTGTGCGTGGCGGCTGCCCCCGGGCCCGGA
AGCGCCTGTGGATACCAAAGCAAGTGGAAATGCCAGATGGAAAAGCCCCGTGTTAGTCAATGCTGTAGAGTTCAGCCAGCCTCGA
GTTTGCAGGTTTACAGAGCTGCCTTGCGCCTGGCTGCTGCTGCTGCTGCATTCCTGCTTCTGCCTCCAGCTGTGACCACCTCCTGCC
ACTCCTGCTCTCACTGTGGGTTCCTGCTCACTCTGTCTCCAGGACAGACTGCCTTCCGGGCAGCCTTCCCTCCTCAAGCCTCTTGGC
CTTTGCAATCCTCTTACCTGGGTCACTGGTGGGATCTCATTTGTGGATCAAGTCGCCCCCAGTGGAGACAAATGTCTGATGGAGTC
TGGCCAAGGCCCTCCTGAGCCTTCACTGGGCCCTGCATGAGAAGCCTGCCAAGGCTGAGGGGCCAGGGAAACGGAGACGAAGCC
CTCAGAGCAGGCCAAGAGGGTGGGAGGTGGGGGGCATTTAGAGGGTTAGATACAGAGCACCCCTTTACAAATACCAGCTACTGG
CTTTTCGTATTACATGTTCATTTTAGATACAACATACTGCACACGCTCCCTTAACGTGTGTTTACGCGTGGGTGGTGTATCCTTCCA
GACGTCTTCCTCACATCTATACATAATATGCATAGATAAAACATTTACCACCAAAACCCATAGTGTTATGTACATATTTGTCTGGC
TGTGTAACTTTAAATAACATACAAATGTATAGAACAGAAGCTTGCCCTCTTTCTGAAATATCTAACGTGGGATTTCAGGCTTTCTG
ATGAGACCTCTGTAGAGGTCAGTGTTTTGCCACCAGAGGTCCTTCAGCCTCCATCTGTTCTCCCACCTACCCACATTCTGGCCCCTG
GCAATTCACAGGGAGTTTAGGAAGTAGACACCAGGGCCCTATTTCCTGGAGACCAGCCTGGTGGCCGATGTCATAGAGTGCGGTG
GGCCTGGGCCGGCCCTGCTCTGGGCCCGTGACCTGCGTGTCTGACTCGGGTCCAGCTGTTCTTCCTGCCAGAGCCTCTTCCTGTGA
GGCGGGGGTAACACAACCTTCTGTGGTGGCTGTGGGATTAATCCGTATGGCTGCATTGTGAGTAAAGCCTGGTGGAAATCTCTGT
CTCCACTGCTTTCCTTTTCCTGCTGTTCACCTTGGCTCCCTCGACACTTAATCCCCCTCCACATGTGTCTGGAGCGGGCAGAGCGGG
GGCAGTTGATAGAAAGGGGGCCGGGTAGTGCCAAGGCTGTTACTTTCCCCCACTGCCTCCCTTGGCTAACTTGAAGTCTGACCCTT
TATACCAGAACTGTAAGACAGTGTGTCAGAATGGATTCAGTTGCAGAGCAGGAAGCCTGGATCCCAGCGCCGGACGGAAATGAG
AGGTCGATGGTGCAGGCTGGTGTGGGGGTTCCTCCACCGTCAGGGCCCAGGCTCCTTCTCAGGTCTCAGTCTCACTCTTCTTAGCA
CGAGGTCAGGTCTCATTCCTTGGCTGCGGGAGCTCCAGCCAGCACACGTTTTAGGAAGAAGGAGGAAGGAAGAAGGTAAAGGGT
GGATGGCAGCTGCCTCCTCCTCTCTTGGAAGCTCACAGAGCGCTGGGTCACAATTCCCTGGGTAGAACTGGATCACACAGGCACC
CCTGTCAGCAAAAGAGGCTGGAAAAAGTATTTCTGAAGCTGAATCAAATTAAGATTCCTGTTACTAAGAAGGGAGTGATTGTATG
GGCGACTACAGGGACCACGGCCATACACGGTGCCTGGAAGACCAAGCTTGTGACAGTGACGAGGATTTGGAGAGGGCAGGGTGA
TGGGGAGCTTTGGGGGGAGTGCATTAGGAACCCTGACCTGGAGAGGGGCAGAATGAAACCTGCGGGCCCCTAACCCTAGTGGGT
TGTTTGAGAAACCTGTCCTACTGTGGCAGGGGGCTGAGTCTTCTCAGGGTCATGCATGAAAACTGAAATTCCTGAAGGCCACACA
CAGCCCCGGAAGTGCTGACTGACAAGGGCACATGCCAGTGATGCAGTTTTCTTTTTTGTCTTCACTTTTGTTGTTCCGCCGTCTTCA
ACACATGGCTCCCAGCTCACAGCAAATGCTGCCCTGGTTCAGCTACCAGGAAGCAGGAGAGGGGAAGGGAGGGCAAGCCTCATT
CTTTATGGAACAAAAGCAGTGGGCAGACAGCCTTCCCTCACGTTCCACTCACTGGAATGTGGTCTGGCTGCCTTCCCTGCAGGAG
GTGGGATGCACCCTCAGTGCAGCAGCCCTGCCCCAGCCAAAAACGTCTCAGCACAGCTGTAAGAAGAGGAAGATGGCTAGAGAC
AGGCAGCCTTCCCTGCAAGGGCAATGAGGCAAGCCTGCCAAAAGCCTCCTTTGGAAATACTGTTTGATTACTTTTCAGAGTTTCTA
TTTAGGAAAAGGGCAAAACCTTTCAGGATCAGGAGTAGGTGAGCGGCGATCAGGCCTCACTCTTCACCGAGGGCCTTCCCTGAGG
AGGGGCCTGCAGGACGCTGGCAGCGGAATGGGGCTGTGTGGCTGCTAGATTAGGTCATGGCAGGGAGACAGCCTCTTCCTGGTTC
TTGCTAGAACAGGCACACTTGGGGCCTTGAGCTCCAGGGAGTTCATGGAAGACATCTGACTACCCTGAGCCCCTTGCTGGAGGGT
TCTGGGGAGTGGCCCACGGCCACCGTCACCCATGGCCACCGTCACCCACAGGGGCCGTGAGGACATCCCTGGCCAGCATCTAACA
CAACCACATGGGATGCCCTAAGCAACTACTGCCCAGCCGAGGGCTGCCTGAATTTCTGACTCACAAATGGTGGGCAATGTGAAAC
GGGTATTTTAAGCTGCTGAGTTCTGCGGGAGTTTGCTGAGCAACAGTAGAAACCAGAACTCTCGGATACTGTGTTCTGTCCTTGAA
ACGGTGGAAGATTTTATGTGACCAGAATGGAATGTTTGAACAAATATTTTGAGAATAGAATTTTAAAACATTTACTCATCAGCATC
CAAGGGTGGGGAGCAGTGTCATCTAGGAGACTGGTTCTATTATTTACGTAGATGTTCTTGAATTAAAGGATGGGAATATTTTTTCC
TTCCAAAACTTTTTTTCAATTTTATATTCTGTTTTTCAAGTTTTTATTATGAAAATATTCAAACTCACAGGGAAGTTGAAAGACTAA
TACAAAGAAGAACCATACTCTTTCCACTGACATGATCCAACGAGGAATATTTTGCCACACGGCAAATATATACCGTATAATTTTCT
GTACCACTTGATAGAAAGGTAAAGAATGAATATTGTTTTTTAAATAACTTTTTTCGTATATAAGTAATATGTGCTTATCGTGTAACT
ACCTAAAAACATTGAAAAATAAAAGGAAAATAAAATTCATACAT

MGAT2 3’UTR sequence:

GTTTACTGTGGTAGCCATTTCCCCACCTAGAAAAAATGGAGGGTGGGGAGATATTAGGGACCATGAACTCTGTAAAAGTTATAGA
AGACTGCAGTGAAAATCACAGTTACAAAAGCGACAGTCTTCTATTTTTGATATTTGTCCAAACAGGACATACAATTGAATAAAAG
AGTTTAGGAACTGGTTTCTGCTTTAATACAAAAACAAAATCTTGTAAAAGGTGTCCAAATACATAGTAATCTTTTCCAGTTATGTC
TGATTAAGATTTAAAACTGAAGGTTTCATTTTGGGAGTAGGGTTTTAAAGCTCAATCTGTTATCTGCTAAAATTGATTATTGTTGAT
ATGAGAGAAGAGGGGAAATTTTATTTAAATTGCATTTATTAATCTTTTTATCTGAAACTTTGTACACTTTTCCACTTTCAAAACCTA
TTTTAAGTACAGCAAAATTTATTTAAAACTGTCATAGCAGTAAAAAGTATTACGATGAAATTGTTAGGGTATTAATGGAACAAAC
CCAGTTTCACTCTCTTGACACACTTATTAGGAAGGGATTGCTTCACTGGTTTAATAATTTAAAAGTTATGTTTGTTAAACACCCTGT
CAGAACAGTCATTTTCAGTATTAGATTCCTGTACTATTGTGTTTTGAGTGTGTTTTGGAACCTTCATAGAACACACTTTCTTTTGGA
ATGTATTTGATTGATAAGAAAGTTTAAACATTGTTTTCACCTCAATGTAGAAATACAGTGGTTTTGTTTTTTTTTTTCTTTTAGTGCT
GACAAAATAAAATACTCATTTTTGCATAAAAAGGTTCCTAATCCTTTTGCAGAATAAGTTTTGTTTACTCTTTATACCAAAATTCAG
TGAAGGCATTCTACAAGTTTTGAGTTAGCATTACATTTTAATATTTACTATTGCTACATTGTATAATTGAGTTTGAAATAAAACCCA
GCTTATGACAATGCA

MGAT3 3’UTR sequence:

GAAGTCTAGAGCTGCATGATCTGATAGGGTTTGTGACAGGGCGGGGGTGGCGGCGGCCCCTAGCGCTATCTCCCTGCCTCCTGCC
GGCTCCTTGGTTCTTGAGGGGACCAGGAGTGGGTGGGGAGTGGGGGTGGGGGTAGGGTTTCCCTACTGAAGCCCTTGTGAATCAA
GGGTCAGGCCTTTGAGCTCAGAAAATATCCCTCCTGTTGGGAGAGGGCGCAGGCCGTGACGTCTGGGTGGCCCTTATGACTGCCA
AGACTGCTGTGGCCAGGAGGTGCCACTGGAGTGTGCGTGGTGGTCCCTGGGTAGCGGGGGAGGGTAGGCAGGATTGGGGAAGAG
AGCCTGCAGGATCTCACCAGGCAGCCTCTGGGGGGTGGCCAGGCCGGGAAAAAGCCCACCATTTGGCATCCCTGGGCCTTGGGCT
CCGTGTGGGAGACCGGCCTGCCAGGAGGACCCAGGGCTCTGTAAGTAGATGCATTTGGGTCCAGGAGGAAGCGTGGACACCTCG
TAGGGAAGAGATGAAAAAGCCACATCCTACCAAGAGGAGGTGCTGAGGGATGCTTTGCAGTGTAGTCAGAAGTGCTGGGCCAGA
TGGAGACAGAACTCCACCCCCTGCCGCAAAGGACAGGACCTGGCTGCCCTGGGATGCTGGTGCCTGAGTCTGTCTCTGTGCACCC
CTCAGGCTGTCGTGAGCCAACACAGGGGCCTGGAGAACCCTGAGGAGCTTTCCTTTTGGTTCTAAACCCGGCGTTGACGTTCCTTC
TCCCTTTCACATTGCTGTCTTGTGGACTGTGCACTCAGTCCTTGCAAGGCCAAGAGTCCAGTTGTAGGTGTGGCCTTGAGGGGGAA
GTGGGGAGGAGAAGACTGACATGAGTCCTCTGCACGGATCCGTCTCTCCCTCCCCATCACCCCTTCCTTCTGACACCCAGTCCCAG
CTGTCCACTGTCCCAGGTGCAGTCACTGTTGTGCCCTTCCTTGGGGCAGGCTGGCTGGGGGCCAGAAAGGGGCCATGAGGCTGTC
TTGGGCCCAAAAAGGGACAATAAGGCCAGTTGTATGCTTCCTGTTCCTCATAGCTTGCCTTGGTGGGGATGTCTTTGTTGGAGTTG
ATTCTGAGCTGCTGTGATTAGGAGACCCTGAAATACAGTGGTTTAAGCAAGATGGAAGCTTGTTTCTAATTAGTCTAGATTGAGAT
GGCCCAGAGCTGGTAGGGCAGCTCTGCGTTTCTTCATACGCACCTTCCAATTCTGGGTACACAGCGGCTGCTCCAGCGCCCACCCT
CCTGTGTGCATCCAAGCCTGGGGGAAGCAGAAATAGACAAGAGGGCACACCCACTTTTTGCTAAAGGCATGAGCCAGAATTGGC
AGGCTCACCTCTGCTGGCCTCTCATTGGCTGGGACTCAGTCACATGGCCACAAGCAGCTGCTAGGGAACCTGGGAAGTGTAGTCT
TCAGCGGGGCCGCCATGTGCCTGGCCTCACCTTGGGAGTTATCTTATTGATGGAGGAGAAGAGAATGGATATGGGGGACCAGTAG
CATCTCTGGGAGAGGGGGAGGGAGCAGCAATAACTCAGTCGTCGGATCCAGCTCTCATTGTCAGAGTTTCCGGAACAGCTTGCTC
CTGTTTCCCTCACTGTGCAGCCCAGGGCTGGGGGCAGTGAGGAGCTTGCAGCTCTGTGGGAAGGGGAAACACCCCCTCCCCTCGG
CCCCTCAGACGCTACCCAATGATGCCGGTTTGCAGAGTTGGCCTGTGGAATGGCTCATGTTTGTGCGTGTGTGTGTGTATATTTAT
GGGCATGGGTGCATGCTTGGTGTGTATTTGTACATGTCTGTATTGCTGTGTCCCTGTAAATACATGCTTGTGTATGGATGGAAGAG
GCCAGGCCCAGGCCTGGCCTCTTCCTCGGGCCTGTGGCCACACCTCCTGCAGCTCCCCAAAATGACTGAGGCAGAAAGCCCTTGG
GGAGCCTAGAAAGCAAAGCTAAAGGGGATGCAGGGTCTGTCTGTCTGTCTGTCTTTCAGTCTGAGGAATGAGAATCCTGACCTGA
GGGCTGTGCAGCTGAGAGCCCACTACCTCCCCAGCCCCTCTCGGCCCCAGCCGCATCATCCCACCTGTCCCCTCCCCCCCACCTCC
AGTGGGGCTTTCTCCAGATGTCTTATGGTTGGGGGTTTCCTGATGGGCCAGGAGAGGAGGGCATCTTCTTGCGACAGCACTGTCTG
GGTTAAGTGCCCAGTGAGGGCATGGTGTGGGGAGCTGGCCTCAGAGGAGCCGCTGGTGGGCAAGCGTGAAGTGGGCTGAGGGGC
TCTGAGCCACTTTGCTCCCATCTAGGGGACTGCCCCCCATGGAACTCCTTTGAAGTCACAGCAGCCTTCCTTTCTGTTTGCTCTTGG
GGCTGAGAGGTGGCTCAAACACTCGGGGTCCCTATGGCTCTGGGTCAATCTAGGCCAGGCTGCACCCCATGGACAGGGAGTCTCA
GGGCTCCTGATCATGCCCAGGCCCTGGCCTGGGGCCTCCCTCCTTGGCAGCTTTCCCACCCCCACGCCCCTGGCATCCTCAGTTGC
TATGGGATGCCCCTCCAGGGCACCAGCTCAGGGCTAAGCGAAGGAAGATAGGAGCAGCTCAGAGCTGCCAGGCTCTGCCTTCCTC
ACAGACCTGGTGGGGCAGGTCCTGTTCACAGCAGCAGGAGTGAAGGCCTGGCCATCGGTGGAGAGGGCAGCTGTCAGAGGGCTG
GGGGCCAGGGCACAGGATTGAAGAGTTTCACATATCATCACAGCATACACTGGGAATTTGGTGGGGGCAGAAGAACCCAGGGCC
ACTCCCTCAATATGAAGGGAAACCAAGCTGAATGTGACCACCGGCACACTGCTGCCATGTCCCATGTCCACCTTTCTCCCCGGGA
ATAACTGGCCCTGAGACCCCTAGACCCAAGGAGGCCTGTCCATGCCAAGCATCCGGGAAGCATGGCTGGCCTTATCCACCCATGG
GTCACGTCGGTTCCCAGGGGCAGCATGGGAGATCTTTGGGGGCAACAGGGAGAGTCTGGGTGGGGAGACGGGACTTGTCCAAGC
AGAAGGCAGGACCCTGGGAAATGCATAATGTAAGGACATCAATAATAGTATTATTTTTTTTGTAAGGGAAAATCAATATGTACAT
TCTGAAATCATTTTCTCTGTAAATGGTTGGATTTCATTTCACCCTTAAAGGATGCTTAAAGGAGAAGATAATATTAATAATAAAA
ACAGCTACAAAGTCTG

MGAT4B 3’UTR sequence:

GCTCTTCCAGATCTTCCTGAAAAAGGCCGACTAAGCTGCGGGCTTCTGAGGGTACCCTGTGGCCAGCCCTGAAGCCCACATTTCTG
GGGGTGTCGTCACTGCCGTCCCCGGAGGGCCAGATACGGCCCCGCCCAAAGGGTTCTGCCTGGCGTCGGGCTTGGGCCGGCCTGG
GGTCCGCCGCTGGCCCGGAGGCCCTAGGAGCTGGTGCTGCCCCCGCCCGCCGGGCCGCGGAGGAGGCAGGCGGCCCCCACACTG
TGCCTGAGGCCCGGAACCGTTCGCACCCGGCCTGCCCCAGTCAGGCCGTTTTAGAAGAGCTTTTACTTGGGCGCCCGCCGTCTCTG
GCGCGAACACTGGAATGCATATACTACTTTATGTGCTGTGTTTTTTATTCTTGGATACATTTGATTTTTTCACGTAAGTCCACATAT
ACTTCTATAAGAGCGTGACTTGTAATAAAGGGTTAATGAAGTGTGTGCCTC

MGAT5B 3’UTR sequence:

GGCTGTCTGTGAATCCGCCTCTGCCGCCCTGCCTGGCACCCACGCTGGCTCTCTCCTGCCGCGGGAGAAAGCACCAGCAGGTTCTG
AGCCCTGGCTGCTTGTCCTCCTCGCAACCCCCCCAGGCCGGAGCTTCCTTCCTTAGCCGGGAAGCTGGCAGAGGAGAGCCGTGCC
CGGGAATAGGAGGAGGCAGCATGCCGAGCCCCTGGGACCTCCCAGGCAGGCTCCGGTTCTCTCCTGGGGACTCACAGAAGCATC
GTGGCCAAGCAGGTGTCGGACTGCTCAGAGTCCGCATGGCCCAGGAGCAGGTGGTCGGAGGCCCCTGGCTTTGTGCAAGGCCGG
ATCTGGGCCAGGTGGCGAAAGGGGCCCAGTCGTTCTTGGGCCCAGGATGGGGCCTCTAGACTTGCAAGGGAGAGGAACAGGGAC
CAGGCTGCCCCACGGTCCCTGAAGGGTCCAAGGAGGGGCCCTCCCCATGGCCCTGGAGAGTGGGCCTGGGTGGTACCTGCTCCAG
GCAGGGAAACTGGGGGCTCGCCCTTCTCCTGTGAGGGGAGCCAGGCACACAGGGCCCATTGGTGTTTGGGATGTGGACAGAGGG
GCAGGGGGCTGGGAGAAGGCTAAGCCGAGGGGTCCTGTTTGTGCCTCCCCTTAGTCCCTTCCCTCCCGATTTCCCGATTCCCCCAC
CCTCCCTCTACACTTGAGGACCACAGTTGGGGGTGTAGGGACCACCCAGACCCTGGTTGAATTGTTTCTCTCTCCTGCTTGTTCCA
ACCCTTTTCACTCTGGGCTTCTCCCAAAACCCATCCTGGCATGACCTGCAACTCCAGGTGGTGGATTTGTTCCAAAGCCTCAATCC
CTACCCCCTCCAAGGGGCAGGTTTCCAGTCCAGCCTCAGAGATCAGGCTCTGGGACCCCTGCCTGGGGGGTGGCCTTCATGCACT
AGCCACTTCCGCAGGTGCTGACTCCCGCACTCCCTGGCATTTTTTGCAGACAAGGGCTTGGGATGGACCCTCAGCCCCATGGTACG
CCCTGCCCAGTTTCCAGTTGCCCTGTCCACTTACCCTAGGTAGCCCCCCACCCCATCAGTGCCGAGTCCTTGTCCCTACCTCCAGCT
TCCTCCAGCCTCAAACCGCCTCTGGATCTAGCTGTCCTTCTCCGAGTGGCACGCCTGCCCCAGGATGCCCCCTTTCCCTCCCCCCCA

TGCCCAGAGCCCCGCCTGCCTCAGCGGGTCAGGCCTTCAGAACACTGCCACCCACCCAGTTTTATAATCCCGCTCCCTCTCCAGGC
AACCCCACCCACCAGCCTAGGCCTGCTCCTCCACCCTTCCCGGGAGGCAGCCCCGGGATGCTGAGAGTTGGTGGAGGGGCCAGGC
TGGACGCTTCCTGTGGGAGTCCCCTCCAGACCTGGCTGGCCCCTGCAGCCACAGAAACCACGATGGCAAAAAATCTCATTGGTTC
TCAAGGACTAACCTGTGGGGGAAAGCAATAGAGACACTCTTTTTCTCTCTTTTTTTTAAAGATTTATTTCTTGAAATAATAAATATT
TTATTGGGATGTG

ALG1 3’UTR sequence:

CCTTTGGTTATGGACACATAACTCCTGGGCCAGAGGCTAAAACCCCAGGACCCCTGCTGTCCTTCCCGCAGCTTCTTCTTGGAGTC
TCAGGGCAAACCCTTTCGAGCAGCACCTCCCAGTGGCCAGAAGCTGAAATGACAGCAGTGGTACTGCCTGGTAAAAGAATTGGTT
CTGTGACCCGGGAAGCTTTGGTTGGCCTTGATTTCTTCTCTGGAGGCTTGGAAACGCTTCCTCTCTTCTTCTGTTCTTCACGCCCCA
TGCCCCTGCTAGCGTATTACTGTTCTGTGACTTCCCTGTGACCTCTGCAGAACTCCTCATCCTGCGTTTGGTCTCCAGGTGTCCCCT
TTCTGCCGTGTTCCTAACATTTTGATTCCTGTCTTGAAAAAAGCACCTGCTGCACCGTAAGCCCAGGGATGTGGCAGCTGCAGTGG
GCTTGGCTTTGTGAGGAACTGAGTGTGTCCACGTTGGGGGAACATCATACTTGATACACACGTTTTTATTTGCACAAAGAAAATGC
TATTTTTGGAGCCAGAATTTTCATGTCTGATTTATGGTGATTTTCTTAAGAACCAGAACTGCTGGCAGAAAGGGGGCACCCACACG
CTTAGATAGCCGATGTCTTATTAGAGGGCAGTTTGTGGTTCCTGATTTGGAAATTAACATTCTCCAAACATTCCAGTCCAATGAAA
GTTTTATCCGCTTTCCCATATAAAAATTCTTCCCATGA

ALG2 3’UTR sequence:

CGATATGTTACCAAACTGCTGGTATAATCAGATTGTTTTTAAGATCTCCATTAATGTCATTTTTATGGATTGTAGACCCAGTTTTGA
AACCAAAAAAGAAACCTAGAATCTAATGCAGAAGAGATCTTTTAAAAAATAAACTTGAGTCTTGAATGTGAGCCACTTTCCTATA
TACCACACCTCCCTGTCCACTTTTCAGAAAAACCATGTCTTTTATGCTATAATCATTCCAAATTTTGCCAGTGTTAAGTTACAAATG
TGGTGTCATTCCATGTTCAGCAGAGTATTTTAATTATATTTTCTCGGGATTATTGCTCTTCTGTCTATAAATTTTGAATGATACTGTG
CCTTAATTGGTTTTCATAGTTTAAGTGTGTATCATTATCAAAGTTGATTAATTTGGCTTCATAGTATAATGAGAGCAGGGCTATTGT
AGTTCCCAGATTCAATCCACCGAAGTGTTCACTGTCATCTGTTAGGGAATTTTTGTTTGTCCTGTCTTTGCCTGGATCCATAGCGAG
AGTGCTCTGTATTTTTTTTAAGATAATTTGTATTTTTGCACACTGAGATATAATAAAAGGTGTTTATCATAAA

ALG3 3’UTR sequence:

CAACACAGCAAGAAAGCCCACTGAAGTCCACCCCTTTCCCTCAGGACCTGAGTCTACCCTCAGGACCTGGGGTTGGTTGGACTCT
GCCCTTCCAAATAAACCTTGCTAAGTCCAACTCTGTGCAACCTACATGGAGGTGGGGGCAGCCGATGCCTGGTCCAGGCTGTGAG
GGACACGTATGGAGCAGATAAAGAATTCACTCAA

ALG5 3’UTR sequence:

GCTTGAGCAAACTCGGAAAATGAATTAGGTTGTTTGCAGTCTTCAGTTGTGTTCTTATGCTTCAGTGTCACATTTCATTTCATTTGA
AACTAAAATTTTAAGTAAAGCTGAAATAAACTTCTTGTCATTGTCTGCCTTTT

ALG11 3’UTR sequence:

GTGACATTCCTATCATCTGTGGAAAAGTTATTTAAGTAATGCCATATCTGTAAAATTAAAGATATTTTATATAAACTGGTTAAACA
CCTTCATATGTAAATATTTTTCTAAATTCAATCTCATTTGTCAAATCATTTTACTTTAGAAAACAGACAAAATTTCCTTTTAGAATA
AAAGGAAGTGTTGAAAAGAAAATGGATGACTAGCCTTCGGCTTCCATTCTTGGTATACATGAGAGAGGCTGGCTGCTGAGATGAA
TGTGAACCAGGTTGCAGAGAATCTGGCTTTGAGCCACCAGGAAGAACTAGTGGATTTGCCAAAAAACTACCCCTTGAGTGAAAAT
GAAGATGAGGGGGACAGTGATGGAGAGAGAAAGCATCAAAAGCTTCTGGAAGCAATCATTTCCCTTGATGGAAAGAATAGGCGG
AAATTGGCTGAGAGGTCTGAGGCTAGTCTGAAAGTGTCAGAGTTCAGTGTCAGTTCTGAAGGATCAGGAGAAAAGCTGGGCCTTG
CAGATCTGCTTGAGCCCGTTAAAACTTCATCTTCTTTGGCCACTGTAAAAAAGCAACTGAATAGAGTCAAATCAAAGAAGGTGGT
GGAGTTACCTCTTAACAAAGAAAAAATTGAACAGATCCACAGAGAAGTAGCATTCAGTAAAACCTCACAGGTCCTCTCCAAATGG
GACCCTATCATCCTGAAGAACCAGCAGGCAGAGCAGCTGGTTTTTCCCCTGGGGAAGGAGCAGCCAGCCATTGCTCCCATTGAAC
ATGCGCTCAGTGGCTGGAAGGCAAGAACTCCCCTGGAGCAGGAAATTTTTAACCTCCTCCATAAGAACAAGCAGCCAGTGACAG
ATCCTTTACTGACTCCCATGGAAAAGGCCTCTCTCCAAGCCATGAGCCTGGAAGAGGCAAAGATGCACCGAGCAGAGCTTCAGAG
GGCTCGGGCTCTGCAGTCCTACTATGAGGCCAAGGCTCGAAAAGAGAAGAAAATCAAAAGTAAAAAGTATCACAAAGTCGTGAA
GAAAGGAAAGGCCAAGAAAGCCTTAAAAGAGTTTGAGCAGCTACAGAAGGTTAATCCAACTGTGGCACTGGAAGAAATGGAAA
AAATTGAAAA

ALG13 3’UTR sequence:

CCAGCTTCTCATTATGTACCTCAGGGTATGTAAGATCCAGCAGTATGAAGTATTCTTGCACTGCCATTTTCTTGCTGTTTTTGTTTTT
AAAAAGTATTTTATGTTAGTGGTTAAATGATTTAGGTGATTAGTGTTTACTATTGTATTTGTCTTTAAAATTATTTTATCTTTTGATT
TAAAATAGTACTTTAAAATTAAGGGGTATTATTTTGGGCTGTGACTAAGGAAATTGAGATGGATGTACAACTAGCCCCATATTGA
GCATACTTCATTGTATTCAGCTGTTTTCCTGTCAGCCATTTGTCAGCTTTATATTAGCTGATGGTACCAATTGATAAAATGAATATA
AAGTATTTCATTGGTTCAAAAATCACACATCATATTAAACCATGCAGAATTGGAGTAACTTCCACTTTTTTCTAGAAAGTAAAACC
AAGAGCCTTTGCTTCTGGATAACTCACTTAATATTAAATTAAAGAGCTCTTCACGTTTCTTGAGAATTATCTGAAGCCAGTTGCATT

CTGTGATATCAGTTTTGAAGGCACATGGTTCTCTGCTTTAGATTTATCCCATATGCTATTGTTTAATACTGGATGTATGTAAGTGTT
TTACTGCACTGTATTGAATTGGTGTCTTTTGCACAGTTAGCAGTAAATAAAAATTAGCATTTAAAATTGCCAAAA

B3GALNT1 3'UTR sequence:

CATGCTAAGGAACACCACATGCCATTATTAACTTCACATTCTACAAAAAGCCTAGAAGGACAGGATACTTTGTGGAAAGTGTTAA
ATAAAGTAGGTACTGTGGAAAATTCATGGGGAGGTCAGTGTGCTGGCTTACACTGAACTGAAACTCATGAAAAACCCAGACTGGA
GACTGGAGGGTTACACTTGTGATTTATTAGTCAGGCCCTTCAAAGATGATATGTGGAGGAATTAAATATAAAGGAATTGGAGGTT
TTTGCTAAAGAAATTAATAGGACCAAACAATTTGGACATGTCATTCTGTAGACTAGAATTTCTTAAAAGGGTGTTACTGAGTTATA
AGCTCACTAGGCTGTAAAAACAAAACAATGTAGAGTTTTATTTATTGAACAATGTAGTCACTTGAAGGTTTTGTGTATATCTTATG
TGGATTACCAATTTAAAAATATATGTAGTTCTGTGTCAAAAAACTTCTTCACTGAAGTTATACTGAACAAAATTTTACCTGTTTTTG
GTCATTTATAAAGTACTTCAAGATGTTGCAGTATTTCACAGTTATTATTATTTAAAATTACTTCAACTTTGTGTTTTTAAATGTTTTG
ACGATTTCAATACAAGATAAAAAGGATAGTGAATCATTCTTTACATGCAAACATTTTCCAGTTACTTAACTGATCAGTTTATTATT
GATACATCACTCCATTAATGTAAAGTCATAGGTCATTATTGCATATCAGTAATCTCTTGGACTTTGTTAAATATTTTACTGTGGTAA
TATAGAGAAGAATTAAAGCAAGAAAATCTGAAGTATTGTCTTGTTTTTAAAAAATACAGTTCCTAGTGTTTTTAGAAGTCACTTAA
TTTGTCTCATTTTTCCACCTGGAAATTAGGAATAATGTAGAATGCAAGGCAGTAATTTCCTTTTGGAAAGGACTCTGAAGGCAGAA
AAGAAGGGAGAGAACCTCATGGGCAGAATATTATAAAAAGAGTGTCATATTCCAGCATTTGAATTGGAAAGAGAAGAGTGAAGA
TCCAAGTTGCATTATTAATCTGCCCTGTGTTTTTTCCTTTTAACAATCAGTTTGAGCTGCTGCTGTTATGAGTTTCTCATCAAGATGA
AAGCCCTAATATGTAAAGTCAAATCCGATTTAAATTTTGTGCTTTTATAGAAAGAAATTTCTTCATAGACGTGGTGATATATCATT
TGTTGGACCTGCTAATAGTAGGTCAAAGGGGAGCACTCCTTGCCCCCTGTTCCTGGGTTTATGCAGTTTTCTTTTTAGAGTTTATAT
AGGGCAAGTGGTTCTTTTTCTCTGAATTACAGGATGGAAAAAGGTCATATCCTTTGTCAGGAAATATAAACTTGAAAGTATGTAGT
CAGCTCTTGTAATACTCATATTTATGATTGTCCTATATGAAAAACAACTTCAGTTAAAACTATAATGTGTGATTCTGTATAACAAG
GTGATGTCTGTTTCCCAGGGCTCAGACCTAATCCAGTTATAATAAAATCAATTAAATGAAATATTCTATAGAATCGATCTATGCCC
TTGTTAATCTCCATCCATATAGGAGTCACGTTCTTTAAGACAGATGGTGGTAGTTATTTTTGTGGCATGGTTAGATTTGACTGGTTT
TGCAGAAGATTACAGTTATGTACTGCATAATGACATATACAATAGTGGTCCCATAAAATTATAATGGAGCAGAAAATCTATTGCC
TCATGATGTTTTAGCCGTTTTAATGTCATAGCCTAGTGCATTACTCACGTGTCTGTGGAGATGCTGGTGTAAACAAACCTACTACA
CTGCCAGTTGTATAAAAGTACAGCACATTCAGTTATGTACAGTATGTAATACTGATAATGACAATAAATGACACCGGTTTGTGTAT
TTACTTTTTATAA

B3GALNT2 3'UTR sequence:

CGATGTCAAGCAAGATAACAGGGACTTGAATTAGCAGAGTCTAAAATCAGGGCAGGCAAACGATAATCTGAGTGCAAGTCTGAG
GAGTCCCAGGGTTTAGCAGTAGACTGTATGGTCTTTCAAGAGAGTTCCAGACTGGCACTTTCACCCAGAACCAATGCGGTGTTTCT
TAATGTTTGCACAAATTTCCTTAAAAATCAACTTGTACTGTAGCATAAGAAAAGTTTTTATTTATCTATTGGAAGATTATCAGAAA
AATACCAAGTTATTTTATAAAAGAAAAAATATTTCTAAATCCTGA

B3GNT3 3'UTR sequence:

GCAATCAGACACAGATCTACTGAGTCAGCATCAGGGTCCCCAGCCTCTGGGCTCCTGTTTCCATAGGAAGGGGCGACACCTTCCT
CCCAGGAAGCTGAGACCTTTGTGGTCTGAGCATAAGGGAGTGCCAGGGAAGGTTTGAGGTTTGATGAGTGAATATTCTGGCTGGC
GAACTCCTACACATCCTTCAAAACCCACCTGGTACTGTTCCAGCATCTTCCCTGGATGGCTGGAGGAACTCCAGAAAATATCCATC
TTCTTTTTGTGGCTGCTAATGGCAGAAGTGCCTGTGCTAGAGTTCCAACTGTGGATGCATCCGTCCCGTTTGAGTCAAAGTCTTACT
TCCCTGCTCTCACCTACTCACAGACGGGATGCTAAGCAGTGCACCTGCAGTGGTTTAATGGCAGATAAGCTCCGTCTGCAGTTCCA
GGCCAGCCAGAAACTCCTGTGTCCACATAGAGCTGACGTGAGAAATATCTTTCAGCCCAGGAGAGAGGGGTCCTGATCTTAACCC
TTTCCTGGGTCTCAGACAACTCAGAAGGTTGGGGGGATACCAGAGAGGTGGTGGAATAGGACCGCCCCCTCCTTACTTGTGGGAT
CAAATGCTGTAATGGTGGAGGTGTGGGCAGAGGAGGGAGGCAAGTGTCCTTTGAAAGTTGTGAGAGCTCAGAGTTTCTGGGGTCC
TCATTAGGAGCCCCCATCCCTGTGTTCCCCAAGAATTCAGAGAACAGCACTGGGGCTGGAATGATCTTTAATGGGCCCAAGGCCA
ACAGGCATATGCCTCACTACTGCCTGGAGAAGGGAGAGATTCAGGTCCTCCAGCAGCCTCCCTCACCCAGTATGTTTTACAGATT
ACGGGGGGACCGGGTGAGCCAGTGACCCCCTGTAGCCCCCAGCTTCAGGCCTCAGTGTCTGCCAGTCAAGCTTCACAGGCATTGT
GATGGGGCAGCCTTGGGGAATATAAAATTTTGTGAAGACTTGGA

B3GNT5 3'UTR sequence:

CTTGTAGGGCTGCGTTTATCTAATAGTACTTGAATGTTGTATGTTTTCACTGTCACTGAGTCAAACCTGGATGAAAAAAACCTTTA
AATGTTCGTCTATACCCTAAGTAAAATGAGGACGAAAGACAAATATTTTGAAAGCCTAGTCCATCAGAATGTTTCTTTGATTCTAG
AAGCTGTTTAATATCACTTATCTACTTCATTGCCTAAGTTCATTTCAAAGAATTTGTATTTAGAAAAGGTTTATATTATTAGTGAAA
ACAAAACTAAAGGGAAGTTCAAGTTCTCATGTAATGCCACATATATACTTGAGGTGTAGAGATGTTATTAAGAAGTTTTGATGTTA
GAATAATTGCTTTTGGAAAATACCAAATGAACGTACAGTACAACATTTCAAGGAAATGAATATATTGTTAGACCAGGTAAGCAAG
TTTATTTTTGTTAAAGAGCACTTGGTGGAGGTAGTAGGGGCAGGGAAAGGTCAGCATAGGAGAGAAAGTTCATGAATCTGGTAAA
ACAGTCTCTTGTTCTTAAGAGGAGATGTAGAAAAATGTGTACAATGTTATTATAAACAGACAAATCACGTCTTACCACATCCATGT
AGCTACTGGTGTTAGAGTCATTAAAATACCTTTTTTTGCATCTTTTTTCAAAGTTTAATGTGAACTTTTAGAAAAGTGATTAATGTT
GCCCTAATACTTTATATGTTTTTAATGGATTTTTTTTTAAGTATTAGAAAATGACACATAACACGGGCAGCTGGTTGCTCATAGGGT
CCTTCTCTAGGGAGAAACCATTGTTAATTCAAATAAGCTGATTTTAATGACGTTTTCAACTGGTTTTTAAATATTCAATATTGGTCT
GTGTTTAAGTTTGTTATTTGAATGTAATTTACATAGAGGAATATAATAATGGAGAGACTTCAAATGGAAAGACAGAACATTACAA
GCCTAATGTCTCCATAATTTTATAAAATGAAATCTTAGTGTCTAAATCCTTGTACTGATTACTAAAATTAACCCACTCCTCCCCAAC

AAGGTCTTATAAACCACAGCACTTTGTTCCAAGTTCAGAGTTTTAAATTGAGAGCATTAAACATCAAAGTTATAATATCTAAAACA
ATTTATTTTTCATCAATAACTGTCAGAGGTGATCTTTATTTCTAAATATTTCAAACTTGAAAACAGAGTAAAAAAGTGATAGAAA
AGTTGCCAGTTTGGGGTTAAAGCATTTTTAAAGCTGCATGTTCCTTGTAATCAAAGAGATGTGTCTGAGATCTAATAGAGTAAGTT
ACATTTATTTTACAAAGCAGGATAAAAATGTGGCTATAATACACACTACCTCCCTTCACTACAGAAAGAACTAGGTGGTGTCTACT
GCTAGGGAGATTATATGAAGGCCAAAATAATGACTTCAGCAAGAGTGACTGAACTCACTCTAAGGCCTTTGACTGCAGAGGCACC
TGTTAGGGAAAATCAGATGTCTCATATAATAAGGTGATGTCGGAAACACGCAAAACAAAACGAAAAAAGATTTCTCAGTATACA
CAACTGAATGATGATACTTACAATTTTTAGCAGGTAGCTTTTTAATGTTTACAGAAATTTTAATTTTTTTCTATTTTGAAATTTGAG
GCTTGTTTACATTGCTTAGATAATTTAGAATTTTTAACTAATGTCAAAACTACAGTGTCAAACATTCTAGGTTGTAGTTACTTTCAG
AGTAGATACAGGGTTTTAGATCATTACAGTTTAAGTTTTCTGACCAATTAAAAAAACATAGAGAACAAAAGCATATTTGACCAAG
CAACAAGCTTATAATTAATTTTTATTAGTTGATTGATTAATGATGTATTGCCTTTTGCCCATATATACCCTGTGTATCTATACTTGG
AAGTGTTTAAGGTTGCCATTGGTTGAAAACATAAGTGTCTCTGGCCATCAAAGTGATCTTGTTTACAGCAGTGCTTTTGTGAAACA
ATTATTTATTTGCTGAAAGAGCTCTTCTGAACTGTGTCCTTTTAATTTTTGCTTAGAATAGAATGGAACAAGTTTAAATTTCAAGGA
AATATGAAGGCACTTCCTTTTTTTCTAAGAAGGAAGTTGCTAGATGATTCCTTCATCACACTTACTTAAAGTACTGAGAAGAGTAT
CTGTAAATAAAAGGGTTCCAACCTTTTAAAAAAGAAGGAAAAAACTTTTTGGTGCTCCAGTGTAGGGCTATCTTTTTAAAAAATGT
CAACAAAGGGAAAATAAACTATCAGCTTGGATGGTCACTTGAATAGAAGATGGTTATACACAGTGTTATTGTTAAAATTTTTTTAC
CTTTTGGTTGGTTTGCATCTTTTTTCCATATTGTTAATTTTATACCAAAATGTTAAATATTTGTATTACTTGAATTTTGCTCTTGTATG
GCAAAATAATTAGTGAGTTTAAAAAAAATCTATAGTTTCCAATAAACAACTGAAAAATTATCATGA

B4GALT1 3’UTR sequence:

GAGCTAGCGTTTTGGTACACGGATAAGAGACCTGAAATTAGCCAGGGACCTCTGCTGTGTGTCTCTGCCAATCTGCTGGGCTGGTC
CCTCTCATTTTTACCAGTCTGAGTGACAGGTCCCCTTCGCTCATCATTCAGATGGCTTTCCAGATGACCAGGACGAGTGGGATATT
TTGCCCCCAACTTGGCTCGGCATGTGAATTCTTAGCTCTGCAAGGTGTTTATGCCTTTGCGGGTTTCTTGATGTGTTCGCAGTGTCA
CCCCAGAGTCAGAACTGTACACATCCCAAAATTTGGTGGCCGTGGAACACATTCCCGGTGATAGAATTGCTAAATTGTCGTGAAA
TAGGTTAGAATTTTTCTTTAAATTATGGTTTTCTTATTCGTGAAAATTCGGAGAGTGCTGCTAAAATTGGATTGGTGTGATCTTTTT
GGTAGTTGTAATTTAACAGAAAAACACAAAATTTCAACCATTCTTAATGTTACGTCCTCCCCCCACCCCCTTCTTTCAGTGGTATGC
AACCACTGCAATCACTGTGCATATGTCTTTTCTTAGCAAAAGGATTTTAAAACTTGAGCCCTGGACCTTTTGTCCTATGTGTGTGGA
TTCCAGGGCAACTCTAGCATCAGAGCAAAAGCCTTGGGTTTCTCGCATTCAGTGGCCTATCTCCAGATTGTCTGATTTCTGAATGT
AAAGTTGTTGTGTTTTTTTTTAAATAGTAGTTTGTAGTATTTTAAAGAAAGAACAGATCGAGTTCTAATTATGATCTAGCTTGATTT
TGTGTTGATCCAAATTTGCATAGCTGTTTAATGTTAAGTCATGACAATTTATTTTTCTTGGCATGCTATGTAAACTTGAATTTCCTA
TGTATTTTTATTGTGGTGTTTTAAATATGGGGAGGGGTATTGAGCATTTTTTAGGGAGAAAAATAAATATATGCTGTAGTGGCCAC
AAATAGGCCTATGATTTAGCTGGCAGGCCAGGTTTTCTCAAGAGCAAAATCACCCTCTGGCCCCTTGGCAGGTAAGGCCTCCCGG
TCAGCATTATCCTGCCAGACCTCGGGGAGGATACCTGGGAGACAGAAGCCTCTGCACCTACTGTGCAGAACTCTCCACTTCCCCA
ACCCTCCCCAGGTGGGCAGGGCGGAGGGAGCCTCAGCCTCCTTAGACTGACCCCTCAGGCCCCTAGGCTGGGGGGTTGTAAATAA
CAGCAGTCAGGTTGTTTACCAGCCCTTTGCACCTCCCCAGGCAGAGGGAGCCTCTGTTCTGGTGGGGGCCACCTCCCTCAGAGGCT
CTGCTAGCCACACTCCGTGGCCCACCCTTTGTTACCAGTTCTTCCTCCTTCCTCTTTTCCCCTGCCTTTCTCATTCCTTCCTTCGTCTC
CCTTTTTGTTCCTTTGCCTCTTGCCTGTCCCCTAAAACTTGACTGTGGCACTCAGGGTCAAACAGACTATCCATTCCCCAGCATGAA
TGTGCCTTTTAATTAGTGATCTAGAAAGAAGTTCAGCCGAACCCACACCCCAACTCCCTCCCAAGAACTTCGGTGCCTAAAGCCTC
CTGTTCCACCTCAGGTTTTCACAGGTGCTCCCACCCCAGTTGAGGCTCCCACCCACAGGGCTGTCTGTCACAAACCCACCTCTGTT
GGGAGCTATTGAGCCACCTGGGATGAGATGACACAAGGCACTCCTACCACTGAGCGCCTTTGCCAGGTCCAGCCTGGGCTCAGGT
TCCAAGACTCAGCTGCCTAATCCCAGGGTTGAGCCTTGTGCTCGTGGCGGACCCCAAACCACTGCCCTCCTGGGTACCAGCCCTCA
GTGTGGAGGCTGAGCTGGTGCCTGGCCCCAGTCTTATCTGTGCCTTTACTGCTTTGCGCATCTCAGATGCTAACTTGGTTCTTTTTC
CAGAAGCCTTTGTATTGGTTAAAAATTATTTTCCATTGCAGAAGCAGCTGGACTATGCAAAAAGTATTTCTCTGTCAGTTCCCCAC
TCTATACCAAGGATATTATTAAAACTAGAAATGACTGCATTGAGAGGGAGTTGTGGGAAATAAGAAGAATGAAAGCCTCTCTTTC
TGTCCGCAGATCCTGACTTTTCCAAAGTGCCTTAAAAGAAATCAGACAAATGCCCTGAGTGGTAACTTCTGTGTTATTTTACTCTT
AAAACCAAACTCTACCTTTTCTTGTTGTTTTTTTTTTTTTTTTTTTTTTTTTTTTTGGTTACCTTCTCATTCATGTCAAGTATGTGGTTCA
TTCTTAGAACCAAGGGAAATACTGCTCCCCCCATTTGCTGACGTAGTGCTCTCATGGGCTCACCTGGGCCCAAGGCACAGCCAGG
GCACAGTTAGGCCTGGATGTTTGCCTGGTCCGTGAGATGCCGCGGGTCCTGTTTCCTTACTGGGGATTTCAGGGCTGGGGGTTCAG
GGAGCATTTCCTTTTCCTGGGAGTTATGACCGCGAAGTTGTCATGTGCCGTGCCCTTTTCTGTTTCTGTGTATCCTATTGCTGGTGA
CTCTGTGTGAACTGGCCTTTGGGAAAGATCAGAGAGGGCAGAGGTGGCACAGGACAGTAAAGGAGATGCTGTGCTGGCCTTCAG
CCTGGACAGGGTCTCTGCTGACTGCCAGGGGCGGGGGCTCTGCATAGCCAGGATGACGGCTTTCATGTCCCAGAGACCTGTTGTG
CTGTGTATTTTGATTTCCTGTGTATGCAAATGTGTGTATTTACCATTGTGTAGGGGGCTGTGTCTGATCTTGGTGTTCAAAACAGAA
CTGTATTTTTGCCTTTAAAATTAAATAATATAACGTGAATAAATGACCCTATCTTTGTAACTGCA

B4GALT3 3’UTR sequence:

CTCTATCTACTGCCAACCACACAGCCCTCCGAGGTTCACACTGACTCCTCCTTCCTGTCTACCTTAATCATGAAACCGAATTCATG
GGGTTGTATTCTCCCCACCCTCAGCTCCTCACTGTTCTCAGAGGGATGTGAGGGAACTGAACTCTGGTGCCGTGCTAGGGGGTAGG
GGCCTCTCCCTCACTGCTGGACTGGAGCTGGGCTCCTGTAGACCTGAGGGGTCCCTCTCTCTAGGGTCTCCTGTAGGGCTTATGAC
TGTGAATCCTTGATGTCATGATTTTATGTGACGATTCCTAGGAGTCCCTGCCCCTAGAGTAGGAGCAGGGCTGGACCCCAAGCCCC
TCCCTCTTCCATGGAGAGAAGAGTGATCTGGCTTCTCCTCGGACCTCTGTGAATATTTATTCTATTTATGGTTCCCGGGAAGTTGTT
TGGTGAAGGAAGCCCCTCCCTGGGCATTTTCTGCCTATGCTGGAATAGCTCCCTCTTCTGGTCCTGGCTCAGGGGGCTGGGATTTT
GATATATTTTCTAATAAAGGACTTTGTCTCGC

B4GALT4 3’UTR sequence:

CAACATCACAGTGGATTTCTGGTTTGGTGCATGACCCTGGGTCTTTTGGTGATGTTTGGAAGAACTGATTCTTTGTTTGCAATAATT
TTGGCCTAGAGACTTCAAATAGTAGCACACATTAAGAACCTGTTACAGCTCATTGTTGAGCTGAATTTTTCCTTTTTGTATTTTCTT
AGCAGAGCTCCTGGTGATGTAGAGTATAAAACAGTTGTAACAAGACAGCTTTCTTAGTCATTTTGATCATGAGGGTTAAATATTGT
AATATGGATACTTGAAGGACTTTATATAAAAGGATGACTCAAAGGATAAAATGAACGCTATTTGAGGACTCTGGTTGAAGGAGAT
TTATTTAAATTTGAAGTAATATATTATGGGATAAAAGGCCACAGGAAATAAGACTGCTGAATGTCTGAGAGAACCAGAGTTGTTC
TCGTCCAAGGTAGAAAGGTACGAAGATACAATACTGTTATTCATTTATCCTGTACAATCATCTGTGAAGTGGTGGTGTCAGGTGAG
AAGGCGTCCACAAAAGAGGGGAGAAAAGGCGACGAATCAGGACACAGTGAACTTGGGAATGAAGAGGTAGCAGGAGGGTGGAG
TGTCGGCTGCAAAGGCAGCAGTAGCTGAGCTGGTTGCAGCTGCTGATAGCCTTCAGGGGAGGACCTGCCCAGGTATGCCTTCCAG
TGATGCCCACCAGAGAATACATTCTCTATTAGTTTTTAAAGAGTTTTTGTAAAATGATTTTGTACAAGTAGGATATGAATTAGCAG
TTTACAAGTTTACATATTAACTAATAATAAATATGTCTATCAAATACCTCTGTAGTAAAATGTGAAAAAGC

B4GALT5 3’UTR sequence:

GAGTACTGAGAGGAGAGAATGTACGTTTGCTTTACCCACCGCCACCAAGAAAGCAGTCCGATGAGATTTTTTTTGGAGGGGGGA
GGGTCTACACAGCAAGAGAACAGAAATACTGTGTCTCATGAAGGATCACAGAGTTCAGGGGGAAAATGTGACAGCACACGCACA
AACGCCTTCACTGGATCAGCCGCTGGAACTGAGGGAGTGAGCTTGGGGACTTCCTTCGTCAGCACTGGCTTTCTGTTTTCACAAGA
CAGACGTCTGTCCCGCTGCTCTCTCCCCATCTCCTACCCCACATCCTGTCTTAGCCGCAGTCTCCAGAACCCATGATGAACTGTGAT
CTGCCGTGGTCCTGCCGTGGTCCTGCCGTGGAGCCTGTCCCTACACATGACCTTGGAGCCTCTTGGCCTTCAGAGCAGAGGCAAAC
CCACCACAGGGCAGCTGCGTTTTAGGAAGAGCAAATGAAACTCCACACCATTCTTCTAGATCTCTGGTGTTCTCTTTGGTTTCATTT
TTTTAAAAAATTACCTTCTTTGGGTGGGGATTGAGGGTGGAGGGGAGGGTGTTTGGGAAAGATAAATAGACATAAATATATAACA
ATCACTTCTTGAAGAAGTATAATTGTAAATAAGCCATGTAAAATGCCTTTTTAAAATTTAATTTTCTAGCTGGCTCCAATTCAAATT
GAGGATTTATGTATTAGGCCACTTACTTGGTTGGCAAGTGCAGGAACTCAGTTAAAATGCAGTTGAAGAATGTCATCTCCCGAATT
GCTGTCACTTTGGCGAGGGAGTGGATATAGGGCATGTCACAAAAGAACAAAATAACCCGACCTTTATTGCTGGGAGCTGGCTTCT
GTCCCTTTCTTCCCCCCCCCACGAGTCTTGCCCTTGACTTCTGCTCTGGATTCACTCTTCCCTGTCGGCCGCGCATGTGCTCATCCCA
CTCTCCGCTAAGCGGGAGGCTGCTGTTAGAGCAGGCTGCTTCCTGCCTAAAGCAGGCCCTTCGGGGCTCGCTGCACACACATCTCT
GGCTCTCCAGGCTTCGTGTTCTGTCTTTTCATCAGCATGGCGGGGCGGGGGGCGGGGGGCGGGGGTGTGTATGGGAATCCCTCCC
CCTCTTACTTTTTCTCTTGTGGAACTTGGCCACAGTTTCTGAACAATGTGCCTACATTACCAGCTGGCTTCAGTGATTCCTCTGTGT
CCCTTTTTGGTTTCTGGAAAGATTCTTTGTCAACATTAGTAACTGATACATAGAACCAAGGAGCACTCAAATAGGGAGCCAGGAG
CCAGGGAGCTGGTGACACTTGTGTGCTGTGGGGCAGCTGGGATCCAGGTAAGACCGGATTGAAGCTTTGAAATTAGACTAACAAA
GCTCCAGACAGCAAGAGCCCAGGTGCACTGCTCACACCCCCACCTGCATTTTGAAGTCATATTATTTTTTGTTTTGTTTTTTAAGAC
GGTCTGGCTCTGTCGCCTAAGCTGGAGTGTGGTGGCACGATCACAGCTCACTGCAGCCTCCATCTCCTAGGCTCAAGCCATTTTCC
CACCTCAGCCTCCCGAGTAGCTGGGACTACAGGTGCACACCACCACACCTGGCTAATTTTTTGTATTTTTAGTAGAGACAGGGGTT
TCTTCCATGTTGCCCAGGCTGGTCTCGAACTCCTGGACTCAAGCAATCCGCCCACCTTGACTTCCCAAAGTGCTGGGATTATGGGC
GGGTGTGAGCCATTGCGCCCAGCCTTGAAGTCATGTTCTAAATTGTATTTGAATTTGTGCCTCTTTGTTTTTCCCCAAACCAAAGCC
CTCAAATTGTAGTCTCTGTCGGCTTCTGCAGAATTCTGGAAAATGCCAGTTTTCCTCCCCCGCCCTTGTTTTCCATAAAACATATTT
ATATATTGTGATGAGGAGTACTTTCTGAAGAGTACTTCGTATTTTTTTTTAATTGCCTTGTTTGCCTTCAACTTCCTTGATTTTCATA
GTTTACATGGGTGTGTGTAGGGGTGTGTGTGTGTATGTGTGTGGGTTAGGGCTTTTTTCGTTGCATGTGATGGTTCTGTGGACATAT
GATCCCCACAAACTGTGGGAGTGATTGGCCAGGCCTTGTTTTGTTTGTTTGTTTGTTTGTGTTTTTGTTCTTTTGAAGAATAGAGTG
GTATTTAGAAAATAAATTGCATTGCAAAGCTCTTATCGGCTCATATGAGAGAGCAGGTTCCTGCCCTTGAAAATGCCGGTAAGCT
ATAGCATATGTTTTTTAAGACTTAAGCATTTCATGCTTTAAAATACCTTCACAAGTGAACATTACACACAGAAGTTCATTTGGTTTT
CCTTTGTTTTATGGTGCATATAGCAATAAAGACCCCCCTCCACCCTGCAACCCCCATCCCCCACCGGGCCTTTGTCCCTGCCTTGGC
TTTTCTCCCCTTCTCATTCTCCTCTCCCCTTTCCTCACTGAAGGCTGTGAGTTGCTTTCAATGTGACAACACTATGATGTCATTTGGA
AGGATTTGCCAGGACAGACTGATTCTGAGTCCTGGGTGCCGTATGTGTATGCGGCAGTGTTGTCAGGCGATCTTGTTTGAAGCTCT
ATGTTGCCATAATTACCATCAAGTACACACTGTTGGCAAAAGGCTAACACCTGACTTTAGAAAATGCTGATTTGAGAACAAAAGG
AAAGGTCTTTTTTCACTGCTTAAAGTGGGGTCACTTTGATACCTTTGCGGTCATGTCTGTGTCTGATGAGTGTAGAATCTCTGGATG
TGCACTGTCAGTCATGTGTCCACCAGGCCTCGAATATCATATGGGAAATGTCATAGTTAAAAACGTACAGCCAGGCCCGTGTGCT
GTTAATAGTGTGAAATTGTCATGTTAAAAAAAAAAACAGGAACCAAATGTGACCTTGTGCATATATTGGTAGCTGAAAATCTTCA
AGGCTACTGATGGGTGGCCCCTTAATCTTGTCTTTGATTGCTGTGTGCAGGGAAAGGTGTCCCCGTTTGTTCATGCTGTTTTGGGGG
GTGGGGGGGTATTTGCAAGAATACTCATTTTGACATAATAGGTCCTCTTGTCAGAGATCCTCTACCACAGACATTAATAGCTGAGC
AGGAGCCACATGGATTGATTGTATCCACTCACCATTGACGATGGCATTGAGCGTAGCTAGCTTATTTCCATCACTACGTGTTTTTG
AGCTTGCTCTTACGTTTTAAGAGGTGCCAGGGGTACATTTTTGCACTGAAATCTAAAGATGTTTTAAAAAACACTTTTCACAAAAA
TAGTCCTTTGTCATTACATTATTTACTCATGTGTTTGTACATTTTTGTATGTTAATTTATGAATGATTTTTTCAGTAAAAAATACATA
TTCAAGAACCAAA

PIGA 3’UTR sequence:

AAGGAAGCCTAGATTGTAAGATTTTAAACATTTGTAATAGTTCTATAAAGACTATGGAAAATAACCTTGCTTTTGGGGGGTTTTTG
TTTTTTTAGAGTTAATTTAGTAAGTTATGCTACCTCTATATCATTCAATATTTTCTGTTGAGGAAAGATAAAAATGTATGCAATTCC
TGAGTGTAGAAACTTCTTGCACTTATTTAAAATTTAGGAGAGAACATTTAAGCCACTCAGGTATGCAATTTTTCAGACTACTGAAA
TCCCTGTAGCAGAGATGTTTTAACATTATATTTTGAGAGCTTTGGGTGCTGAAGGGCCAAACGTTTTCTGGGCATTTTTTGGCCAGT
TTTTAATGTAACACCATTAGACACTCACCAGATGTTTACAAGTTTTCTTTAGGGGAACTACAACAATTATATGAACTGTTTTATATC
ATGTTCATATACATTTATTAGGAATCTAAATCATGTCTTTGAACATTTATTAGGTTCACTCAGTAGGTGTTACATGTAATTAACAGG
TTCCTTGAGTAAGATAGTCCATCAGTTACCAGCACATTTTGAACCCCTGCTCTGTGTAGAATGTTGAACTAGATGCTTCCCGCCATT
AAGGACCAGGGGTGCATTCACTCTTTGTTTACCATTCAAATGGCTTACTTCATCATAATTGTGGTTGATATGAGATCAATATCCAA
CATGCCAAAAATGCTCATGCCAGTTAATGCCAGGAAAAAAATCACCGACACACTACTAGTACTTTGTTCCTGTTGTATGCATTCTC

CTAGGTAGAGCCTCCATCTTCAGTTGTGTTTGTGAAGGTATTTTTTGCTTTTTAAATACTGGGGACCGATATCACTGTTGATAGTGC
AGAGAAACCCTCCACATTTTTCAGTGCATAATTGAGTTTTCTATAAATGCCTTCGTGTTTTCTGAGCAGAATGTACGAGGTGTGCC
ATCCCAAAACCAGCTGCTACCCTGTCCTTTTAATGTAAGTCACTCCCCTTCACTGTGGCCTCGCTGATGTCTGATAAGTATTGTCAG
TGTGCAAAAGGCTTTACTTCAGAATGGTTTATTTATAGCAAACTAAGTTGAAAATTTTAGAAACAGTCTTTGTGGGTGGATGTTAT
TAACTGTCATTGTTGTTGCCCAGAGCCATGGGTTTTTTAACCCCAAATTATCCACATGGTGTGTATTATGAATTCTTTGAACTCTTA
AGGTTTTTGTGAGAAAAGGACTGTGAATTCAAAACAATAAGGCACTTGTGGGTGCACTACATAGATTCTGACAGTGTTGTGATTCT
GTATAGGATTTTTAAAAATGACAACATTCACAAAATTTATTACTTTTTAAAAAATAACATGCCTATTAACTGGTTGCACTGATATA
AAAGAAATATATTTGTGTTTTGTTTGTACTAAAATGCAAAAGCAAGAGTGCAATTTTTAAAATCTAGAAGTTAGGGGTTTTGTTGG
AGAAAAATGGACTGATCTTTAAACTATTCAGTCTTACTGGGATTTTTATGCATAGAAACTCACATATAAACATGAAATAAACAGT
GCCAGTATTCATAGGAAAGTGAGAAACTGTAATATTTGGCCATTATTCTATTCAACAGGTTTTAGAGGCATGCCACCATTTTTTCC
TTATATTTTTGCTTAATTTTTTTAAATTGTCATTTAATTCTTAAACTGTCATTTATTTGAGATGGAAATAAGATCTAAAGTTAGTTGC
CTTTGCCTGTAAAACATGTGATTTGCAAATTATTATTTTTCTTTTTTTTAACAAATGGAAGTAAATTTGTTTCACGTAAATCTTAATT
TTCAACCTTTCTGGATACCTTAATTGTAACTGTCAGTTTGCACTGGTCGGTATATGGAAACACATTGCTCTACCCTGCTACTTAGTT
GATTTTAAAGTGAATTTACAGTGATGAGAAATTTGTGAAAAATATATTGTATTTCTTTTGATGTTTCAAAAGGTTGCCTATGAAAA
ACTGATTTGTTAAAACATGCTACATGTCCAAAAATAAAGACCAGAATGACATTTTGATAATTTTC

PIGK 3'UTR sequence:

GACTTGATGATGAATGAAGAATGCATGGAGGACTGCAAACTTGGATAATAATTTATGTCATTATATATTTTTAAAAATGTGTTTCT
CTTGTATGAATTGGAAATAAGTATAAGGAAACTAAATTTGAATCAACTATTAATTTTATAACTTAAAGAAAAATAATTGTTAATGC
AACTGCTTAATGGCACTAAATATATTCCAGTTTTGTATTTTGTGTATTATAAAAGCGAATGAGACAGAGATCAGAATACATTGACT
GTTTTTGAAAATAGTAATTTCCCCTTATCCCCTTTTCATTTGGAAAAGAAACAATTGTGAAGACATTAAATTCTCACTAACAGAAG
TAACTTTGGTTAATTATTTTTTGTATATCCTCCCAATCTTTTGACTTATGCACATATTTTTTCCCAATATGGAGATCATATGGAATGT
ACTATTTTGTAATGTCTTTTTTCATTTTACAATGTATTATCAACCTTTTCCCTCTCAAAAATACATTGTGAATGACTGCATAGTATTC
ACTTTATGAATATTTAATTCATTTCACAGTCTTCTATTGTTGGACCACTTACATTGTACCAAATGTTTTCCTTTGGTTTATTCTTTAA
TGTATTAATATTTTACTGCTGGTCACTCATGGAATCCTGCAGCTTTAATTAAAAGCAAAGATGAAAAATTGGTTTTTTAATCTATG
GCACTGACAATCTCCAGGACCTTATATGTTTGTTGTCAGTTTATTTGGGAAATTTTAGACCTTTGATAATTTCACGTACTGACTGCT
CAAGAGAAACATACCCCATTGTTTTTCATTTGTAAGCGTTCTGTGATCTTCTACAATTGGTCACGTCCTCTTCATTTTCCATCTTGA
AAGAGAGAGCCAACAAGGACTTTATTTCATTCTGTTTTAGGTAAACCTCCTTGCCCACTGGCTGTATCTATACTTTCCTTGAGAAA
AATCCCATAAAGTGGATGGACCTGTGAAGAAAATGTATGCTTATGGCCTAGCCTTCATGTCTGGCTGATGTATCCTATAAGGCAGT
AAGCCCCTTTTCTAGTCTCTGGTAAGATGCAAGAGCTCATATCCCCATCACTGACATTTTAGTTTGGAAATAATATTGAGACTGTG
CTATGACCAACCCCTGATGTTGTTTTTTCTTTTCAAACTTTTGCATATGAGTAGAGGAAAAGCCTAAAAGTTAAGTATTTATGTCTG
GGGGGATACCTTCAGGTGTCTTATCTGTTTTATGCAAGAATTTATGTGTTCATCTTTATTCAGTGCAAAGATTTTTTTTAAATTTTG
TTTATAATTGTAGGTAACATTAAGACAACTCTTCCTCCACAAGAAAACCTCCTAAAATTAATATTCCTTAAGATTTGTTTTTCCTTT
TGCACTTATAATATTACCTTTTAATTGCATGCAAGATTGTCATACTTTTCAAAAGGCAAAGGATTGACTGTGTTATCTCCCTAGTTA
GAACAAATGATATTGAGGCTTTTTGCCAGCTCTGAATCTTTATTTTAATTGATCTTTTTATTGATGTGTTATATAAATGAGGAAGAA
AAATTTTGTCTGATTATGTGAAGGATCTTTCTGTACATGAAAAGAAGGGAAAATAAACTTGCAATTGAATAGACTGATTATAGTA
GCACTGAGACACAAAAAGATTGACCATGTTGCCCTCCAGACACTCATACAAGGTCGTGGACACCACGGTGAGGCGGAGCTATTTA
GGGTGGTAAAGGAATTATGATTGTTCTTGAGCCAAAGTAATTTAGTTTGAATATAATGAAACATACCCTGTAAAGACTGCTAGAA
AGTAAAAGGATTCGTCTTCAGAGGTTGTAGAAGGTGCCCTTCTTAGTTAAAACCAAACTGGGAAAAGTAATACTGGATAAAATAT
TCAGGATAAATTTTGCCTCAGCAGAATTTCAAAGGGCAGTTGTTCCTCTGTTTCATTATTGAATCTTCAGAATATAGTTAAAGCCA
AAAGCTTAAAATATGTTAAATGTTTCACTTATAACCATAATCTTTTTACATAGAGCATACTCTGCCTTCATAATAACTAAATCCTCT
GCATGTGGTAGATGAGTACGTTTAGGAAATATTGTCAGTGCAATTAAATGGCCTACACTTTAAACAGTATCATAAAAACAAATCC
TTAAATATATTCTACTTGAGTCACAAAAGCTGAACAACAGAAAGGTGTTTTGTTTTTGCCTTTCTCACAGTGTTGTGGTGAGAATC
AGATGAGATAGTATTTTGACTAAACACTTCTGAAATTGTAAATATATGGTGGCATTATTGTTCTTATGTCGGCTTAGGAGGATACC
AAAGGGGAAGTTAATGGTCACAGTGCACTTATGTAGCTTTCTAAGCTACTCAATGTGATTCTTGTTCTCTTTGCTGTTCTTTTTCTC
CTCCCCCATGGTGTCCTTCAGAGAGAAAAGGAATGTAGATAAATGAATCCCTGCAGATGTGTCCTGACATTTCAGGGAGGGACAG
GGTATAATGATGCCATCCTGCAAAGGCAGCCTGTGTGAGAAAAAGAAATCAAATAATGTGGATTTTAAAATTACGAAAGACATTC
ATTTGCAGTTTATGAAAGGAAAATGTAGTTTGGATACAAAGCTGATTAAATTGGATCAAGAAATATTAGAATTAAATGCAAAAAA
TAATCCATGCATTTATGGTTTTGATTTTTATATATTCCCAGCTAGTTGAAAATGATGATTCCCACAAGAAGCATAACTCAGCTTGTT
TCTGCTTACTGAGTATTTTCTACTATGGTATATATTGATAACATTTCTTCCATTATGTATGTTGTATACCAGAGTTACAGTTACTGTG
GGAATCATAATTTGAAATTTTGACTCCTGTGTTTCTGGAATCTTTACAACAAATGTTGCATTAACATATAACTTTTTTCAGTTGACT
TTACCAAAATTAAGCCCATCTTTAGTAGATACTGTTTTAACATGTGAAAGAAATACGTTATAAACATACCCACAAGATATGGCTATA
AAACAATGAGATCAGTATCCATTTTTGCTTTAAAGAATTGGCCTTATTGCTTCAGTGTCACATCTCATACTCAAGGGCATTTACTAC
AAAGAAAGAGTTCTCCAATATTGCTGTTCTGTTGCTGCCTGCCCTATTTACACATGTACCTGCTACTTAAATAGGAAAGCCTTTCA
ATTCATGGACAATACACCTTGGTGGTAACCAGGCTTTTATTTTTATTTTTTTTTCTTAGTGTAAAAACTGTACTGTTTTGGAAATGT
GCTGTGAAATATTAGGTTTAACTGTGTAGATCCTAGAATAAGGGGATTTATATAGATGAAGTTGTAACCAAGAAACTGGTTATTA
AAAATTTATTTACTCCAAACATGGAA

Sequence 2. Plasmid Map of pSFmiR-gene-3'UTR and sequence of 3'-UTR of different glycosylation genes.

References

1. Schmiedel, J. M.; Klemm, S. L.; Zheng, Y.; Sahay, A.; Bluthgen, N.; Marks, D. S.; van Oudenaarden, A., Gene expression. MicroRNA control of protein expression noise. *Science* **2015,** *348* (6230), 128-32.
2. Liu, B.; Li, J.; Cairns, M. J., Identifying miRNAs, targets and functions. *Brief Bioinform* **2014,** *15* (1), 1-19.
3. Paul, P.; Chakraborty, A.; Sarkar, D.; Langthasa, M.; Rahman, M.; Bari, M.; Singha, R. S.; Malakar, A. K.; Chakraborty, S., Interplay between miRNAs and human diseases. *J Cell Physiol* **2018,** *233* (3), 2007-2018.
4. Bartel, D. P., Metazoan MicroRNAs. *Cell* **2018,** *173* (1), 20-51.
5. Wolter, J. M.; Kotagama, K.; Pierre-Bez, A. C.; Firago, M.; Mangone, M., 3'LIFE: a functional assay to detect miRNA targets in high-throughput. *Nucleic Acids Res* **2014,** *42* (17), e132.
6. Bracken, C. P.; Li, X.; Wright, J. A.; Lawrence, D. M.; Pillman, K. A.; Salmanidis, M.; Anderson, M. A.; Dredge, B. K.; Gregory, P. A.; Tsykin, A.; Neilsen, C.; Thomson, D. W.; Bert, A. G.; Leerberg, J. M.; Yap, A. S.; Jensen, K. B.; Khew-Goodall, Y.; Goodall, G. J., Genome-wide identification of miR-200 targets reveals a regulatory network controlling cell invasion. *EMBO J* **2014,** *33* (18), 2040-56.
7. Kurcon, T.; Liu, Z.; Paradkar, A. V.; Vaiana, C. A.; Koppolu, S.; Agrawal, P.; Mahal, L. K., miRNA proxy approach reveals hidden functions of glycosylation. *Proc Natl Acad Sci U S A* **2015,** *112* (23), 7327-32.
8. Agarwal, V.; Bell, G. W.; Nam, J. W.; Bartel, D. P., Predicting effective microRNA target sites in mammalian mRNAs. *Elife* **2015,** *4*.
9. Betel, D.; Koppal, A.; Agius, P.; Sander, C.; Leslie, C., Comprehensive modeling of microRNA targets predicts functional non-conserved and non-canonical sites. *Genome Biol* **2010,** *11* (8), R90.
10. Vogel, C.; Marcotte, E. M., Insights into the regulation of protein abundance from proteomic and transcriptomic analyses. *Nat Rev Genet* **2012,** *13* (4), 227-32.
11. Ostlund, G.; Sonnhammer, E. L., Quality criteria for finding genes with high mRNA-protein expression correlation and coexpression correlation. *Gene* **2012,** *497* (2), 228-36.
12. Gumienny, R.; Zavolan, M., Accurate transcriptome-wide prediction of microRNA targets and small interfering RNA off-targets with MIRZA-G. *Nucleic Acids Res* **2015,** *43* (18), 9095.
13. Reczko, M.; Maragkakis, M.; Alexiou, P.; Grosse, I.; Hatzigeorgiou, A. G., Functional microRNA targets in protein coding sequences. *Bioinformatics* **2012,** *28* (6), 771-6.
14. Wang, X., Improving microRNA target prediction by modeling with unambiguously identified microRNA-target pairs from CLIP-ligation studies. *Bioinformatics* **2016,** *32* (9), 1316-22.

15. Chi, S. W.; Zang, J. B.; Mele, A.; Darnell, R. B., Argonaute HITS-CLIP decodes microRNA-mRNA interaction maps. *Nature* **2009,** *460* (7254), 479-86.
16. Hafner, M.; Landthaler, M.; Burger, L.; Khorshid, M.; Hausser, J.; Berninger, P.; Rothballer, A.; Ascano, M., Jr.; Jungkamp, A. C.; Munschauer, M.; Ulrich, A.; Wardle, G. S.; Dewell, S.; Zavolan, M.; Tuschl, T., Transcriptome-wide identification of RNA-binding protein and microRNA target sites by PAR-CLIP. *Cell* **2010,** *141* (1), 129-41.
17. Eichhorn, S. W.; Guo, H.; McGeary, S. E.; Rodriguez-Mias, R. A.; Shin, C.; Baek, D.; Hsu, S. H.; Ghoshal, K.; Villen, J.; Bartel, D. P., mRNA destabilization is the dominant effect of mammalian microRNAs by the time substantial repression ensues. *Mol Cell* **2014,** *56* (1), 104-15.
18. Mukherji, S.; Ebert, M. S.; Zheng, G. X.; Tsang, J. S.; Sharp, P. A.; van Oudenaarden, A., MicroRNAs can generate thresholds in target gene expression. *Nat Genet* **2011,** *43* (9), 854-9.
19. Lemus-Diaz, N.; Boker, K. O.; Rodriguez-Polo, I.; Mitter, M.; Preis, J.; Arlt, M.; Gruber, J., Dissecting miRNA gene repression on single cell level with an advanced fluorescent reporter system. *Sci Rep* **2017,** *7*, 45197.
20. Ziauddin, J.; Sabatini, D. M., Microarrays of cells expressing defined cDNAs. *Nature* **2001,** *411* (6833), 107-10.
21. Wheeler, D. B.; Carpenter, A. E.; Sabatini, D. M., Cell microarrays and RNA interference chip away at gene function. *Nat Genet* **2005,** *37 Suppl*, S25-30.
22. Kittler, R.; Pelletier, L.; Heninger, A. K.; Slabicki, M.; Theis, M.; Miroslaw, L.; Poser, I.; Lawo, S.; Grabner, H.; Kozak, K.; Wagner, J.; Surendranath, V.; Richter, C.; Bowen, W.; Jackson, A. L.; Habermann, B.; Hyman, A. A.; Buchholz, F., Genome-scale RNAi profiling of cell division in human tissue culture cells. *Nat Cell Biol* **2007,** *9* (12), 1401-12.
23. Genovesio, A.; Giardini, M. A.; Kwon, Y. J.; de Macedo Dossin, F.; Choi, S. Y.; Kim, N. Y.; Kim, H. C.; Jung, S. Y.; Schenkman, S.; Almeida, I. C.; Emans, N.; Freitas-Junior, L. H., Visual genome-wide RNAi screening to identify human host factors required for Trypanosoma cruzi infection. *PLoS One* **2011,** *6* (5), e19733.
24. Castel, D.; Pitaval, A.; Debily, M. A.; Gidrol, X., Cell microarrays in drug discovery. *Drug Discov Today* **2006,** *11* (13-14), 616-22.
25. Erfle, H.; Neumann, B.; Liebel, U.; Rogers, P.; Held, M.; Walter, T.; Ellenberg, J.; Pepperkok, R., Reverse transfection on cell arrays for high content screening microscopy. *Nat Protoc* **2007,** *2* (2), 392-9.
26. Sturzl, M.; Konrad, A.; Sander, G.; Wies, E.; Neipel, F.; Naschberger, E.; Reipschlager, S.; Gonin-Laurent, N.; Horch, R. E.; Kneser, U.; Hohenberger, W.; Erfle, H.; Thurau, M., High throughput screening of gene functions in mammalian cells using reversely transfected cell arrays: review and protocol. *Comb Chem High Throughput Screen* **2008,** *11* (2), 159-72.
27. Rantala, J. K.; Makela, R.; Aaltola, A. R.; Laasola, P.; Mpindi, J. P.; Nees, M.; Saviranta, P.; Kallioniemi, O., A cell spot microarray method for production of high density siRNA transfection microarrays. *BMC Genomics* **2011,** *12*, 162.
28. Kim, H. C.; Kim, G. H.; Cho, S. G.; Lee, E. J.; Kwon, Y. J., Development of a cell-defined siRNA microarray for analysis of gene function in human bone marrow stromal cells. *Stem Cell Res* **2016,** *16* (2), 365-76.
29. Bajar, B. T.; Wang, E. S.; Lam, A. J.; Kim, B. B.; Jacobs, C. L.; Howe, E. S.; Davidson, M. W.; Lin, M. Z.; Chu, J., Improving brightness and photostability of green and red fluorescent proteins for live cell imaging and FRET reporting. *Sci Rep* **2016,** *6*, 20889.
30. Kohen, N. T.; Little, L. E.; Healy, K. E., Characterization of Matrigel interfaces during defined human embryonic stem cell culture. *Biointerphases* **2009,** *4* (4), 69-79.

CHAPTER 3

DEVELOPMENT OF MIRFLUR HIGH-THROUGHPUT PLATFORM FOR MAPPING MIRNAS-GENE INTERACTOME NETWORK

This chapter contains content published in **Thu, C.T**., Chung, J. Y., Dhawan, D., Vaiana, C. A., and Mahal, L. K. High-Throughput miRFluR Platform Identifies miRNA Regulating B3GLCT That Predict Peters' Plus Syndrome Phenotype, Supporting the miRNA Proxy Hypothesis. *ACS Chemical Biology,* **2021**, *16*, 1900-1907**.**

3.1 ABSTRACT

MicroRNAs (miRNAs, miRs) are small endogenous non-coding RNAs that finely tune protein expression at the posttranscriptional level. Each miR has the capacity to potentially regulate several hundreds of mRNAs, thus creating a large and complex regulatory network to control specific biological processes. It was clearly established that miRs significantly modulate numerous pathophysiological processes including proliferation, differentiation, metabolism and apoptosis. Through their interactions with mRNAs, they can regulate both mRNA and protein levels by impacting the translational process and/or stability of mRNA. They are critical regulators of glycosylation, one of the most diverse and abundant posttranslational modifications. miRs have predicted the biological functions of glycosylation enzymes, leading to the "miRNA proxy hypothesis" which states, "if a miR drives a specific biological phenotype…, the targets of that miR will drive the same biological phenotype." The capacity to test this powerful hypothesis is hampered by our lack of understanding of miR target. Computational tools to identify miR targets usually suffer from low accuracy and a high false prediction rate.

This chapter focuses on the development of a high-throughput experimental platform to analyze miR-target interactions, miRFluR. We utilized this system to analyze the interactions of the entire human miRNAome with beta-3-glucosyltransferase (B3GLCT), a glycosylation enzyme whose loss underpins the congenital disorder Peters' Plus Syndrome. Although this enzyme is predicted by multiple prediction algorithms to be highly targeted by miRs, only 27 miRs downregulate B3GLCT leading to a >96% false positive rate for prediction. Functional enrichment analysis of these validated miR networks predicts phenotypes associated with Peters' Plus Syndrome, although B3GLCT is not in their known target network. Thus, the biological functions

of B3GLCT can be predicted by the miRNA network that regulate B3GLCT, providing support for the miRNA Proxy Hypothesis.

3.2 INTRODUCTION

miRs are emerging as critical regulators of the glycome [1-4]. Glycosylation is one of the most abundant and diverse post-translational modifications with roles in almost every disease state [5]. However, identifying which glycosylation enzyme underlies which glycan epitope and concordant biology is still a barrier to our understanding of the glycome. Previous work from our laboratory integrated a public gene and miR expression dataset from the National Cancer Institue, NCI60 cancer cell line, with glycomic lectin array data to identify miR regulatory networks that control glycosylation to argue that miRs are key regulators of the glycome [2]. Downregulation of miR targets often recapitulates the phenotype induced by a miR. Our laboratory realized that this might enable us to identify biological phenotypes of specific glycogenes, a point we demonstrated in work by Kurcon *et al.* [3]. In this work, it was shown that the currently used methods (transcriptomic profiling and crosslinking assay) to identify miRNA targets failed to observe any actual glycosylation enzyme targets (B3GLCT, ST3Gal5 and ST6GALNAC5) of hsa-miR-200b-3p because of their low abundance. This work also pinpointed that glycosylation enzymes targeted by the miR-200 family, which controls epithelia to mesenchymal transition (EMT) and migration, also regulate EMT and migration. This led us to the formulation of the "miRNA proxy hypothesis" which states, "if a miR drives a specific biological phenotype…, the targets of that miR will drive the same biological phenotype. Thus, miRs can be used to identify (by proxy) the biological functions of specific glycosylation enzymes (or other proteins)." [1] The lab used this approach to identify glycosylation enzymes controlling cell cycle, providing additional evidence for our hypothesis [4]. Testing of this hypothesis and utilization of this approach to identify the biological functions of glycosylation enzymes requires a thorough knowledge of miR:target interactions. However, in the original work, only 3 out of the 11 miR:target interactions identified by prediction were accurate, and 4 unpredicted interactions were discovered [2]. The high false positive rates of prediction observed, coupled with significant false negatives, points to the need for more accurate data on miR regulation of glycosylation enzymes the hypothesis can be tested.

Herein, I discuss the creation of our second generation high-throughput platform, miRFluR. As discussed, this technology grew from previous work (Chapter 2).

3.3 B3GLCT GENE AND BIOLOGICAL FUNCTIONS

The B3GLCT gene encodes the beta-1,3-glucosyltransferase that mediates the transfer of glucose into O-linked fucosylglycans on proteins with thrombospondin type-1 repeats (TSRs). The biosynthesis of glucosyl-β(1→3)-fucose disaccharide on a TSR is initiated by the enzyme *O*-fucosyltransferase-2 (POFUT2), which transfers fucose to serine or threonine residues within the TSR. B3GLCT subsequently attaches a glucosyl residue to the O-linked fucosylglycan product (**Figure 3.1**).

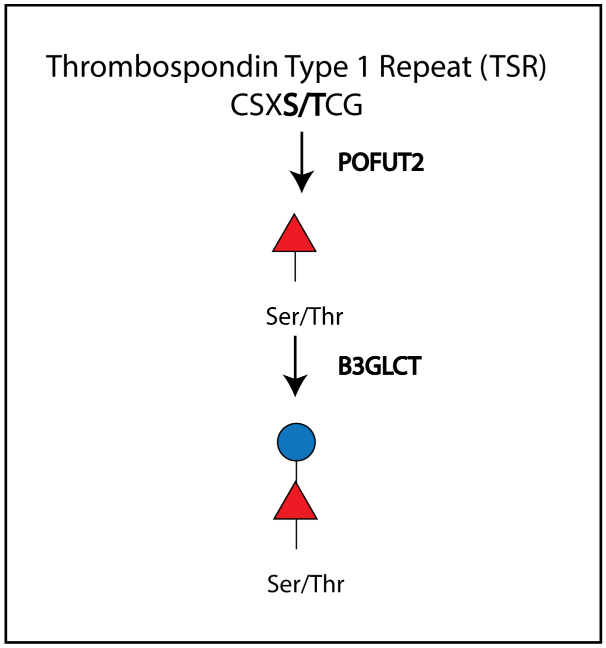

Figure 3.1. Biosynthesis pathways for TSRs: B3GLCT adds glucose to O-linked fucosylglycans occurring on TSRs.

The ER has a canonical quality-control system to identify, proof-read and tag improperly-folded proteins. POFUT2 and B3GLCT are found to mediate a non-canonical ER quality-control mechanism that recognizes folded TSRs and stabilizes them further by glycosylation [6 7]. Vasudevan *et al* demonstrated that the addition of fucosyl groups by POFUT2 enzyme sequentially stabilized TSRs in model substrates [6]. The subsequent attachment of a glucosyl residue by B3GLCT further stabilizes the folded TSRs in an additive manner and promoted ER exit. Both O-fucosylation and O-glucosylation occur co-translationally in the ER. While POFUT2 is required for the proper secretion of all targets containing TSRs, B3GLCT only impacts a subset of targets.

Mutations in the coding region of B3GLCT results in Peter Plus syndrome (PPS) with the c.660+1G>A being the most common mutation identified [8 9 10]. PPS is a rare, autosomal-recessive congenial disorder characterized by anterior segment dysgenesis of the eye, dysmorphic facial features, and variable other systemic anomalies. Patients with classic PPS display eye and ear abnormalities, short stature, cleft lip, cleft palate, distinctive facial features, intellectual disability, and developmental delay (**Figure. 3.2**).

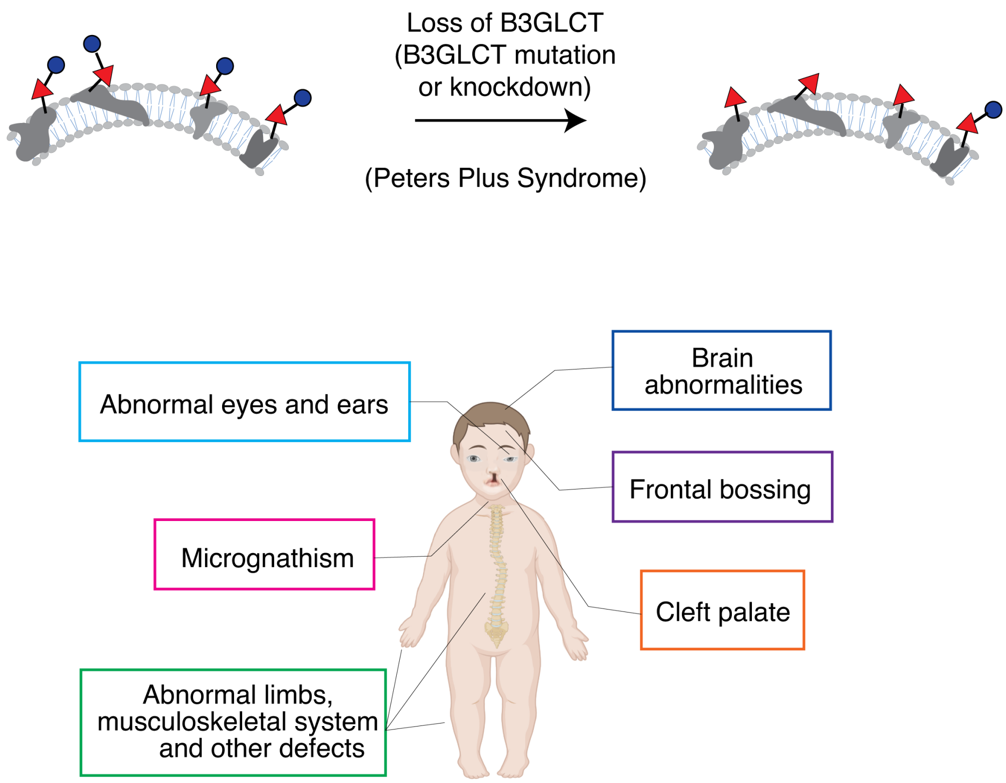

Figure 3.2. B3GLCT mutations and Peters' Plus syndrome: B3GLCT mutations or B3GLCT knockdown resulted in the loss of B3GLCT functions leading to Peters's Plus syndrome characterized by eye and ear abnormalities, short stature, cleft lip, cleft palate, distinctive facial features, and intellectual disability.

3.4 DEVELOPMENT OF HIGH-THROUGHPUT MIRFLUR PLATFORM FOR IDENTIFICATIONS OF THE MIR-GENE INTERACTOME

3.4.1 Development of high-throughput fluorescent ratiometric assay to identify miR:3'UTR interaction (miRFluR) platform

In my previous chapter, I created pSFmiR-3'UTR sensors with miRFP670 and mClover3 as our reporters based on the original sensor, pFMIR-B3GLCT that our previous lab member, Dr. Chris Vaiana created. This pSFmiR version is adapted to be compatible with our Genepix scanner system for the miRfect cell microarray platform. However, due to the technical issues with the miRfect system, I adapted our assay into a 384-well plate platform using fluorescent plate reader, to create a more robust and accurate method to identify miR:3'UTR interactions. At first, I tested the pSFmiR-B3GLCT in this new platform. However, the fluorescence signals of miRFP670 were too low when measured by the fluorescent reader. We then tested another sensor that I created with the mClover3-mRuby3 pair, pSFmiRv2-mClover3-mRuby3. However, the fluorescent signal readout are not consistent with multiple replicates in the plate. From literature, we found that the cellular endoplasmic reticulum (ER) became abnormal and acquired a low organized smooth ER (OSER) score compared to normal cells after transfection. mRuby3 which has a tendency to oligomerize under physiologic conditions. As a result, we decided to test the original sensors, pFMIR-B3GLCT, in the 384 well plate. We obtained good fluorescent signals from both Cerulean and mCherry and proceed to the optimization of the assay.

Principles of miRFluR platform: In pFmiR (pFmiR-3'UTR, **Figure 3.3, Sequence 1**), the 3'UTR of a gene of interest is cloned downstream of Cerulean, our reporter protein. A second fluorescent protein, mCherry, is incorporated into the same plasmid, to control for transfection efficiency and any non-specific effects of the miR on the transfected cells. The pFmiR plasmid and the miR mimics are co-transfected into Hek-293T cells in a 384-well plate assay. The ratio of Cerulean/mCherry fluorescence in miR transfected cells is normalized to the data from a non-targeting control (NTC) and reflects the extent of miR-target regulation (**Figure 3.3**). For miRs that repress protein expression, a loss of Cerulean fluorescence is expected, with a concomitant reduction in the normalized fluorescence ratio. Our miRFluR assay enables rapid analysis of miR libraries without the need for additional manipulation and reagents post-transfection.

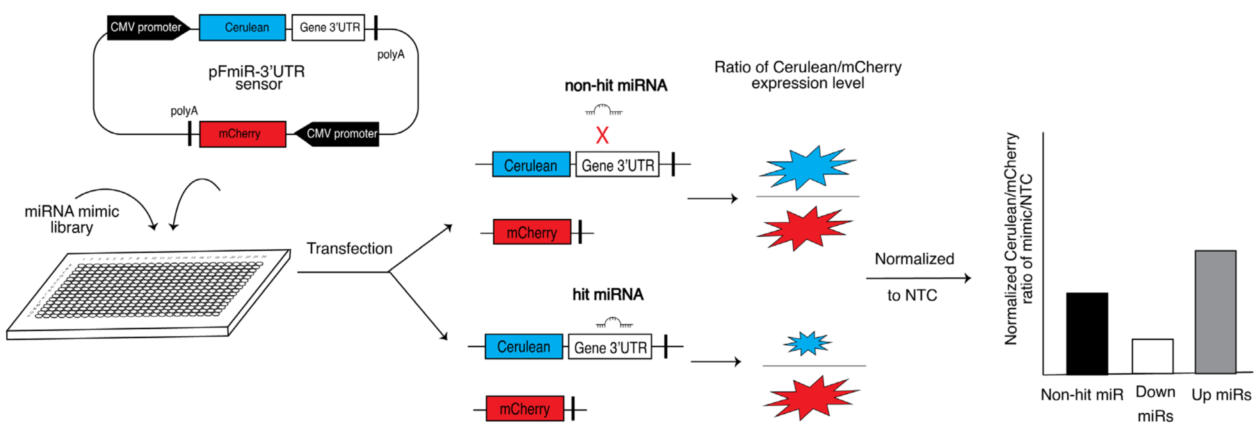

Figure 3.3. Schematic illustration of the miRFluR high-throughput assay.

Comparison of 384 well plate platform and miRfect system:

	miRfect system	384 well plate
Advantages	• Higher-throughput platform: miR-lipofectamine complexes spots (around 150-200 nm in diameter) are simultaneously	• More accurate and reliable results: miRs and reagents are separated by wells.

	printed in multiples slides for subsequent transfection with different plasmid sensors. • Less reagents and consumables are required.	• Cells do not need to be fixed post-transfection.
Disadvantages	• MiR-matrix spots are in the same slide which is prone to cross-contamination. Thus, this impacts the accuracy and reproducibility of the assay. • Spot morphology can impact the results. • Cells are required to be fixed post-transfection and before fluorescent readout. • Cells could get detached from the slide surface during handling processes especially with less adherent cell lines. • Slides could not be stored and used for long time since the transfectibility and stability of	• Lower throughput than miRfect platform. • More reagents and consumables are needed.

	miR transfected complexes reduces.	

Establishment of miRFluR platform

To establish that our sensor worked as expected, I compared the Cerulean/mCherry fluorescence ratios upon co-transfection of our sensor with either NTC, the positive control miR-200b-3p or the known negative control miR-200a-3p (**Figure 3.4**) [3]. I observed a clear downregulation of Cerulean, but not mCherry, by miR-200b-3p but not NTC1 or miR-200a-3p. I next analyzed our sensor using the Mission miRNA mimic library v.21 (Sigma), which contained all human miRs included in miRbase version 21. This library has 2,754 miR mimics. These mimics were aliquoted into 384-well plates in triplicate, for a total of 32 plates. Each plate contained NTC, miR-200b-3p and miR-200a-3p as controls. miRs were co-transfected with pFmiR plasmid into Hek-293T cells using lipofectamine 2000. After 48 h, plates were read by a fluorescence plate reader. For each plate, the average ratiometric data for each miR was normalized to the average ratiometric data for the NTC in that plate. Higher error measurements were observed in 5 plates, and these were omitted from further analysis. Comparison of the miR-200a-3p and miR-200b-3p data for the remaining 27 plates showed high reproducibility in the data, with significant repression of B3GLCT observed for miR-200b-3p as compared to miR-200a-3p, in line with our previous work (**Figure 3.5**). Upon co-transfection of pMIR-B3GLCT with miRs to cells, if a miR regulates that gene of interest via binding to the 3'UTR, a loss or gain of fluorescence should be observed for Cerulean in comparison to the signal from mCherry. Ratiometric analysis of Cerulean/mCherry fluorescence reports the extent of miR:target regulation. The fluorescence signals were measured by using a microplate reader. This allows the production of highly quantitative, high-throughput screening data to experimentally identify miR hits for a specific gene. (**Figure 3.3**)

After optimization for the transfection condition (plasmid amount, miRNA concentration and lipofectamine 2000), the co-transfection of pMIR-B3GLCT and miRNA mimic with lipofectamine 2000 was performed directly in 384 well-plates containing 2754 human miRNA mimics (total of 32 384-well plates). Microscopic images of the transfections were captured for the controls (**Figure 3.4**). We indeed observed a significant decrease of Cerulean signal in comparison to mCherry in the case of miR-200b-3p. Meanwhile, the ratio of Cerulean signal to mCherry of miR-200a-3p was similar to NTC1. This indicated that the sensor is working properly with our assay and also allowed us to identify the effect of miR on protein expression as the result of changing fluorescence response.

To increase the throughput of our assay, fluorescence signals are measured by microplate reader instead of microscopic imaging. This not only provides a platform for faster measurement but also does not required image analysis. The question was whether the result from reading fluorescence in microplate reader could recapitulate what we saw from microscopic imaging. To examine this point, we did multiple control assay with NTC1, miR-200a-3p and miR-200b-3p. The results confirmed the decrease of miR-200b-3p in comparison to NTC1 and miR-200a-3p negative controls. All data were obtained for B3GLCT from 32 384-well miR plates. We omitted 5 plates due to the high measurement errors. We then examined plate to plate variations. After analyzing the data for NTC1, miR-200a-3p and miR-200b-3p within each plate, the effects of miR-200b-3p are consistent across all plates in comparison to NTC1 and miR-200a-3p. (**Figure 3.5A, B and C**)

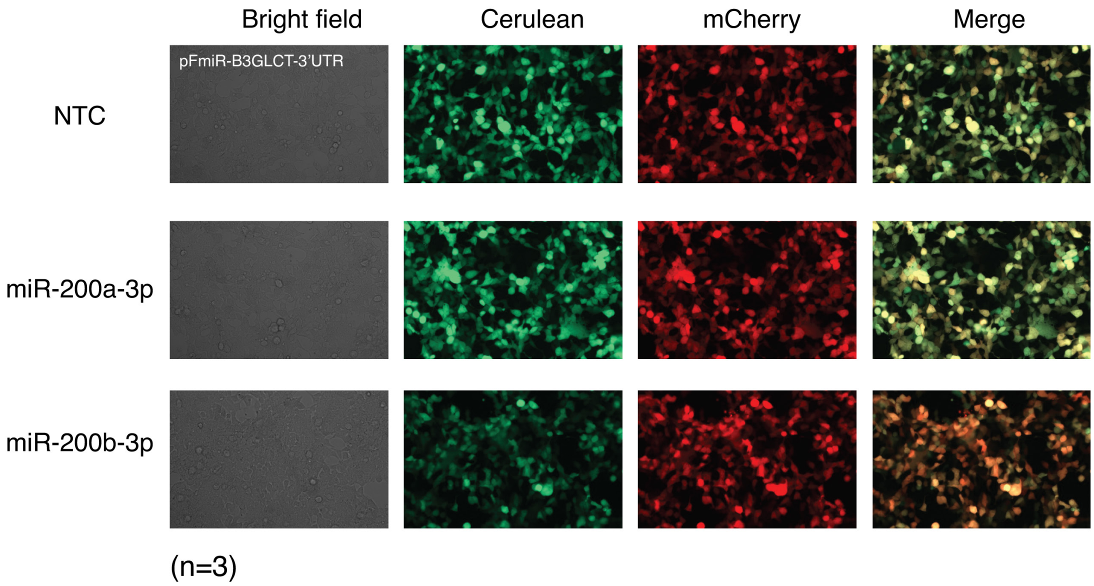

Figure 3.4. Fluorescence microscopy images of *HEK-293T* cells co-transfected with pFmiR-B3GLCT and either NTC, miR-200a-3p or miR-200b-3p, 48 h post-transfection. Images shown are representative of n=3 replicates.

A

miR-200b-3p			
	Normalization	Error propagation	%error
miR-200b-3p	0.767048598	0.014137905	1.843156374
miR-200b	0.676551902	0.031326854	4.630369725
miR-200b	0.713829821	0.035631635	4.991614864
miR-200b	0.669219212	0.026358103	3.938635136
miR-200b	0.672992456	0.02059831	3.060704395
miR-200b	0.699464173	0.038214279	5.463364749
miR-200b	0.718240277	0.072391696	10.07903606
miR-200b	0.64356795	0.031839783	4.947384801
miR-200b	0.646406619	0.037396326	5.785263533
miR-200b	0.662219997	0.030781561	4.648237993
miR-200b	0.719738924	0.05243425	7.285176409
miR-200b	0.709599104	0.043369307	6.111804088
miR-200b	0.735768007	0.043649855	5.93255679
miR-200b	0.666840152	0.02310209	3.464411911
miR-200b	0.768685844	0.066576748	8.661112851
miR-200b	0.755783405	0.07470162	9.883998402
miR-200b	0.739645717	0.075075554	10.15020469
miR-200b	0.638166899	0.047116447	7.383091616
miR-200b	0.708659151	0.065076343	9.18302437
miR-200b	0.661266394	0.025064195	3.790332517
miR-200b	0.689017251	0.066826737	9.698848139
miR-200b	0.7393283	0.034425117	4.656269351
miR-200b	0.70026707	0.038629613	5.516411472
miR-200b	0.785476645	0.035890433	4.569255308
miR-200b	0.737934828	0.06388929	8.657849987
miR-200b	0.696491419	0.03178056	4.562950668
miR-200b	0.654762617	0.031589121	4.824515103
Mean	**0.702850842**		
Std	**0.04143727**		
%Error	**5.895599396**		

B

miR-200a-3p			
	Normalization	Error propagation	%error
miR-200a-3p	0.947124211	0.026486147	2.796480801
miR-200a	0.939230496	0.040182151	4.278199097
miR-200a	0.982178462	0.064678495	6.585208069
miR-200a	0.933873215	0.023811672	2.549775659
miR-200a	0.941848343	0.019081983	2.026014444
miR-200a	0.930808362	0.034008023	3.653600978
miR-200a	0.908982787	0.036401727	4.004666261
miR-200a	0.905344453	0.044684118	4.935593056
miR-200a	0.961996483	0.055940062	5.814996552
miR-200a	0.953781912	0.027272032	2.859357174
miR-200a	0.934837632	0.023642711	2.529071426
miR-200a	0.901809435	0.030817419	3.417287275
miR-200a	0.960293889	0.045865886	4.776234311
miR-200a	0.938272869	0.030964305	3.300138556
miR-200a	0.914919478	0.0620637	6.783514998
miR-200a	0.929329977	0.070187238	7.552456074
miR-200a	0.87424585	0.04614545	5.278315077
miR-200a	0.911154901	0.054828775	6.017503212
miR-200a	0.940868696	0.053513721	5.687692841
miR-200a	0.932056153	0.048062303	5.156588787
miR-200a	0.977233858	0.049461106	5.061337705
miR-200a	0.931733133	0.045221201	4.853449966
miR-200a	0.969747681	0.060388311	6.227218917
miR-200a	0.904708055	0.027015463	2.986097358
miR-200a	0.930560668	0.022670768	2.436248278
miR-200a	0.888243546	0.043537581	4.901536426
200a	0.857118061	0.045275602	5.28230642
Mean	**0.929714911**		
Std	**0.029756257**		
%Error	**3.200578657**		

C

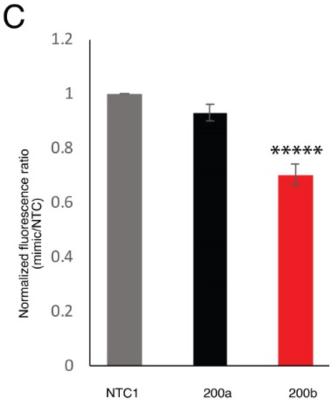

Figure 3.5. Reproducibility of the miRFluR high-throughput analysis system. Normalization data and quantitative analysis of miR-200b-3p (A) and miR-200a-3p (B) normalized to NTC1 with triplicates for each data point over 27 384 well-plates. (C) Bar graph represented the reproducibility of the assay. Unpaired Student's t test; *****p << 0.0001.

I next analyzed the remaining miR data for B3GLCT. I first removed any miRs that had high errors in the measurement (median error +2 standard deviation (S.D.) across all plates), leaving us with data for 2,071 miRs. We calculated Z-scores using the remaining NTC normalized ratiometric data. In line with previous work by Wolter et al using luciferase assays[11], we set the threshold for hits at 20% change (either up or down) and a Z-score of +/-1.960, which corresponds to the 95% confidence interval. Using these thresholds, I identified 27 miRs that downregulated expression, all of which met the 20% threshold. To our surprise, we also identified 11 miRs that were potential upregulators **(Figure 3.6 and Table 3.2**). Although a few upregulatory miRs have been described in the literature[12, 13], most are thought to activate expression in senescent cells[14, 15]. To validate our findings, I first rescreened a small set of 12 miRs (**Figure 3.7 and 3.8**). All miRs are found to recapitulate the findings observed in the library screen.

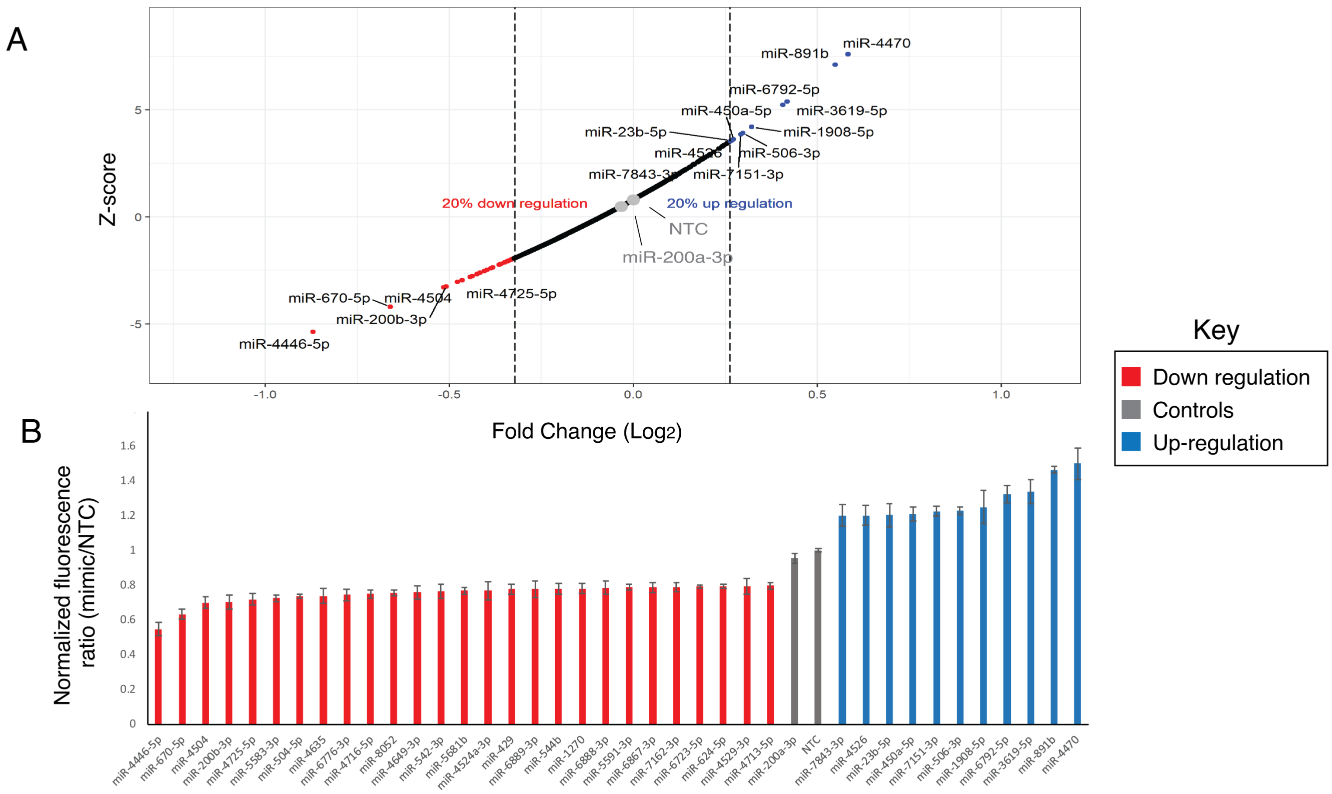

Figure 3.6. Identification and validation of hits for B3GLCT. (A) Plot of Z-score versus log2(fold change) for 2074 miRs against the 3'-UTR of B3GLCT. miRs within the 95 % confidence interval and with a minimum impact of +/- 20 % are labeled (red: downregulatory, grey: controls (NTC and hsa-miR-200a-3p), blue: upregulatory). (B) Bar graph of ratiometric data for miRs indicated in A. Error bars represent propagated error.

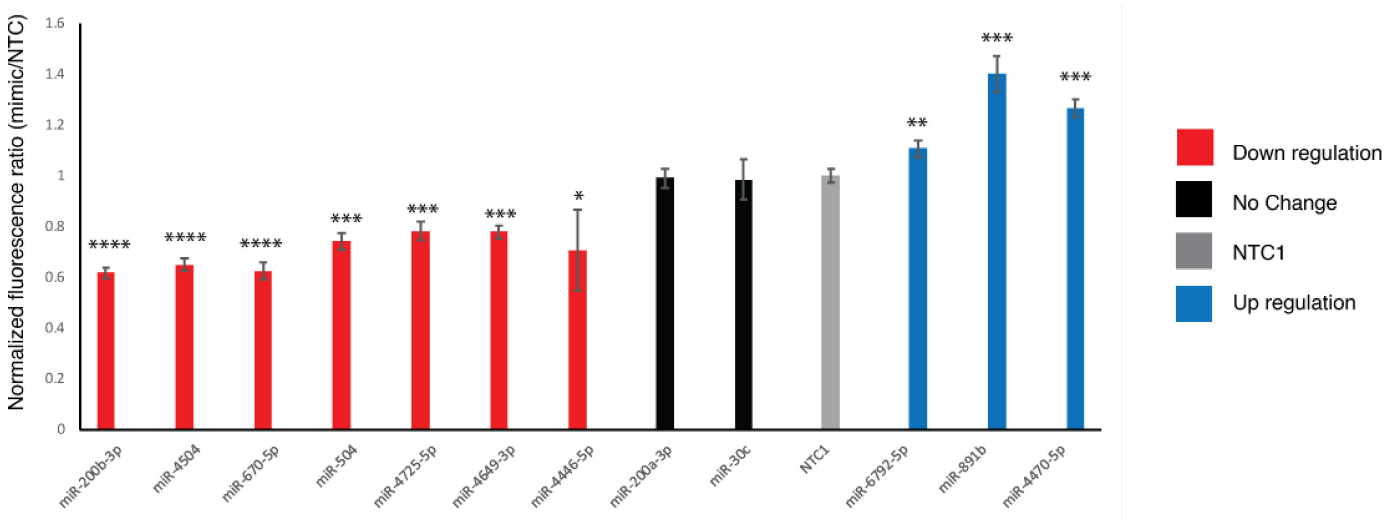

Figure 3.7. Small scale validation of miR subsets. Cells were co-transfected with pFmiR-B3GLCT and indicated miRs. Data shown is from 3 biological replicates. Error bars represent standard deviations. Statistical analysis was done against NTC1. Student's t-test for comparing the means between a miR and the negative control (miR-200a-3p); *$p<0.05$, ** $p<0.01$, *** $p<0.001$ and **** $p<0.0001$.

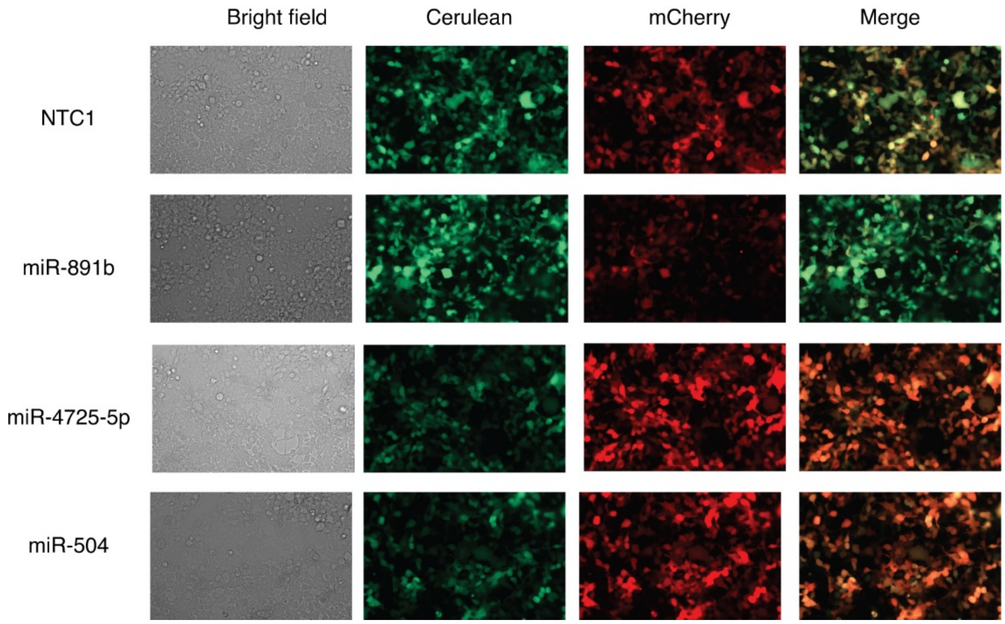

Figure. 3.8. Fluorescence microscopy images of co-transfection of pMIR-B3GLCT with NTC1, miR-891b, miR-4725-5p and miR-504 48 hours post-transfection. Data is representative of n=3 experiments.

I next performed Western blot analysis for the protein levels of B3GLCT in HEK-293T transfected with the subset of downregulatory (miR-200b-3p, miR-504, miR-4504, miR-4649-3p, miR-4725-5p) and upregulatory (miR-891b and miR-4470-5p) miRs that passed our secondary screen. I used miR-200a-3p and NTC as negative controls (**Figure 3.9, Figure 3.10 and Table 3.1**). In general, the B3GLCT protein levels followed the expected results from our sensor assay, with one exception (miR-4649-3p). The downregulatory miR-4649-3p did not show significant inhibition. I tested whether the mRNA levels of B3GLCT changed with miR transfection (**Figure 3.11, Table 3.4 and Table 3.5**). Although generally mRNA levels are thought to correspond to protein expression, the correlation is not absolute and miRs have been shown to impact mRNA in ways not reflected in the protein levels[11]. For all inhibitory miRs, I observed a clear loss of mRNA expression for B3GLCT. Conversely, the upregulatory miR, miR-891b, elevated mRNA expression in line with its impact on the protein. Interestingly, miR-4470-5p, which up-regulated both protein and sensor expression, clearly repressed mRNA levels for B3GLCT. This argues for multiple pathways to protein regulation through differential mRNA regulation by miRNA.

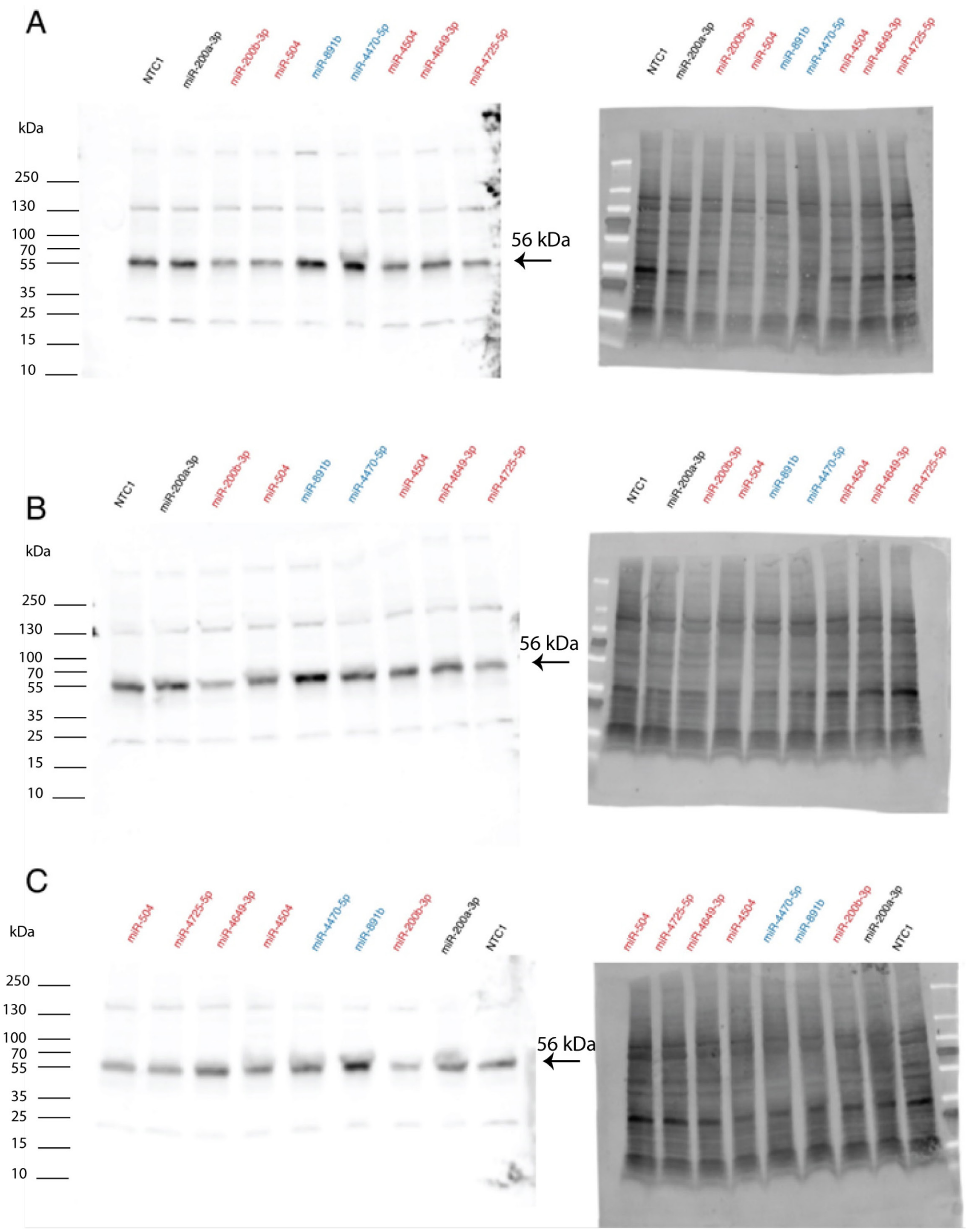

Figure 3.9. (A-C) B3GLCT Western blot analysis and accompanying Ponceau S stain for the 3 biological replicates.

	Relative expression of B3GLCT				
	Replicate 1	Replicate 2	Replicate 3	Mean	Standard error
NTC	1.000000	1.000000	1.000000	1.000000	0.000000
miR-200a-3p	1.094828	1.086474	1.044100	1.075134	0.027199
miR-200b-3p	0.624814	0.537807	0.547072	0.569898	0.047784
miR-504	0.717978	0.974680	0.733903	0.808854	0.143830
miR-4504	0.830806	0.862380	0.793719	0.828968	0.034368
miR-4649-3p	0.962720	0.941172	1.064173	0.989355	0.065684
miR-4725-5p	0.609225	0.579229	0.725140	0.637865	0.077057
miR-891b	1.501843	1.582876	1.774619	1.619779	0.140082
miR-4470-5p	1.437434	1.170618	1.410259	1.339437	0.146832

Table 3.1. Quantification of Western blot (n=3). 1,2 and 3 correspond to A, B and C in **Figure 3.10**.

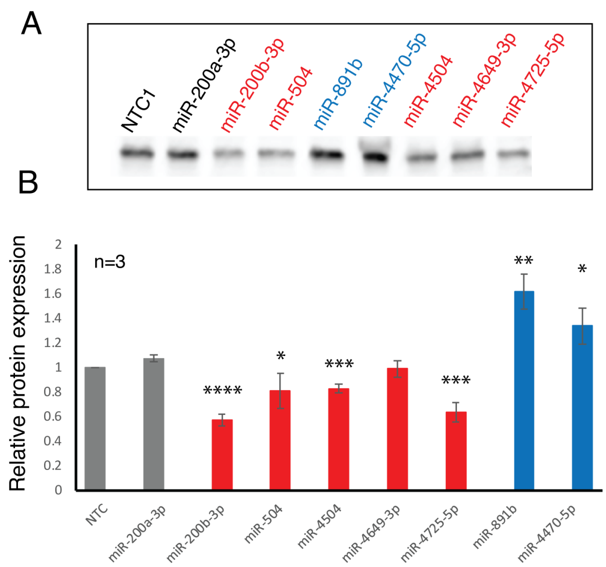

Figure 3.10. Validation of hits for B3GLCT. (A) Western blot analysis of B3GLCT in HEK273T transfected with 50 nM miR mimics or NTC, 48 hours post-transfection. (B) Quantification of Western blot analysis for three independent experiments. B3GLCT expression was normalized to total protein levels from Ponceau staining and set over normalized NTC for each blot. Statistical analysis was done against miR-200a-3p as a negative control. Ponceau and whole Westerns corresponding to the data are shown in **Figure 3.9**. Error bars represent standard deviations.

Student's t-test for comparing the means between a miR and the negative control (miR-200a-3p); *p<0.05, ** p <0.01, *** p <0.001 and **** p <0.0001. n=3 indicates the biological replicates.

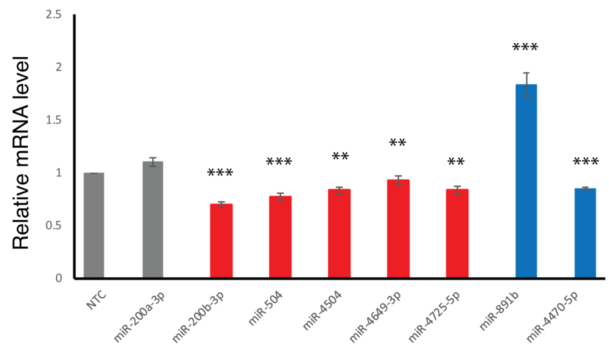

Figure 3.11. Identification and validation of hits for B3GLCT. (E) RT-qPCR analysis for relative B3GLCT mRNA expression levels. All samples are normalized to GAPDH within the sample and then to NTC for that run. Results shown are from three independent experiments. Statistical analysis was done against miR-200a-3p as a negative control. Error bars represent standard deviations. Student's t-test; *p<0.05, ** p <0.01, *** p <0.001 and **** p <0.0001.

3.5 COMPARISON TO BIOINFORMATICS TOOLS SHOWED TOO MANY FALSE TARGETS FOR MIRS

Identification of miRs that target a specific protein is heavily based on prediction from algorithms. I tested how accurately two of the most popular miR prediction programs, Targetscan 7.2 [16] and miRwalk 3.0 [17-19], predicted B3GLCT regulators. For both algorithms, we only examined miR predictions for miR within our final dataset. Targetscan 7.2 predicted 480 unique miR interactions with the 3'-UTR of B3GLCT (**Figure 3.13A**). Of those, only 17 (3.5%) were identified as hits within our screen. All 17 were repressors. Of the repressors, 17/27 (~2/3) were identified by Targetscan. Overall, there was a weak but significant correlation between the Targetscan score, where available, and the level of protein repression observed for miRNAs where a score existed (**Figure 3.13D,** R= 0.25, p = 1×10^{-9}). It should be noted, that although Targetscan 7.2 analyzes the miRs from miRbase v 21, only 559 of the 2,071 miRs from our analysis even have a context score in Targetscan. Scores were not available for the 10 non-predicted downregulatory miRs or the 10 upregulatory miRs. Among the unpredicted downregulators were miR-504-5p, miR-4649-3p and miR-4725-5p, all of which showed clear repression of B3GLCT in our assays (**Figure 3.6 and 3.8**). Thus, the actual correlation is far lower. For miRwalk 3.0, 781 unique miR interactions were predicted. Of these, only 13 were observed (1.7%, **Figure 3.13B**). In this case, 1 of the upregulators (miR-6792-5p) was among the predicted hits. No correlation was observed between the score in miRwalk 3.0 and miR regulation of the sensor (**Figure 3.13E**). Only 9 of the hits were predicted by both algorithms, which only predicted 185 miRs in common between the two (**Figure 3.13C**). In previous work, a higher concordance between prediction and testing (~16[20]-63 %[11]) was observed. However in these analyses, multiple 3'-UTRs were tested against a selected set of miRs skewed towards highly abundant miRs and cancer-related genes. Although the majority of repressor miRs were predicted by both algorithms (63%-Targetscan, ~41%-miRwalk), there is a high rate of false positives.

In order to understand why most miR prediction algorithms do not perform well in predicting miR targets, the underlying features and statistical modeling should be examined. Targetscan relied heavily on the conservation of binding sites with canonical seed regions. The rational for that is although non-canonical interactions are observed in both in vivo UV-crosslinking and computational approaches, the mRNA repression was not mediated by these interactions. However, no effect on mRNA was observed with non-canonical sites even with observable interactions. Thus, they concluded the functional sites are mostly canonical to control protein production. This approach assumes that protein abundance is reflected in the transcriptome. However, this has proven to be incorrect[21]. For low abundance genes, which include glycogenes (e.g. B3GLCT) and most cell surface receptors, it is known that measurable transcript levels are not accurate to protein abundance [22]. Indeed the concordance between changes in measurable transcript and protein levels in response to miRs is far lower for low abundance transcripts [21]. The context score (++) for specific sites in Targetscan is the sum of the contribution of 14 features (site type, supplementary pairing, local AU, minimum distance, sRNA1A*, sRNA1C*, sRNA1G*, sRNA8A*, sRNA8C*, sRNA8G*, site8A*, site8C*, site8G*, 3' UTR length*, SA*, ORF length*, ORF 8mer count*, 3' UTR offset 6mer count*, TA (target site abundance), SPS (seed-pairing stability), PCT (probability of conserved targeting)*). These features are chosen based on the seed site efficacy and structural accessibility for the strongest overall targeting efficacy. However, it was observed that canonical sites are not necessarily those with the highest affinity in comparison to non-canonical sites [23-26] and other biological factors (like RNA binding proteins, transcriptional machinery…) could impact miRNA targeting efficacy, Targetscan fails to take into consideration.

For miRwalk, it integrates Targetscan (context scores), miRDB and validated miRTarBase in its algorithm framework, then implements a random-forest based learning approach (TarPmiR) to predict miR target sites. miRDB performs using MirTarget2 algorithm, which models only site context and ignores the multiple binding site properties or cooperative interactions between them. This algorithm also ignores some important canonical sites in the miR:target interactions. The utilization of diverse algorithms in miRwalk increases the number of possible miR: target interactions with the expansion to both 5'UTR and coding region. However, this combination does not improve its performance since all of its components possess low accuracy and sensitivity to predict miR target sites. This indicates that widening criteria and features to build prediction algorithms does not necessarily improve performance and the correct identification of miR targets, especially when the underlying biological mechanisms driving biologically relevant actions and functions of miRs remain largely unknown. Thus, prediction algorithms still possess low sensitivity and accuracy to predict miR target interactions. Our analysis here is the first to test a broad swath of the human miRome against a single gene using a protein-based outcome. More such datasets will be essential to advance our knowledge or miRNA regulation and create more accurate prediction algorithms.

Interestingly, targets resulting from the intersection of two lists of predictions (176 targets) are not more likely to be present in the intersection of two other lists (9 out of 176; 5%). Thus, intersecting results do not improve the probability of predicting true positives and it may lead to declined sensitivity because of possibly omitting valid interactions.

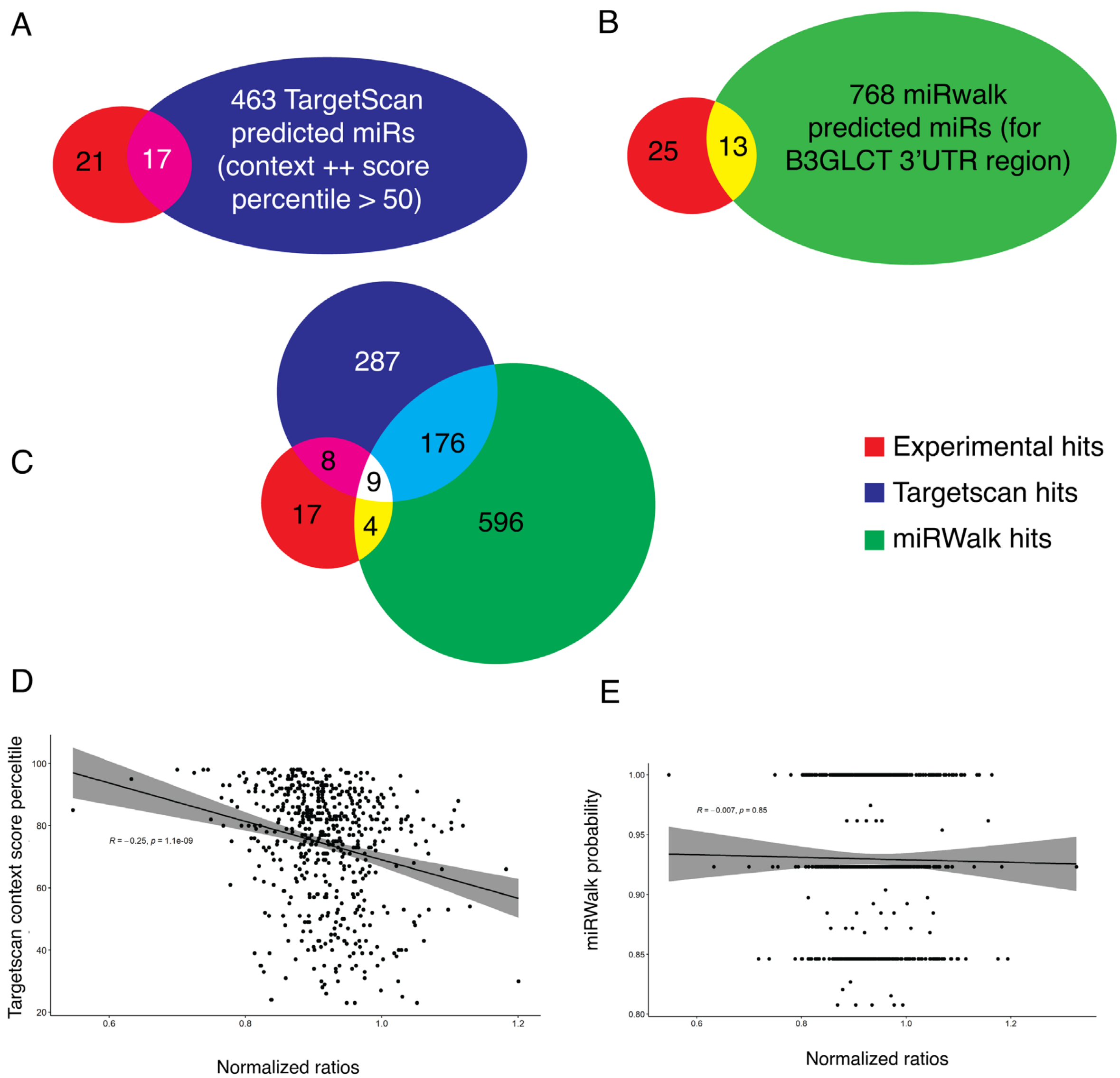

Figure 3.13. Comparison of experimental results to prediction datasets from TargetScan (A) or miRWalk (B). (C) Overlap of experimental results and predictions from both Targetscan and miRWalk. (D) Correlation between Targetscan context++ score percentile and our experimental results. A significant but small negative correlation was observed (R = -0.25, p~10-9) with data for which Targetscan context scores++ exist. (E) Correlation between miRWalk score and our experimental results. No correlation was observed.

3.6 MIRNA HITS CAN PREDICT THE BIOLOGICAL FUNCTIONS OF B3GLCT AND THE SUPPORT FOR MIRNA PROXY HYPOTHESIS

We next tested whether miRs that downregulate B3GLCT can predict the phenotypic outcome of losing this enzyme (i.e. Peters' Plus Syndrome) through analysis of their other protein targets in line with our miRNA proxy hypothesis. To this end, I analyzed the gene target network, and enrichment in associated disease phenotypes, of the 27 validated downregulatory miRs using miRNet [27, 28]. miRNet is a platform for building and analyzing miRNA networks that integrates information from multiple databases. For my analysis, I configured miRNet to only consider validated miR-target interactions from miRTarbase. Interactions in this database are experimentally confirmed by reporter assays, western blot, or microarray experiments [29, 30]. None of the 27 miRs fed into the system were known in miRTarbase to target B3GLCT. The resulting gene target network for our downregulatory miRs was analyzed using miRNet for disease associations found in DisGeNET [31]. The network was functionally enriched in phenotypes associated with features of Peters' Plus Syndrome (**Figure 3.14, Table 3.3**). The only non-Peters' plus phenotype observed in the predicted set were a subset of cancer phenotypes. Whether this is due to a real role for B3GLCT in these specific cancers, or is an outcome of the bias of the current datasets towards cancer genes is unknown. Overall, my analysis supports the miRNA proxy hypothesis, predicting a role for B3GLCT in the disease outcomes related to Peters' Plus Syndrome through the miRs that downregulate this enzyme.

Previous reports documented patients with classic PPS phenotypes had B3GLCT mutations in the coding region, but also found cases where patients affected with PPS-like phenotypes had no mutations in B3GLCT [8]. The molecular mechanisms for those cases are still awaiting discovery and our analysis of B3GLCT here may help to explain this phenomenon. The miRNA network regulating B3GLCT and their gene target regulatory network, when disturbed, may give rise to an outcome that recapitulates the B3GLCT loss of function.

A

PATHWAY	P-VALUE
Preauricular dimple	7.49E-05
Preauricular sinus	7.49E-05
Malignant mesothelioma	9.22E-05
Cleft Palate	0.000101
Acquired scoliosis	0.000122
Preauricular Fistulae, Congenital	0.000133
Curvature of spine	0.000162
Uranostaphyloschisis	0.000296
Frontal bossing	0.00038
Flatfoot	0.000432

PATHWAY	P-VALUE
Congenital small ears	0.000492
Hemangiosarcoma	0.00106
Acquired flat foot	0.00128
Muscle Cramp	0.00128
Adenoma	0.00133
Micrognathism	0.00136
Mandibular hypoplasia	0.00136
Hypoplastic mandible condyle	0.00136
Lymphoma, Follicular	0.00189
Intellectual Disability	0.00195

PATHWAY	P-VALUE
Sezary Syndrome	0.00197
Dull intelligence	0.00296
Orbital separation excessive	0.00321
Low intelligence	0.00359
Colonic Neoplasms	0.00371
Poor school performance	0.00385
Ventricular Septal Defects	0.00424
Aplasia/Hypoplasia of the lungs	0.00468
Mental Retardation	0.00473

B

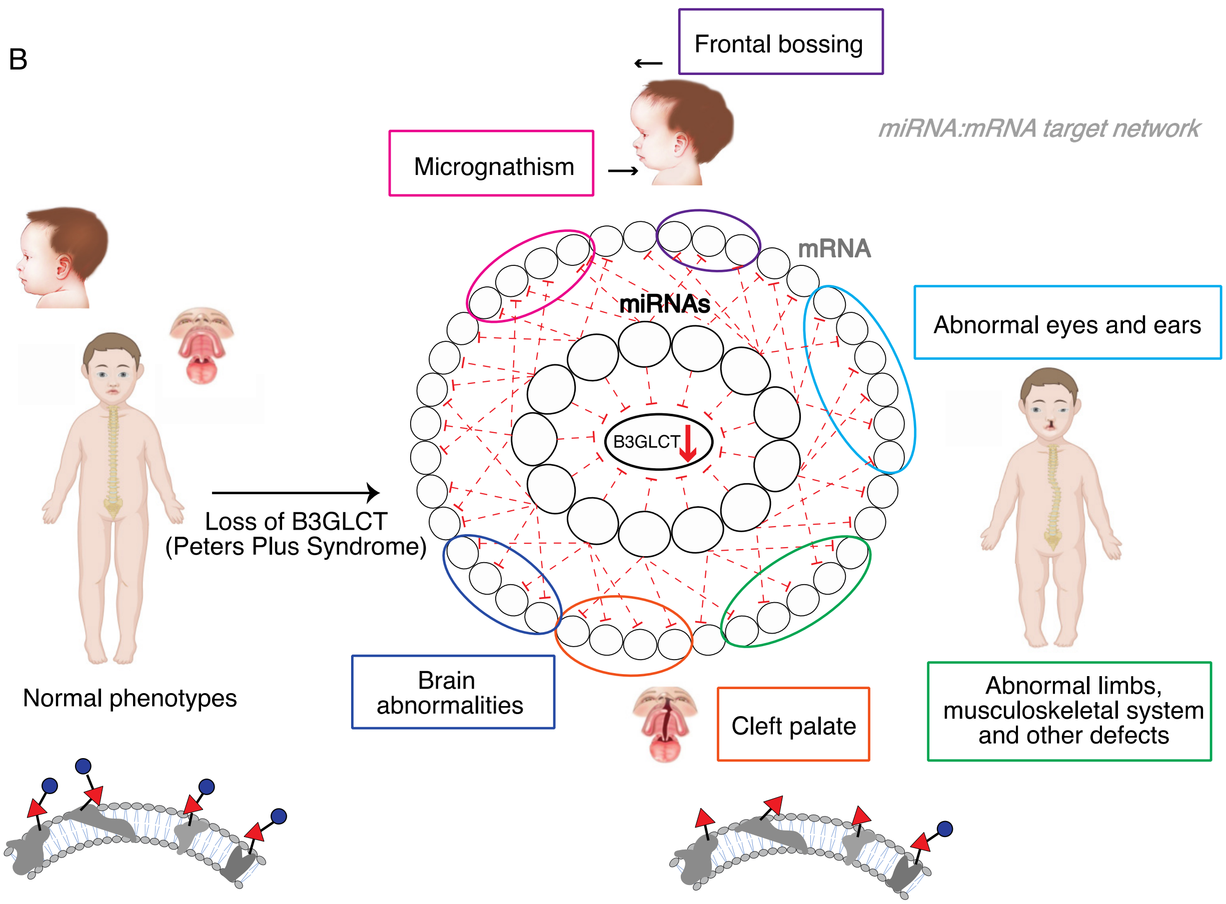

Figure 3.14. Phenotypic network analysis of miRs downregulating B3GLCT. (A) Table of enriched disease phenotypes resulting from miRNet analysis of B3GLCT downregulatory miRs. Table is color coded to phenotypes seen in Peter's Plus Syndrome as in (B). (B) Schematic of B3GLCT downregulating miR-mRNA target network as it applies to identification of disease

phenotypes observed in Peters' Plus Syndrome. miRs that downregulate B3GLCT target the mRNA of genes enriched in the disease networks (circled in corresponding colors) shown in (A).

3.7 CONCLUSION

Our current understanding of miR regulation of protein expression has been hampered by limited data on miR:mRNA target interactions. Herein, we created a high-throughput experimental platform, miRFluR, to rapidly analyze miR interactions with the 3'-UTR of a gene of interest. We used this dual fluorescence platform to perform the first comprehensive analysis of miR regulation of a gene, B3GLCT, through its 3'-UTR. Our analysis found both downregulatory and upregulatory miRs for B3GLCT, which we validated at the protein and mRNA levels. We anticipated that this gene would be highly regulated, based on the predictions from multiple algorithms [3, 16, 32]. However, we found a wide discrepancy between prediction and our assay, with < 4% of predicted miRs targeting this enzyme (>96 % false positive rate). Although it is widely held that miRs target hundreds to thousands of genes, our results would argue that prediction algorithms vastly overstate miR regulation. This low performance of prediction algorithms stems from the chosen features, which do not reflect the correct biological impacts of miRs in specific contexts. Functional enrichment analysis of miRs downregulating B3GLCT identified disease phenotypes included in Peters' Plus Syndrome, the known disorder caused by mutation of this gene, in line with our miRNA Proxy hypothesis. One limitation of this analysis is that the dataset underpinning miRNet and other such network analysis algorithms has a lack of validated interactions[29, 30]. As our information on true miR:target interactions grow, our ability to harness this data to understand the biological functions of the glycome and other genes will improve. Furthermore, our analysis on B3GLCT may help to explain PPS-like phenotypes with no genetic mutation on B3GLCT. MiRNA network regulates B3GLCT and their gene target regulatory network, when disturbed, can give rise to the outcome that recapitulates B3GLCT loss of function.

With this system biology approach, our capacity to understand different layers of regulation and how they balance or compensate each other will advance.

3.8 MATERIALS AND EXPERIMENTAL METHODS

3.8.1 Cloning of pFmiR-B3GLCT-3'UTR

B3GLCT 3'UTR was cloned from cDNA using primers:

B3GLCTc_fwd: CTAGCATCAGGGTGACCTG

B3GLCT_rev: GATCCTTTTCATTACATAATAAAG

and standard PCR conditions. The DNA fragment was cloned using the NheI and BamHI sites downstream of Cerulean in our pFmiR-empty backbone using standard ligation protocols. Plasmid maps and sequences for pFmiR and pFmiR-B3GLCT-3'-UTR can be found in **Figure S1** and **Figure S2**, respectively.

3.8.2 MiRFluR High-throughput Assay.

The Human miRNA Mimic library version 21 (MISSION, Sigma) was resuspended in nuclease-free water and aliquoted into black 384-well, clear optical bottom tissue-culture treated plates (Nunc). Each plate contained 3 replicates of every miRNA (1.8 pmol/well). Including controls (NTC, miR-200a-3p, miR-200b-3p).

To each well in the plate was added 25 ng of pMIR-B3GLCT plasmid in 5 µl Opti-MEM (Gibco) and 0.11 µl lipofectamine 2000 (Invitrogen) in 5 µl Opti-MEM (Gibco). The solution was allowed to incubate at room temperature for 25 min. Then, *HEK293T* cells (25 µl per well, 400 cells/ µl in non-phenol red Dulbecco's Modified Eagle Medium (DMEM) with FBS 10%) were added to the plate. Plates were then incubated at 37°C, 5% CO_2. After 48 hours, the fluorescence signals of Cerulean (excitation: 433 nm; emission: 475 nm) and mCherry (excitation: 587 nm; emission: 610 nm) were measured using the bottom read option in a FlexStation 3 Multi-mode microplate reader (Molecular Devices).

3.8.3 Data Processing

We calculated the ratio Cerulean fluorescence (Cer) over mCherry fluorescence (Cer/mCh) for each well in each plate. For each miR, triplicate values were averaged and the standard deviation (S.D.) obtained. We calculated a % error for each miR as 100 x S.D./mean. . As a quality control measure, we removed any plates or miRs that had high errors in the measurement (median error +2 S.D. across all plates). This left us with data for 2,071 miRs. The Cer/mCh ratio for each miR was then normalized to the Cer/mCh ratio for the NTC within that plate and error was propagated. Data from all plates was then combined and Z-scores were calculated. A Z-score of +/-1.960, corresponding to a 2-tailed p-value of 0.05, was used as a threshold for significance. In addition, we set a second threshold of +/- 20% impact by the miR, in line with previous work [11, 20].

3.8.4 Microscopy imaging

HEK293T cells were seeded in 35 mm glass-bottom dishes (80,000 cells per well), cultured for 24 h, and co-transfected with pFmiR-B3GLCT-3'UTR and miRNA mimics (50 nM, Sigma MISSION) using Lipofectamine 2000 (Life Technologies). After 48 h, cells were imaged in the mCherry and Cerulean channels using the 20x lens on a Zeiss LSM 980 miscroscope. All experiments were done in biological triplicate.

3.8.5 Western Blot

HEK293T cells were seeded in six-well plates (80,000 cells per well), cultured for 24 h, and transfected with miRNA mimics (50 nM, Sigma MISSION) using Lipofectamine 2000 (Life Technologies). Cells were washed and harvested 48 hours post-transfection. Cells were then lysed in cold RIPA buffer supplemented with protease inhibitors and 50 µg of protein were run on SDS-PAGE. Standard Western Blot analysis using α-B3GLCT (IHC-plus anti-human B3GALTL antibody, 1:500) and α-rabbit-HRP (2°, 1:5,000, Abcam)] was performed [2]. Blots were developed using Clarity and Clarity Max Western ECL substrate (Bio-Rad).

3.8.6 RT-PCR

Total RNA was isolated using RNeasy kit (Qiagen) according to the manufacturer's instructions. RNA concentrations were measured using NanoDrop, and isolated RNA was reverse-transcribed (Applied Biosystems Power SYBR Green PCR). Real-time quantitative PCR (qPCR) was performed using the SYBR Green method and cycle threshold values (Ct) were obtained using an Applied Biosystem (ABI) 7500 Real-Time PCR machine and normalized to GAPDH.

Primer	Sequence (5' → 3')
B3GLCT-qRT-F	GGTCTGATTAGTGCCTTCTACTG
B3GLCT-qRT-R	TGGTTAGGCTTACACCATTCC
GAPDH-qRT-F	GGTGTGAACCATGAGAAGTATGA
GAPDH-qRT-R	GAGTCCTTCCACGATACCAAAG

[i] B3GLCT, beta 3-glucosyltransferase; GAPDH, glyceraldehyle-3-phosphate dehydrogenase; RT-qPCR, Reverse transcription quantitative polymerase chain reaction; F, forward; R, reverse.

3.8.7 Network Analysis Using miRNet.

Downregulatory miRs (27 miRs, **Figure 2B**) were input into miRNet (www.mirnet.ca) [26,27] using the following parameters: Organism: human miRs, ID type: miRbase ID, Targets: Genes(miRTarbase v 8.0). The Diseases Phenotype Enrichment function was used for **Figure 4**.

Appendix 3A. Plasmid maps and sequences

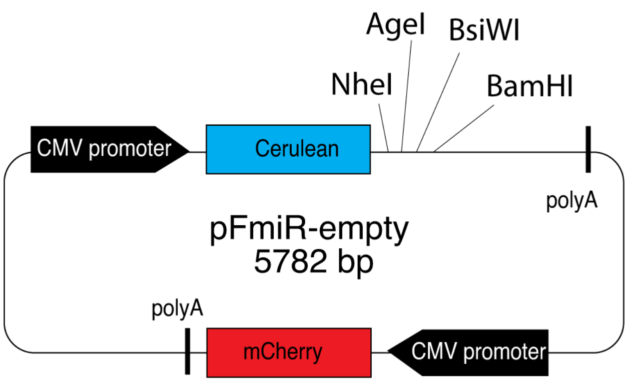

List of features:

mCherry (2539..3249)
CMV promoter 1 (236..852)
CMV promoter 2 (1916..2532)
Cerulean (918..1637)
polyA_1 (1688..1914)
polyA_2 (3272..3498)

Sequence 1_pFmiR-empty:

GACGGATCGGGAGATCTCCCGATCCCCTATGGTCGACTCTCAGTACAATCTGCTCTGATGCCGCATAGTTAAGCCAGTATCTGCTC
CCTGCTTGTGTGTTGGAGGTCGCTGAGTAGTGCGCGAGCAAAATTTAAGCTACAACAAGGCAAGGCTTGACCGACAATTGCATGA
AGAATCTGCTTAGGGTTAGGCGTTTTGCGCTGCTTCGCGATGTACGGGCCAGATATACGCGTTGACATTGATTATTGACTAGTTAT
TAATAGTAATCAATTACGGGGTCATTAGTTCATAGCCCATATATGGAGTTCCGCGTTACATAACTTACGGTAAATGGCCCGCCTGG
CTGACCGCCCAACGACCCCCGCCCATTGACGTCAATAATGACGTATGTTCCCATAGTAACGCCAATAGGGACTTTCCATTGACGTC
AATGGGTGGACTATTTACGGTAAACTGCCCACTTGGCAGTACATCAAGTGTATCATATGCCAAGTACGCCCCCTATTGACGTCAAT
GACGGTAAATGGCCCGCCTGGCATTATGCCCAGTACATGACCTTATGGGACTTTCCTACTTGGCAGTACATCTACGTATTAGTCAT
CGCTATTACCATGGTGATGCGGTTTTGGCAGTACATCAATGGGCGTGGATAGCGGTTTGACTCACGGGGATTTCCAAGTCTCCACC
CCATTGACGTCAATGGGAGTTTGTTTTGGCACCAAAATCAACGGGACTTTCCAAAATGTCGTAACAACTCCGCCCCATTGACGCAA
ATGGGCGGTAGGCGTGTACGGTGGGAGGTCTATATAAGCAGAGCTCTCTGGCTAACTAGAGAACCCACTGCTTACTGGCTTATCG
AAATTAATACGACTCACTATAGGGAGACCCAAGCTTGGTACCGAGCTCGGATCGATATCATGGTGAGCAAGGGCGAGGAGCTGTT
CACCGGGGTGGTGCCCATCCTGGTCGAGCTGGACGGCGACGTAAACGGCCACAAGTTCAGCGTGTCCGGCGAGGGCGAGGGCGA
TGCCACCTACGGCAAGCTGACCCTGAAGTTCATCTGCACCACCGGCAAGCTGCCCGTGCCCTGGCCCACCCTCGTGACCACCCTG
ACCTGGGGCGTGCAGTGCTTCGCCCGCTACCCCGACCACATGAAGCAGCACGACTTCTTCAAGTCCGCCATGCCCGAAGGCTACG
TCCAGGAGCGCACCATCTTCTTCAAGGACGACGGCAACTACAAGACCCGCGCCGAGGTGAAGTTCGAGGGCGACACCCTGGTGA
ACCGCATCGAGCTGAAGGGCATCGACTTCAAGGAGGACGGCAACATCCTGGGGCACAAGCTGGAGTACAACGCCATCAGCGACA
ACGTCTATATCACCGCCGACAAGCAGAAGAACGGCATCAAGGCCAACTTCAAGATCCGCCACAACATCGAGGACGGCAGCGTGC
AGCTCGCCGACCACTACCAGCAGAACACCCCCATCGGCGACGGCCCCGTGCTGCTGCCCGACAACCACTACCTGAGCACCCAGTC
CGCCCTGAGCAAAGACCCCAACGAGAAGCGCGATCACATGGTCCTGCTGGAGTTCGTGACCGCCGCCGGGATCACTCTCGGCATG
GACGAGCTGTACAAGTAATAAGCTAGCACACCGGTCGTCTAGCAATGCGATCCACGTACGTAGGATCCCGACTGTGCCTTCTAGT
TGCCAGCCATCTGTTGTTTGCCCCTCCCCCGTGCCTTCCTTGACCCTGGAAGGTGCCACTCCCACTGTCCTTTCCTAATAAAATGAG
GAAATTGCATCGCATTGTCTGAGTAGGTGTCATTCTATTCTGGGGGGTGGGGTGGGGCAGGACAGCAAGGGGGAGGATTGGGAA
GACAATAGCAGGCATGCTGGGGATGCGGTGGGCTCTATGGACATTGATTATTGACTAGTTATTAATAGTAATCAATTACGGGGTC
ATTAGTTCATAGCCCATATATGGAGTTCCGCGTTACATAACTTACGGTAAATGGCCCGCCTGGCTGACCGCCCAACGACCCCCGCC
CATTGACGTCAATAATGACGTATGTTCCCATAGTAACGCCAATAGGGACTTTCCATTGACGTCAATGGGTGGACTATTTACGGTAA
ACTGCCCACTTGGCAGTACATCAAGTGTATCATATGCCAAGTACGCCCCCTATTGACGTCAATGACGGTAAATGGCCCGCCTGGC
ATTATGCCCAGTACATGACCTTATGGGACTTTCCTACTTGGCAGTACATCTACGTATTAGTCATCGCTATTACCATGGTGATGCGGT
TTTGGCAGTACATCAATGGGCGTGGATAGCGGTTTGACTCACGGGGATTTCCAAGTCTCCACCCCATTGACGTCAATGGGAGTTTG
TTTTGGCACCAAAATCAACGGGACTTTCCAAAATGTCGTAACAACTCCGCCCCATTGACGCAAATGGGCGGTAGGCGTGTACGGT
GGGAGGTCTATATAAGCAGAGCTCTCTGGCTAACTAGAGAACCCACTGCTTACTGGCCCCGGGATGGTGAGCAAGGGCGAGGAG
GATAACATGGCCATCATCAAGGAGTTCATGCGCTTCAAGGTGCACATGGAGGGCTCCGTGAACGGCCACGAGTTCGAGATCGAGG
GCGAGGGCGAGGGCCGCCCCTACGAGGGCACCCAGACCGCCAAGCTGAAGGTGACCAAGGGTGGCCCCCTGCCCTTCGCCTGGG
ACATCCTGTCCCCTCAGTTCATGTACGGCTCCAAGGCCTACGTGAAGCACCCCGCCGACATCCCCGACTACTTGAAGCTGTCCTTC
CCCGAGGGCTTCAAGTGGGAGCGCGTGATGAACTTCGAGGACGGCGGCGTGGTGACCGTGACCCAGGACTCCTCCCTGCAGGAC

GGCGAGTTCATCTACAAGGTGAAGCTGCGCGGCACCAACTTCCCCTCCGACGGCCCCGTAATGCAGAAGAAGACCATGGGCTGG
GAGGCCTCCTCCGAGCGGATGTACCCCGAGGACGGCGCCCTGAAGGGCGAGATCAAGCAGAGGCTGAAGCTGAAGGACGGCGGC
CACTACGACGCTGAGGTCAAGACCACCTACAAGGCCAAGAAGCCCGTGCAGCTGCCCGGCGCCTACAACGTCAACATCAAGTTG
GACATCACCTCCCACAACGAGGACTACACCATCGTGGAACAGTACGAACGCGCCGAGGGCCGCCACTCCACCGGCGGCATGGAC
GAGCTGTACAAGTAATCTAGAGCTCGCTGATCAGCCTCGACTGTGCCTTCTAGTTGCCAGCCATCTGTTGTTTGCCCCTCCCCCGT
GCCTTCCTTGACCCTGGAAGGTGCCACTCCCACTGTCCTTTCCTAATAAAATGAGGAAATTGCATCGCATTGTCTGAGTAGGTGTC
ATTCTATTCTGGGGGGTGGGGTGGGGCAGGACAGCAAGGGGGAGGATTGGGAAGACAATAGCAGGCATGCTGGGGATGCGGTGG
GCTCTATGGCTTCTGAGGCGGAAAGAACCAGCTGGGGCTCGAGTGCATTCTAGTTGTGGTTTGTCCAAACTCATCAATGTATCTTA
TCATGTCTGTATACCGTCGACCTCTAGCTAGAGCTTGGCGTAATCATGGTCATAGCTGTTTCCTGTGTGAAATTGTTATCCGCTCAC
AATTCCACACAACATACGAGCCGGAAGCATAAAGTGTAAAGCCTGGGGTGCCTAATGAGTGAGCTAACTCACATTAATTGCGTTG
CGCTCACTGCCCGCTTTCCAGTCGGGAAACCTGTCGTGCCAGCTGCATTAATGAATCGGCCAACGCGCGGGGAGAGGCGGTTTGC
GTATTGGGCGCTCTTCCGCTTCCTCGCTCACTGACTCGCTGCGCTCGGTCGTTCGGCTGCGGCGAGCGGTATCAGCTCACTCAAAG
GCGGTAATACGGTTATCCACAGAATCAGGGGATAACGCAGGAAAGAACATGTGAGCAAAAGGCCAGCAAAAGGCCAGGAACCG
TAAAAAGGCCGCGTTGCTGGCGTTTTTCCATAGGCTCCGCCCCCCTGACGAGCATCACAAAAATCGACGCTCAAGTCAGAGGTGG
CGAAACCCGACAGGACTATAAAGATACCAGGCGTTTCCCCCTGGAAGCTCCCTCGTGCGCTCTCCTGTTCCGACCCTGCCGCTTAC
CGGATACCTGTCCGCCTTTCTCCCTTCGGGAAGCGTGGCGCTTTCTCAATGCTCACGCTGTAGGTATCTCAGTTCGGTGTAGGTCGT
TCGCTCCAAGCTGGGCTGTGTGCACGAACCCCCCGTTCAGCCCGACCGCTGCGCCTTATCCGGTAACTATCGTCTTGAGTCCAACC
CGGTAAGACACGACTTATCGCCACTGGCAGCAGCCACTGGTAACAGGATTAGCAGAGCGAGGTATGTAGGCGGTGCTACAGAGT
TCTTGAAGTGGTGGCCTAACTACGGCTACACTAGAAGGACAGTATTTGGTATCTGCGCTCTGCTGAAGCCAGTTACCTTCGGAAAA
AGAGTTGGTAGCTCTTGATCCGGCAAACAAACCACCGCTGGTAGCGGTGGTTTTTTTGTTTGCAAGCAGCAGATTACGCGCAGAA
AAAAAGGATCTCAAGAAGATCCTTTGATCTTTTCTACGGGGTCTGACGCTCAGTGGAACGAAAACTCACGTTAAGGGATTTTGGT
CATGAGATTATCAAAAAGGATCTTCACCTAGATCCTTTTAAATTAAAAATGAAGTTTTAAATCAATCTAAAGTATATATGAGTAAA
CTTGGTCTGACAGTTACCAATGCTTAATCAGTGAGGCACCTATCTCAGCGATCTGTCTATTTCGTTCATCCATAGTTGCCTGACTCC
CCGTCGTGTAGATAACTACGATACGGGAGGGCTTACCATCTGGCCCCAGTGCTGCAATGATACCGCGAGACCCACGCTCACCGGC
TCCAGATTTATCAGCAATAAACCAGCCAGCCGGAAGGGCCGAGCGCAGAAGTGGTCCTGCAACTTTATCCGCCTCCATCCAGTCT
ATTAATTGTTGCCGGGAAGCTAGAGTAAGTAGTTCGCCAGTTAATAGTTTGCGCAACGTTGTTGCCATTGCTACAGGCATCGTGGT
GTCACGCTCGTCGTTTGGTATGGCTTCATTCAGCTCCGGTTCCCAACGATCAAGGCGAGTTACATGATCCCCCATGTTGTGCAAAA
AAGCGGTTAGCTCCTTCGGTCCTCCGATCGTTGTCAGAAGTAAGTTGGCCGCAGTGTTATCACTCATGGTTATGGCAGCACTGCAT
AATTCTCTTACTGTCATGCCATCCGTAAGATGCTTTTCTGTGACTGGTGAGTACTCAACCAAGTCATTCTGAGAATAGTGTATGCG
GCGACCGAGTTGCTCTTGCCCGGCGTCAATACGGGATAATACCGCGCCACATAGCAGAACTTTAAAAGTGCTCATCATTGGAAAA
CGTTCTTCGGGGCGAAAACTCTCAAGGATCTTACCGCTGTTGAGATCCAGTTCGATGTAACCCACTCGTGCACCCAACTGATCTTC
AGCATCTTTTACTTTCACCAGCGTTTCTGGGTGAGCAAAAACAGGAAGGCAAAATGCCGCAAAAAAGGGAATAAGGGCGACACG
GAAATGTTGAATACTCATACTCTTCCTTTTTCAATATTATTGAAGCATTTATCAGGGTTATTGTCTCATGAGCGGATACATATTTGA
ATGTATTTAGAAAAATAAACAAATAGGGGTTCCGCGCACATTTCCCCGAAAAGTGCCACCTGACGTC

With the multiple cloning sites

...ACAAGTAATAAGCTAGCACACCGGTCGTCTAGCAATGCGATCCACGTACGTAGGATCCC

Cerulean *NheI* *AgeI* *BsiWI* *BamHI*

GACTGTG….

Sequence 1. Plasmid Map of pFmiR-empty and sequence.

Appendix 3B. pFmiR-B3GLCT-3'UTR plasmid map and 3'UTR sequence

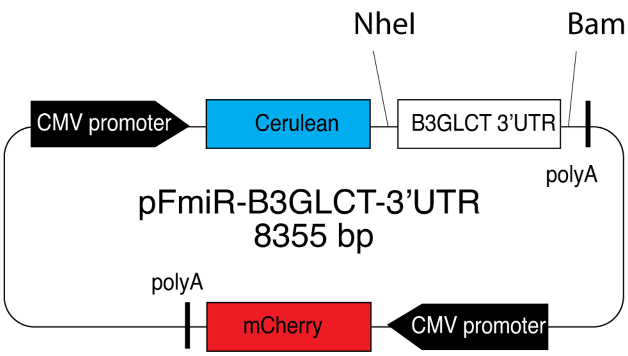

3'UTR sequence:

GCTAGCATCAGGGTGACCTGTGCGCCTAGCCTGCTCAGGGAGTGAACTGGAGACTGTGGCCTCATCCCACTGTGCTGTGCTCACA
ACACTTGTGTCTGCCACATGGCATTGGGTGCTTCCTGACTTTAGGGGGAGATTTTATGTATGGTATTTTTTGACAGAGGAAGAAAA
GGGGTCACAGGAGAAACATTTTTTTTTCTGGGAAAAATCACTTGCTTTTGACTTATGCAGTTGTTTTAACACTTAGTGATGACTGTG
TATTCTCCAAGCTGTGATACAGCAGTTTTTTTTTATTGTCACAGGGAAATAAATGGTACCAGAAGTCCCTTTCCTGTTCTGTCTCTT
CATTGTAATGGAAGTTTCAGTTGGGCATGAGCCTGGAGAGATGTGACTGTCTACAGTTCTATTTGTATATATAAAAAGAAGACTG
AAAGTCTTTTGACATGGATATTGTGAATGGTATGAACTTTTAAACCATATTATTGATGATGAAAATTATTTCCTGGGAACTCAGTA
GGAATAATACCGTATTAAGGAATAATACTGTACATAAAACATCATGAAACCCTAGATATGAAATCCCCTGAAGTCTGTAATCATG
GTGGTTATGTTTTGTCTATTCTTTTGCTGTTTGTGCCTCATAAAAAGAGAATGAGGTCTTCTGCTAGAGCTTCGTATTGCTTTGGAA
GTTCATCTGTGTTTTATTTCTCCCTGAAGCCCTATCTTTATGGCTTACTTGTAACATGAAAGTAGTAGATGCTGCCAGAAAATAGTG
TCCTCAATATTTTAAAACAATGTTGACATGTTTTGTTCAAGTCAGCAAGCTCTATGTGAGTCTCAGGAAGTGAATTAAATTTGGAC
CTTATGTTTTACTCTTGTTTTTTTTTTTTTTTTTAAATGTTACTTAATGACTCTCTCCTGACTCAGGAGAGAAACCCCTTGTGGAAGGA
CAGCATGGTGATCAGGCAATTTCTCTGGGTTCCCAAAGAATGACATTTGAACACAGTATTTTGAAACAGCTCTAGTTTTCAAATTA
TATCTTTAATATATAGTAATGTAACATATTCAGTATTAATGTATAAAAAGCACTCTAATTATATAATTCAGTTTTTGTAAAGGTATT
TGCATAAAATTTAATATGTCTTAAACTAATTTTGGTAAATTACTTCTTTTTTTTCTTTTTAATAAAAACTGTTACTCATTAACTTTGC
TTATAATGCTTTTTATAGCCCAGCACAGAATTTAAAGCCATACCACCAAAAGTACCTGTGTGTGTTAATATGTTTTTCTTGTAGCAT
AGATTGACTATTTGCAATAGTATTAGTATTTACCATTTTTCCAAATTAGCAACTACCAGACCTCACGTGTTGCAGTGATAACACAA
TGCATTGGATTCAGTTTTGTGAAAATGGATTCTGTGGCCATCCAAGGGATGTATCAGGGATGATCAGCTGATGAGAGGCTCCAGA
AGGATTTCTAGATCGCTTCAAGCCTATACTGATGGCCTTAGCTTTGTTCAGTCATTGTAACTGGGATTGTTGTCATTGCTACCGTGG
TAGTCACCTTCATGTCATCTATAATAGTACTCCTGGAGAGCCCTGGCTGCCTACACCAGTGGAAAAGAGTCTCCAGTTCTGCTCTG
GCCTACTAACTGTTACCACTGAGAGAACAACATGTTCATTTGACATGATTGAAGCTGGCATCCGTATATGAAGATCCTTGTCAAGC
TTTCTTCTGTGGTCTGATTAGTGCCTTCTACTGATACCGGGGCACCTCCTCTGGTACTTTTAAGTGTTTTGTTAATTATATTTACTTT
TTGGAATGGTGTAAGCCTAACCACAAGTAAAAGATCTTTGCCTAAGTTTTTGATTTCTCAAATATTGTGTTCATTAGTCTAGACTG
GGAATGGGGAGGGGAAATGGGGAAAATGAATGAATGAAATCAGAAAAAAGTCAGCGGCTCAGTAAATACAGTTTAAAGAGAGA
ATAATTACTTCAGAGCTACCCTTTTAAGAGAAAACCATCAGAAATTGATAATGTTTATATAAAGTTTATAAAGCCATTGTGTTTTG
TTATATAACAAATCAGAGATGTTATTTTAGAATCGATTCCCATCTAAAGAACTCAATTTTGAGTCTGACATTTCCAGGACCAGATA
TTGTCTTACTCACATTTCCTTTGCTTTGAAATAGGGCTTTCCTTCCAAATGGCTATTTTTAGGCTAGGGATGTTAACATCAGGGATT
TGTGTGTGGAATAACTGGAATGTCATTTTTGCTTTTAAGCCATTTCTGATGATATAGCCAAAGCAGGTTGTCTGACTATGTAGGAT
TTTTACATCTTGAAACTAAATCAGAAATCCAGACATGAAAATAACCTTTCTAGAATGCCTAGGAGCAGAAAACAATAATAGCATG
CTAAATCACAAATGATGCTATGTATGGGTATGTAAATATCAGTGCTGTCTGCATTTCTGGGTTTATTGAAGACCTCTTGTTGTATAT
ATCCTCAAAAATTAATGTAATTGACATCTTCAAGAATGTTTCTATTGTCTTCCATTCATAATCAGAGATGTAATTTGTATGGACTAA
ATAAAAACTTTATTATGTAATGAAAAG

Sequence 2. Plasmid Map of pFmiR-B3GLCT-3'UTR and sequence of 3'-UTR of B3GLCT.

Table 3.2. Identification of downregulatory and upregulatory miRs for B3GLCT from miRFluR assay.

miRNAs	Normalization	Error prop	%error	Z-score
miR-4446-5p	0.547	0.040	7.244	-4.952
miR-670-5p	0.633	0.029	4.548	-3.892
miR-4504	0.700	0.034	4.836	-3.062
miR-200b	0.703	0.039	5.496	-3.025
miR-4725-5p	0.718	0.032	4.485	-2.835
miR-5583-3p	0.725	0.019	2.584	-2.756
miR-6846-3p	0.730	0.074	10.185	-2.684
miR-6764-5p	0.733	0.054	7.394	-2.656
miR-504-5p	0.736	0.013	1.802	-2.618
miR-4635	0.738	0.044	5.935	-2.587
miR-4450	0.742	0.056	7.529	-2.545
miR-6776-3p	0.745	0.034	4.518	-2.503
miR-4716-5p	0.749	0.023	3.103	-2.450
miR-8052	0.755	0.016	2.160	-2.378
miR-4649-3p	0.759	0.039	5.082	-2.327
miR-542-3p	0.765	0.039	5.105	-2.259
miR-5681b	0.767	0.018	2.396	-2.227
miR-4524a-3p	0.768	0.052	6.781	-2.225
miR-429	0.777	0.029	3.750	-2.111
miR-6889-3p	0.778	0.047	6.032	-2.099
miR-544b	0.780	0.032	4.078	-2.076
miR-1270	0.780	0.029	3.745	-2.076
miR-4423-3p	0.782	0.075	9.595	-2.051
miR-6888-3p	0.785	0.039	4.976	-2.015
NTC1	1.000	0.009	0.876	
miR-7843-3p	1.201	0.062	5.154	3.122
miR-4526	1.202	0.059	4.919	3.135
miR-23b-5p	1.203	0.068	5.648	3.151
miR-1827	1.203	0.102	8.504	3.152
miR-1911-3p	1.205	0.133	11.068	3.174
miR-450a-5p	1.207	0.041	3.408	3.207
miR-1911-5p	1.208	0.124	10.265	3.211
miR-181c-5p	1.216	0.148	12.175	3.313

miR-583	1.218	0.149	12.274	3.336
miR-7151-3p	1.224	0.028	2.302	3.414
miR-590-5p	1.226	0.139	11.329	3.438
miR-506-3p	1.229	0.022	1.780	3.471
miR-1908-5p	1.249	0.095	7.582	3.724
miR-187-5p	1.259	0.153	12.119	3.842
miR-6855-5p	1.270	0.111	8.763	3.977
miR-17-5p	1.279	0.112	8.779	4.093
miR-188-5p	1.310	0.161	12.271	4.474
miR-6895-5p	1.313	0.142	10.850	4.512
miR-183-3p	1.319	0.109	8.257	4.590
miR-6792-5p	1.325	0.051	3.848	4.659
miR-187-3p	1.328	0.137	10.279	4.702
miR-6856-3p	1.330	0.113	8.491	4.725
miR-3619-5p	1.336	0.070	5.223	4.800
miR-582-3p	1.338	0.145	10.816	4.820
miR-4430	1.360	0.146	10.709	5.087
miR-183-5p	1.393	0.292	20.961	5.501
miR-6878-3p	1.443	0.154	10.683	6.112
miR-891b	1.463	0.018	1.254	6.365
miR-4470	1.499	0.091	6.042	6.803

Table 3.3. Disease enrichment analysis of 27 downregulatory miRs for B3GLCT in miRNet

Pathway	Total	Expected	Hits	Pval
Preauricular dimple	17	2.15	9	7.49E-05
Preauricular sinus	17	2.15	9	7.49E-05
Malignant mesothelioma	70	8.87	21	9.22E-05
Adult onset	33	4.18	13	9.65E-05
Cleft Palate	107	13.6	28	0.000101
Acquired scoliosis	153	19.4	36	0.000122
Preauricular Fistulae, Congenital	18	2.28	9	0.000133
Curvature of spine	155	19.6	36	0.000162
Uranostaphyloschisis	86	10.9	23	0.000296
Frontal bossing	82	10.4	22	0.00038
Flatfoot	33	4.18	12	0.000432
Congenital small ears	29	3.67	11	0.000492

Hemangiosarcoma	11	1.39	6	0.00106
Acquired flat foot	32	4.05	11	0.00128
Muscle Cramp	32	4.05	11	0.00128
Adenoma	19	2.41	8	0.00133
Micrognathism	160	20.3	34	0.00136
Mandibular hypoplasia	160	20.3	34	0.00136
Hypoplastic mandible condyle	160	20.3	34	0.00136
Lymphoma, Follicular	12	1.52	6	0.00189
Intellectual Disability	378	47.9	67	0.00195
Sezary Syndrome	20	2.53	8	0.00197
Dull intelligence	330	41.8	59	0.00296
Orbital separation excessive	131	16.6	28	0.00321
Low intelligence	326	41.3	58	0.00359
Mental deficiency	326	41.3	58	0.00359
Colonic Neoplasms	79	10	19	0.00371
Poor school performance	327	41.4	58	0.00385
Ventricular Septal Defects	63	7.98	16	0.00424
Aplasia/Hypoplasia of the lungs	10	1.27	5	0.00468
Mental Retardation	330	41.8	58	0.00473
Small head	192	24.3	37	0.00511
Liver neoplasms	70	8.87	17	0.00532
Gastroesophageal reflux disease	43	5.45	12	0.00565
Global developmental delay	313	39.6	55	0.00592
Byzanthine arch palate	113	14.3	24	0.00667
Cognitive delay	315	39.9	55	0.00677
Squamous cell carcinoma	66	8.36	16	0.00688
Mental and motor retardation	316	40	55	0.00724
Heartburn	39	4.94	11	0.00728
Low posterior hairline	34	4.31	10	0.00753
Distal amyotrophy	29	3.67	9	0.00756
Bladder Neoplasm	50	6.33	13	0.00774
Muscle hypotonia	311	39.4	54	0.00814
Neoplastic Cell Transformation	57	7.22	14	0.00988
Precancerous Conditions	46	5.83	12	0.01
Renal Insufficiency	46	5.83	12	0.01
Alcoholic Intoxication	16	2.03	6	0.0105
Abnormally-shaped vertebrae	16	2.03	6	0.0105
Renal failure in adulthood	41	5.19	11	0.0108
Isolated cases	36	4.56	10	0.0115
Bilateral fifth finger clinodactyly	58	7.35	14	0.0116
Curvature of little finger	58	7.35	14	0.0116
Proximal muscle weakness	26	3.29	8	0.0123
Dilated ventricles (finding)	65	8.23	15	0.0139

Diffuse Large B-Cell Lymphoma	17	2.15	6	0.0145
Broad thumbs	17	2.15	6	0.0145
Cataract	121	15.3	24	0.0156
Liver carcinoma	121	15.3	24	0.0156
Downward slant of palpebral fissure	90	11.4	19	0.0158
Prostatic Neoplasms	260	32.9	45	0.0159

Table 3.4 RT-PCR with 3 biological replicates

Replicate 1	Delta Ct	Error prop (delta Ct)	2^-delta Ct	Error prop (2^delta ct)		relative (/ref.)	Error prop.
NTC1	7.358854294	0.058438507	0.006092059	0.000246768		1	0.057284822
miR-200a-3p	7.162140846	0.038838774	0.006982015	0.000187963		1.146084524	0.055741609
miR-200b-3p	7.901312828	0.091189692	0.004182807	0.000264386		0.686599859	0.051545367
miR-504	7.806370735	0.093613745	0.004467332	0.000289877		0.733304124	0.056092931
miR-4504	7.650029182	0.076310553	0.004978652	0.000263343		0.817236254	0.054446569
miR-4649-3p	7.519591331	0.085243231	0.005449761	0.000322005		0.894567941	0.064084685
miR-4725-5p	7.651560783	0.092579754	0.004973369	0.000319148		0.816369116	0.061951301
miR-891b	6.491556168	0.060372043	0.011113398	0.000465059		1.824243263	0.106244321
miR-4470-5p	7.56333828	0.043874601	0.005286988	0.000160786		0.867849038	0.043958401
Replicate 2	Delta Ct	Error prop (delta Ct)	2^-delta Ct	Error prop (2^delta ct)		relative (/ref.)	Error prop.
NTC1	6.666665108	0.057404844	0.009843144	0.000391659		1	0.056271566
miR-200a-3p	6.549961344	0.090344484	0.010672475	0.000668332		1.08425475	0.080445291
miR-200b-3p	7.222418736	0.031457839	0.006696306	0.000146012		0.680301593	0.030867247
miR-504	7.046149775	0.077890451	0.007566544	0.000408514		0.768712127	0.05155598
miR-4504	6.980326325	0.032778975	0.007919767	0.000179942		0.804597289	0.03686665
miR-4649-3p	6.805610943	0.106756282	0.008939371	0.000661494		0.908182514	0.076303122
miR-4725-5p	7.009653091	0.072323683	0.007760401	0.000389036		0.788406741	0.050460233
miR-891b	5.874842408	0.047618897	0.017041045	0.000562472		1.731260354	0.089502985
miR-4470-5p	6.918618787	0.09709403	0.008265863	0.000556296		0.839758455	0.065654911
Replicate 3	Delta Ct	Error prop (delta Ct)	2^-delta Ct	Error prop (2^delta ct)		relative (/ref.)	Error prop.
NTC1	7.006746292	0.081765842	0.007776053	0.000440714		1	0.080151632
miR-200a-3p	6.906258583	0.102561345	0.008336985	0.000592677		1.072135841	0.097475637
miR-200b-3p	7.454258919	0.055236301	0.005702227	0.000218321		0.733306063	0.050155281
miR-504	7.318007469	0.097732428	0.006267008	0.000424546		0.805936916	0.071184126
miR-4504	7.193367004	0.098582405	0.006832518	0.00046688		0.87866144	0.078005246
miR-4649-3p	7.025995255	0.026451112	0.007672991	0.000140681		0.986746251	0.058778085
miR-4725-5p	7.137515068	0.099496382	0.007102216	0.000489809		0.913344622	0.081530531
miR-891b	6.037761688	0.032019563	0.015221331	0.000337826		1.957462411	0.119143835
miR-4470-5p	7.24985218	0.058105494	0.006570176	0.000264618		0.844924368	0.058746679

Table 3.5. Quantification of 3 RT-PCR replicates

	Replicate 1		Replicate 2		Replicate 3		Mean of 3 rep.	Error prop	Std error of mean
	Mean	Error prop	Mean	Error prop	Mean	Error prop			
NTC	1	0.057284822	1	0.056271566	1	0.080151632	1	0.03781876	0
miR-200a-3p	1.146084524	0.055741609	1.08425475	0.080445291	1.072135841	0.097475637	1.100825038	0.04604354	0.039661477
miR-200b-3p	0.686599859	0.051545367	0.680301593	0.030867247	0.733306063	0.050155281	0.700069172	0.02608802	0.028955747
miR-504	0.733304124	0.056092931	0.768712127	0.05155598	0.805936916	0.071184126	0.769317722	0.03475568	0.036320183
miR-4504	0.817236254	0.054446569	0.804597289	0.03686665	0.87866144	0.078005246	0.833498328	0.03400718	0.03961964
miR-4649-3p	0.894567941	0.064084685	0.908182514	0.076303122	0.986746251	0.058778085	0.929832235	0.0385629	0.049756839
miR-4725-5p	0.816369116	0.061951301	0.788406741	0.050460233	0.913344622	0.081530531	0.839373493	0.03805176	0.065568816
miR-891b	1.824243263	0.106244321	1.731260354	0.089502985	1.957462411	0.119143835	1.837655343	0.06100446	0.113695891
miR-4470-5p	0.867849038	0.043958401	0.839758455	0.065654911	0.844924368	0.058746679	0.850843954	0.03281951	0.014951634

3.9 REFERENCES

1. Thu, C. T.; Mahal, L. K., Sweet Control: MicroRNA Regulation of the Glycome. *Biochemistry* **2020,** *59* (34), 3098-3110.
2. Agrawal, P.; Kurcon, T.; Pilobello, K. T.; Rakus, J. F.; Koppolu, S.; Liu, Z.; Batista, B. S.; Eng, W. S.; Hsu, K. L.; Liang, Y.; Mahal, L. K., Mapping posttranscriptional regulation of the human glycome uncovers microRNA defining the glycocode. *Proc Natl Acad Sci U S A* **2014,** *111* (11), 4338-43.
3. Kurcon, T.; Liu, Z.; Paradkar, A. V.; Vaiana, C. A.; Koppolu, S.; Agrawal, P.; Mahal, L. K., miRNA proxy approach reveals hidden functions of glycosylation. *Proc Natl Acad Sci U S A* **2015,** *112* (23), 7327-32.
4. Vaiana, C. A.; Kurcon, T.; Mahal, L. K., MicroRNA-424 Predicts a Role for beta-1,4 Branched Glycosylation in Cell Cycle Progression. *J Biol Chem* **2016,** *291* (3), 1529-37.
5. Varki, A., Biological roles of glycans. *Glycobiology* **2017,** *27* (1), 3-49.
6. Vasudevan, D.; Takeuchi, H.; Johar, S. S.; Majerus, E.; Haltiwanger, R. S., Peters plus syndrome mutations disrupt a noncanonical ER quality-control mechanism. *Curr Biol* **2015,** *25* (3), 286-295.
7. Holdener, B. C.; Percival, C. J.; Grady, R. C.; Cameron, D. C.; Berardinelli, S. J.; Zhang, A.; Neupane, S.; Takeuchi, M.; Jimenez-Vega, J. C.; Uddin, S. M. Z.; Komatsu, D. E.; Honkanen, R.; Dubail, J.; Apte, S. S.; Sato, T.; Narimatsu, H.; McClain, S. A.; Haltiwanger, R. S., ADAMTS9 and ADAMTS20 are differentially affected by loss of B3GLCT in mouse model of Peters plus syndrome. *Hum Mol Genet* **2019,** *28* (24), 4053-4066.
8. Weh, E.; Reis, L. M.; Tyler, R. C.; Bick, D.; Rhead, W. J.; Wallace, S.; McGregor, T. L.; Dills, S. K.; Chao, M. C.; Murray, J. C.; Semina, E. V., Novel B3GALTL mutations in classic Peters plus syndrome and lack of mutations in a large cohort of patients with similar phenotypes. *Clin Genet* **2014,** *86* (2), 142-8.
9. Maillette de Buy Wenniger-Prick, L. J.; Hennekam, R. C., The Peters' plus syndrome: a review. *Ann Genet* **2002,** *45* (2), 97-103.
10. Hennekam, R. C.; Van Schooneveld, M. J.; Ardinger, H. H.; Van Den Boogaard, M. J.; Friedburg, D.; Rudnik-Schoneborn, S.; Seguin, J. H.; Weatherstone, K. B.; Wittebol-Post, D.; Meinecke, P., The Peters'-Plus syndrome: description of 16 patients and review of the literature. *Clin Dysmorphol* **1993,** *2* (4), 283-300.
11. Wolter, J. M.; Kotagama, K.; Pierre-Bez, A. C.; Firago, M.; Mangone, M., 3'LIFE: a functional assay to detect miRNA targets in high-throughput. *Nucleic Acids Res* **2014,** *42* (17), e132.
12. Liu, J.; Li, Y.; Chen, X.; Xu, X.; Zhao, H.; Wang, S.; Hao, J.; He, B.; Liu, S.; Wang, J., Upregulation of miR-205 induces CHN1 expression, which is associated with the aggressive behaviour of cervical cancer cells and correlated with lymph node metastasis. *BMC Cancer* **2020,** *20* (1), 1029.
13. Wang, L.; Zhang, S.; Zhang, W.; Cheng, G.; Khan, R.; Junjvlieke, Z.; Li, S.; Zan, L., miR-424 Promotes Bovine Adipogenesis Through an Unconventional Post-Transcriptional Regulation of STK11. *Front Genet* **2020,** *11*, 145.
14. Vasudevan, S.; Tong, Y.; Steitz, J. A., Switching from repression to activation: microRNAs can up-regulate translation. *Science* **2007,** *318* (5858), 1931-4.

15. Valinezhad Orang, A.; Safaralizadeh, R.; Kazemzadeh-Bavili, M., Mechanisms of miRNA-Mediated Gene Regulation from Common Downregulation to mRNA-Specific Upregulation. *Int J Genomics* **2014,** *2014*, 970607.
16. Agarwal, V.; Bell, G. W.; Nam, J. W.; Bartel, D. P., Predicting effective microRNA target sites in mammalian mRNAs. *Elife* **2015,** *4*.
17. Dweep, H.; Sticht, C.; Pandey, P.; Gretz, N., miRWalk--database: prediction of possible miRNA binding sites by "walking" the genes of three genomes. *J Biomed Inform* **2011,** *44* (5), 839-47.
18. Dweep, H.; Gretz, N.; Sticht, C., miRWalk database for miRNA-target interactions. *Methods Mol Biol* **2014,** *1182*, 289-305.
19. Sticht, C.; De La Torre, C.; Parveen, A.; Gretz, N., miRWalk: An online resource for prediction of microRNA binding sites. *PLoS One* **2018,** *13* (10), e0206239.
20. Zhou, P.; Xu, W.; Peng, X.; Luo, Z.; Xing, Q.; Chen, X.; Hou, C.; Liang, W.; Zhou, J.; Wu, X.; Songyang, Z.; Jiang, S., Large-scale screens of miRNA-mRNA interactions unveiled that the 3'UTR of a gene is targeted by multiple miRNAs. *PLoS One* **2013,** *8* (7), e68204.
21. Baek, D.; Villen, J.; Shin, C.; Camargo, F. D.; Gygi, S. P.; Bartel, D. P., The impact of microRNAs on protein output. *Nature* **2008,** *455* (7209), 64-71.
22. Ostlund, G.; Sonnhammer, E. L., Quality criteria for finding genes with high mRNA-protein expression correlation and coexpression correlation. *Gene* **2012,** *497* (2), 228-36.
23. Didiano, D.; Hobert, O., Perfect seed pairing is not a generally reliable predictor for miRNA-target interactions. *Nat Struct Mol Biol* **2006,** *13* (9), 849-51.
24. Lal, A.; Navarro, F.; Maher, C. A.; Maliszewski, L. E.; Yan, N.; O'Day, E.; Chowdhury, D.; Dykxhoorn, D. M.; Tsai, P.; Hofmann, O.; Becker, K. G.; Gorospe, M.; Hide, W.; Lieberman, J., miR-24 Inhibits cell proliferation by targeting E2F2, MYC, and other cell-cycle genes via binding to "seedless" 3'UTR microRNA recognition elements. *Mol Cell* **2009,** *35* (5), 610-25.
25. Chi, S. W.; Zang, J. B.; Mele, A.; Darnell, R. B., Argonaute HITS-CLIP decodes microRNA-mRNA interaction maps. *Nature* **2009,** *460* (7254), 479-86.
26. Hafner, M.; Landthaler, M.; Burger, L.; Khorshid, M.; Hausser, J.; Berninger, P.; Rothballer, A.; Ascano, M., Jr.; Jungkamp, A. C.; Munschauer, M.; Ulrich, A.; Wardle, G. S.; Dewell, S.; Zavolan, M.; Tuschl, T., Transcriptome-wide identification of RNA-binding protein and microRNA target sites by PAR-CLIP. *Cell* **2010,** *141* (1), 129-41.
27. Fan, Y.; Siklenka, K.; Arora, S. K.; Ribeiro, P.; Kimmins, S.; Xia, J., miRNet - dissecting miRNA-target interactions and functional associations through network-based visual analysis. *Nucleic Acids Res* **2016,** *44* (W1), W135-41.
28. Chang, L.; Zhou, G.; Soufan, O.; Xia, J., miRNet 2.0: network-based visual analytics for miRNA functional analysis and systems biology. *Nucleic Acids Res* **2020,** *48* (W1), W244-W251.
29. Hsu, S. D.; Lin, F. M.; Wu, W. Y.; Liang, C.; Huang, W. C.; Chan, W. L.; Tsai, W. T.; Chen, G. Z.; Lee, C. J.; Chiu, C. M.; Chien, C. H.; Wu, M. C.; Huang, C. Y.; Tsou, A. P.; Huang, H. D., miRTarBase: a database curates experimentally validated microRNA-target interactions. *Nucleic Acids Res* **2011,** *39* (Database issue), D163-9.
30. Huang, H. Y.; Lin, Y. C.; Li, J.; Huang, K. Y.; Shrestha, S.; Hong, H. C.; Tang, Y.; Chen, Y. G.; Jin, C. N.; Yu, Y.; Xu, J. T.; Li, Y. M.; Cai, X. X.; Zhou, Z. Y.; Chen, X. H.; Pei, Y. Y.; Hu, L.; Su, J. J.; Cui, S. D.; Wang, F.; Xie, Y. Y.; Ding, S. Y.; Luo, M. F.; Chou, C. H.; Chang, N. W.; Chen, K. W.; Cheng, Y. H.; Wan, X. H.; Hsu, W. L.; Lee, T. Y.; Wei,

F. X.; Huang, H. D., miRTarBase 2020: updates to the experimentally validated microRNA-target interaction database. *Nucleic Acids Res* **2020,** *48* (D1), D148-D154.
31. Pinero, J.; Ramirez-Anguita, J. M.; Sauch-Pitarch, J.; Ronzano, F.; Centeno, E.; Sanz, F.; Furlong, L. I., The DisGeNET knowledge platform for disease genomics: 2019 update. *Nucleic Acids Res* **2020,** *48* (D1), D845-D855.
32. Dweep, H.; Gretz, N., miRWalk2.0: a comprehensive atlas of microRNA-target interactions. *Nat Methods* **2015,** *12* (8), 697.

CHAPTER 4

INVESTIGATING THE MIRNA REGULATORY LANDSCAPE OF OGT AND OGA VIA THE 3'UTR AND 5'UTR REGIONS

4.1 ABSTRACT

The addition of a single β-D-N-acetylglucosamine to serine or threonine residues on thousands of intracellular proteins is called O-linked GlcNAcylation (O-GlcNAcylation). O-GlcNAc occurs in diverse organisms including bacteria, protozoans and metazoans. This dynamic post-translational modification contributes to cellular processes including epigenetic modifications, transcription, metabolism, and cell signaling that play significant roles in development and normal physiology. O-GlcNAcylation is catalyzed by O-GlcNAc transferase (OGT) and the modification is removed by O-GlcNAcase (OGA). These enzymes are highly regulated at multiple levels, but little is known about their regulation by microRNAs (miRs). In this work, we built a comprehensive dataset of OGT and OGA regulation via both their 3'UTR and 5'UTRs. Downregulation was almost exclusively mediated through binding to the 3'UTR. While the majority of miRNA regulators of OGT and OGA showed no overlap, we observed significant co-regulation of OGT and OGA by a subset of miRs.

In summary, this work provides a better understanding of OGT and OGA regulation through miRNA binding via both the 3'UTR and 5'UTR regions and compares the impact of miRNA regulation via these regions.

4.2 INTRODUCTION

A myriad of cytoplasmic, nuclear and mitochondrial proteins are reversibly modified by O-GlcNAc on serine or threonine residues. Unlike canonical O-glycosylation, O-GlcNAc is a dynamic glycan modification found on cytoplasmic, mitochondrial and nuclear proteins[1]. O-GlcNAcylation is dynamically cycled by only two proteins: O-GlcNAc transferase (OGT) and O-GlcNAcase (OGA), which catalyze the addition and removal of O-GlcNAc respectively **(Figure 4.1**). O-GlcNAcylation is often compared to phosphorylation since they both dynamically modify the serine/threonine residues of thousands of proteins. However, unlike phosphorylation, O-GlcNAcylation utilizes just two enzymes instead of hundreds of phosphatases and kinases with their own substrate specificity and selectivity. Thus, OGT and OGA must display complex mechanisms of regulation and substrate selection.

O-GlcNAcylation is highly dependent on the availability of UDP-GlcNAc, which is generated from the hexosamine biosynthesis pathway (HBP). Thus, O-GlcNAcylation is considered a nutrient sensor of cell metabolic status that is highly regulated and responsive to environmental factors. This modification dynamically regulates all fundamental and developmental processes in the cell including stress response, epigenetics, signal transduction, cell proliferation, transcription, metabolism and proteostasis[1-13] (**Figure. 4.1**). Previously, studies have indicated that this modification has significant impacts on protein functions including cellular localization, stability, protein-protein interactions and has an extensive and intricate crosstalk with phosphorylation to modulate cellular signaling[14]. Due to the prevalence of O-GlcNAc, dysregulation of O-GlcNAcylation is associated with a diverse set of diseases including cancer, neurodegeneration, cardiovascular diseases, immunity and diabetes[3-13].

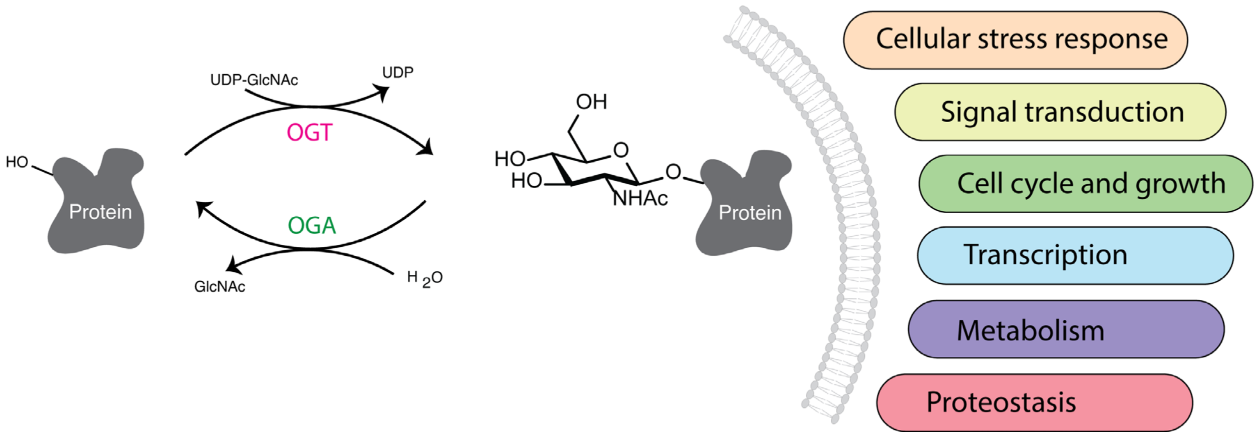

Figure 4.1. O-GlcNAcylation and functions. O-GlcNAc transferase (OGT) catalyzes the transfer of an N-acetylglucosamine (GlcNAc) from UDP-GlcNAc to a serine or threonine residue on a protein substrate (gray). O-GlcNAcase (OGA) catalyzes the removal of O-GlcNAc from protein substrates. This modification occurs mainly in the nucleus, cytoplasm and mitochondria.

Despite the significance and ubiquitous nature of O-GlcNAc, the study of this modification remains challenging due to technical difficulties in its detection and quantification. OGT is alternatively spliced to produce 3 isoforms: nuclear cytoplasmic OGT (ncOGT, 116 kDa, 13 TPRs), mitochondrial isoform (mOGT, 103 kDa, 9 TPRs), and a short OGT (sOGT, 70 kDa, 2-3 TPR) [15, 16]. The number of TPRs depends on the species and the type of alternatively spliced isoforms. Recently, studies have shown alternative splicing further regulates OGT expression in response to changes in O-GlcNAc levels through intron retention[17]. OGA is a 130 kDa protein with an N-terminal glycoside hydrolase (GH) catalytic domain, a stalk domain and C-terminal histone acetyltransferase (pseudoHAT) domain. OGA mRNA also undergoes alternative splicing in the HAT domain to produce a shorter form of OGA (sOGA) that only contains N-terminal O-GlcNAcase domains. Full length OGA localizes in the cytoplasm and nucleus while sOGA targets to the ER and nascent lipid droplets[18].

OGT and OGA expression levels are known to change O-GlcNAc homeostasis and lead to numerous human diseases. However, how OGT and OGA expression levels are regulated is a fundamental question that requires further investigation and study. In the effort to address that question, previous studies demonstrated that OGT and OGA are regulated at both transcriptional and post-transcriptional levels via CREB/P300 transcription factors and intron retention respectively[17, 19]. However, regulation of OGT/OGA by miRNA has been little explored. In recent years, 10 miR:mRNA interactions have been identified for the main transcript of OGT, regulating the enzyme in a variety of diseases from cancer to cardiovascular disease [2, 20-30]. Several of the miRs identified to hit OGT directly impact cell proliferation and are involved in cancer progression. Examples include miR-483 in gastric cancer and miR-485-5p in esophageal and colorectal cancers[20, 21]. Other identified functions of miRs targeting OGT include reducing tumor angiogenesis (miR-7[30]), inhibiting cell invasion (miR-24[25]), and modulating glucose-induced inflammation (miR-200a/b[22]).

In contrast to OGT, OGA is not predicted to be a highly regulated gene. To date, only one miR-mRNA interaction has been identified for this glycogene. miR-539 is up-regulated in the failing heart, and targets OGA, increasing O-GlcNAcylation during heart failure[31]. O-GlcNAcylation is highly dynamic in the heart, as are the transcript levels of both OGT and OGA. miR-24, which is involved in cardiovascular function has also been shown to modulate OGT[32], although not in the context of cardiovascular disease. Currently we still have a limited understanding of the regulation of OGT and OGA, but it is increasingly clear that miRs may play a strong role in the dynamic expression of these enzymes and the resulting O-GlcNAcylation levels. Given the critical importance of O-GlcNAcylation to a wide variety of diseases, miR regulation of these enzymes warrants a more thorough examination.

In my previous chapters, I have discussed the significance and development of miRFluR high-throughput platform to map miR:target interactomes. My exploration of the regulatory network of miRs via the 3'UTR region of B3GLCT opened up many questions. Is the 3'UTR a dominant and prevalent domain when considering miR regulation? What about the coding and 5'UTR regions? What is the interplay between the 3'UTR and 5'UTR? How do miRs regulate OGT and OGA to control O-GlcNAc levels? Herein, we investigate the miRNA regulatory network of OGT and OGA by miRs via both the 3'UTR and 5'UTR regions.

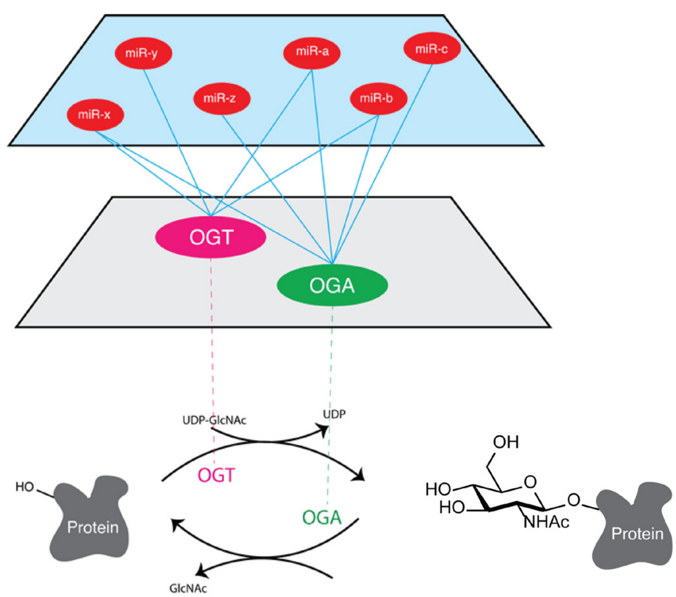

Figure 4.2. Regulatory network of OGA and OGA by miRNAs.

4.3 ROLES OF 5'UTR IN GENE REGULATION

mRNAs have both 5' and 3'-untranslated regions (5'UTR and 3'UTR). The 5'UTR is important in regulating gene expression as it is the translational initiation site. The 5'UTR consists of multiple components including the 5'cap, several open reading frames (ORFs), multiple AUGs start sites and internal ribosomal entry sites (IRESs) (**Figure 4.3**) [33]. All these features are important in regulating mRNA translation via altering mRNA stability, ribosomal accessibility, mRNA circularization or interacting with translational machinery. The 5'UTR typically possess a high GC content and a higher degree of secondary structure, which consequently influences the rate of mRNA translation. Additionally, both the 5'UTR and 3'UTR harbor numerous binding sites for RNA binding proteins that either suppress or enhance translation.

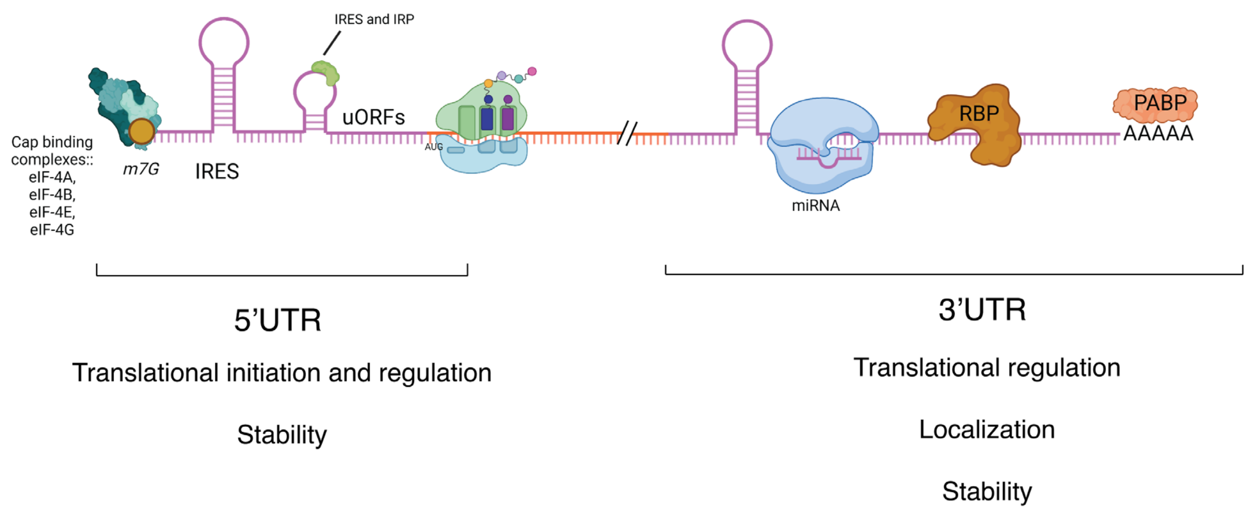

Figure 4.3. Roles of the 5'UTR and 3'UTR in translational regulation.

Contemporary studies demonstrated that miRNA targeting in mammalian cells occurs chiefly through pairing with the typically unstructured and AU-rich elements in the 3'UTR [34] [35]. However, translational repression through targeting the 5'UTR has been demonstrated, at least in the context of an artificially genetic-encoded reporter construct, which indicated that miRNA targeting of the 5'UTR is feasible [36]. Although the interaction between miRNA and the 5'UTR remains largely unexplored, several studies found upregulation upon miRNA binding. For instance, miR-10a induces upregulation of several ribosomal protein (Rps16, Rps6, and Rpl9) [37]. Another example is the upregulation of insulin expression through competitive binding of miR-196b to the same RNA element in the 5'UTR as HuD, a repressor, leading to de-repression (**Figure 4.4**) [38]. In addition, the interaction of the liver specific miRNA, miR-122, to the 5'UTR of Hepatitis C (HCV) RNA is required for viral replication [39]. These studies suggest a paradigm in which binding to the 5'UTR could result in mechanistic effects divergent from 3'UTR binding.

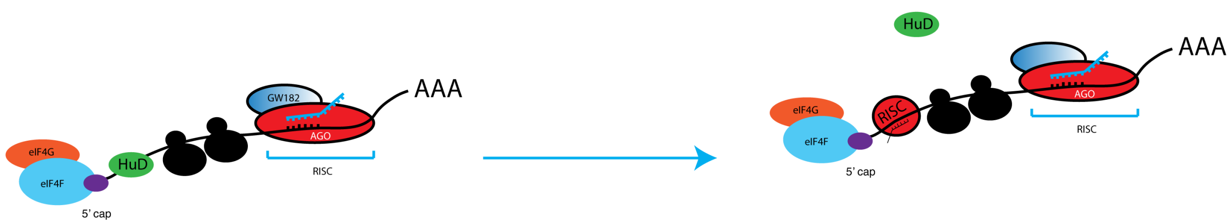

Figure 4.4. miRNA impacts RNA binding protein (HuD) to upregulate mRNA expression.

4.4 GENERATING THE RATIOMETRIC FLUORESCENT REPORTERS FOR MAPPING MIR-TARGET IN THE 3'UTR AND 5'UTR REGIONS OF OGT AND OGA

OGT has 3 isoforms (ncOGT, mOGT and sOGT) with 7 known transcripts. They contain identical catalytic regions but different TPR motif numbers. ncOGT is the major form of OGT. It is currently most studied and considered as most important functionally. Previous reports showed the absence of mOGT in multiple biological systems and ncOGT was found to be necessary and sufficient for O-GlcNAcylation of mitochondrial proteins [40]. The ncOGT transcript (1046 amino acids) contains the longest 3'UTR region. The mOGT 3'UTR is shorter and identical to 5'part of the ncOGT 3'UTR. Thus, a subset of miR regulating the ncOGT 3'UTR potentially also regulates the mOGT 3'UTR. sOGT transcript does not contain 3'UTR region. The 5'UTR regions of ncOGT, mOGT and sOGT are not homologous, which indicates possibly distinct regulatory patterns. Thus, I also generated pFmiR-mOGT 5'UTR and pFmiR-sOGT 5'UTR reporters. However, we mainly focus on ncOGT due to its prevalence and containing longest 3'UTR.

As discussion in Chapter 3, the pFmiR-3'UTR sensor is a dual color genetically-encoded fluorescent reporter for identification of miR targets[41]. In brief, the 3'UTR of the gene of interest is inserted downstream after the stop codon of Cerulean under the first CMV promoter to create pFmiR-ncOGT and OGA 3'UTR (**Figure 4.5, see Plasmid maps and sequences**). mCherry serves as a reference for transfection efficiency and any non-specific effects for a more reliable and accurate quantitative approach.

For our 5'UTR reporter, we still utilized Cerulean as the sensing module and mCherry as the control but instead of the 3'UTR domain, the 5'UTR of OGT or OGA was inserted upstream of the Cerulean start codon (pFmiR-OGT 5'UTR and pFmiR-OGA 5'UTR, **Figure 4.5, see Plasmid maps and sequences**).

I also generated a full version of both the 5'UTR and 3'UTR of OGT and OGA cloned into the reporter (pFmiR-OGT 3+5'UTR and pFmiR-OGA 3+5'UTR, **Figure 4.5, see Plasmid maps and sequences**). I next utilized our miRFluR platform to identify miR hits for each reporter. In brief, the specific pFmiR reporter is co-transfected with miR mimics into *HEK293T* cells in 384-well plate format. The fluorescent ratio of Cerulean/mCherry was then normalized to the non-targeting control (NTC) which is indicative of the extent of miR-target regulation. (**Figure 4.5B**).

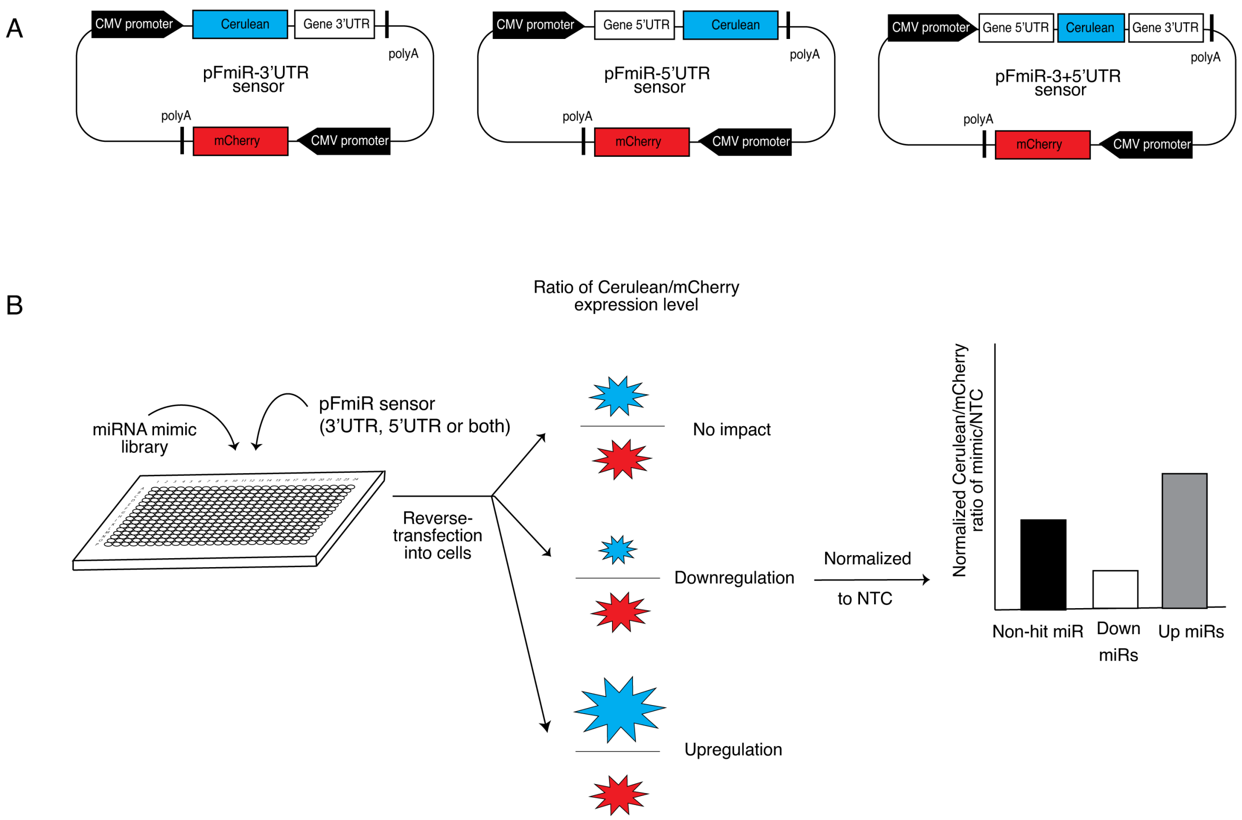

Figure 4.5. MiRFluR platform extending to the 5'UTR. (A) Plasmid maps for mapping miRs with the 3'UTR and 5'UTR regulatory regions. (B) Schematic illustration of miRFluR platform.

4.5 GENERAL MIRFLUR ASSAY FOR PFMIR REPORTERS

The miRFluR assay was performed for 6 pFmiR reporters (pFmiR-OGT 3'UTR, pFmiR-OGA 3'UTR, pFmiR-OGT 5'UTR, pFmiR-OGA 5'UTR, pFmiR-OGT 3+5'UTR and pFmiR-OGA 3+5'UTR) using miR mimic library v.21 (2601 miRs, miRIDIAN, Horizon Discovery) aliquoted in 24 384 well plates. Briefly, the reporter was transfected into HEK-293T cells along with miRs in a 384 well format. The data was then collected in triplicate, filtered and analysed as described in Chapter 3. In brief, we first omitted any data with high errors of measurement (median error ±

2 S. D. across all plates). Z-scores were then calculated for the remaining ratiometric normalized data for the reporters.

4.6 INVESTIGATION OF OGT REGULATION VIA 5'UTR AND 3'UTR REGIONS UTILIZING MIRFLUR PLATFORM

4.6.1 Comprehensive mapping of miR-target regulatory network via 3'UTR and 5'UTR of OGT

In Chapter 3, we set the threshold for hits at 20% change for downregulatory miRs and 95% confidence interval for upregulatory miRs. With that threshold, we found a high number of hits for OGT 3'UTR (160 downregulatory miRs and 67 upregulatory miRs out of 2080 data points, 11% hits) (**Figure 4.6**). Consistent with our miRFluR assay result, miR-7-5p, miR-101-5p, miR-15b-3p, miR-483-3p and miR-24-3p were found to regulate OGT. A dominant number of downregulatory miRs were identified in comparison to upregulators for the 3'UTR (70% downregulators). In contrast, regulation in the 5'UTR of OGT is heavily skewed towards the upregulatory miRs, in contrast to the 3'UTR (**Figure 4.7**). For the reporters with both the 5'UTR and 3'UTR domains, a dominant impact of 3'UTR was clearly observed, as most of the downregulatory miRs from the 3'UTR were detected (**Figure 4.8**).

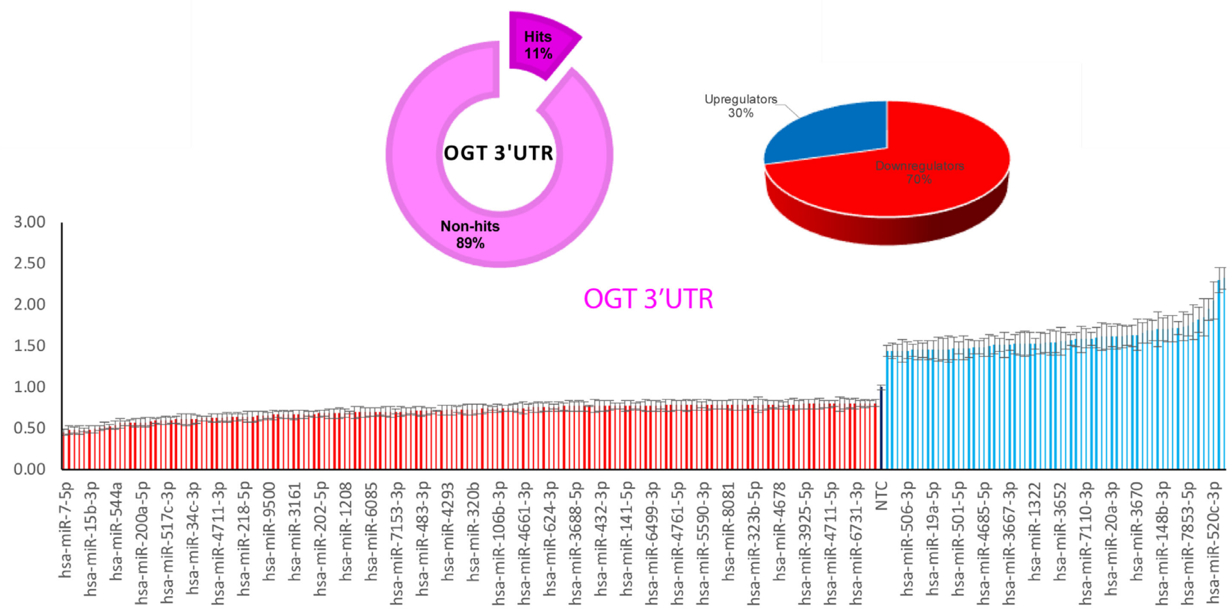

Figure 4.6. Identification and validation of hits for OGT 3'UTR. Pie graphs represent hit miR versus non hit miR percentages and downregulatory versus upregulatory miRs. Bar graph indicates the ratiometric data for miRs. Error bars represent propagated error.

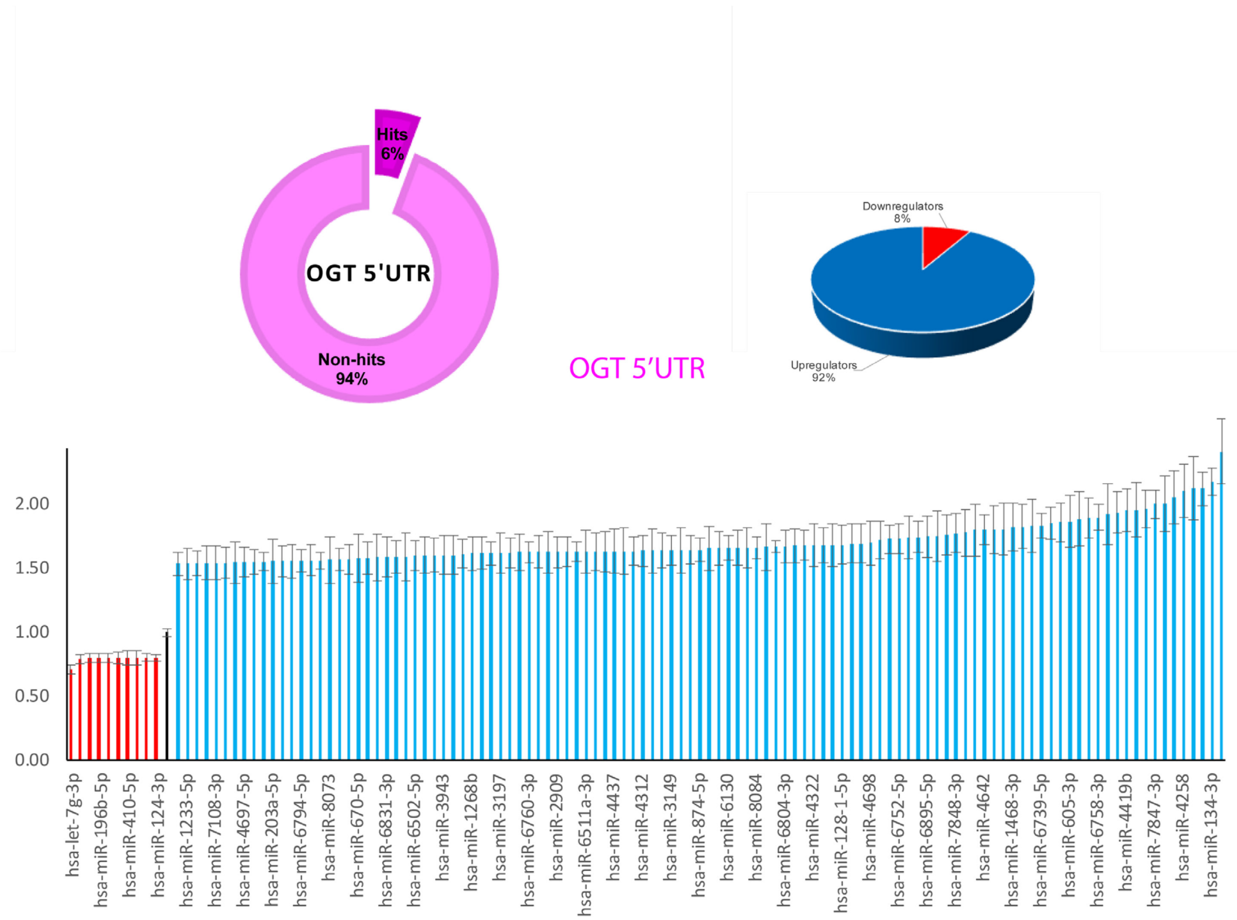

Figure 4.7. Identification and validation of hits for OGT 5'UTR. Pie graphs represent hit miR versus non hit miR percentages and downregulatory versus upregulatory miRs. Bar graph indicates the ratiometric data for miRs. Error bars represent propagated error.

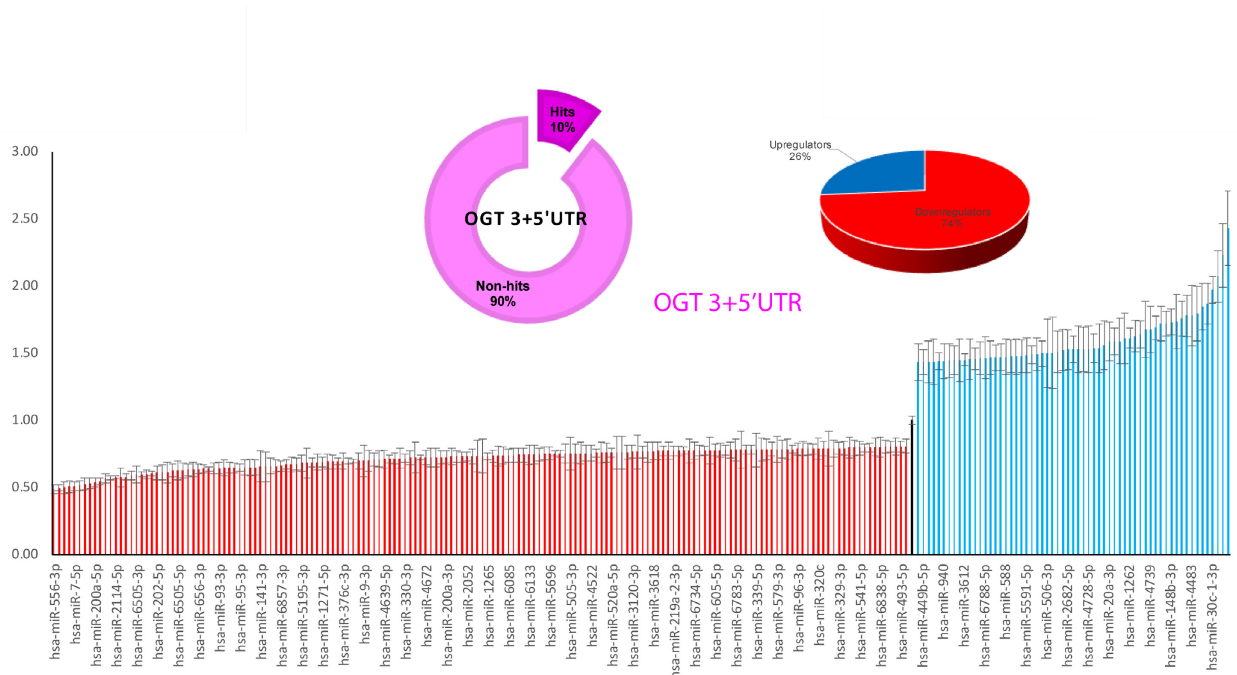

Figure 4.8. Identification and validation of hits for OGT 3+5'UTR. Pie graphs represent hit miR versus non hit miR percentages and downregulatory versus upregulatory miRs. Bar graph indicates the ratiometric data for miRs. Error bars represent propagated error.

I then performed Western blot analysis for the protein levels of OGT in *MDA-MB-231* transfected with the subset of downregulatory miRs from the 3'UTR dataset (miR-7-5p, miR-200a-3p, let-7g-3p, miR-95) and in the 5'UTR dataset (miR-196b-5p, miR-4639-5p, miR-196a-5p, miR-449c-3p and miR-4713-3p), and upregulatory miRs from the 3+5'UTR (miR-20a-3p, miR-30c-2-3p, miR-134-3p, miR-135b, miR-576 and miR-765) dataset that passed our threshold. I used NTC as a negative control (**Figure 4.9, Figure 4.10, Figure 4.11 and Table 3.1**). The protein levels followed the expected results from our sensor assay for miR-20a-3p, miR-30c-2-3p, miR-576 and miR-765 for upregulation. miR-7-5p, miR-200a-3p, let-7g-3p, miR-95 all repressed OGT, especially let-7g-3p. The downregulatory miR-4713 did not show significant inhibition.

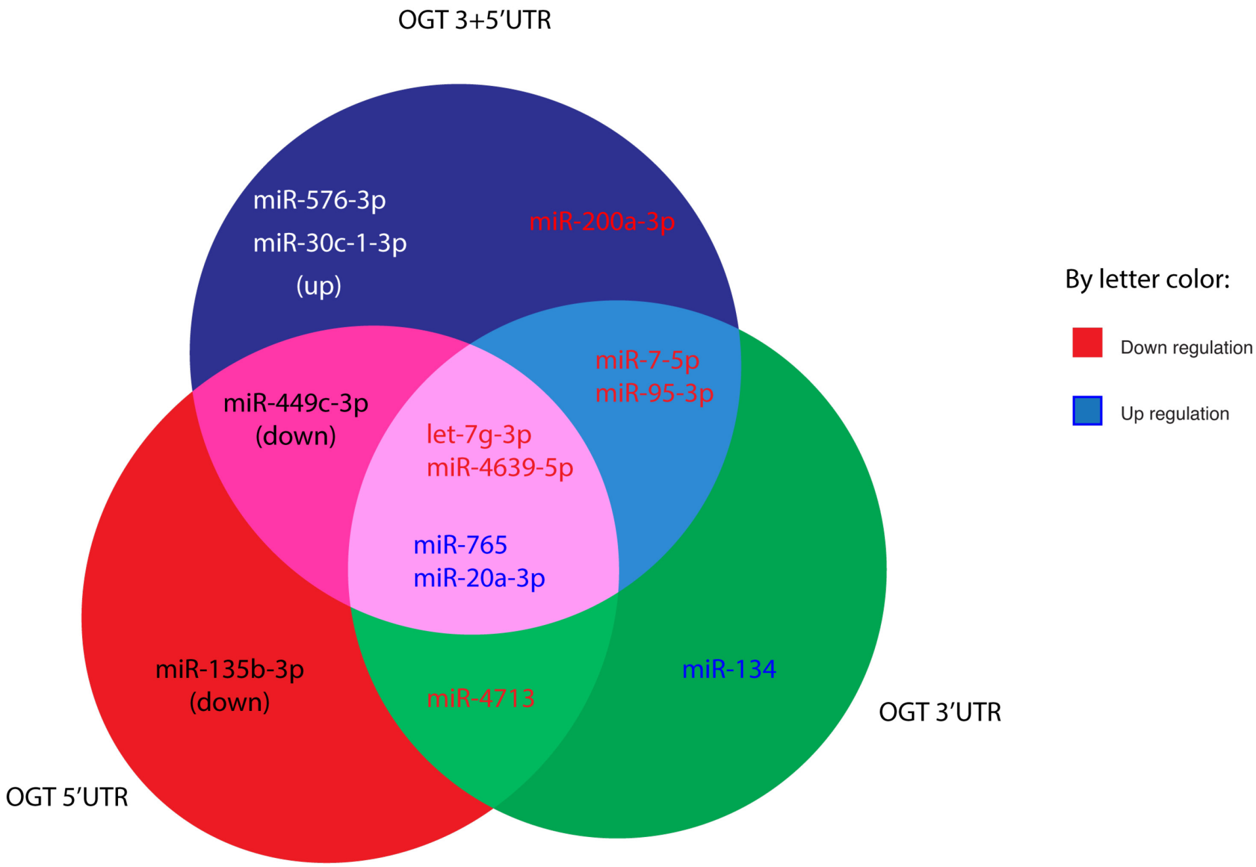

Figure 4.9. miRs were chosen for OGT validation.

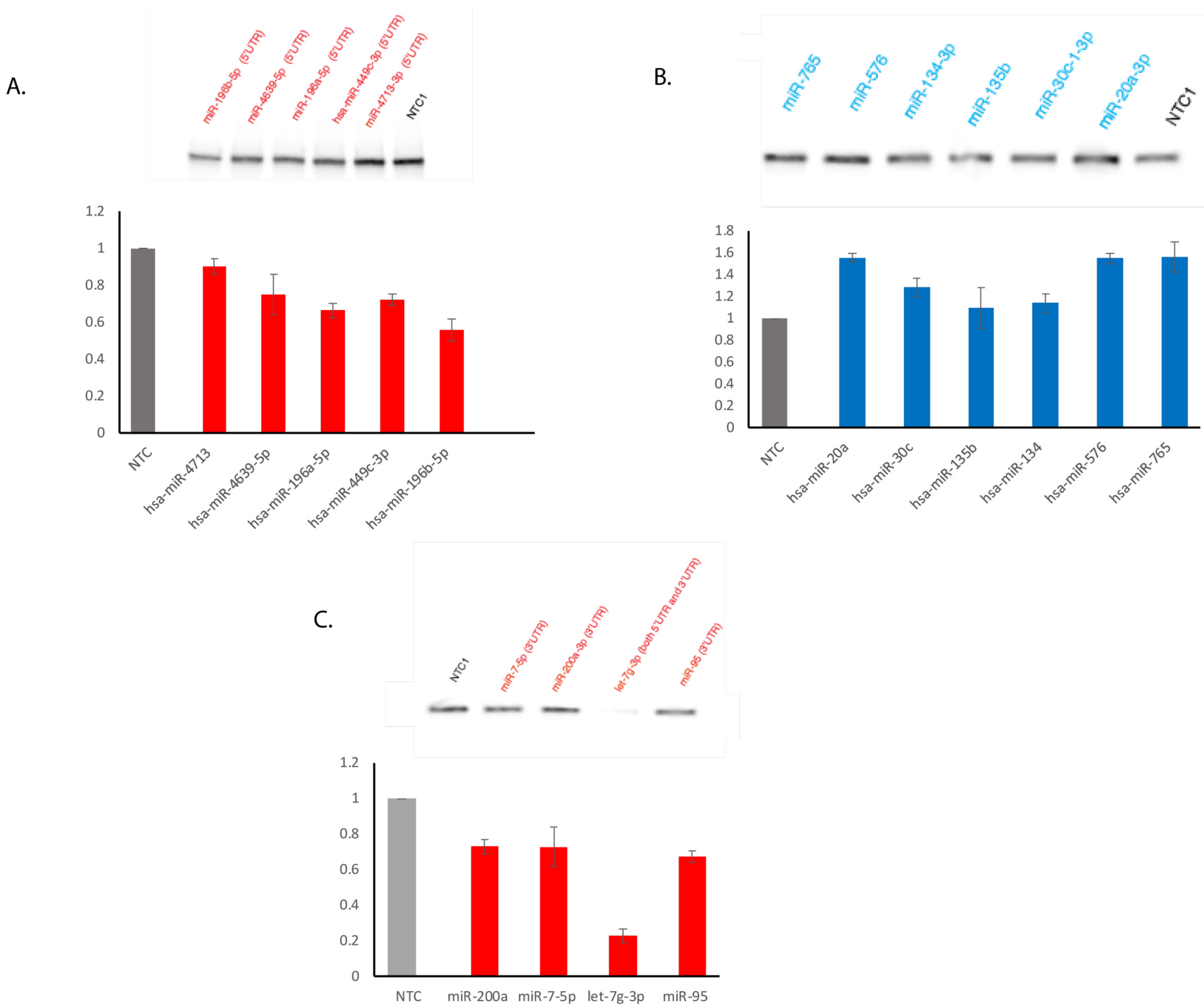

Figure 4.10. Validation of hits for OGT. (A), (B), (C) Western blot analysis of OGT in *MDA-MB-231* transfected with 50 nM miR mimics or NTC, 48 hours post-transfection and quantification of Western blot analysis for three independent experiments. OGT expression was normalized to total protein levels from Ponceau staining and set over normalized NTC for each blot. Ponceau and whole Westerns corresponding to the data are shown in **Appendix 4A**.

I also plotted OGT 3'UTR and 5'UTR data to compare. The graph represents data available for both 3'UTR and 5'UTR reporters. The OGT 3+5'UTR dataset was used to define downregulators and upregulators. Most of downregulatory miRs shown dowregulation in the 3’UTR region but not the 5’UTR. Only let-7g-3p repressed OGT in both 3’UTR and 5’UTR. For upregulation, most of the miRs indicated protein enhancement in both 3’UTR and 5’UTR.

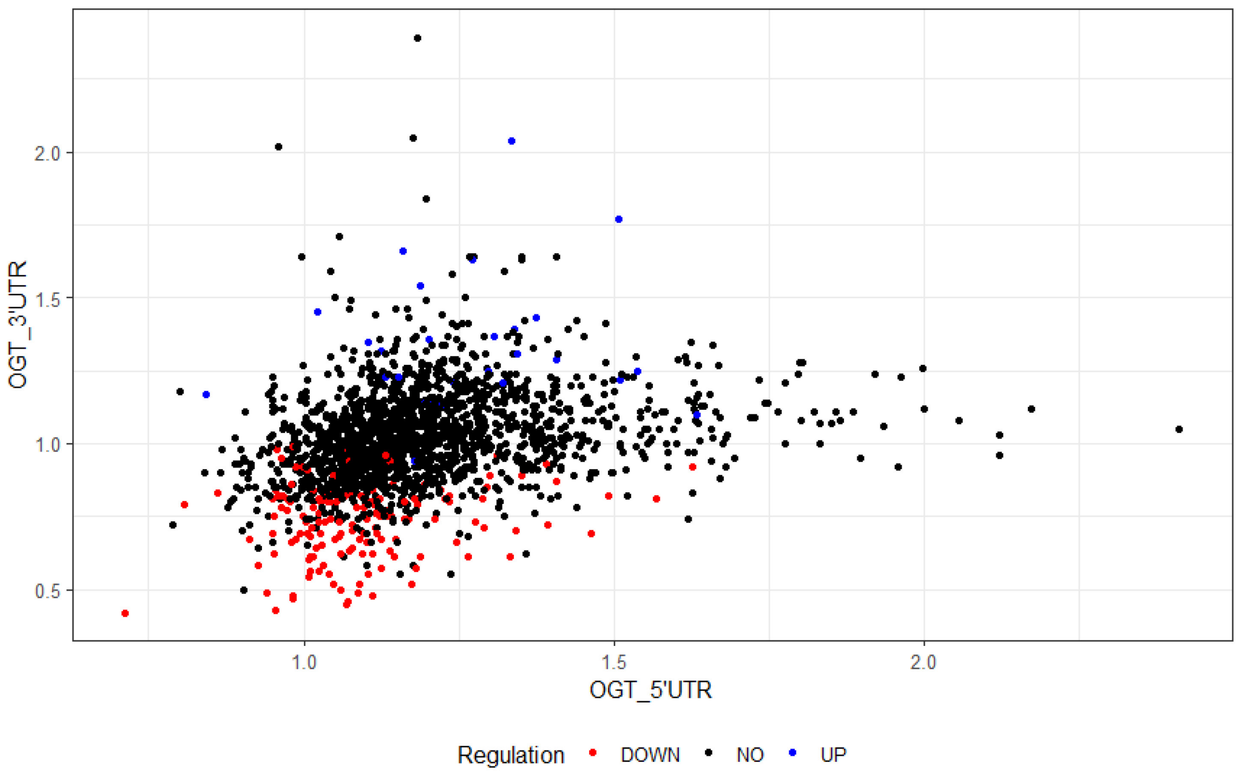

Figure 4.11. Comparison between OGT 3’UTR and OGT 5’UTR. Color code represents regulation by the OGT 3’+5’UTR dataset.

4.7 INVESTIGATION OF OGA REGULATION VIA 5’UTR AND 3’UTR REGIONS UTILIZING MIRFLUR PLATFORM

4.7.1 Generating the ratiometric fluorescent reporter data for mapping miR-target in the 3’UTR and 5’UTR regions

The miRFluR assay was performed for 3 pFmiR reporters (pFmiR-OGA 3’UTR, pFmiR-OGA 5’UTR, and pFmiR-OGA 3+5’UTR). I found a high fluctuation in NTC in the plates for

OGA and NTC repressed the reporter thus the dataset was normalized to the median of each plate. To validate this, I used the B3GLCT dataset in previous chapter. I plotted the correlation between the negative controls for B3GLCT, miR-200a-3p and NTC, with the median of each plate. High correlation was found between the negative controls and the median of each plate.

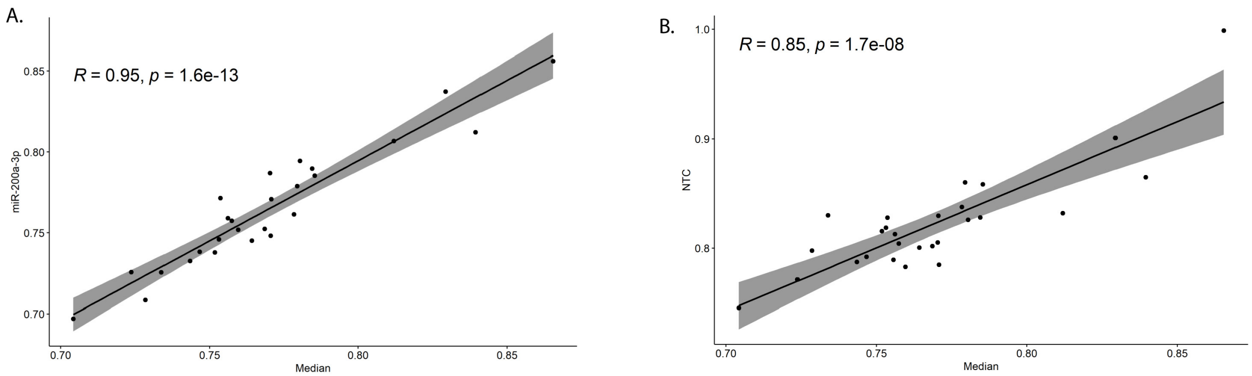

Figure 4.12. Correlation between two negative controls, (A) miR-200a-3p and (B) NTC, with the median of each plate for B3GLCT.

For the OGA 3'UTR, data for 1291 miRs was acquired after filter (**Figure 4.12**). Downregulatory miRs were dominant in comparison to upregulators for 3'UTR region. More upregulators were identified in comparison to OGT but the observed trend was similar to OGT. Similarly, most miR hits were found to upregulate OGA in the 5'UTR domain (**Figure 4.13**). The dominant impact of 3'UTR was detected in the OGA 3+5'UTR repression dataset. Thus, the 3'UTR is the more dominant domain in regulating both OGT and OGA repression by miRNAs.

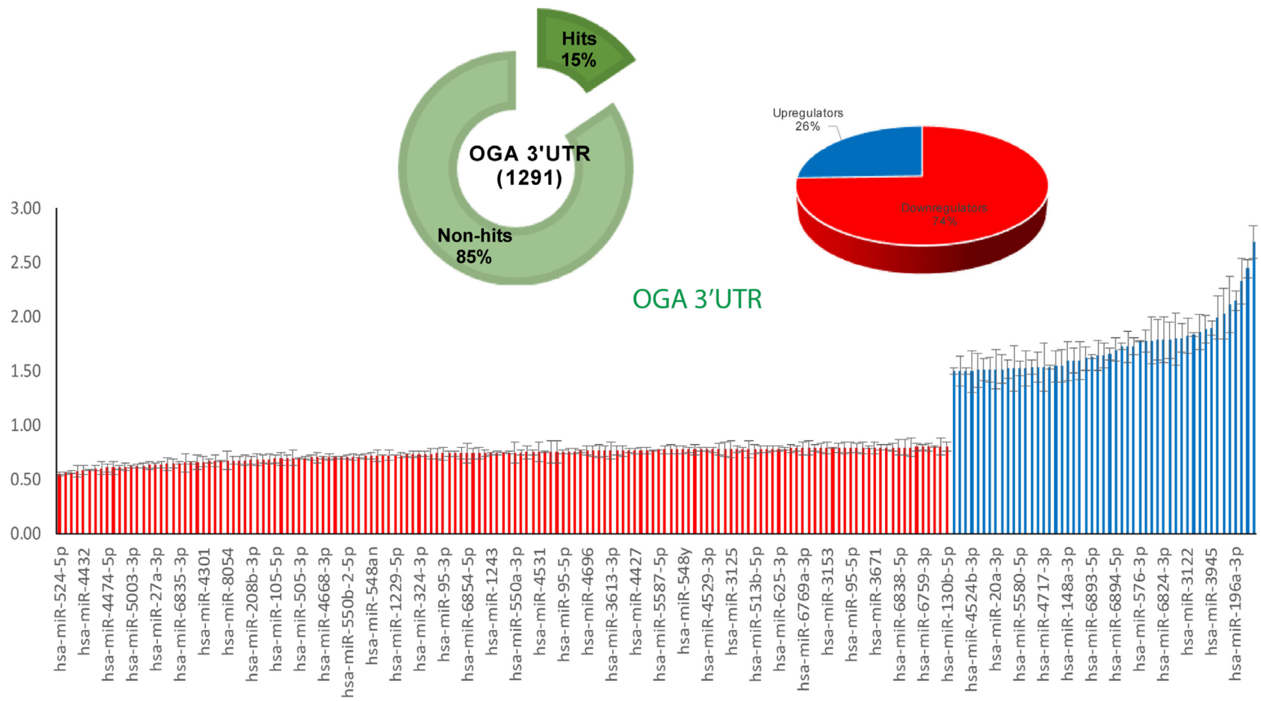

Figure 4.13. Identification and validation of hits for OGA 3'UTR. Pie graphs represent hit miR versus non hit miR percentages and downregulatory versus upregulatory miRs. Bar graph indicates the ratiometric data for miRs. Error bars represent propagated error.

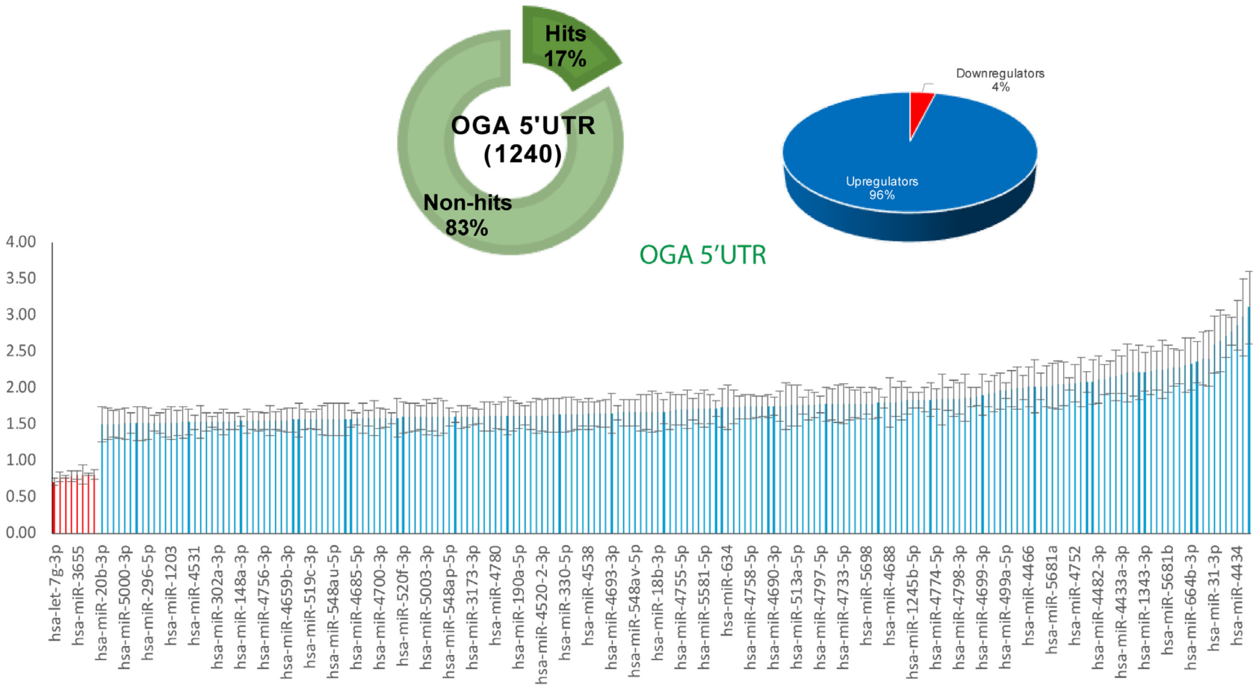

Figure 4.14. Identification and validation of hits for OGA 5'UTR. Pie graphs represent hit miR versus non hit miR percentages and downregulatory versus upregulatory miRs. Bar graph indicates the ratiometric data for miRs. Error bars represent propagated error.

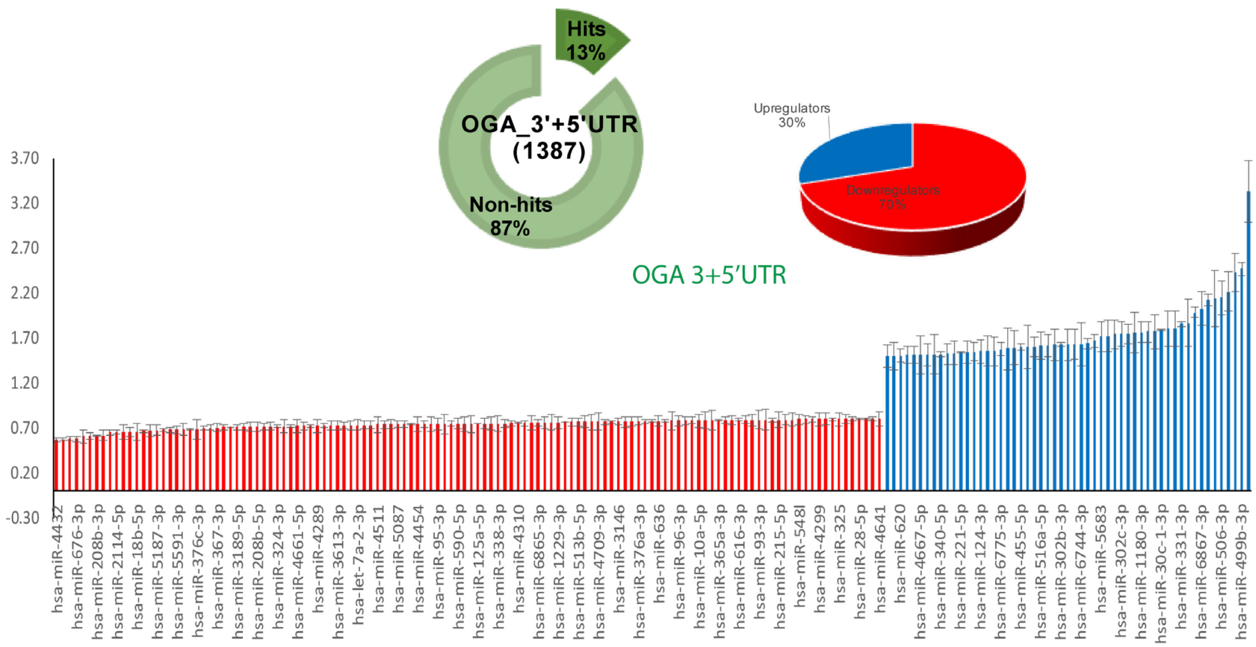

Figure 4.15. Identification and validation of hits for OGA 3+5'UTR. Pie graphs represent hit miR versus non hit miR percentages and downregulatory versus upregulatory miRs. Bar graph indicates the ratiometric data for miRs. Error bars represent propagated error.

I next performed Western Blot analysis for the protein expression of OGA in *HeLa* and *MDA-MB-231* cell lines for validation (**Figure 4.16, Figure 4.17, Table 4.1, Appendix 4B-D**). Briefly, cells were transfected with 3 downregulatory miRs for the 3'UTR region (miR-27a, miR-520d-5p and miR-524-5p), 3 downregulatory miRs for the 5'UTR (miR-140, miR-3655 and miR-3127), 10 upregulatory miRs (for both the 5'UTR and 3'UTR) and NTC as the negative control. The OGA protein levels generally followed the anticipated results from the reporter data with the exception of miR-3655. The result was also consistent with *MDA-MB-231* cell lines (**Appendix 4D**).

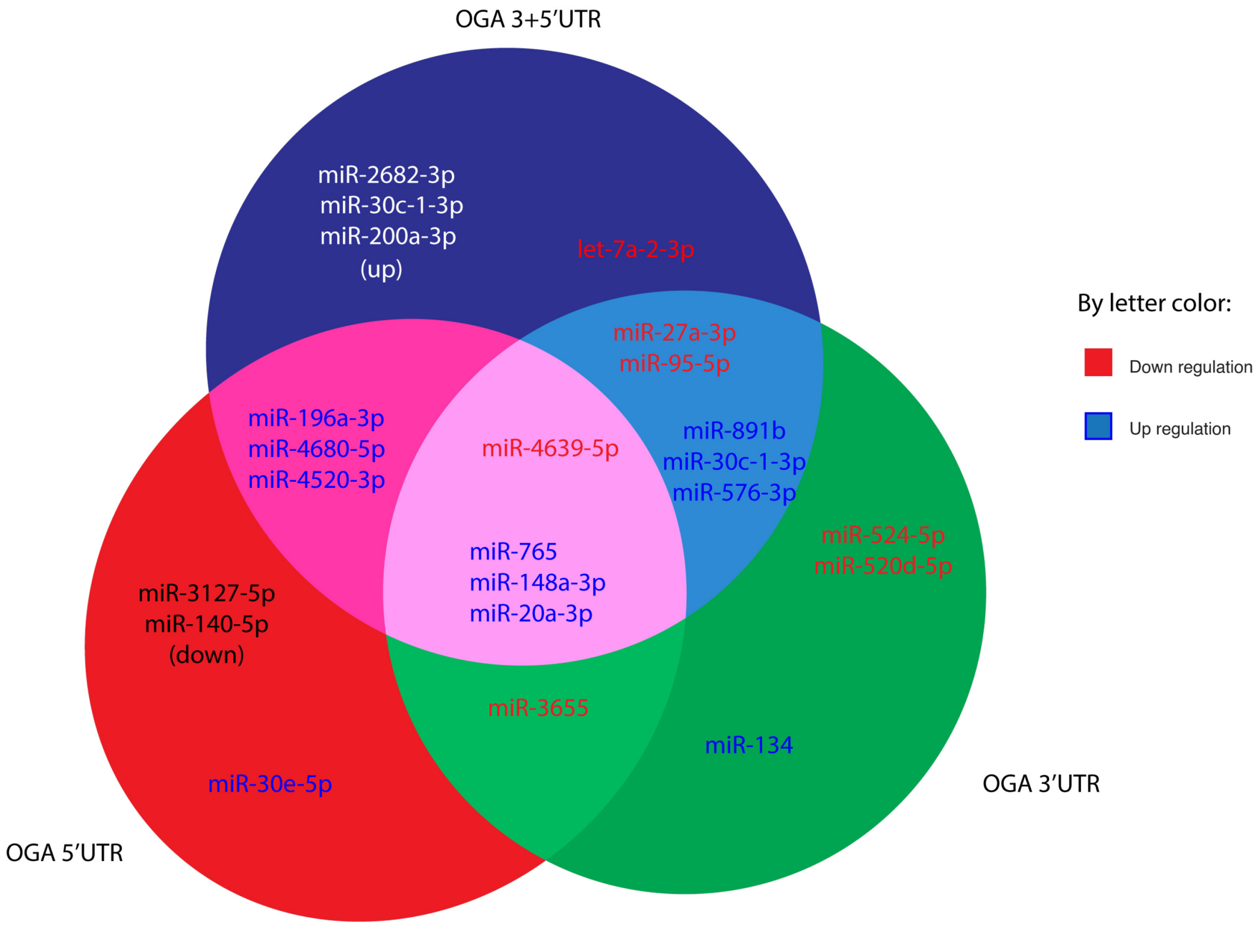

Figure 4.16. miRs were chosen for OGA validation.

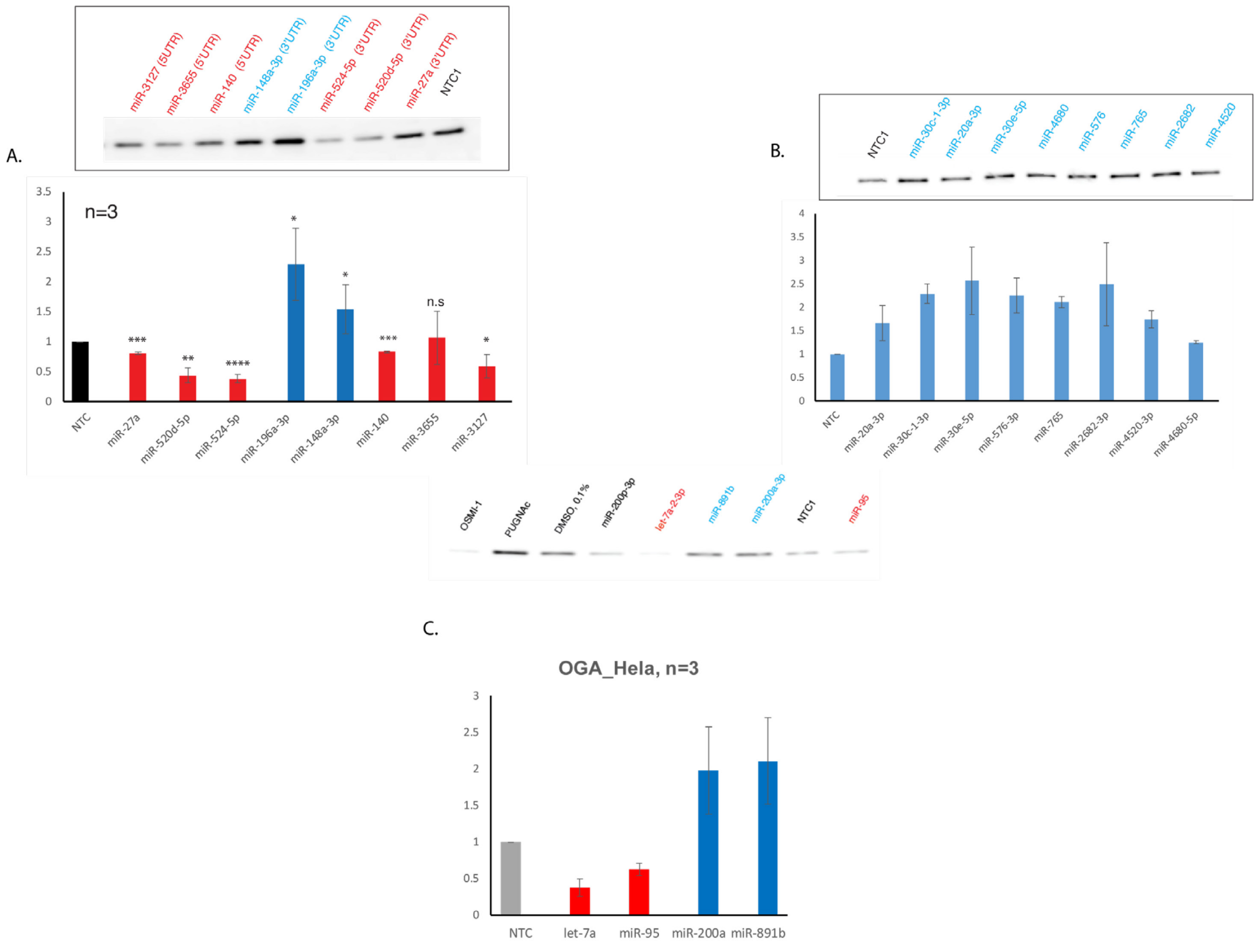

Figure 4.17. Validation of hits for OGA. Western blot analysis of OGA in *HeLa* transfected with 50 nM miR mimics or NTC, 48 hours post-transfection. Quantification of Western blot analysis were shown for three independent experiments. OGA expression was normalized to total protein levels from Ponceau staining and set over normalized NTC for each blot. Ponceau and whole Westerns corresponding to the data are shown in **Appendix 4B-D**.

Similarly to OGT, the OGA 3'UTR and 5'UTR data were also compared. The graph regpresents data available on both 3'UTR, 5'UTR and 3'+5'UTR (**Figure 4.18**). The downregulatory and upregulatory miRs were labeled by using the OGA 3+5'UTR dataset. Most of downregulatory miRs shown dowregulation in the 3'UTR region. The downregulatory miRs showed more scattered ratios than OGT but were still predominantly observed in the OGA 3'UTR dataset. For upregulation, higher condordance of upregulation between 3'UTR and 5'UTR was observed than in OGT datasets. This observation indicates a possible synergy between 3'UTR and 5'UTR in protein upregulation.

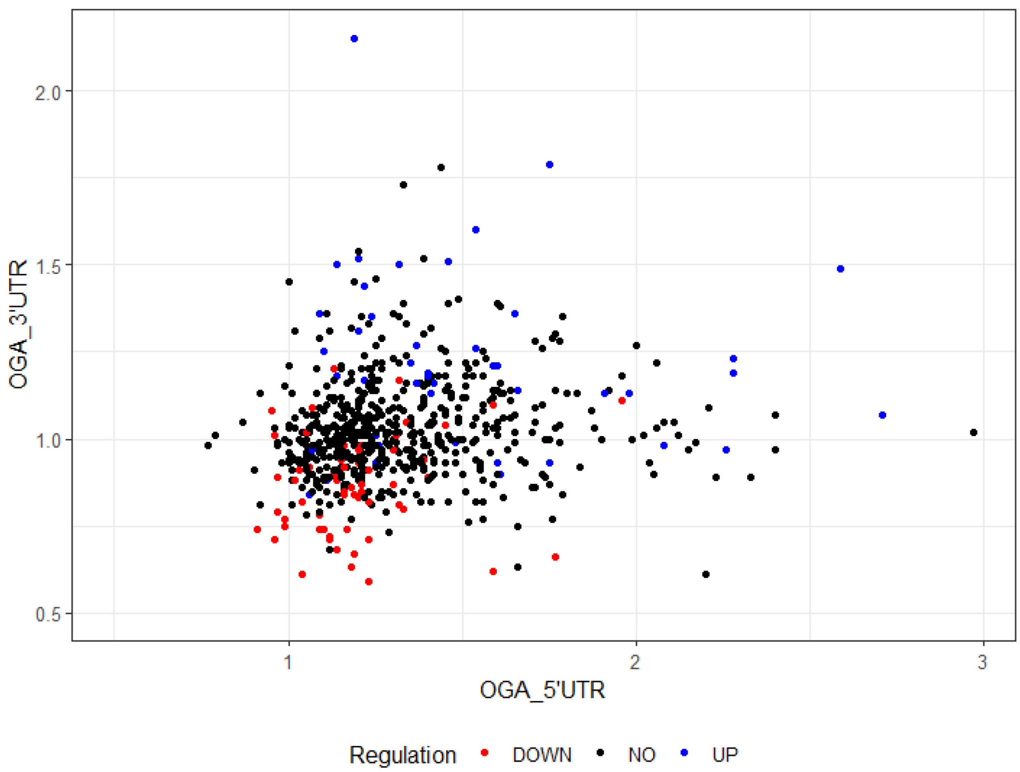

Figure 4.18. Comparison between OGA 3'UTR and OGA 5'UTR. Color code represents regulation by the OGA 3'+5'UTR dataset.

I also analyzed the binding sites of miRs in the 3'UTR and 5'UTR of both OGT and OGA by RNAhybrid algorithm (**Figure 4.19**, **Table 4.3-4.11**) and found that the "seed" binding sites were primarily present in the downregulatory miRs but not upregulatory miRs. The seed sites found in upregulators are also weaker, mostly 6mer instead of 8mer or 7mer. Thus, current miR target prediction algorithms (TargetScan, miRwalk,…), which utilize "seed" as a significant criteria, would predominantly identify downregulatory miRs.

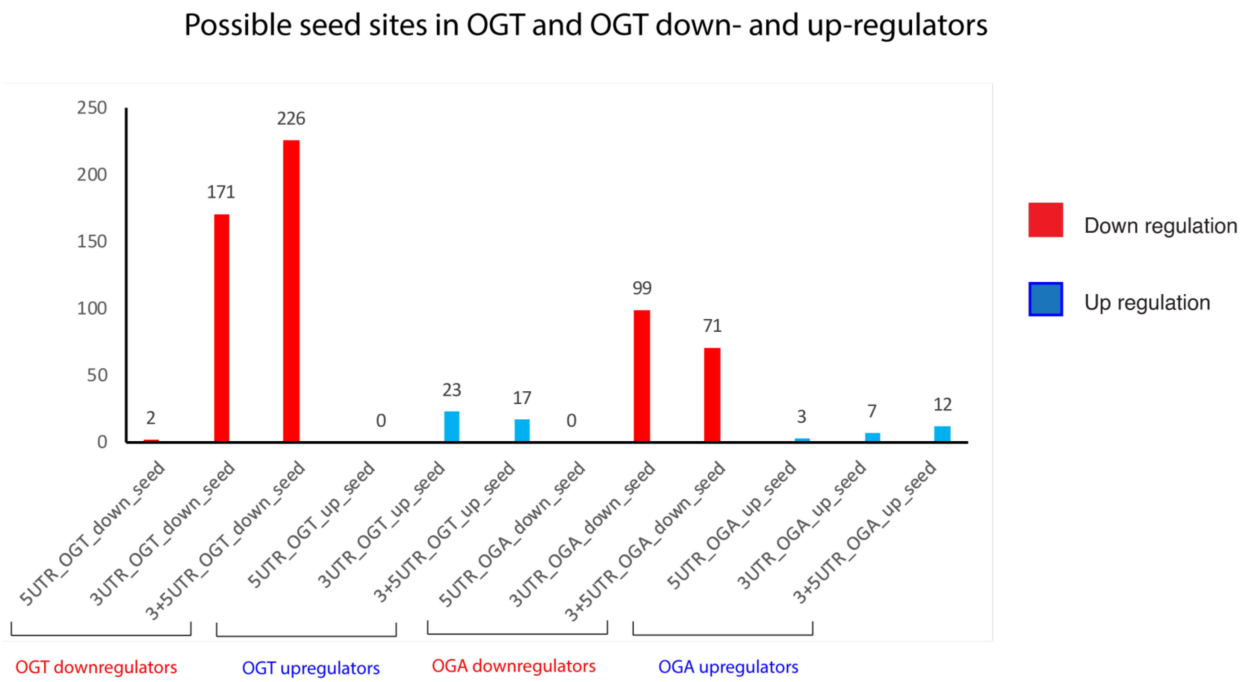

Figure 4.19. Possible seed sites analysis for OGT and OGA.

4.8 POST-TRANSCRIPTIONAL CO-REGULATION OF OGT AND OGA BY MIRNAS

4.8.1 Transcriptional co-regulation of OGT, OGA and O-GlcNAc homeostasis

In previous studies, accumulated evidence indicated that OGT and OGA are highly regulated at both the transcriptional and translational stages. Transcription is regulated by limiting the amount of mRNA produced via transcription factors (activators or repressors) or premature termination of transcription. Post-transcriptional regulation allows for more rapid and dynamic changes in cellular concentrations of encoded proteins. Thus, this regulation is crucial in maintaining cellular homeostasis and executing proper environmental responses. Since O-GlcNAc is significant in controlling the environmental responses of the cell, we would expect a high degree of transcriptional and post-transcriptional regulation of OGT and OGA. Previous studies have shown that OGT and OGA are highly correlated at the transcriptional level in different human cancers especially pancreatic adenocarcinoma (PDAC) [19]. OGT and OGA are known to be linked through transcriptional regulation. Specifically, OGA enhances *ogt* transcription via histone acetyltransferase p300 and C/EBPβ cooperative interactions. Furthermore, OGA, C/EBPβ and ERK signaling are found to regulate *ogt* expression in PDAC.

4.8.2 Translational co-regulation of OGT and OGA by miRNAs

We utilized the ratiometic fluorescent signals which indicated the level of regulation by miRs for both OGT and OGA to reveal the relationship between their regulatory networks. Interestingly, I found a high level of correlation between OGT and OGA after plotting 3'+5'UTR OGT versus 3'+5'UTR OGA data (**Figure 4.20**). To validate this finding, the dataset for B3GLCT regulation was plotted against OGT and OGA as a control (**Figure 4.21**). Their correlations were not significant.

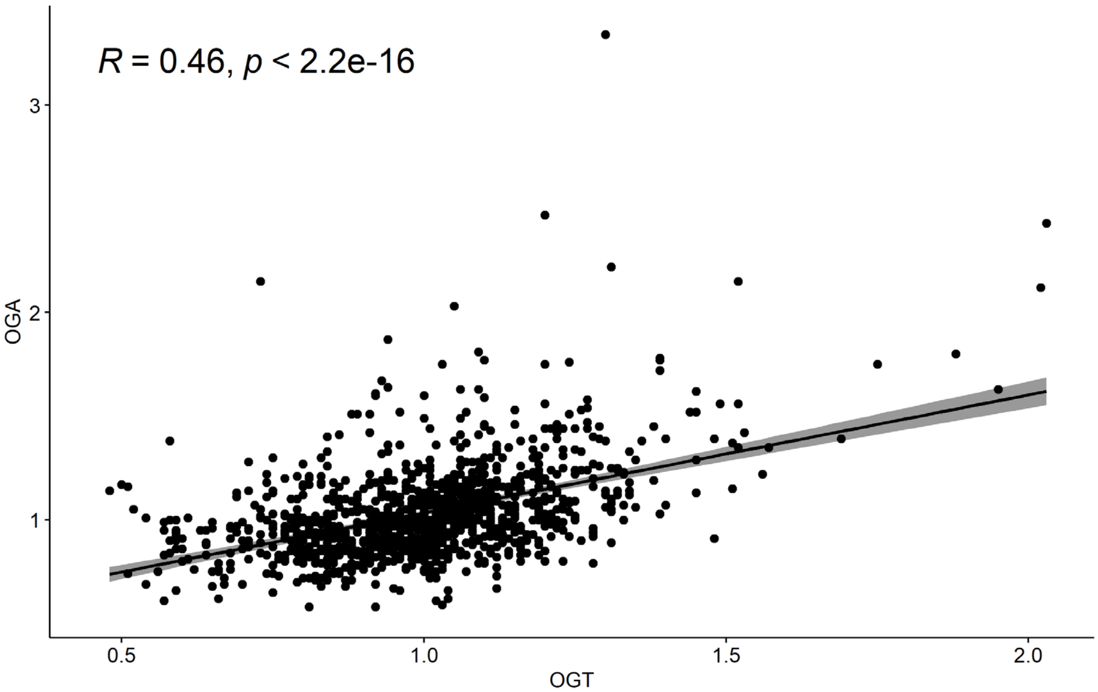

Figure 4.20. Pearson's correlation of OGT and OGA (data from 3+5'UTR reporters).

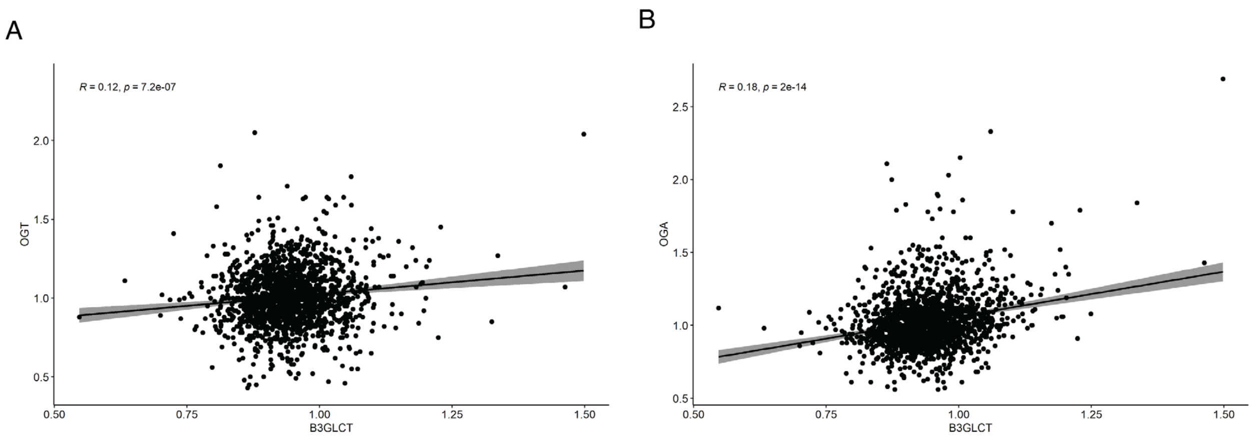

Figure 4.21. Pearson's correlation of OGT and OGA with B3GLCT (data from 3'UTR reporters).

In summary, OGT and OGA are highly co-regulated in both a transcriptional and post-transcriptional manner. While the transcriptional mechanism is known via CREB/P300 transcription factors, the exact mechanism behind the co-regulation of OGT and OGA by miRs requires further investigation. Could these miRs target a protein subset to cooperatively repress or enhance the translation of OGT and OGA or impact splicing factors to regulate OGT and OGA productive forms? In addition, the mutual regulation of OGA and OGT could also contribute to the maintenance of O-GlcNAc homeostasis (**Figure 4.22**).

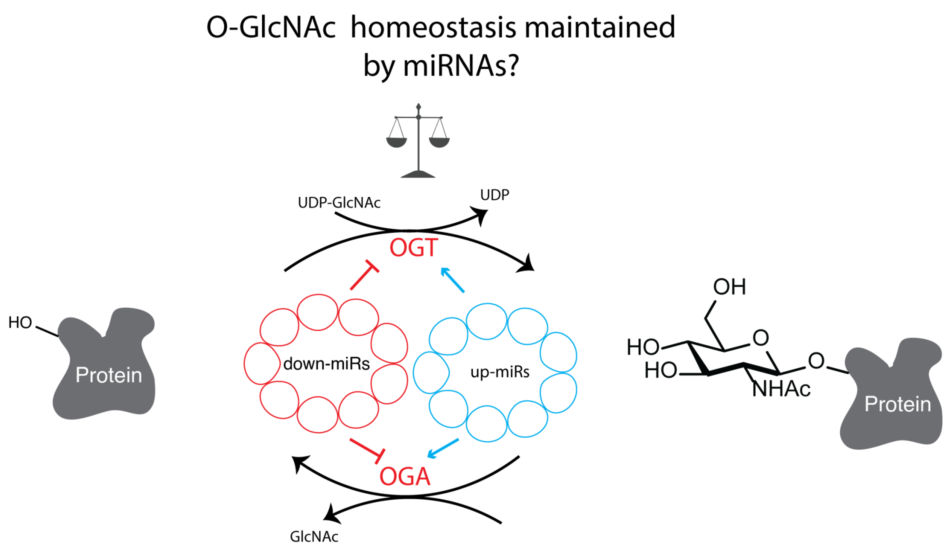

Figure 4.22. Downregulatory and upregulatory miRs co-regulate OGT and OGA to maintain O-GlcNAc homeostasis?

4.9 GENERATING THE RATIOMETRIC FLUORESCENT REPORTER FOR MAPPING MIR-TARGET IN THE CODING REGION FOR ncOGT

Functional miR-binding sites are mainly focused in the 3'UTR regions meanwhile the coding and 5'UTR regions are largely unexplored. Thus, I also generated pFmiR sensors to investigate miR regulation of the OGT coding region (**Figure 4.21**). The reporter was cloned by fusing the nucleocytoplasmic OGT coding sequence with Cerulean sensing module with a known linker peptide to maintain biological integrity and aid protein folding and stability. Unfortunately, we found a low signal to noise ratio of Cerulean expression over background fluorescence. This may be due to genetic regulatory elements in OGT that may govern the basal expression level of Cerulean. These regulatory elements possess structural and folding features, RNA binding protein partners or other regulatory factors (e.g., endogeneous miRs…) which can influence Cerulean expression. Furthermore, OGT is known to have numerous protein binding partners which could also contribute to the complexity of the question.

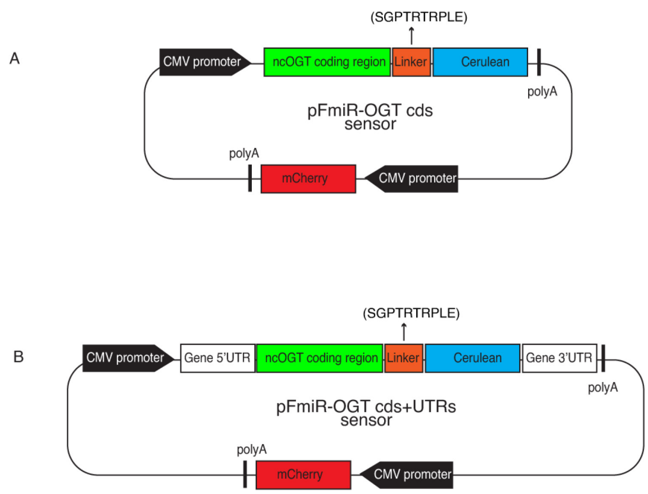

Figure 4.21. MiRFluR platform extending to the coding region. (A) Plasmid maps for mapping miRs with OGT coding regulatory regions. (B) Plasmid maps for mapping miRs with full OGT regulatory regions.

4.10 CONCLUSIONS

OGT and OGA expression levels are known to change O-GlcNAc homeostasis and lead to numerous human diseases. However, how OGT and OGA expression levels are regulated is a fundamental question that requires further investigation and study. In the effort to address that question, few previous works demonstrated that OGT and OGA are regulated in both a transcriptional and post-transcriptional manner via CREB/P300 transcription factors and intron retention respectively[17, 19]. Nonetheless, the comprehensive regulatory network of OGT and OGA by miRs has not yet been explored. Furthermore, our current understanding of miRs is mainly focused on the 3'UTR regulatory element while miR regulation of the 5'UTR is largely neglected. Thus, for our investigation, we utilized genetically encoded ratiometric fluorescent reporters (pFmiR) integrated with our miRFluR platform to comprehensively map miR regulation of OGT and OGA in both the 3'UTR and 5'UTR. The results indicated that OGT and OGA are highly regulated by miRs. For both OGT and OGA, we observed that the down-regulatory miRs are mostly targeting and downregulating via the 3'UTR region, while up-regulatory miRs are binding and upregulating through both regions. However, the 3'UTR is the more dominant domain for miR regulation in general. A selection of miRs hitting OGT and OGA were validated by Western blot. In addition, we also found the post-transcriptional layer of regulation of OGT and OGA by miRs is highly correlated, which could contribute to the maintenance of O-GlcNAc homeostasis. While the transcriptional mechanism is known via CREB/P300 transcription factors, the exact mechanism of how some miRs co-regulate OGT and OGA remains to be elucidated.

4.11 MATERIALS AND EXPERIMENTAL METHODS

4.11.1 Cloning of pFmiR-OGT-3'UTR, pFmiR-OGT-5'UTR, pFmiR-OGT-3+5'UTR, pFmiR-OGA-3'UTR, pFmiR-OGA-5'UTR, pFmiR-OGA-3+5'UTR

OGT 3'UTR, OGT 5'UTR, OGA 3'UTR and OGA 5'UTR was cloned from cDNA using primers:

OGT 3’UTR_fwd: CCACATGATTAAGCCTGTTG

OGT 3’UTR_rev: GATCCCCGTATTAAAGGGAAATC

OGT 5’UTR_fwd: ATTTCAAGACCGTACTAGGTAG

OGT 5’UTR_rev: CTGGAGCTTCTCGAGGGAG

OGA 3’UTR_fwd: CTGTGACATTTGTTGACACTG

OGA 3’UTR_rev: ACAAGCATTCACTTCAAGTTTTATTTTG

OGA 5’UTR_fwd: GGTCTGCAGCGCAAGCGC

OGA 5’UTR_rev: CCTCCTGCCCCCGGCCGC

under standard PCR conditions. The 3’UTR DNA fragment was cloned using the NheI and BamHI sites downstream of Cerulean in our pFmiR-empty backbone using standard ligation protocols and the 5’UTR DNA fragment was inserted to pFmiR-empty backbone using the EcoRV and HindIII sites upstream of Cerulean. Plasmid maps and sequences for pFmiR-empty, pFmiR-OGT-3’UTR, pFmiR-OGT-5’UTR, pFmiR-OGT-3+5’UTR, pFmiR-OGA-3’UTR, pFmiR-OGA-5’UTR, pFmiR-OGA-3+5’UTR can be found in **Plasmid maps and Sequences**.

4.11.2 FluoRmiR High-throughput Assay.

The Human miRNA Mimic library version 21 (miRDIAN, Horizon Discovery) was resuspended in nuclease-free water and aliquoted into black 384-well, clear optical bottom tissue-culture treated plates (Nunc). Each plate contained 3 replicates of every miRNA (1.8 pmol/well).

To each well in the plate was added 25 ng of pMIR-B3GLCT plasmid in 5 µl Opti-MEM (Gibco) and 0.11 µl lipofectamine 2000 (Invitrogen) in 5 µl Opti-MEM (Gibco). The solution was allowed to incubate at room temperature for 25 min. Then, *HEK293T* cells (25 µl per well, 400 cells/ µl in non-phenol red Dulbecco's Modified Eagle Medium (DMEM) with FBS 10%) were added to the plate. Plates were then incubated at 37°C, 5% CO_2. After 48 hours, the fluorescence signals of Cerulean (excitation: 433 nm; emission: 475 nm) and mCherry (excitation: 587 nm; emission: 610 nm) were measured using the bottom read option in a FlexStation 3 Multi-mode microplate reader (Molecular Devices).

4.11.3 Data Processing

We calculated the ratio Cerulean fluorescence (Cer) over mCherry fluorescence (Cer/mCh) for each well in each plate. For each miR, triplicate values were averaged and the standard deviation (S.D.) obtained. We calculated a % error for each miR as 100 x S.D./mean. . As a quality control measure, we removed any plates or miRs that had high errors in the measurement (median error +2 S.D. across all plates). The Cer/mCh ratio for each miR was then normalized to the Cer/mCh ratio for the NTC within that plate and error was propagated. Data from all plates was then combined and Z-scores were calculated. A Z-score of +/-1.960, corresponding to a 2-tailed p-value of 0.05, was used as a threshold for significance. In addition, we set a second threshold of +/- 20% impact by the miR, in line with previous work [42, 43].

4.11.4 Western Blot

Mammalian cells were seeded in six-well plates (80,000 cells per well), cultured for 24 h, and transfected with miRNA mimics (50 nM, miRIDIAN, Horizon Discovery) using Lipofectamine 2000 (Life Technologies). Cells were washed and harvested 48 hours post-transfection.

Cells were then lysed in cold RIPA buffer supplemented with protease inhibitors and 50 µg of protein were run on SDS-PAGE. Standard Western Blot analysis using α-OGT (abcam antibody, 1:1000) or α-OGA (Sigma) and then, α-rabbit-HRP (2°, 1:5,000, Abcam)] was performed [44]. Blots were developed using Clarity and Clarity Max Western ECL substrate (Bio-Rad).

Appendix 4A. OGT Western Blot

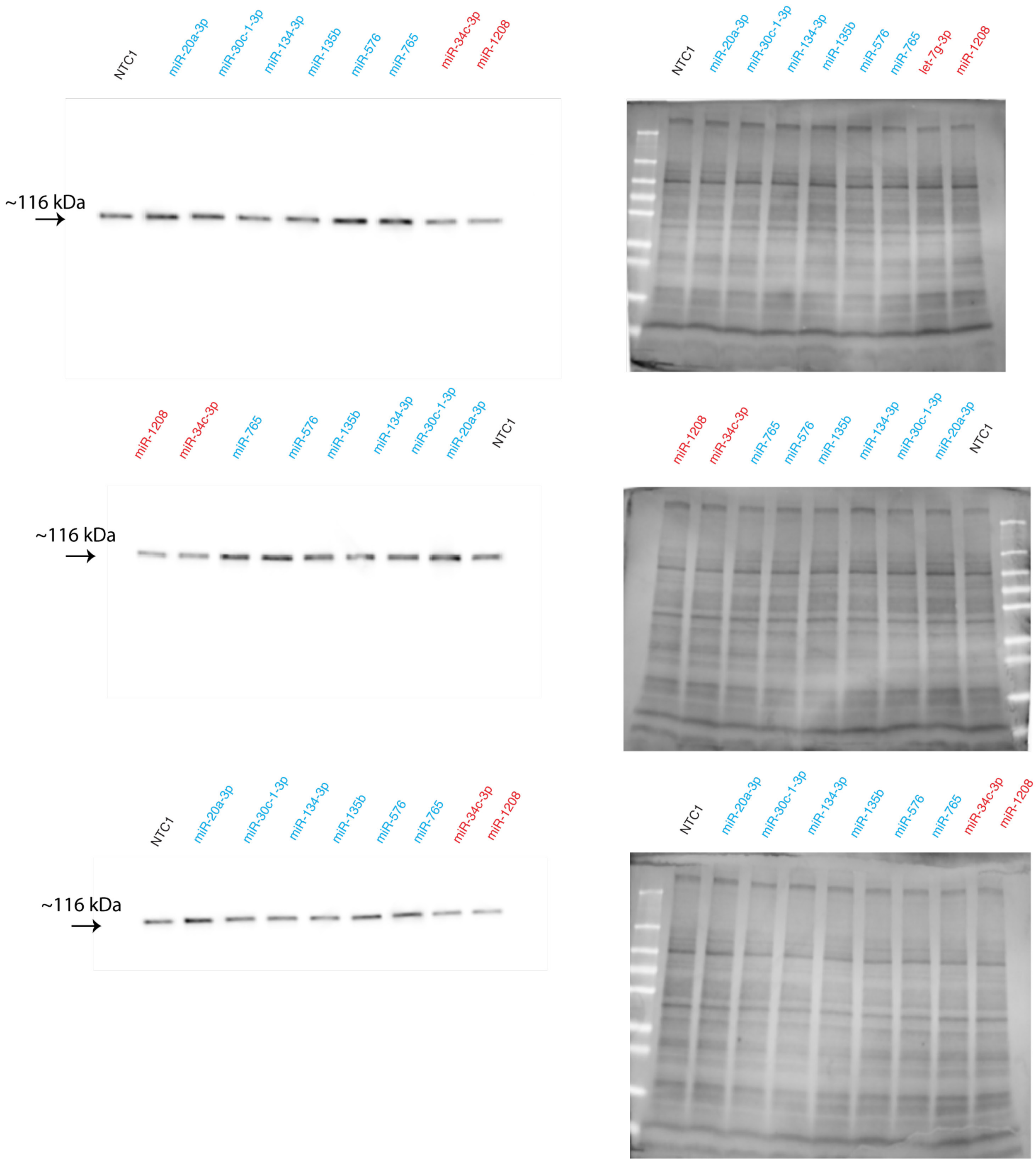

Appendix 4A. OGT Western blot analysis and accompanying Ponceau S stain for the 3 biological replicates in *MDA-MB-231*.

Appendix 4B-D. OGA Western Blot

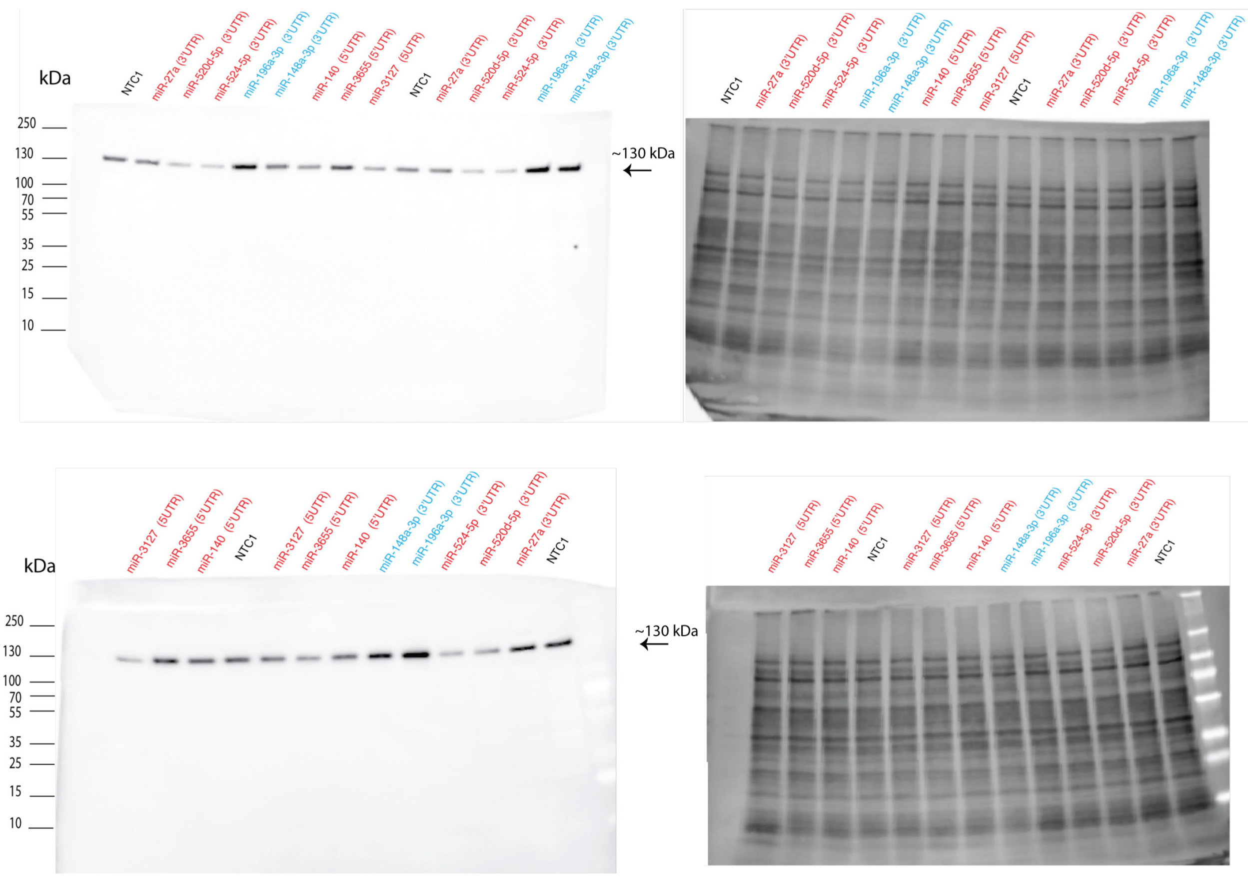

Appendix 4B. OGA Western blot analysis and accompanying Ponceau S stain for the 3 biological replicates in *HeLa*.

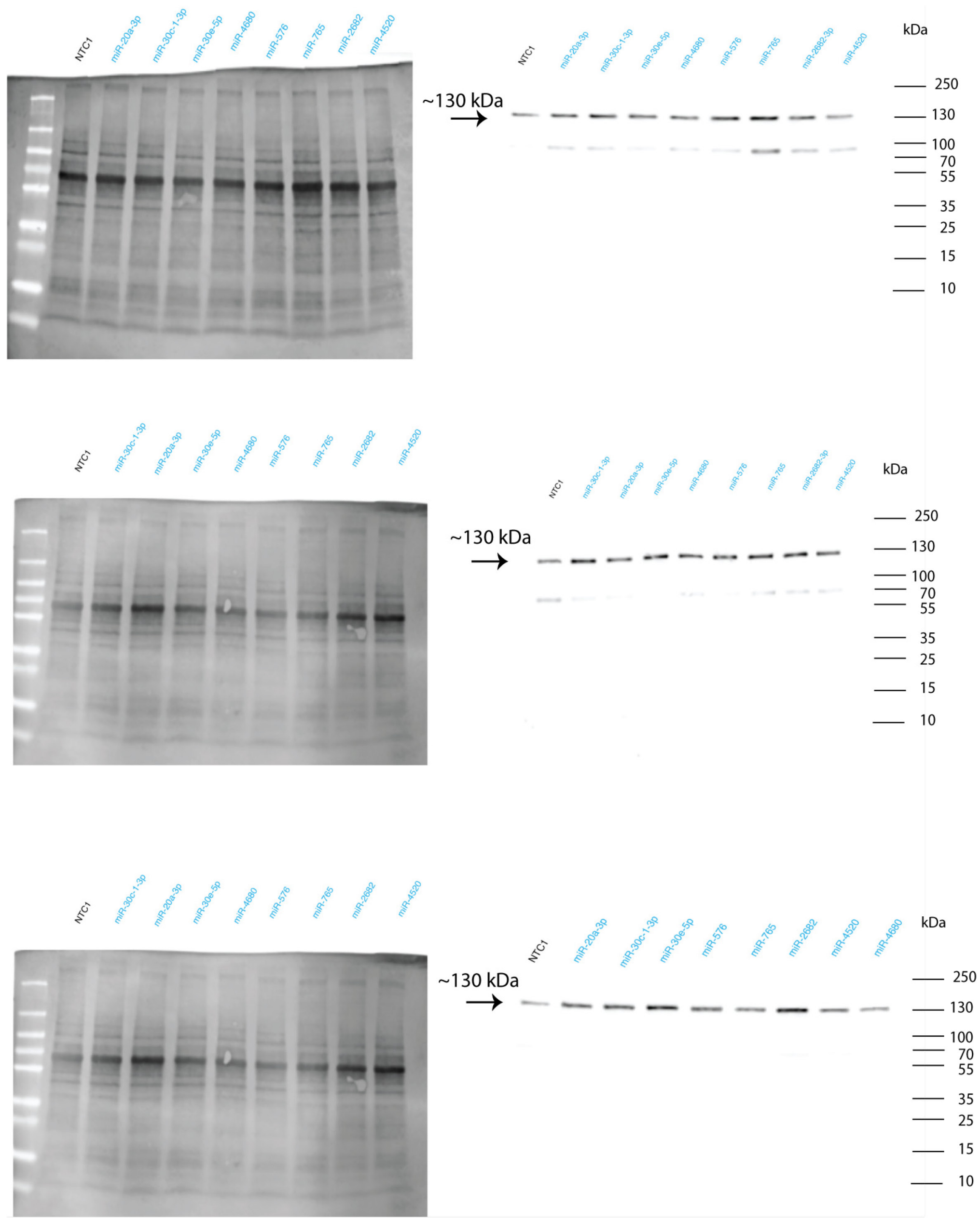

Appendix 4C. OGA Western blot analysis and accompanying Ponceau S stain for the 3 biological replicates in *HeLa*.

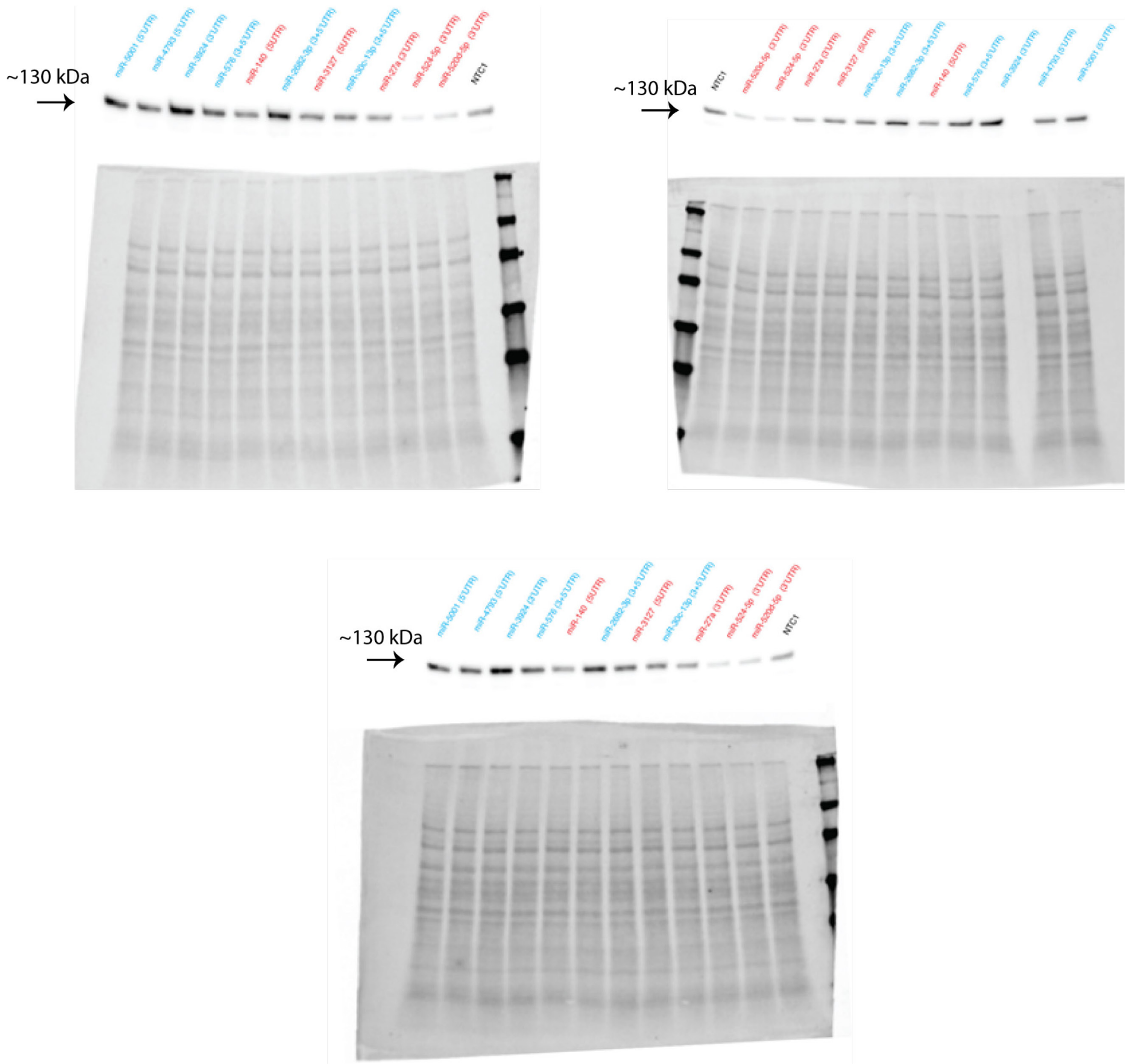

Appendix 4D. OGA Western blot analysis and accompanying Ponceau S stain for the 3 biological replicates in *MDA-MB-231*.

Appendix 4E. 5 Plasmid maps and sequences

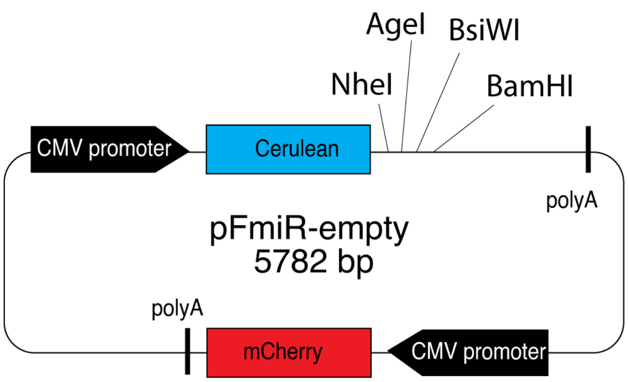

List of features:

mCherry (2539..3249)
CMV promoter 1 (236..852)
CMV promoter 2 (1916..2532)
Cerulean (918..1637)
polyA_1 (1688..1914)
polyA_2 (3272..3498)

Sequence 1_pFmiR-empty:

GACGGATCGGGAGATCTCCCGATCCCCTATGGTCGACTCTCAGTACAATCTGCTCTGATGCCGCATAGTTAAGCCAGTATCTGCTC
CCTGCTTGTGTGTTGGAGGTCGCTGAGTAGTGCGCGAGCAAAATTTAAGCTACAACAAGGCAAGGCTTGACCGACAATTGCATGA
AGAATCTGCTTAGGGTTAGGCGTTTTGCGCTGCTTCGCGATGTACGGGCCAGATATACGCGTTGACATTGATTATTGACTAGTTAT
TAATAGTAATCAATTACGGGGTCATTAGTTCATAGCCCATATATGGAGTTCCGCGTTACATAACTTACGGTAAATGGCCCGCCTGG
CTGACCGCCCAACGACCCCCGCCCATTGACGTCAATAATGACGTATGTTCCCATAGTAACGCCAATAGGGACTTTCCATTGACGTC
AATGGGTGGACTATTTACGGTAAACTGCCCACTTGGCAGTACATCAAGTGTATCATATGCCAAGTACGCCCCCTATTGACGTCAAT
GACGGTAAATGGCCCGCCTGGCATTATGCCCAGTACATGACCTTATGGGACTTTCCTACTTGGCAGTACATCTACGTATTAGTCAT
CGCTATTACCATGGTGATGCGGTTTTGGCAGTACATCAATGGGCGTGGATAGCGGTTTGACTCACGGGGATTTCCAAGTCTCCACC
CCATTGACGTCAATGGGAGTTTGTTTTGGCACCAAAATCAACGGGACTTTCCAAAATGTCGTAACAACTCCGCCCCATTGACGCAA
ATGGGCGGTAGGCGTGTACGGTGGGAGGTCTATATAAGCAGAGCTCTCTGGCTAACTAGAGAACCCACTGCTTACTGGCTTATCG
AAATTAATACGACTCACTATAGGGAGACCCAAGCTTGGTACCGAGCTCGGATCGATATCATGGTGAGCAAGGGCGAGGAGCTGTT
CACCGGGGTGGTGCCCATCCTGGTCGAGCTGGACGGCGACGTAAACGGCCACAAGTTCAGCGTGTCCGGCGAGGGCGAGGGCGA
TGCCACCTACGGCAAGCTGACCCTGAAGTTCATCTGCACCACCGGCAAGCTGCCCGTGCCCTGGCCCACCCTCGTGACCACCCTG
ACCTGGGGCGTGCAGTGCTTCGCCCGCTACCCCGACCACATGAAGCAGCACGACTTCTTCAAGTCCGCCATGCCCGAAGGCTACG
TCCAGGAGCGCACCATCTTCTTCAAGGACGACGGCAACTACAAGACCCGCGCCGAGGTGAAGTTCGAGGGCGACACCCTGGTGA
ACCGCATCGAGCTGAAGGGCATCGACTTCAAGGAGGACGGCAACATCCTGGGGCACAAGCTGGAGTACAACGCCATCAGCGACA
ACGTCTATATCACCGCCGACAAGCAGAAGAACGGCATCAAGGCCAACTTCAAGATCCGCCACAACATCGAGGACGGCAGCGTGC
AGCTCGCCGACCACTACCAGCAGAACACCCCCATCGGCGACGGCCCCGTGCTGCTGCCCGACAACCACTACCTGAGCACCCAGTC
CGCCCTGAGCAAAGACCCCAACGAGAAGCGCGATCACATGGTCCTGCTGGAGTTCGTGACCGCCGCCGGGATCACTCTCGGCATG
GACGAGCTGTACAAGTAATAAGCTAGCACACCGGTCGTCTAGCAATGCGATCCACGTACGTAGGATCCCGACTGTGCCTTCTAGT
TGCCAGCCATCTGTTGTTTGCCCCTCCCCCGTGCCTTCCTTGACCCTGGAAGGTGCCACTCCCACTGTCCTTTCCTAATAAAATGAG
GAAATTGCATCGCATTGTCTGAGTAGGTGTCATTCTATTCTGGGGGGTGGGGTGGGGCAGGACAGCAAGGGGGAGGATTGGGAA
GACAATAGCAGGCATGCTGGGGATGCGGTGGGCTCTATGGACATTGATTATTGACTAGTTATTAATAGTAATCAATTACGGGGTC
ATTAGTTCATAGCCCATATATGGAGTTCCGCGTTACATAACTTACGGTAAATGGCCCGCCTGGCTGACCGCCCAACGACCCCCGCC
CATTGACGTCAATAATGACGTATGTTCCCATAGTAACGCCAATAGGGACTTTCCATTGACGTCAATGGGTGGACTATTTACGGTAA
ACTGCCCACTTGGCAGTACATCAAGTGTATCATATGCCAAGTACGCCCCCTATTGACGTCAATGACGGTAAATGGCCCGCCTGGC
ATTATGCCCAGTACATGACCTTATGGGACTTTCCTACTTGGCAGTACATCTACGTATTAGTCATCGCTATTACCATGGTGATGCGGT
TTTGGCAGTACATCAATGGGCGTGGATAGCGGTTTGACTCACGGGGATTTCCAAGTCTCCACCCCATTGACGTCAATGGGAGTTTG
TTTTGGCACCAAAATCAACGGGACTTTCCAAAATGTCGTAACAACTCCGCCCCATTGACGCAAATGGGCGGTAGGCGTGTACGGT
GGGAGGTCTATATAAGCAGAGCTCTCTGGCTAACTAGAGAACCCACTGCTTACTGGCCCCGGGATGGTGAGCAAGGGCGAGGAG
GATAACATGGCCATCATCAAGGAGTTCATGCGCTTCAAGGTGCACATGGAGGGCTCCGTGAACGGCCACGAGTTCGAGATCGAGG
GCGAGGGCGAGGGCCGCCCCTACGAGGGCACCCAGACCGCCAAGCTGAAGGTGACCAAGGGTGGCCCCCTGCCCTTCGCCTGGG
ACATCCTGTCCCCTCAGTTCATGTACGGCTCCAAGGCCTACGTGAAGCACCCCGCCGACATCCCCGACTACTTGAAGCTGTCCTTC
CCCGAGGGCTTCAAGTGGGAGCGCGTGATGAACTTCGAGGACGGCGGCGTGGTGACCGTGACCCAGGACTCCTCCCTGCAGGAC

GGCGAGTTCATCTACAAGGTGAAGCTGCGCGGCACCAACTTCCCCTCCGACGGCCCCGTAATGCAGAAGAAGACCATGGGCTGG
GAGGCCTCCTCCGAGCGGATGTACCCCGAGGACGGCGCCCTGAAGGGCGAGATCAAGCAGAGGCTGAAGCTGAAGGACGGCGGC
CACTACGACGCTGAGGTCAAGACCACCTACAAGGCCAAGAAGCCCGTGCAGCTGCCCGGCGCCTACAACGTCAACATCAAGTTG
GACATCACCTCCCACAACGAGGACTACACCATCGTGGAACAGTACGAACGCGCCGAGGGCCGCCACTCCACCGGCGGCATGGAC
GAGCTGTACAAGTAATCTAGAGCTCGCTGATCAGCCTCGACTGTGCCTTCTAGTTGCCAGCCATCTGTTGTTTGCCCCTCCCCCGT
GCCTTCCTTGACCCTGGAAGGTGCCACTCCCACTGTCCTTTCCTAATAAAATGAGGAAATTGCATCGCATTGTCTGAGTAGGTGTC
ATTCTATTCTGGGGGGTGGGGTGGGGCAGGACAGCAAGGGGGAGGATTGGGAAGACAATAGCAGGCATGCTGGGGATGCGGTGG
GCTCTATGGCTTCTGAGGCGGAAAGAACCAGCTGGGGCTCGAGTGCATTCTAGTTGTGGTTTGTCCAAACTCATCAATGTATCTTA
TCATGTCTGTATACCGTCGACCTCTAGCTAGAGCTTGGCGTAATCATGGTCATAGCTGTTTCCTGTGTGAAATTGTTATCCGCTCAC
AATTCCACACAACATACGAGCCGGAAGCATAAAGTGTAAAGCCTGGGGTGCCTAATGAGTGAGCTAACTCACATTAATTGCGTTG
CGCTCACTGCCCGCTTTCCAGTCGGGAAACCTGTCGTGCCAGCTGCATTAATGAATCGGCCAACGCGCGGGGAGAGGCGGTTTGC
GTATTGGGCGCTCTTCCGCTTCCTCGCTCACTGACTCGCTGCGCTCGGTCGTTCGGCTGCGGCGAGCGGTATCAGCTCACTCAAAG
GCGGTAATACGGTTATCCACAGAATCAGGGGATAACGCAGGAAAGAACATGTGAGCAAAAGGCCAGCAAAAGGCCAGGAACCG
TAAAAAGGCCGCGTTGCTGGCGTTTTTCCATAGGCTCCGCCCCCCTGACGAGCATCACAAAAATCGACGCTCAAGTCAGAGGTGG
CGAAACCCGACAGGACTATAAAGATACCAGGCGTTTCCCCCTGGAAGCTCCCTCGTGCGCTCTCCTGTTCCGACCCTGCCGCTTAC
CGGATACCTGTCCGCCTTTCTCCCTTCGGGAAGCGTGGCGCTTTCTCAATGCTCACGCTGTAGGTATCTCAGTTCGGTGTAGGTCGT
TCGCTCCAAGCTGGGCTGTGTGCACGAACCCCCCGTTCAGCCCGACCGCTGCGCCTTATCCGGTAACTATCGTCTTGAGTCCAACC
CGGTAAGACACGACTTATCGCCACTGGCAGCAGCCACTGGTAACAGGATTAGCAGAGCGAGGTATGTAGGCGGTGCTACAGAGT
TCTTGAAGTGGTGGCCTAACTACGGCTACACTAGAAGGACAGTATTTGGTATCTGCGCTCTGCTGAAGCCAGTTACCTTCGGAAAA
AGAGTTGGTAGCTCTTGATCCGGCAAACAAACCACCGCTGGTAGCGGTGGTTTTTTTGTTTGCAAGCAGCAGATTACGCGCAGAA
AAAAAGGATCTCAAGAAGATCCTTTGATCTTTTCTACGGGGTCTGACGCTCAGTGGAACGAAAACTCACGTTAAGGGATTTTGGT
CATGAGATTATCAAAAAGGATCTTCACCTAGATCCTTTTAAATTAAAAATGAAGTTTTAAATCAATCTAAAGTATATATGAGTAAA
CTTGGTCTGACAGTTACCAATGCTTAATCAGTGAGGCACCTATCTCAGCGATCTGTCTATTTCGTTCATCCATAGTTGCCTGACTCC
CCGTCGTGTAGATAACTACGATACGGGAGGGCTTACCATCTGGCCCCAGTGCTGCAATGATACCGCGAGACCCACGCTCACCGGC
TCCAGATTTATCAGCAATAAACCAGCCAGCCGGAAGGGCCGAGCGCAGAAGTGGTCCTGCAACTTTATCCGCCTCCATCCAGTCT
ATTAATTGTTGCCGGGAAGCTAGAGTAAGTAGTTCGCCAGTTAATAGTTTGCGCAACGTTGTTGCCATTGCTACAGGCATCGTGGT
GTCACGCTCGTCGTTTGGTATGGCTTCATTCAGCTCCGGTTCCCAACGATCAAGGCGAGTTACATGATCCCCCATGTTGTGCAAAA
AAGCGGTTAGCTCCTTCGGTCCTCCGATCGTTGTCAGAAGTAAGTTGGCCGCAGTGTTATCACTCATGGTTATGGCAGCACTGCAT
AATTCTCTTACTGTCATGCCATCCGTAAGATGCTTTTCTGTGACTGGTGAGTACTCAACCAAGTCATTCTGAGAATAGTGTATGCG
GCGACCGAGTTGCTCTTGCCCGGCGTCAATACGGGATAATACCGCGCCACATAGCAGAACTTTAAAAGTGCTCATCATTGGAAAA
CGTTCTTCGGGGCGAAAACTCTCAAGGATCTTACCGCTGTTGAGATCCAGTTCGATGTAACCCACTCGTGCACCCAACTGATCTTC
AGCATCTTTTACTTTCACCAGCGTTTCTGGGTGAGCAAAAACAGGAAGGCAAAATGCCGCAAAAAAGGGAATAAGGGCGACACG
GAAATGTTGAATACTCATACTCTTCCTTTTTCAATATTATTGAAGCATTTATCAGGGTTATTGTCTCATGAGCGGATACATATTTGA
ATGTATTTAGAAAAATAAACAAATAGGGGTTCCGCGCACATTTCCCCGAAAAGTGCCACCTGACGTC

With the multiple cloning sites

...ACAAGTAATAAGCTAGCACACCGGTCGTCTAGCAATGCGATCCACGTACGTAGGATCCC

Cerulean ***NheI*** ***AgeI*** ***BsiWI*** ***BamHI***

GACTGTG….

Sequence 1. Plasmid Map of pFmiR-empty and sequence.

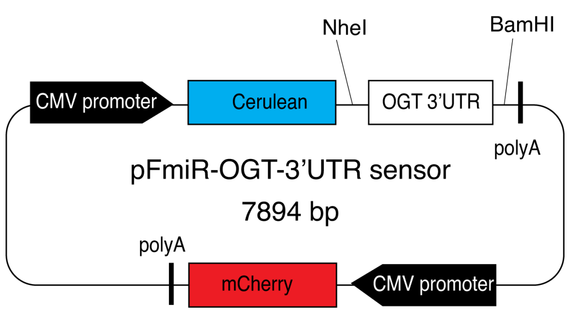

OGT 3’UTR:

CACATGATTAAGCCTGTTGAAGTCACTGAGTCAGCATAAATAAAGACTGCACAGGAGAATTACCCCTATACCTGAGCCTCAACCT
TCTGGGGGAAAGGGAACTAGATAACATACTTCTTACTTGTCTGTACAGTACCTTGTTGCAGATGGGTGATATATAATGGTAATAGA
ATAGCACAGCCAGACTTGCTTCCTGCATGGTAGGGAGAGACACAAAAGATGGGAAACTGCTTTTCCACAAGGAATCTCCGTAGAA
TTTTGCGGCGACCAGATGGTGCATAGGTCTGGAAGGTCTGATCTCCCTTGGTCTTCCATGGGATGGTTAGTGTGGAGGGGAGATAT
AGATTGTCCGGCCGCTTTGTGATTCCATGGATTGATTCAGTCTTCTGGATTTTTTTTTCTTTATATTTTGGGTACTGGAGCTTTTAAA
AATGTTTGGTTTCAGGTATTTTTATTCATGTGAAGTGTATATGATTCTCTTGAGATAAGGTTTTAAGCTAAAATGTTACTCCCTGTT
TTAGTTTCTGAACTCTGACAGATTGACAGGGACTTTGCTGGTGTAGTCTTTTTATAGGTTTTATAAACCACTTGAGCCTATATCAGT
CGTTTTAGTGTCTGACCTAATATTTGGAGCTATCAGTGCTTTGTTGATTTAGATGATGACTCAAGATTTTTTCTGGTCCATTTCCCAT
TTCCTTTTCTTCCCTGACCCCCATACCCTCACCCTTAAAATTCTCCTGTAACTCAACTAACAAAATCAAGCCTGATTCAAAACATCC
TAGGGTGTTTTAAACACACCATCTGGTGCCAAATGAAGATTTTTAGGAGTGATTACTAATTATCAAGGGCACAGTTGTGGTACTGT
CATTGATAATAATATAGTTTTTTTTTTTTTCCTAATTTTGACCTGTTTCACCAGTGTTTTACCCTTGACTGCCCCTTCTATGCTGCTTC
CAAAAGTGATAGTGTGTGTAAGATTTTTACCTTCCTTTCTAAAGTTTTTTTTTTTTTTTTTTAAGTGAGTCCTGTTCTTCCTATTTCTT
TCAGCAGAAATGAAATCCCAGGTAAGTATAAGTATTCAAGTATTTGATCAGTAAGTCACAGTTATCTCCAGTGCATTAAATAACCT
TCATCAAGAAATAGGTTATAGGTAAAATCTCTGAAGGATCATCTATGTATTCAAGTAATTATTTTTTAGATAATAACTGTCTTCTG
GACTTGGTCTTGAAGTCTGTACAGATTCAGCCTCAGTAGTAGCGAACTGCACTGCTGTTTGGTTTGGAGTACAAATTAGACTTATA
GTCCTCCTGGAACTTGAGTTATTAAAATCATAGGAATAAAATTATGGGATCTCAACAAAGGGTCGAGGGTTTGAGGCTTAAACAA
GCCAACATATGAATATATGTTTTGTCTCGCTATACTGCACTTACGCTATCCAGTTGCAGGTAATTTTTTGTCTGCTAGTAGTGTTCT
AGATTATGTCTTTCCAAAGCGCTGAGGCTGTGCACCTATTCTGTAGTTGCAGCTGATGCCTGAATGTATCCTAGCTGACAAATTAT
TGATTAATAAGAACTTGAATTTCTGGAAGATTCTTACTGTTAACCAAATTTTGAGCAAGGAGTCTCAAAGGTAATTCTGAACCAGA
ATTACATGTTAATGAACAGTGTACCTTTTAACAGTGTAAATCACGGAATATCCGTGAAGGGATTTCTTAATTTATTTTTTACCGGTT
GATTGAAATATCAGTTAAAGGTTGCCAGCATGGTTGCAGATAAACTGATGTTTGAAATTCGCTGAAATACTTAATGTGGAATAGG
ATAATATACTTCCAATGCCCTCAAGGCTGTGACCTTACAGCCATTTTACATAGCACATCATTCCTCCTATAGGGATGAACTTTTTCC
TGGCACGAAAAGTAGCCGCTCTGGTTGAAGCTTTGCTTATTGTAACAGGCTTTTATTTCCAGGTAATATGTCTTGGAAGACTTAAT
TCTGATTAGAGATATAGATATTACTGGAAACTAATTGTTTTTTTTCTATTGTACTCTGCTTTATCAAAGAAGTAAAACATTTAAATC
GTACTACAGAAATTAAGATGTTGTCTTGCGATCCTTAATAAATGAATGATTTCCCTTTAATACGGGGATC

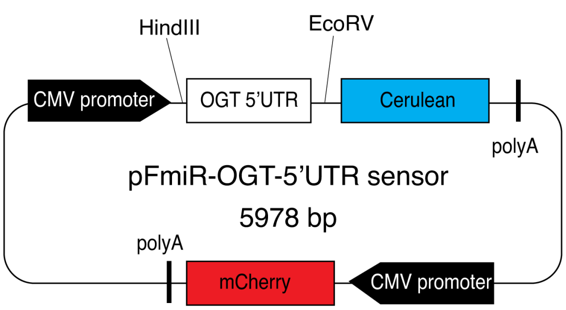

OGT 5’UTR:

ATTTCAAGACCGTACTAGGTAGATGGTCAATTAGAGTTCCCAGGGTTTGAAGCCTGTAACTGCTGCCGCCGCTCAAGCCCTCCAGA
GCATTGCTACGGCTGCTGCCCTTGTACTACTACCTCCAAATACGTTCTTGCTGGTAGTGGCGGCAGCAGGACCAATTACCTCTTTTT
TGCTCTCCCTCGAGAAGCTCCAG

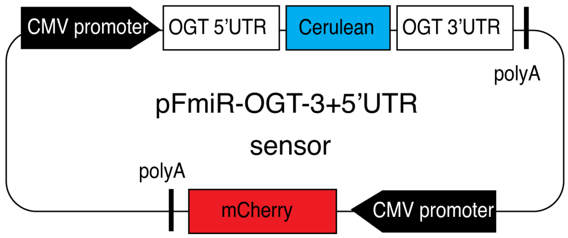

OGT 5'UTR:

ATTTCAAGACCGTACTAGGTAGATGGTCAATTAGAGTTCCCAGGGTTTGAAGCCTGTAACTGCTGCCGCCGCTCAAGCCCTCCAGA
GCATTGCTACGGCTGCTGCCCTTGTACTACTACCTCCAAATACGTTCTTGCTGGTAGTGGCGGCAGCAGGACCAATTACCTCTTTTT
TGCTCTCCCTCGAGAAGCTCCAG

OGT 3'UTR:

CACATGATTAAGCCTGTTGAAGTCACTGAGTCAGCATAAATAAAGACTGCACAGGAGAATTACCCCTATACCTGAGCCTCAACCT
TCTGGGGGAAAGGGAACTAGATAACATACTTCTTACTTGTCTGTACAGTACCTTGTTGCAGATGGGTGATATATAATGGTAATAGA
ATAGCACAGCCAGACTTGCTTCCTGCATGGTAGGGAGAGACACAAAAGATGGGAAACTGCTTTTCCACAAGGAATCTCCGTAGAA
TTTTGCGGCGACCAGATGGTGCATAGGTCTGGAAGGTCTGATCTCCCTTGGTCTTCCATGGGATGGTTAGTGTGGAGGGGAGATAT
AGATTGTCCGGCCGCTTTGTGATTCCATGGATTGATTCAGTCTTCTGGATTTTTTTTTCTTTATATTTTGGGTACTGGAGCTTTTAAA
AATGTTTGGTTTCAGGTATTTTTATTCATGTGAAGTGTATATGATTCTCTTGAGATAAGGTTTTAAGCTAAAATGTTACTCCCTGTT
TTAGTTTCTGAACTCTGACAGATTGACAGGGACTTTGCTGGTGTAGTCTTTTTATAGGTTTTATAAACCACTTGAGCCTATATCAGT
CGTTTTAGTGTCTGACCTAATATTTGGAGCTATCAGTGCTTTGTTGATTTAGATGATGACTCAAGATTTTTTCTGGTCCATTTCCCAT
TTCCTTTTCTTCCCTGACCCCCATACCCTCACCCTTAAAATTCTCCTGTAACTCAACTAACAAAATCAAGCCTGATTCAAAACATCC
TAGGGTGTTTTAAACACACCATCTGGTGCCAAATGAAGATTTTTAGGAGTGATTACTAATTATCAAGGGCACAGTTGTGGTACTGT
CATTGATAATAATATAGTTTTTTTTTTTTTCCTAATTTTGACCTGTTTCACCAGTGTTTTACCCTTGACTGCCCCTTCTATGCTGCTTC
CAAAAGTGATAGTGTGTGTAAGATTTTTACCTTCCTTTCTAAAGTTTTTTTTTTTTTTTTTAAGTGAGTCCTGTTCTTCCTATTTCTT
TCAGCAGAAATGAAATCCCAGGTAAGTATAAGTATTCAAGTATTTGATCAGTAAGTCACAGTTATCTCCAGTGCATTAAATAACCT
TCATCAAGAAATAGGTTATAGGTAAAATCTCTGAAGGATCATCTATGTATTCAAGTAATTATTTTTTAGATAATAACTGTCTTCTG
GACTTGGTCTTGAAGTCTGTACAGATTCAGCCTCAGTAGTAGCGAACTGCACTGCTGTTTGGTTTGGAGTACAAATTAGACTTATA
GTCCTCCTGGAACTTGAGTTATTAAAATCATAGGAATAAAATTATGGGATCTCAACAAAGGGTCGAGGGTTTGAGGCTTAAACAA
GCCAACATATGAATATATGTTTTGTCTCGCTATACTGCACTTACGCTATCCAGTTGCAGGTAATTTTTTGTCTGCTAGTAGTGTTCT
AGATTATGTCTTTCCAAAGCGCTGAGGCTGTGCACCTATTCTGTAGTTGCAGCTGATGCCTGAATGTATCCTAGCTGACAAATTAT
TGATTAATAAGAACTTGAATTTCTGGAAGATTCTTACTGTTAACCAAATTTTGAGCAAGGAGTCTCAAAGGTAATTCTGAACCAGA
ATTACATGTTAATGAACAGTGTACCTTTTAACAGTGTAAATCACGGAATATCCGTGAAGGGATTTCTTAATTTATTTTTTACCGGTT
GATTGAAATATCAGTTAAAGGTTGCCAGCATGGTTGCAGATAAACTGATGTTTGAAATTCGCTGAAATACTTAATGTGGAATAGG
ATAATATACTTCCAATGCCCTCAAGGCTGTGACCTTACAGCCATTTTACATAGCACATCATTCCTCCTATAGGGATGAACTTTTTCC
TGGCACGAAAAGTAGCCGCTCTGGTTGAAGCTTTGCTTATTGTAACAGGCTTTTATTTCCAGGTAATATGTCTTGGAAGACTTAAT
TCTGATTAGAGATATAGATATTACTGGAAACTAATTGTTTTTTTTCTATTGTACTCTGCTTTATCAAAGAAGTAAAACATTTAAATC
GTACTACAGAAATTAAGATGTTGTCTTGCGATCCTTAATAAATGAATGATTTCCCTTTAATACGGGGATC

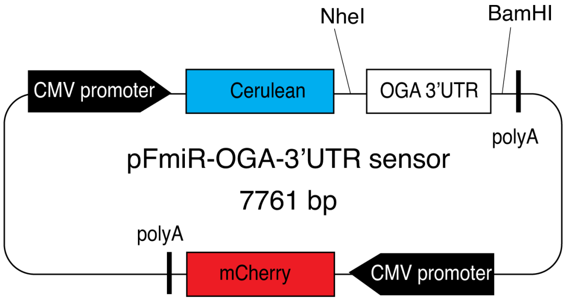

OGA 3'UTR:

CATTTGTTGACACTGTGAACTGTCCAAAAGTCTCTTAACTGCACCTTGTGAATGGTAGTTGAGGTCTTCATACAGTTCAGCCTCTA
GAATGGTAACAAATCAGCCAATTGGATTCGAAACAAAGAAGACTATGTAAAACTCACCCATCACACTTTGAGACTACTCACTGGT
TGGAAGAATATAGTATTGCAGCAAATCCTGTATGAAAGAGAGATGTGGGCTTCCTTTTTGAGTCTTGTGTTAGGTGCTGAGACCTT
TTACATGGGCTTATACAGGGAGAGAGTCTTCAATAAATGTAGTCAGCACTATTTTCTGCATCCAGTGTGGTTGCGTTTCTCACCTG
AGAGTAATCAAGATAACATCTGTCATCTTCCTTGGTTTATTGAGTGAAATGCCTCTCAGTCTTAGGGGACATGGCAGAGATGAAA
GAAAGAAAGAGTGGGTTTCAGAAGTGTCAGGGTGGAGTGATTCCAAGTGGGATGGTTGTGGCATTAGTTTAAGCTGAATAAATAA
TTTCAATTTGGGGCAGTTATTCTGCTTTTTGTAAAGCCGTGGCCAATTGTCTCCTGTAATGACTGTTGGTTCAGGCATGTTGTACTT
TGTAGGGACAAATGTGCATTTGTTTGTGGCAAAAGCCTACAATTGACAAACTTGTAAATTTCTTTGTATATAAACTAGCTGTAACC
TGACTATCCTTTGTGTTTACTGTTTTTGTAAATTTTTTTCCTCTATAAATGAAAGGGTGTTGGTTCAGAATGGCACTTTGAATAATG
TAAACCAGTGAAAAGTGGATTTTCTTTACTTTTGTCTTTGGGTTTGGGGTTGTTTTTGTTCTTTTTGAAGTTTTATTATTTTTAAAGT
GCCTCCCACCTAGGCGTAGGCCATGACCATTTGGGGTACGAGAGCCTAATTTTGTAGGACTTAATCTGTTGAAAAGTGCAGTTACT
TCTGGAAATTAACCTCAATATTAGGTCAGCATGTGAAATGTTGGATTTGACATGTCAGGTAGGGTTCAGGGACTGATTGGTCCCAT
TTGCCCTCAGGTCAGTTGTTTAATCTCAAGACCTGTTACTACTGATTTTATTAAATCAGAGTCTTTAATTCTTGCATGTTTGTATCTA
ATTTCTGAATGAATGAGCACACTTTAACCAGTTATTTACAGTTACCTTTTTCCTTTAACCGGATTGTGAAAGCTTCATGTATTTTAA
TTTAGATTCTGTGTTTTTAAGGGTTCTGAGCATGAAGCTGGCAGATAGTCGGCAGGACTCATTTTTTCATCATGGCTGGCTGATTTC
TCCATAGATTGATAACAGTATTTTGTTATCTTGCTTCTCTGTAGTTTTGCATCAGCTGTTTAACTTTGAGCTGAGTGAGGGGAGAGG
GGTAAAGAGAAAGAAACTTAAGTTTTCTTTCACAGAACTCCACCATTGTGGGCTTTGAGAGAGCCCTAAAGCATTGTACCTAGTG
GTACCTAGTGACTTCCAACCAAAGCCTTTGAGTATGCACTAAATAGGTGAGAAGAAAGGAGAGAAGGTTTTTAGGTTAGAAACCT
TTAACCGATAGAAGGATATGGTATGTTGTAAAGCTGGAACCAAGTTTGCATTTTTGAGGGCTTGAGATGAAGGGAAGACTCTTAC
CAGATAGTAAGACAGCTGAGTTTTCCTCAGTTTTCTCGTCTTAACACTAGTGGACAATTCTAGCATTTTGTTTGGAGGATTTCAGA
GTTAACCTCATGGAATTCAGGATTTTTTAGCAAGTTTGCTTTTGGTTTTATCTTGGCTTTTAGTAATCATGTTGGCTGGTCTGGTCAC
AGGTGACTGTGAAACAGATGCCCTGGTCTTGCTTTCATCACTCTAGGATCATGAAGTGCTATGCTATTTCCTGGTTATGAATATTA
AGGTTGGAATTACATTTTTATTGATTGTTTGGATCAGAGCTCAGTTCCTGTAGAAAACGAACTGTAAAAGACCATGCAAGAGGCA
AAATAAAACTTGAAGTGAATGCTTGT

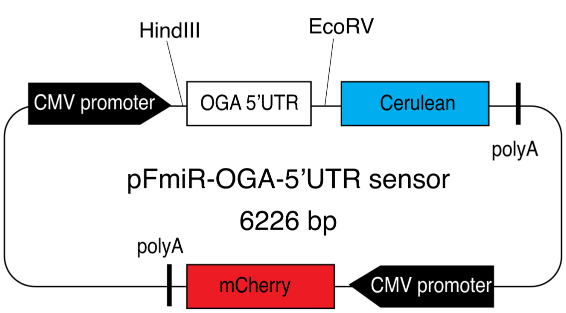

OGA 5'UTR:

GGTCTGCAGCGCAAGCGCAGTGCGGATAAACAGGAAGCGGGCGGTGGAGGCAGCAGCAGAGGGAGAGCTCGGGGCTTGGAGGG
GAAACAGCGGAAGACCTAAGATTATCGGGAGGGCAGCAGAGGCAGAGAACGAGGACAGGACCCTTGGCCGTCTTCTTCCAGGGA

ACGAGAGGTCACAGCCTCGCTCTCCGCTTAGGCTTCTGGCGCCCCAGCTTAAAGCCGAGGCTGCGGCTGACAAAGGGCTCGCGCC
GGTGCCGCCGCCCTTCTCATCCGGGCATTCGGGTCCCTGCGGAGAGGGAGGGGGAAGGGCAGAGGGGGAGGGGAAGGAGCCGG
AGGGGCGCACACTTGGAGCTGAAGCCCTCTCCAGGGCTCCGGGCCGGTGCCCCAACGGACAGAGGTCGAGGAGGACCCGCAGAG
GTGGCAGCGGCCGGGGGCAGGAGG

OGA 3’UTR:

CATTTGTTGACACTGTGAACTGTCCAAAAGTCTCTTAACTGCACCTTGTGAATGGTAGTTGAGGTCTTCATACAGTTCAGCCTCTA
GAATGGTAACAAATCAGCCAATTGGATTCGAAACAAAGAAGACTATGTAAAACTCACCCATCACACTTTGAGACTACTCACTGGT
TGGAAGAATATAGTATTGCAGCAAATCCTGTATGAAAGAGAGATGTGGGCTTCCTTTTTGAGTCTTGTGTTAGGTGCTGAGACCTT
TTACATGGGCTTATACAGGGAGAGAGTCTTCAATAAATGTAGTCAGCACTATTTTCTGCATCCAGTGTGGTTGCGTTTCTCACCTG
AGAGTAATCAAGATAACATCTGTCATCTTCCTTGGTTTATTGAGTGAAATGCCTCTCAGTCTTAGGGGACATGGCAGAGATGAAA
GAAAGAAAGAGTGGGTTTCAGAAGTGTCAGGGTGGAGTGATTCCAAGTGGGATGGTTGTGGCATTAGTTTAAGCTGAATAAATAA
TTTCAATTTGGGGCAGTTATTCTGCTTTTTGTAAAGCCGTGGCCAATTGTCTCCTGTAATGACTGTTGGTTCAGGCATGTTGTACTT
TGTAGGGACAAATGTGCATTTGTTTGTGGCAAAAGCCTACAATTGACAAACTTGTAAATTTCTTTGTATATAAACTAGCTGTAACC
TGACTATCCTTTGTGTTTACTGTTTTTGTAAATTTTTTTCCTCTATAAATGAAAGGGTGTTGGTTCAGAATGGCACTTTGAATAATG
TAAACCAGTGAAAAGTGGATTTTCTTTACTTTTGTCTTTGGGTTTGGGGTTGTTTTTGTTCTTTTTGAAGTTTTATTATTTTTAAAGT
GCCTCCCACCTAGGCGTAGGCCATGACCATTTGGGGTACGAGAGCCTAATTTTGTAGGACTTAATCTGTTGAAAAGTGCAGTTACT
TCTGGAAATTAACCTCAATATTAGGTCAGCATGTGAAATGTTGGATTTGACATGTCAGGTAGGGTTCAGGGACTGATTGGTCCCAT
TTGCCCTCAGGTCAGTTGTTTAATCTCAAGACCTGTTACTACTGATTTTATTAAATCAGAGTCTTTAATTCTTGCATGTTTGTATCTA
ATTTCTGAATGAATGAGCACACTTTAACCAGTTATTTACAGTTACCTTTTTCCTTTAACCGGATTGTGAAAGCTTCATGTATTTTAA
TTTAGATTCTGTGTTTTTAAGGGTTCTGAGCATGAAGCTGGCAGATAGTCGGCAGGACTCATTTTTTCATCATGGCTGGCTGATTTC
TCCATAGATTGATAACAGTATTTGTTATCTTGCTTCTCTGTAGTTTTGCATCAGCTGTTTAACTTTGAGCTGAGTGAGGGGAGAGG
GGTAAAGAGAAAGAAACTTAAGTTTTCTTTCACAGAACTCCACCATTGTGGGCTTTGAGAGAGCCCTAAAGCATTGTACCTAGTG
GTACCTAGTGACTTCCAACCAAAGCCTTTGAGTATGCACTAAATAGGTGAGAAGAAAGGAGAGAAGGTTTTTAGGTTAGAAACCT
TTAACCGATAGAAGGATATGGTATGTTGTAAAGCTGGAACCAAGTTTGCATTTTTGAGGGCTTGAGATGAAGGGAAGACTCTTAC
CAGATAGTAAGACAGCTGAGTTTTCCTCAGTTTTCTCGTCTTAACACTAGTGGACAATTCTAGCATTTTGTTTGGAGGATTTCAGA
GTTAACCTCATGGAATTCAGGATTTTTTAGCAAGTTTGCTTTTGGTTTTATCTTGGCTTTTAGTAATCATGTTGGCTGGTCTGGTCAC
AGGTGACTGTGAAACAGATGCCCTGGTCTTGCTTTCATCACTCTAGGATCATGAAGTGCTATGCTATTTCCTGGTTATGAATATTA
AGGTTGGAATTACATTTTTATTGATTGTTTGGATCAGAGCTCAGTTCCTGTAGAAAACGAACTGTAAAAGACCATGCAAGAGGCA
AAATAAAACTTGAAGTGAATGCTTGT

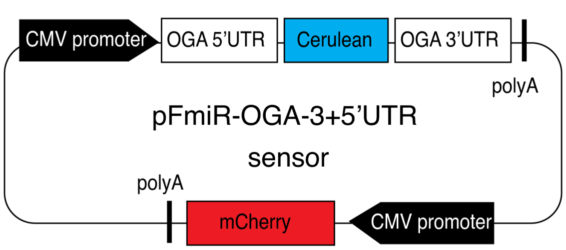

OGA 5’UTR:

GGTCTGCAGCGCAAGCGCAGTGCGGATAAACAGGAAGCGGGCGGTGGAGGCAGCAGCAGAGGGAGAGCTCGGGGCTTGGAGGG
GAAACAGCGGAAGACCTAAGATTATCGGGAGGGCAGCAGAGGCAGAGAACGAGGACAGGACCCTTGGCCGTCTTCTTCCAGGGA
ACGAGAGGTCACAGCCTCGCTCTCCGCTTAGGCTTCTGGCGCCCCAGCTTAAAGCCGAGGCTGCGGCTGACAAAGGGCTCGCGCC
GGTGCCGCCGCCCTTCTCATCCGGGCATTCGGGTCCCTGCGGAGAGGGAGGGGGAAGGGCAGAGGGGGAGGGGAAGGAGCCGG

AGGGGCGCACACTTGGAGCTGAAGCCCTCTCCAGGGCTCCGGGCCGGTGCCCCAACGGACAGAGGTCGAGGAGGACCCGCAGAG GTGGCAGCGGCCGGGGGCAGGAGG

Table 4.1 Quantification of OGA with 3 replicates associated with **Figure 4.15**

	Relative expression of OGA				
	Replicate 1	Replicate 2	Replicate 3	Mean	Standard deviation
NTC	1	1	1	1	0
miR-27a	0.783167898	0.818383815	0.812598138	0.804717	0.018884623
miR-520d-5p	0.424236675	0.318776704	0.566535026	0.436516	0.124334771
miR-524-5p	0.354872531	0.339366198	0.460641085	0.38496	0.065998777
miR-196a-3p	2.735257616	2.54479499	1.605790372	2.295281	0.604662708
miR-148a-3p	1.377535808	2.005785306	1.237375997	1.540232	0.40922591
miR-140	0.819426922	0.850335368	0.827974609	0.832579	0.01596036
miR-3655	1.514178789	1.0528534	0.629836005	1.065623	0.442309656
miR-3127	0.573709387	0.41153999	0.797426084	0.594225	0.193759366

Table 4.2 Quantification of OGA associated with **Figure 4.16**

	Relative expression of OGA				
	Replicate 1	Replicate 2	Replicate 3	Mean	Standard deviation
NTC	1	1	1	1	0
let-7a	0.289593	0.511534	0.335163	0.378763	0.117219
miR-95	0.70804	0.624814	0.537807	0.623554	0.085124
miR-200a	2.647619	1.513154	1.774619	1.978464	0.594068
miR-891b	2.756701	1.586129	1.986308	2.109713	0.594963

Table 4.3. Analysis of downregulatory miR binding seed sites in OGT 3'UTR regions

miRNA	Ratio	dG_hybrid	LogitProb	TargetMatch	MirMatch
hsa-miR-4729	0.74	-16.8	0.897	GC UCCU AUAAAUGA	CG AGGG UAUUUACU
hsa-miR-3682-5p	0.52	-12.9	0.8917	AGAAGUA	UCUUCAU
hsa-miR-548c-3p	0.76	-18.3	0.8754	CAAAAGUGAU UG AGAUUUUU	GUUUUCAUUA AC UCUAAAAA
hsa-miR-4772-3p	0.66	-21	0.8667	UCUG CAG GUUGCAG	AGAC GUC CAACGUC
hsa-miR-4705	0.77	-20.5	0.8639	UUACCGG UGAUUGA	AAUGGUU ACUAACU
hsa-miR-202-5p	0.61	-15.6	0.8591	GAGU CAUAGGAA	UUCA GUAUCCUU
hsa-miR-3164	0.71	-17	0.8502	UAUUU UC AAGUCACA	GUAAA GG UUCAGUGU
hsa-miR-599	0.78	-19.9	0.8443	UGGUA GA GACACAA	ACUAU UU CUGUGUU
hsa-miR-4712-5p	0.46	-18.1	0.8442	GUACUGGA	CAUGACCU
hsa-miR-205-3p	0.53	-22.6	0.8433	GA UUUG UUCGCUGAAAU	CU AAGU AGGUGACUUUA
hsa-miR-5003-3p	0.69	-19.5	0.8425	UCCUGGCA GAAAAGUA	GGGGUUGU CUUUUCAU
hsa-miR-483-3p	0.71	-19.1	0.8374	AAGAU AGGAGUGA	UUCUG UCCUCACU
hsa-miR-4476	0.62	-26.4	0.8354	GU GUCCU GUUCUUCCU	CG CAGGG UAGGAAGGA
hsa-miR-4696	0.61	-20.6	0.832	AGAUG UUGUCUUGCG	UCUAC GGCAGAACGU
hsa-miR-3155a	0.8	-24.1	0.8262	GGUUU CCACU GAGCCU	UCAAG GGUGA CUCGGA
hsa-miR-1264	0.66	-18.6	0.825	CAGGU G CUUGG AAGACUU	GUCCA C GAGUU UUCUGAA
hsa-miR-3161	0.69	-19.1	0.8169	UCU G CUCUG UUUAUCA	AGA C GAGAC GAAUAGU
hsa-miR-93-3p	0.58	-19.1	0.8161	AAGUG GU UCAGCAG	UUCAC CG AGUCGUC
hsa-miR-3064-5p	0.74	-23.5	0.8149	GUA AU GC ACAGCCAGA	CGU UG UG UGUCGGUCU
hsa-miR-767-5p	0.77	-29.4	0.8128	UGC GGCGACC AUGGUGCA	ACG CUGUUGG UACCACGU
hsa-miR-4422	0.65	-14	0.8118	GUACU C UGCUUU	CAUGA G ACGAAA
hsa-miR-551a	0.74	-22.1	0.8111	UGGGA UCAA GGGUCG	ACCUU GGUU CCCAGC
hsa-miR-770-5p	0.57	-24.5	0.8008	UGG UCUU AUAU GGUACUGGA	ACC GGGA UGUG CCAUGACCU
hsa-miR-4772-3p	0.66	-24.1	0.7988	UUGA UCAG GCA GGUUGCAG	GACU AGUC CGU UCAACGUC
hsa-miR-770-5p	0.57	-18.7	0.7977	GAUAU UACUGGA	CUGUG AUGACCU
hsa-miR-5571-5p	0.78	-14.7	0.7959	AG CU C GAGAAUU	UC GA G CUCUUAA
hsa-miR-770-5p	0.57	-26.2	0.7919	GGC A UGUGGUACUG	CCG U GCACCAUGAC
hsa-miR-3941	0.56	-21.6	0.7904	UAUG UCC AGU UGUGUGUAA	AUAC AGG UCA ACACACAUU
hsa-miR-5579-3p	0.67	-19.8	0.7901	GAU GGU UUUAAGCUAA	CUA CCA GAAUUCGAUU
hsa-miR-624-3p	0.67	-20.4	0.7889	CAGUACCUUGU	GUUAUGGAACA
hsa-miR-7-5p	0.45	-22.1	0.7858	GAUC UUGGUCUUCCA	UUAG GAUCAGAAGGU
hsa-miR-4712-5p	0.46	-21.2	0.7849	GAU AGAGAU UACUGGA	UUA UCUCUG AUGACCU
hsa-miR-466	0.64	-19.1	0.7844	GUG GUGUGUGUA	CGC CAUACACAU
hsa-miR-5195-3p	0.57	-22.8	0.7817	UCU UUAGAGA ACUGGA	GGG AGUCUCU UGACCU
hsa-miR-520a-5p	0.71	-19.1	0.7815	AAG ACUU UUUCUGGA	UUC UGAA GGAGACCU
hsa-miR-520a-5p	0.71	-21.4	0.7707	AAAGUA CC CUCUGG	UUUCAU GG GAGACC

hsa-miR-542-3p	0.8	-22.3	0.7669	CAGUUGU G CUGUCAU	GUCAAUA U GACAGUG
hsa-miR-15b-3p	0.49	-11.9	0.7653	GGAU UGAUUC	UUUA ACUAAG
hsa-miR-502-3p	0.52	-25.9	0.7643	GAAUUUU GC CCA GGUGCAU	CUUAGGA CG GGU CCACGUA
hsa-miR-320b	0.76	-23.6	0.7639	GCC CUCU G AGCUUU	CGG GAGA U UCGAAA
hsa-miR-501-3p	0.61	-24.7	0.7596	AGAAUUUU GC CC GGUGCAU	UCUUAGGA CG GG CCACGUA
hsa-miR-1271-5p	0.61	-25.9	0.7544	GGGUGUUU CU GGUGCCAA	CUCACGAA GA CCACGGUU
hsa-miR-548c-3p	0.76	-12.4	0.748	CA GGUG UG AGAUUUUU	GU UCAU AC UCUAAAAA
hsa-miR-4643	0.69	-20.1	0.747	GGUAUUU UCAUGUG	UCGUAAA AGUACAC
hsa-miR-4661-3p	0.8	-17.1	0.7465	GAU UCU UG GAUCCU	CUG AGA AC CUAGGA
hsa-miR-452-3p	0.79	-26.2	0.7437	CUUACU UCU UUGCAGAUGGG	GAAUGA AGA AACGUCUACUC
hsa-let-7g-3p	0.42	-19.5	0.7436	GUCUGUACAG	CGGACAUGUC
hsa-miR-1264	0.66	-19.3	0.7398	GG GU CAAAU AGACUU	CC CG GUUUA UCUGAA
hsa-miR-1208	0.61	-15.4	0.7352	CCU UU AACAGUG	GGA AG UUGUCAC
hsa-miR-96-5p	0.62	-21.8	0.7349	GUGU UGGUGCCAAA	CACG AUCACGGUUU
hsa-miR-15b-3p	0.49	-14.9	0.7334	AGU GUA AUGAUUC	UCG CGU UACUAAG
hsa-miR-320c	0.77	-21.1	0.7214	GCC CUCU G AGCUUU	UGG GAGA U UCGAAA
hsa-miR-548u	0.74	-19.2	0.7207	GC G UGUAGUCUUU	CG C ACGUCAGAAA
hsa-miR-5571-5p	0.78	-16	0.7185	GGAG CUC G AGAAUU	CCUC GAG C UCUUAA
hsa-miR-1304-5p	0.7	-21.9	0.7164	UAC CU CUG AGCCUCAA	GUG GA GAC UCGGAGUU
hsa-miR-200a-5p	0.58	-19.2	0.7154	UCC AGUG GU UG GUAAGAU	AGG UCGU CA GC CAUUCUA
hsa-miR-544a	0.55	-13.9	0.7153	CUU CUA GCAGAA	GAA GAU CGUCUU
hsa-miR-548at-3p	0.8	-12.2	0.7134	C GAG UA GGUUUU	G UUC AU CCAAAA
hsa-miR-3118	0.76	-17.4	0.7129	AG AUUU UCA AGUCACA	UC UAAA AGU UCAGUGU
hsa-miR-1208	0.61	-21.4	0.7107	UCUG CC UGUU UGAACAGUG	AGGC GG ACAG ACUUGUCAC
hsa-miR-548ag	0.8	-14	0.7102	UAG G UA UUACCUU	GUC U GU AAUGGAA
hsa-miR-205-3p	0.53	-15.8	0.7064	UUUUAC UU AUUGAAAU	GAAGUG AG UGACUUUA
hsa-miR-141-5p	0.77	-19.6	0.7046	AAC UUG CUGGAAGAU	UUG GAC GACCUUCUA
hsa-miR-556-3p	0.43	-26.4	0.7037	AGAUGGGU UAAUGGUAAUA	UCUACUCG AUUACCAUUAU
hsa-let-7g-3p	0.42	-23.6	0.7032	GGU UG GUCUGUACAG	CCG AC CGGACAUGUC
hsa-miR-4710	0.69	-31	0.7023	GACC CC CCCUCACCC	UUGG GG GGGAGUGGG
hsa-miR-141-5p	0.77	-22.2	0.7014	UCCAG UGU UUGGAAGA	AGGUU ACA GACCUUCU
hsa-miR-106b-3p	0.74	-26.6	0.7012	CAGUAAGU AUCU CAGUGC	GUCGUUCA UGGG GUCACG
hsa-miR-520a-5p	0.71	-21	0.7	AGA ACU UCUUCUGGA	UCU UGA GGGAGACCU
hsa-miR-7-5p	0.45	-21.7	0.6997	UAA GAGUC CUG UCUUCC	GUU UUUAG GAU AGAAGG
hsa-miR-3143	0.7	-15	0.696	GAA AGAA UUAC AUGUUA	CUU UCUU AAUG UACAAU
hsa-miR-4780	0.74	-21.6	0.6942	UUAGG GAUUA UCAAGGG	GAUCC CUAGU AGUUCCC
hsa-miR-7-5p	0.45	-19	0.694	GAUAA ACU GUCUUCU	UUGUU UGA CAGAAGG
hsa-miR-676-5p	0.74	-21.3	0.6934	GCA AGU CC GGUUGAAG	CGU UCA GG CCAACUUC
hsa-miR-4711-3p	0.55	-18	0.6928	UC GC GGG AGACAC	AG CG UCU UCUGUG
hsa-miR-4476	0.62	-18.8	0.6915	GU UGU U AGAU CCUUCCU	CG ACA G UUUA GGAAGGA
hsa-miR-548c-3p	0.76	-7.9	0.6864	GU GGU GG AUUUUU	CG UCA CU UAAAAA
hsa-miR-3064-5p	0.74	-22.7	0.6852	UGUG ACC ACAGCCA	ACGU UGG UGUCGGU
hsa-miR-103a-2-5p	0.69	-15.9	0.685	UAUUGUA AAGAAGU	GUGACAU UUCUUCG

hsa-miR-625-3p	0.76	-10.5	0.6812	UAUAGUU	AUAUCAG
hsa-miR-550b-2-5p	0.69	-22.7	0.6781	GU UUACU UC GGGCACA	CA AAUGA GG UCCGUGU
hsa-miR-452-3p	0.79	-22.1	0.6773	CUUACU UCU UUGCAGAUG	GAAUGA AGA AACGUCUAC
hsa-miR-520a-5p	0.71	-19.9	0.6756	GGA G AUU UCUUCUGGA	UCU C UGA GGGAGACCU
hsa-miR-3202	0.65	-17.9	0.6754	UAAG UUUUU CCUUCC	AUUU GAGAA GGAAGG
hsa-miR-4696	0.61	-15.5	0.6712	GGUA UGUCUUG	UCAU GCAGAAC
hsa-miR-5590-3p	0.77	-10.9	0.6708	GUC C UGGA CUUUAU	CGG G ACUU GAAAUA
hsa-miR-4772-3p	0.66	-23.1	0.6704	CUG UUA GC AGUUGCAGG	GAC AGU CG UCAACGUCC
hsa-miR-298	0.8	-18.1	0.6667	AGA U CUG CUUCUG	UCU A GAC GAAGAC
hsa-miR-3691-3p	0.71	-18.7	0.6649	AGA AU AC GU GGACUUGGU	UCU UA UG CG UCUGAACCA
hsa-miR-876-5p	0.75	-17.2	0.6647	UUCA CAGA GAAAUCC	AAGU GUUU CUUUAGG
hsa-miR-3143	0.7	-19.4	0.6628	GAGA AAG GUUUUA AAUGUUA	CUUU UUC CGAAAU UUACAAU
hsa-miR-1243	0.72	-18.5	0.6623	CUC CUAUA UG AUCCAGUU	GAG GAUAU AC UAGGUCAA
hsa-miR-548ag	0.8	-15.3	0.6617	UACAG UACCUU	GUGUU AUGGAA
hsa-miR-2392	0.77	-23.3	0.6611	GCCU UUCA CAUCCUA	UGGA GAGU GUAGGAU
hsa-miR-5571-5p	0.78	-18.2	0.6611	GGA CUCC AGAAUU	CCU GAGG UCUUAA
hsa-miR-15b-3p	0.49	-13	0.661	AGC UGAUUC	UCG ACUAAG
hsa-miR-4696	0.61	-17.1	0.657	GGUA UGUCUUG A	UCAU GCAGAAC U
hsa-miR-101-5p	0.7	-12.2	0.6561	UUAG AUAACUG	AGUC UAUUGAC
hsa-let-7a-2-3p	0.49	-21.1	0.656	GGA GG CU G AG CUGUACAG	CCU UC GA C UC GACAUGUC
hsa-miR-3155a	0.8	-20.8	0.6541	CCUAU C GAGCCU	GGGUG G CUCGGA
hsa-miR-2114-5p	0.62	-18.2	0.6525	GUUUC GA AGGGACU	CGAAG CU UCCCUGA
hsa-miR-200a-5p	0.58	-14.9	0.6518	GUACU UAAGAUG	CGUGA AUUCUAC
hsa-miR-550a-3p	0.73	-16.9	0.6517	GUG G G G GUAAGAU	CAC C C C CAUUCUG
hsa-miR-501-3p	0.61	-17.4	0.6514	AG AUCU CC GUGCAUU	UC UAGG GG CACGUAA
hsa-miR-625-3p	0.76	-11.1	0.6468	CUAUAG	GAUAUC
hsa-miR-7-5p	0.45	-18.7	0.6456	CA GA GAUU AGUCUUCU	GU UU UUAG UCAGAAGG
hsa-miR-4422	0.65	-17	0.6435	GG GCU UC GUGCUUU	CC UGA AG UACGAAA
hsa-miR-15b-3p	0.49	-14.1	0.6419	AGA GU GCGA AAUGAUUU	UCU CG CGUU UUACUAAG
hsa-miR-4293	0.75	-16.6	0.6414	UUGU CAGGCU	GACA GUCCGA
hsa-miR-452-3p	0.79	-19.7	0.6311	GCUU UU UU UAGAUGA	UGAA AA AA GUCUACU
hsa-miR-924	0.74	-17.2	0.6273	GUAA AUGUC G AAGACUU	CGUU UGUAG U UUCUGAG
hsa-miR-548c-3p	0.76	-11.3	0.6268	GAUUGA GAUUUUU	UUAACU CUAAAAA
hsa-miR-517a-3p	0.69	-24.6	0.6229	GCAC CUA AGGGAU GCACGA	UGUG GAU UCCCUA CGUGCU
hsa-miR-517b-3p	0.67	-24.6	0.6229	GCAC CUA AGGGAU GCACGA	UGUG GAU UCCCUA CGUGCU
hsa-miR-548c-3p	0.76	-10	0.6209	AG UGAU AGAUUUUU	UC AUUA UCUAAAAA
hsa-miR-556-3p	0.43	-15	0.618	GGCU GGUAAUAU	UCGA CCAUUAUA
hsa-miR-149-5p	0.8	-25.1	0.6174	GGGUGA AUGG AGCCAGA	CUCACU UGCC UCGGUCU
hsa-miR-767-5p	0.77	-26.3	0.6154	GUGUUU ACA ACCA UGGUGC	UACGAG UGU UGGU ACCACG
hsa-miR-218-5p	0.58	-22.9	0.6137	AUGGU UAGA AGCACAG	UACCA AUCU UCGUGUU
hsa-miR-5186	0.78	-16.4	0.6105	CUG UUUC AC AAUCUC	GAC AAAG UG UUAGAG
hsa-miR-5590-3p	0.77	-13.6	0.61	UUGUU GUAC GCUUUAU	AACGG UAUG UGAAAUA

hsa-miR-15b-3p	0.49	-18	0.609	GGC GC GUGAUUC	UCG CG UACUAAG
hsa-miR-136-3p	0.73	-19.8	0.6034	GCUU UUGA GAUGAUG	UGAG AACU CUACUAC
hsa-miR-544a	0.55	-17.4	0.6001	ACUUG CUG UGCAGA	UGAAC GAU ACGUCU
hsa-miR-517c-3p	0.6	-21.9	0.5965	GCAC CUA AGGGAU GCACGA	UGUG GAU UUCCUA CGUGCU
hsa-miR-556-3p	0.43	-13.7	0.5962	AGUUG GGUAAU	UCGAU CCAUUA
hsa-miR-3155a	0.8	-19.3	0.5908	UUCUC CUGU A AGCCUG	AAGGG GACG U UCGGAC
hsa-miR-3117-5p	0.75	-21.8	0.5894	AUAU A UCGU UAGUGUCU	UAUA U AGCA AUCACAGA
hsa-miR-493-5p	0.8	-16.5	0.5877	CUUACU UGUACAG	GGAUGG ACAUGUU
hsa-miR-483-3p	0.71	-15	0.5854	GAG AGGAGU	CUC UCCUCA
hsa-miR-103a-3p	0.8	-24.7	0.5851	GCCC C AUGCUGCU	CGGG G UACGACGA
hsa-miR-205-3p	0.53	-15.7	0.5819	AUUUC UC UGAAAUC	UGAAG AG ACUUUAG
hsa-miR-421	0.5	-19.7	0.5804	GC UCAGU UUUGUUGAU	CG GGUUA AGACAACUA
hsa-miR-3117-5p	0.75	-15.3	0.5777	GCU GUAGUGUU	UGA UAUCACAG
hsa-miR-4278	0.79	-19	0.5739	AGG G CCCCUA	UCC C GGGGAU
hsa-miR-3673	0.76	-18.8	0.5722	UCCG UGUG AUUCCAU	AGGC AUAU UAAGGUA
hsa-miR-544a	0.55	-16.9	0.5673	GUUAAAGG UGCAGA	CGAUUUUU ACGUCU
hsa-miR-561-5p	0.78	-15	0.5664	CAG GUUU CCUUGA	GUU CAAA GGAACU
hsa-miR-4761-5p	0.73	-19.5	0.564	C GU UGUAC ACCUUGU	G CG ACGUG UGGAACA
hsa-miR-676-5p	0.74	-15.5	0.5637	UGU UUCUGG GG UUGAAG	ACG AGGACU CC AACUUC
hsa-miR-5095	0.79	-14.9	0.563	UUC CCUGUAA	AAG GGACAUU
hsa-miR-1290	0.78	-14.2	0.5611	UCCUGG UU AAAAUC	GGGACU AG UUUUAG
hsa-miR-4704-5p	0.64	-20.3	0.5606	CA UUGCA UGCU UAGUGUU	GU AGUGU ACGG AUCACAG
hsa-miR-1243	0.72	-15.4	0.5601	CAC UUAU UCCAGU	GUG GAUA AGGUCA
hsa-miR-29a-3p	0.67	-16.6	0.5589	AAC CA UGGUGC	UUG GU ACCACG
hsa-miR-548ao-3p	0.68	-16.2	0.5567	UGU UGG C GGUCUU	ACG AUC G CCAGAA
hsa-miR-3161	0.69	-19.1	0.5565	AUCUGG GCC UG UUU UUAUCA	UAGACC CGG AC AAG AAUAGU
hsa-miR-520a-5p	0.71	-20.9	0.5565	AGA GGUGC UCUGGA	UCU UCAUG AGACCU
hsa-miR-3202	0.65	-18.1	0.5537	CUU CU CCCUUCUA	GAG GA GGGAAGGU
hsa-miR-3143	0.7	-16.3	0.5509	GGG GGAGC UUUUA AAUGUU	CUU CUUCG GAAAU UUACAA
hsa-miR-548u	0.74	-17.1	0.5505	CGC GUGAUU CAGUCUU	GCG CAUUAA GUCAGAA
hsa-miR-4772-3p	0.66	-21.6	0.5498	CUGA C G GCA AGUUGCAG	GACU G C CGU UCAACGUC
hsa-miR-556-3p	0.43	-15.2	0.5491	UGAGC GA GGUAAU	ACUCG UU CCAUUA
hsa-miR-4764-5p	0.78	-18.3	0.5467	UGAUUC ACAUCC	AUUGAG UGUAGG
hsa-miR-3619-3p	0.69	-16.7	0.5464	UCA GC GU GA UGGUCC	GGU CG CG CU ACCAGG
hsa-miR-555	0.72	-18.1	0.5385	CAGU UUACCCU	GUCG AAUGGGA
hsa-miR-4510	0.74	-24	0.5374	AGCUA AU UUACUCCCU	UUGGU UA GAUGAGGGA
hsa-miR-1304-5p	0.7	-16.7	0.5311	UAC UC CA UG CCUCAAG	GUG AG GU AC GGAGUUU
hsa-miR-320c	0.77	-14.4	0.5283	U UCUU AUUU AGCUUUU	G AGAG UGGG UCGAAAA
hsa-miR-1290	0.78	-14.4	0.522	UCCUG CUA AAAAUC	GGGAC GGU UUUUAG
hsa-miR-298	0.8	-26.5	0.5189	GGAGAA CCU CCUG CUUCUG	CCUCUU GGA GGAC GAAGAC
hsa-miR-24-3p	0.68	-22.1	0.5162	CUGC GAG CUGAGCC	GACG CUU GACUCGG
hsa-miR-5187-3p	0.66	-11.1	0.5146	AAG GAUUCA	UUC CUAAGU

hsa-miR-548ar-3p	0.8	-8.7	0.5132	GUAAGA CU AGUUUU	CGUUUU GA UCAAAA
hsa-miR-493-5p	0.8	-17.8	0.5107	UGGA GGUCU UC UGUACAG	ACUU UCGGA GG ACAUGUU
hsa-miR-4705	0.77	-17.8	0.5091	CGGC GCU GUGAUU	GUCG UGG CACUAA
hsa-miR-15a-5p	0.8	-18.8	0.5061	AC GCC UGCUGCU	UG UGG ACGACGA
hsa-miR-502-3p	0.52	-18.7	0.5056	GAUC GUC CAG GUGCAUU	UUAG CGG GUC CACGUAA
hsa-miR-548u	0.74	-17.2	0.5032	CGC GUGAUU CAGUCUU UG	GCG CAUUAA GUCAGAA AC
hsa-miR-548ag	0.8	-18	0.5008	CAGAA AC ACAGU UACCUUU	GUCUU UG UGUUA AUGGAAA
hsa-miR-7-5p	0.45	-14.9	0.3993	CA UC CU UCUUCC	GU AG GA AGAAGG

Table 4.4. Analysis of downregulatory miR binding seed sites in OGT 5'UTR regions

miRNA	Ratio	dG_hybrid	LogitProb	TargetMatch	MirMatch
hsa-miR-196a-5p	0.8	-18.4	0.5014	CCC AC ACUACCU	GGG UG UGAUGGA
hsa-miR-196b-5p	0.8	-18.4	0.5014	CCC AC ACUACCU	GGG UG UGAUGGA

Table 4.5. Analysis of downregulatory miR binding seed sites in OGT 3+5'UTR regions

miRNA	Ratio	dG_hybrid	LogitProb	TargetMatch	MirMatch
hsa-miR-4475	0.79	-21.5	0.9109	AAUGAAUG UCCCUU	UUACUUAC AGGGAA
hsa-miR-3672	0.75	-20.6	0.9	GCA GAGUCUCA	UGU CUCAGAGU
hsa-miR-4729	0.64	-16.8	0.897	GC UCCU AUAAAUGA	CG AGGG UAUUUACU
hsa-miR-3682-5p	0.58	-12.9	0.8917	AGAAGUA	UCUUCAU
hsa-miR-665	0.75	-24.3	0.8803	CUU AG CCUCCUGG	GAG UC GGAGGACC
hsa-miR-4772-3p	0.59	-21	0.8667	UCUG CAG GUUGCAG	AGAC GUC CAACGUC
hsa-miR-202-5p	0.57	-15.6	0.8591	GAGU CAUAGGAA	UUCA GUAUCCUU
hsa-miR-624-5p	0.6	-29.9	0.8567	GGGCACA GU UGGUACUG	CUUGUGU CA ACCAUGAU
hsa-miR-5696	0.75	-13.2	0.8527	GUC GC CU UAAAUGA	UAG UG GA AUUUACU
hsa-miR-3675-3p	0.73	-19.2	0.8477	UUGG GA UUCU UUAGAGAU	AACC CU AAGG AAUCUCUA
hsa-miR-599	0.7	-19.9	0.8443	UGGUA GA GACACAA	ACUAU UU CUGUGUU
hsa-miR-4712-5p	0.5	-18.1	0.8442	GUACUGGA	CAUGACCU
hsa-miR-205-3p	0.72	-22.6	0.8433	GA UUUG UUCGCUGAAAU	CU AAGU AGGUGACUUUA
hsa-miR-5003-3p	0.68	-19.5	0.8425	UCCUGGCA GAAAAGUA	GGGGUUGU CUUUUCAU
hsa-miR-4687-3p	0.8	-28.6	0.8391	UGCCCUC CC ACAGCCA	ACGGGGG GG UGUCGGU
hsa-miR-4476	0.64	-26.4	0.8354	GU GUCCU GUUCUUCCU	CG CAGGG UAGGAAGGA
hsa-miR-4696	0.58	-20.6	0.832	AGAUG UUGUCUUGCG	UCUAC GGCAGAACGU
hsa-miR-93-3p	0.66	-19.1	0.8161	AAGUG GU UCAGCAG	UUCAC CG AGUCGUC
hsa-miR-339-5p	0.79	-26.1	0.8157	UGA CUCU GA GACAGGGA	ACU GAGG CU CUGUCCCU
hsa-miR-3064-5p	0.78	-23.5	0.8149	GUA AU GC ACAGCCAGA	CGU UG UG UGUCGGUCU
hsa-miR-382-3p	0.78	-21	0.8056	AAG UGUUGUCU G UGAAUGAUU	UUC ACAACAGG C ACUUACUAA
hsa-miR-4519	0.8	-27.7	0.8049	CAGCC C GU GCACUGCUG	GUCGG G CG CGUGACGAC

hsa-miR-770-5p	0.59	-24.5	0.8008	UGG UCUU AUAU GGUACUGGA	ACC GGGA UGUG CCAUGACCU
hsa-miR-4772-3p	0.59	-24.1	0.7988	UUGA UCAG GCA GGUUGCAG	GACU AGUC CGU UCAACGUC
hsa-miR-770-5p	0.59	-18.7	0.7977	GAUAU UACUGGA	CUGUG AUGACCU
hsa-miR-5571-5p	0.77	-14.7	0.7959	AG CU C GAGAAUU	UC GA G CUCUUAA
hsa-miR-5007-3p	0.6	-18.6	0.7931	AGGGUUUG G CAUAUGA	UCUCAAAC C GUAUACU
hsa-miR-770-5p	0.59	-26.2	0.7919	GGC A UGUGGUACUG	CCG U GCACCAUGAC
hsa-miR-200a-3p	0.73	-20.5	0.7913	ACA UACC ACAGUGU	UGU AUGG UGUCACA
hsa-miR-5579-3p	0.74	-19.8	0.7901	GAU GGU UUUAAGCUAA	CUA CCA GAAUUCGAUU
hsa-miR-624-3p	0.72	-20.4	0.7889	CAGUACCUUGU	GUUAUGGAACA
hsa-miR-2052	0.75	-15.1	0.7887	CUG UCAAAACA	GAC AGUUUUGU
hsa-miR-7-5p	0.51	-22.1	0.7858	GAUC UUGGUCUUCCA	UUAG GAUCAGAAGGU
hsa-miR-4712-5p	0.5	-21.2	0.7849	GAU AGAGAU UACUGGA	UUA UCUCUG AUGACCU
hsa-miR-34b-3p	0.61	-14.5	0.7831	UGGU AG AGUGAUU	ACCG UC UCACUAA
hsa-miR-5195-3p	0.57	-22.8	0.7817	UCU UUAGAGA ACUGGA	GGG AGUCUCU UGACCU
hsa-miR-1265	0.71	-21.8	0.7815	AACAA GC UGAUU ACAUCCU	UUGUU UG ACUGG UGUAGGA
hsa-miR-520a-5p	0.77	-19.1	0.7815	AAG ACUU UUUCUGGA	UUC UGAA GGAGACCU
hsa-miR-2467-5p	0.71	-23.7	0.779	GC CAGG G CUA C GAGCCUCA	CG GUUC C GAU G CUCGGAGU
hsa-miR-141-3p	0.66	-19.8	0.7766	CA UACC ACAGUGU	GU AUGG UGUCACA
hsa-miR-520a-5p	0.77	-21.4	0.7707	AAAGUA CC CUCUGG	UUUCAU GG GAGACC
hsa-miR-4436b-3p	0.77	-22.2	0.7678	UACUUC UGCCCU	GUGAAG ACGGGA
hsa-miR-542-3p	0.79	-22.3	0.7669	CAGUUGU G CUGUCAU	GUCAAUA U GACAGUG
hsa-miR-3155b	0.74	-23.5	0.7664	CCACU GAGCCU	GGUGA CUCGGA
hsa-miR-330-3p	0.72	-22.9	0.7661	UUUG A GCU GUGCUUUGU	AGAC U CGG CACGAAACG
hsa-miR-15b-3p	0.58	-11.9	0.7653	GGAU UGAUUC	UUUA ACUAAG
hsa-miR-502-3p	0.71	-25.9	0.7643	GAAUUUU GC CCA GGUGCAU	CUUAGGA CG GGU CCACGUA
hsa-miR-641	0.74	-22	0.7641	GUG UUCUA UUAUGUCUUU	CAC GAGAU GAUACAGAAA
hsa-miR-330-3p	0.72	-24.4	0.7631	CUCU GG G GCUUUGC	GAGA CC C CGAAACG
hsa-miR-603	0.64	-25.6	0.7621	CAAAAGUGAU AGUGUGUG	GUUUUCAUUA UCACACAC
hsa-miR-501-3p	0.78	-24.7	0.7596	AGAAUUUU GC CC GGUGCAU	UCUUAGGA CG GG CCACGUA
hsa-miR-9-3p	0.71	-17.4	0.7551	GCU UGGUUG AGCUUUG	UGA GCCAAU UCGAAAU
hsa-miR-1271-5p	0.71	-25.9	0.7544	GGGUGUUU CU GGUGCCAA	CUCACGAA GA CCACGGUU
hsa-miR-4795-3p	0.59	-21	0.7475	CAG GUGGU UGAUAAUA	GUC CACCG AUUAUUAU
hsa-miR-4643	0.71	-20.1	0.747	GGUAUUU UCAUGUG	UCGUAAA AGUACAC
hsa-miR-4661-3p	0.71	-17.1	0.7465	GAU UCU UG GAUCCU	CUG AGA AC CUAGGA
hsa-let-7g-3p	0.49	-19.5	0.7436	GUCUGUACAG	CGGACAUGUC
hsa-miR-148a-5p	0.79	-12.6	0.7424	AGAACUU	UCUUGAA
hsa-miR-1208	0.58	-15.4	0.7352	CCU UU AACAGUG	GGA AG UUGUCAC
hsa-miR-96-5p	0.68	-21.8	0.7349	GUGU UGGUGCCAAA	CACG AUCACGGUUU
hsa-miR-15b-3p	0.58	-14.9	0.7334	AGU GUA AUGAUUC	UCG CGU UACUAAG
hsa-miR-5197-3p	0.68	-23	0.7327	U GA UGAUUCAG UCUUCU	A CU ACUGAGUC AGAAGA
hsa-miR-4460	0.66	-19.6	0.7232	AGGU UUUAU AACCACU	UCCA AAGUG UUGGUGA
hsa-miR-200a-3p	0.73	-19.8	0.7217	ACAU GUUA GA CAGUGU	UGUA CAAU CU GUCACA
hsa-miR-320c	0.8	-21.1	0.7214	GCC CUCU G AGCUUU	UGG GAGA U UCGAAA

hsa-miR-4461	0.78	-20.3	0.7203	AGC AGUCUCAA	UCG UCAGAGUU
hsa-miR-4760-3p	0.75	-14.7	0.7197	GAAC UGAAUUU	CUUG ACUUAAA
hsa-miR-641	0.74	-21.6	0.7192	GGCUUU UCC UAUGUCUU	CUGAGA AGG AUACAGAA
hsa-miR-5571-5p	0.77	-16	0.7185	GGAG CUC G AGAAUU	CCUC GAG C UCUUAA
hsa-miR-1304-5p	0.59	-21.9	0.7164	UAC CU CUG AGCCUCAA	GUG GA GAC UCGGAGUU
hsa-miR-200a-5p	0.54	-19.2	0.7154	UCC AGUG GU UG GUAAGAU	AGG UCGU CA GC CAUUCUA
hsa-miR-544a	0.66	-13.9	0.7153	CUU CUA GCAGAA	GAA GAU CGUCUU
hsa-miR-3167	0.67	-19.2	0.7139	CA CAG UGAAAUCC	GU GUC ACUUUAGG
hsa-miR-548at-3p	0.69	-12.2	0.7134	C GAG UA GGUUUU	G UUC AU CCAAAA
hsa-miR-1208	0.58	-21.4	0.7107	UCUG CC UGUU UGAACAGUG	AGGC GG ACAG ACUUGUCAC
hsa-miR-548ag	0.71	-14	0.7102	UAG G UA UUACCUU	GUC U GU AAUGGAA
hsa-miR-490-3p	0.74	-20.7	0.7075	GGC UUUCCAGGU	UCG GGAGGUCCA
hsa-miR-205-3p	0.72	-15.8	0.7064	UUUUAC UU AUUGAAAU	GAAGUG AG UGACUUUA
hsa-miR-141-5p	0.5	-19.6	0.7046	AAC UUG CUGGAAGAU	UUG GAC GACCUUCUA
hsa-miR-541-5p	0.77	-16.5	0.7046	AUCG ACAG AGA AUCCUU	UGGC UGUC UCU UAGGAA
hsa-miR-556-3p	0.46	-26.4	0.7037	AGAUGGGU UAAUGGUAAUA	UCUACUCG AUUACCAUUAU
hsa-let-7g-3p	0.49	-23.6	0.7032	GGU UG GUCUGUACAG	CCG AC CGGACAUGUC
hsa-miR-4710	0.77	-31	0.7023	GACC CC CCCUCACCC	UUGG GG GGGAGUGGG
hsa-miR-141-5p	0.5	-22.2	0.7014	UCCAG UGU UUGGAAGA	AGGUU ACA GACCUUCU
hsa-miR-4514	0.77	-20.5	0.7014	CCUA UCU UGCCUG	GGGU AGG ACGGAC
hsa-miR-106b-3p	0.74	-26.6	0.7012	CAGUAAGU AUCU CAGUGC	GUCGUUCA UGGG GUCACG
hsa-miR-21-5p	0.77	-16.9	0.7	GAUA GGUUU UAAGCUA	UUGU UCAGA AUUCGAU
hsa-miR-520a-5p	0.77	-21	0.7	AGA ACU UCUUCUGGA	UCU UGA GGGAGACCU
hsa-miR-7-5p	0.51	-21.7	0.6997	UAA GAGUC CUG UCUUCC	GUU UUUAG GAU AGAAGG
hsa-miR-4795-3p	0.59	-21.3	0.6989	CAG GUGGU UAAUAAUAU	GUC CACCG AUUAUUAUA
hsa-miR-5582-3p	0.78	-12.2	0.6985	CCU C UAAAGUUUU	GGA G AUUUCAAAA
hsa-miR-3143	0.74	-15	0.696	GAA AGAA UUAC AUGUUA	CUU UCUU AAUG UACAAU
hsa-miR-640	0.8	-23.3	0.6955	AGGU AGGU UCU GGAUCAU	UCCG UCCA AGG CCUAGUA
hsa-miR-4780	0.75	-21.6	0.6942	UUAGG GAUUA UCAAGGG	GAUCC CUAGU AGUUCCC
hsa-miR-7-5p	0.51	-19	0.694	GAUAA ACU GUCUUCU	UUGUU UGA CAGAAGG
hsa-miR-3616-3p	0.7	-21.7	0.6936	UGUG GA AAUGCCCUC	ACGU CU UUACGGGAG
hsa-miR-676-5p	0.77	-21.3	0.6934	GCA AGU CC GGUUGAAG	CGU UCA GG CCAACUUC
hsa-miR-4711-3p	0.52	-18	0.6928	UC GC GGG AGACAC	AG CG UCU UCUGUG
hsa-miR-4476	0.64	-18.8	0.6915	GU UGU U AGAU CCUUCCU	CG ACA G UUUA GGAAGGA
hsa-miR-338-5p	0.8	-11.1	0.6912	UACU G ACUA UAUUGU	GUGA U UGGU AUAACA
hsa-miR-4686	0.8	-18.2	0.6894	CC UUCAGCAGA	GG GGGUCGUCU
hsa-miR-9-3p	0.71	-15.7	0.6892	UUUUC GU UCU GCUUUAU	GAAAG CA AGA CGAAAUA
hsa-miR-4672	0.65	-21.4	0.6854	UGCUUC GU UAGU UGUGUAA	ACGGAG CA GUCG ACACAUU
hsa-miR-3064-5p	0.78	-22.7	0.6852	UGUG ACC ACAGCCA	ACGU UGG UGUCGGU
hsa-miR-103a-2-5p	0.8	-15.9	0.685	UAUUGUA AAGAAGU	GUGACAU UUCUUCG
hsa-miR-362-3p	0.73	-20.5	0.6841	UG UCC UGA UAG GUGUGU	AC AGG ACU AUC CACACA
hsa-miR-4724-5p	0.8	-22.4	0.6816	G GCUU AUUCC UGG UUCAGU	C CGAG UGAGG ACC AAGUCA
hsa-miR-16-1-3p	0.74	-13.4	0.6799	GU CGC AUACUG	CG GUG UAUGAC

hsa-miR-550b-2-5p	0.74	-22.7	0.6781	GU UUACU UC GGGCACA	CA AAUGA GG UCCGUGU
hsa-miR-641	0.74	-12.1	0.678	GAU UGUCUU	CUG ACAGAA
hsa-miR-2467-5p	0.71	-22.5	0.6778	AGUC AGGUU AAC GAGCCU	UCGG UCCGA UUG CUCGGA
hsa-miR-4461	0.78	-13.9	0.6765	UUAU GG UCUCAA	GAUG UC AGAGUU
hsa-miR-520a-5p	0.77	-19.9	0.6756	GGA G AUU UCUUCUGGA	UCU C UGA GGGAGACCU
hsa-miR-3202	0.66	-17.9	0.6754	UAAG UUUUU CCUUCC	AUUU GAGAA GGAAGG
hsa-miR-5696	0.75	-12.6	0.6721	UCAG C AAAUGA	AGUC G UUUACU
hsa-miR-4696	0.58	-15.5	0.6712	GGUA UGUCUUG	UCAU GCAGAAC
hsa-miR-4661-5p	0.76	-19.1	0.6709	CG AUCC GCAGG GCUAGU	GU UAGG UGUCU CGAUCA
hsa-miR-5590-3p	0.73	-10.9	0.6708	GUC C UGGA CUUUAU	CGG G ACUU GAAAUA
hsa-miR-4772-3p	0.59	-23.1	0.6704	CUG UUA GC AGUUGCAGG	GAC AGU CG UCAACGUCC
hsa-miR-4686	0.8	-20.4	0.6686	CAG CCU GCAGAUG	GUC GGG CGUCUAU
hsa-miR-3691-3p	0.68	-18.7	0.6649	AGA AU AC GU GGACUUGGU	UCU UA UG CG UCUGAACCA
hsa-miR-876-5p	0.68	-17.2	0.6647	UUCA CAGA GAAAUCC	AAGU GUUU CUUUAGG
hsa-miR-330-3p	0.72	-14.4	0.6641	UCU UUGUA CU UGCUUU	AGA GACGU GG ACGAAA
hsa-miR-3143	0.74	-19.4	0.6628	GAGA AAG GUUUUA AAUGUUA	CUUU UUC CGAAAU UUACAAU
hsa-miR-1243	0.66	-18.5	0.6623	CUC CUAUA UG AUCCAGUU	GAG GAUAU AC UAGGUCAA
hsa-miR-548ag	0.71	-15.3	0.6617	UACAG UACCUU	GUGUU AUGGAA
hsa-miR-5571-5p	0.77	-18.2	0.6611	GGA CUCC AGAAUU	CCU GAGG UCUUAA
hsa-miR-15b-3p	0.58	-13	0.661	AGC UGAUUC	UCG ACUAAG
hsa-miR-5007-3p	0.6	-11.7	0.6593	GU UAUAUGAU	CA GUAUACUA
hsa-miR-4696	0.58	-17.1	0.657	GGUA UGUCUUG A	UCAU GCAGAAC U
hsa-let-7a-2-3p	0.51	-21.1	0.656	GGA GG CU G AG CUGUACAG	CCU UC GA C UC GACAUGUC
hsa-miR-3155b	0.74	-20.8	0.6541	CCUAU C GAGCCU	GGGUG G CUCGGA
hsa-miR-2114-5p	0.59	-18.2	0.6525	GUUUC GA AGGGACU	CGAAG CU UCCCUGA
hsa-miR-200a-5p	0.54	-14.9	0.6518	GUACU UAAGAUG	CGUGA AUUCUAC
hsa-miR-452-5p	0.75	-21.1	0.6515	CAGU CCUUU AACAGU	GUCA GGAGA UUGUCA
hsa-miR-501-3p	0.78	-17.4	0.6514	AG AUCU CC GUGCAUU	UC UAGG GG CACGUAA
hsa-let-7f-2-3p	0.79	-11.8	0.651	GUG A UGUAUA	CAU U ACAUAU
hsa-miR-7-5p	0.51	-18.7	0.6456	CA GA GAUU AGUCUUCU	GU UU UUAG UCAGAAGG
hsa-miR-338-5p	0.8	-17.8	0.645	CGCUC GGU GCU UAUUGU	GUGAG UCG UGG AUAACA
hsa-miR-15b-3p	0.58	-14.1	0.6419	AGA GU GCGA AAUGAUUU	UCU CG CGUU UUACUAAG
hsa-miR-493-3p	0.77	-14.5	0.6417	UG A AU ACCUUC	AC U UG UGGAAG
hsa-miR-493-3p	0.77	-20.6	0.6322	CCUG GC C CA ACCUUC	GGAC CG G GU UGGAAG
hsa-miR-5197-3p	0.68	-12.5	0.6321	GAU AU U UCUUCU	CUA UG A AGAAGA
hsa-miR-330-3p	0.72	-22.3	0.6312	UUGU GGCC GCUUUGU	GACG CCGG CGAAACG
hsa-miR-4528	0.64	-21.7	0.6303	U CAGAU G AUAUAUAAUGG	A GUCUA U UGUAUAUUACU
hsa-miR-9-3p	0.71	-17.4	0.6269	AUUUU GGU AGCUUU	UGAAA CCA UCGAAA
hsa-miR-517b-3p	0.74	-24.6	0.6229	GCAC CUA AGGGAU GCACGA	UGUG GAU UCCCUA CGUGCU
hsa-miR-3148	0.8	-17.7	0.62	GAG ACACA AG U UUUUCCA	UUC UGUGU UC A AAAAGGU
hsa-miR-556-3p	0.46	-15	0.618	GGCU GGUAAUAU	UCGA CCAUUAUA
hsa-miR-34b-3p	0.61	-11.9	0.6129	AGUGAU	UCACUA
hsa-miR-5696	0.75	-14.4	0.6116	CAUC GG UGC AAAUGA	GUAG CU AUG UUUACU

hsa-miR-5186	0.77	-16.4	0.6105	CUG UUUC AC AAUCUC	GAC AAAG UG UUAGAG
hsa-miR-5590-3p	0.73	-13.6	0.61	UUGUU GUAC GCUUUAU	AACGG UAUG UGAAAUA
hsa-miR-15b-3p	0.58	-18	0.609	GGC GC GUGAUUC	UCG CG UACUAAG
hsa-miR-505-3p	0.76	-22	0.6076	GGAG AUCAGUG UGUUGAU	CCUU UGGUCGU ACAACUG
hsa-miR-141-3p	0.66	-18.4	0.6061	UCU ACCA GA CAGUGU	AGA UGGU CU GUCACA
hsa-miR-16-1-3p	0.74	-12.8	0.6059	GC A AAUACU	CG U UUAUGA
hsa-miR-4795-3p	0.59	-9.4	0.6059	AUUCA AGU UU GAUAAUA	UAGGU UCA GA UUAUUAU
hsa-miR-490-3p	0.74	-22.2	0.6049	CAGCA GA UC CCAGGU	GUCGU CU GG GGUCCA
hsa-miR-660-5p	0.72	-21.1	0.6042	CC UGCA AUGGGUG	GG ACGU UACCCAU
hsa-miR-136-3p	0.64	-19.8	0.6034	GCUU UUGA GAUGAUG	UGAG AACU CUACUAC
hsa-miR-2467-5p	0.71	-25.3	0.6009	GGUC AAG CUG ACAG AGCCUCA	UCGG UUC GAU UGUC UCGGAGU
hsa-miR-181a-2-3p	0.8	-14.2	0.6002	AGC UCAGUG	UUG AGUCAC
hsa-miR-544a	0.66	-17.4	0.6001	ACUUG CUG UGCAGA	UGAAC GAU ACGUCU
hsa-miR-526b-5p	0.69	-20.7	0.5993	GGAG AGUGCUUU U CUCAAGA	UCUU UCACGAAG G GAGUUCU
hsa-miR-517c-3p	0.73	-21.9	0.5965	GCAC CUA AGGGAU GCACGA	UGUG GAU UUCCUA CGUGCU
hsa-miR-556-3p	0.46	-13.7	0.5962	AGUUG GGUAAU	UCGAU CCAUUA
hsa-miR-26a-2-3p	0.8	-22.8	0.5935	GAAAUA UAAU GGAAUAGG	CUUUGU AUUA UCUUAUCC
hsa-miR-3117-5p	0.8	-21.8	0.5894	AUAU A UCGU UAGUGUCU	UAUA U AGCA AUCACAGA
hsa-miR-3913-3p	0.75	-18.7	0.5861	UGG GC GAU UGAUGUUU	ACC UG CUA ACUACAGA
hsa-miR-103a-3p	0.75	-24.7	0.5851	GCCC C AUGCUGCU	CGGG G UACGACGA
hsa-miR-3148	0.8	-14.4	0.5851	GAG UAUA UACUGG UUUUUUCUA	UUC GUGU GUGGUC AAAAAAGGU
hsa-miR-205-3p	0.72	-15.7	0.5819	AUUUC UC UGAAAUC	UGAAG AG ACUUUAG
hsa-miR-141-3p	0.66	-21.2	0.5813	GUCU GCUAG UAGUGUU	UAGA UGGUC GUCACAA
hsa-miR-421	0.56	-19.7	0.5804	GC UCAGU UUUGUUGAU	CG GGUUA AGACAACUA
hsa-miR-493-3p	0.77	-19.4	0.5804	CC GUGCAU ACCUUCA	GG CGUGUG UGGAAGU
hsa-miR-3120-3p	0.74	-25.8	0.5788	GCCU GU CUGCAC UGCUGU	CGGA CA GAUGUG ACGACA
hsa-miR-3117-5p	0.8	-15.3	0.5777	GCU GUAGUGUU	UGA UAUCACAG
hsa-miR-802	0.73	-17	0.5763	AUAAGG CU UGUUACU	UGUUCC GA ACAAUGA
hsa-miR-3155b	0.74	-17.8	0.5761	UCUC CUGU A AGCCUG	AGGG GACG U UCGGAC
hsa-miR-567	0.71	-22.2	0.5759	CUG UUCUGG G AACAUACU	GAC AGGACC C UUGUAUGA
hsa-miR-4519	0.8	-16.3	0.5757	AG UG G ACUGCU	UC AC C UGACGA
hsa-miR-200a-3p	0.73	-21	0.5747	UUGU UGCUAG UAGUGUU	AGCA AUGGUC GUCACAA
hsa-miR-5197-5p	0.77	-19.6	0.5714	UCAAGG GUGA GCCAUU	AGUUCU UACU CGGUAA
hsa-miR-5591-3p	0.54	-13.8	0.571	UGGGUA	ACCCAU
hsa-miR-26a-2-3p	0.8	-17	0.5705	AGAU GUGAU AGAAUAG	UUUG CAUUA UCUUAUC
hsa-miR-544a	0.66	-16.9	0.5673	GUUAAAGG UGCAGA	CGAUUUUU ACGUCU
hsa-miR-676-5p	0.77	-15.5	0.5637	UGU UUCUGG GG UUGAAG	ACG AGGACU CC AACUUC
hsa-miR-641	0.74	-11.1	0.563	UUUUA UA UGUCUU	GAGAU AU ACAGAA
hsa-miR-4704-5p	0.77	-20.3	0.5606	CA UUGCA UGCU UAGUGUU	GU AGUGU ACGG AUCACAG
hsa-miR-1243	0.66	-15.4	0.5601	CAC UUAU UCCAGU	GUG GAUA AGGUCA
hsa-miR-29a-3p	0.8	-16.6	0.5589	AAC CA UGGUGC	UUG GU ACCACG
hsa-miR-520a-5p	0.77	-20.9	0.5565	AGA GGUGC UCUGGA	UCU UCAUG AGACCU

hsa-miR-3202	0.66	-18.1	0.5537	CUU CU CCCUUCUA	GAG GA GGGAAGGU
hsa-miR-3143	0.74	-16.3	0.5509	GGG GGAGC UUUUA AAUGUU	CUU CUUCG GAAAU UUACAA
hsa-miR-4772-3p	0.59	-21.6	0.5498	CUGA C G GCA AGUUGCAG	GACU G C CGU UCAACGUC
hsa-miR-493-3p	0.77	-19.9	0.5498	CCU GGC GU GACCUU	GGA CCG CA CUGGAA
hsa-miR-141-3p	0.66	-17.9	0.5495	AUUUU ACC G CAGUGUU	UAGAA UGG C GUCACAA
hsa-miR-3148	0.8	-11.3	0.5495	UUUUUCC	AAAAAGG
hsa-miR-556-3p	0.46	-15.2	0.5491	UGAGC GA GGUAAU	ACUCG UU CCAUUA
hsa-miR-4764-5p	0.8	-18.3	0.5467	UGAUUC ACAUCC	AUUGAG UGUAGG
hsa-miR-4776-5p	0.73	-24.5	0.5457	AGCU UGCU G UUCUGG	UCGG ACGG U AGGACC
hsa-miR-362-3p	0.73	-17	0.5379	UG UCC UGA GUGUGU	AC AGG ACU CACACA
hsa-miR-3148	0.8	-14.9	0.5364	G AU A UCAGU UUUUUCU	C UG U GGUCA AAAAAGG
hsa-miR-148a-5p	0.79	-18.3	0.5318	GG UUGGAGU G CUU GGAACUU	UC AGCCUCA C GAG UCUUGAA
hsa-miR-1304-5p	0.59	-16.7	0.5311	UAC UC CA UG CCUCAAG	GUG AG GU AC GGAGUUU
hsa-miR-200a-3p	0.73	-15.8	0.5295	AUU ACC G CAGUGUU	UAG UGG C GUCACAA
hsa-miR-5000-3p	0.79	-17.7	0.5295	UCUAA GUUU AAGU GUCCUG	AGGUU CAAG UUCA CAGGAC
hsa-miR-4686	0.8	-24.7	0.5286	AAUAUCAG AAGGU CCA GCAGAUA	UUGUGGUC UUUCG GGU CGUCUAU
hsa-miR-3913-3p	0.75	-16.5	0.5284	UGG GC GAU UGAUGU	ACC UG CUA ACUACA
hsa-miR-320c	0.8	-14.4	0.5283	U UCUU AUUU AGCUUUU	G AGAG UGGG UCGAAAA
hsa-miR-493-3p	0.77	-20.3	0.5282	CCU GGC GU GACCUU CA	GGA CCG CA CUGGAA GU
hsa-miR-4761-3p	0.69	-25	0.5262	GGAUAA AUGCCCUC	CCUGUU UACGGGAG
hsa-miR-3148	0.8	-14.6	0.5259	GU AU ACU AG UUUUUUCU	CG UG UGG UC AAAAAAGG
hsa-miR-5591-3p	0.54	-17.2	0.5248	GUU GC AUGGGUG	CGA CG UACCCAU
hsa-miR-665	0.75	-22.7	0.5213	AGGG CUU UUUCCUGG	UCCC GAG GGAGGACC
hsa-miR-4999-3p	0.8	-17.2	0.5186	GC GUA UUGUC GUAGUG	UG CAU AACAG CAUCAC
hsa-miR-3148	0.8	-18.9	0.5177	AGCACA CAU UAG UUUUUCC	UCGUGU GUG GUC AAAAAGG
hsa-miR-24-3p	0.63	-22.1	0.5162	CUGC GAG CUGAGCC	GACG CUU GACUCGG
hsa-miR-3689f	0.78	-13.8	0.516	CC GG G AUAUCA	GG CC C UAUAGU
hsa-miR-5187-3p	0.65	-11.1	0.5146	AAG GAUUCA	UUC CUAAGU
hsa-miR-502-3p	0.71	-18.7	0.5056	GAUC GUC CAG GUGCAUU	UUAG CGG GUC CACGUAA
hsa-miR-4721	0.6	-24.8	0.5016	UCGCUG UACUU GGA GCCCUC	GGUGGC GUGGA CCU CGGGAG
hsa-miR-5094	0.79	-18.7	0.5012	AGGUU CA GGU ACUGAU	UCCAA GU CCG UGACUA
hsa-miR-548ag	0.71	-18	0.5008	CAGAA AC ACAGU UACCUUU	GUCUU UG UGUUA AUGGAAA
hsa-miR-7-5p	0.51	-14.9	0.3993	CA UC CU UCUUCC	GU AG GA AGAAGG

Table 4.6. Analysis of downregulatory miR binding seed sites in OGA 3'UTR regions

miRNA	Ratio	dG_hybrid	LogitProb	TargetMatch	MirMatch
hsa-miR-582-5p	0.71	-18.3	0.9035	UCA GAC CUU UUGACAUU	UU CAA G
hsa-miR-582-3p	0.72	-19.4	0.8837	AAGUUGGUCAAU	CCAAGUCAAC
hsa-miR-130b-5p	0.8	-21.4	0.8768	CAU ACGUUGU CUUUCUC	C CC A
hsa-miR-3125	0.78	-19	0.8615	A AGGUG CG AAGGAGAU	AG G U

hsa-miR-4729	0.63	-16.1	0.8513	GAAGGG UAUUUACU	AUC UUGUC
hsa-miR-5582-3p	0.8	-18.5	0.8314	GAUCC GU GAAUUUCAAAAU	G GU
hsa-miR-628-5p	0.61	-22.4	0.8291	GGAG AUUUAUA CAGUCGU	AUC A
hsa-miR-595	0.62	-22	0.8276	UGU UGC CGUGUGAAG	UCUG GG
hsa-miR-5696	0.76	-12	0.8239	AG GAU AUUUACU	CCGU UCU GA C
hsa-miR-539-3p	0.77	-19.4	0.7979	UUUCUU UAAC AGG ACAUACU	A A
hsa-miR-27a-3p	0.63	-22.6	0.7941	GCC UCG UGACACUU	C UUGAA G
hsa-miR-802	0.8	-15	0.7853	UCC AC UUAGA ACAAUGA	UGU U A C
hsa-miR-520d-5p	0.56	-10.7	0.7702	A GGAAACAU	CUUUCCCGA G C
hsa-miR-524-5p	0.56	-10.7	0.7702	A GGAAACAU	CUCUUUCACGA G C
hsa-miR-520d-5p	0.56	-14.6	0.7699	AGGGAAACAU	CUUUCCCGA C
hsa-miR-3973	0.72	-29.4	0.7652	UCCG UACGACAUGAAACA	GAU AU
hsa-miR-27b-3p	0.7	-21.6	0.7571	CG CU GA UCG UGACACUU	U U A G
hsa-miR-4709-3p	0.68	-21.1	0.7532	AUGUCUC AGAAGUU	CG GUGGAGG
hsa-miR-524-5p	0.56	-15.1	0.7483	ACG AGGGAAACAU	CUCUUUC A C
hsa-miR-4735-3p	0.66	-20.7	0.7466	CAGA CGUGGAA	UA UUAAACU A
hsa-miR-3613-3p	0.77	-21.1	0.7409	UUC ACCCGAA AAAAAC	C CCA AAA A
hsa-miR-519c-5p	0.77	-21.7	0.7377	GUC UUUCG GAAG GGAGAUCU	C C
hsa-miR-523-5p	0.78	-21.7	0.7377	GUC UUUCG GAAG GGAGAUCU	C C
hsa-miR-4432	0.59	-18.8	0.7358	GUAG GUCUCAGAAA	UCC AAC
hsa-miR-548aq-5p	0.68	-22.3	0.7333	UUUUU CGUUAAUGAA	CCG GU AG
hsa-miR-3613-3p	0.77	-24.2	0.7306	CCCAA CCC AA AAAAACA	CUU G AAA
hsa-miR-548am-5p	0.78	-22	0.7285	UUUUU GCGUUAAUGAA	CCG G AA
hsa-miR-520h	0.74	-15.2	0.7271	UGAG GUGAAAC	AUUUCCCUUC A
hsa-miR-4474-5p	0.61	-11.4	0.719	C UCUGAU	ACACAGACUAGUA U
hsa-miR-3133	0.75	-10.6	0.7089	ACC AA AAGAAAU	UA C AAUUCUC
hsa-miR-548ao-3p	0.61	-24.6	0.6996	ACGUUU UCAUCAGU CCAGAA	G A
hsa-miR-4696	0.77	-18.7	0.6956	GUC UAGG AGAACGU	UCUACU A C
hsa-miR-485-3p	0.79	-16.6	0.6952	CUCU CC UCU CG ACAUA	U GC
hsa-miR-3973	0.72	-10.8	0.6855	UGAAAC	GAUUCCGAUUACGACA A
hsa-miR-4668-3p	0.71	-17.8	0.6839	UU UUUUU CCUAAAAG	GACCUU UG
hsa-miR-520d-5p	0.56	-19.9	0.6756	UCCCG GGGAAACAU	CUU AA C
hsa-miR-520d-5p	0.56	-16	0.6754	GA GGGAAACAU	CUUUCCC A C
hsa-miR-5191	0.71	-18.7	0.6708	UCG A GA GAUAGGA	UG AGUAA AG
hsa-miR-3133	0.75	-21.9	0.6689	AACCCAAA UUC CAAGAAA	U A U U
hsa-miR-524-5p	0.56	-17.4	0.6669	AC GA GGGAAACAU	CUCUUUC A C
hsa-miR-515-3p	0.78	-23.1	0.6599	GC AGGUUUU CCGUGAG	UU G CUU
hsa-miR-5003-3p	0.62	-20.1	0.6583	GGGUUG UUGGAU CUUUUCAU	G
hsa-miR-4432	0.59	-19.7	0.6563	UCCG C UCUCAGAA	UAGAA G A
hsa-miR-155-3p	0.76	-18.2	0.6518	C GAUUA ACAUCCU	ACAAUUA U C
hsa-miR-640	0.78	-18.4	0.6503	UCCG CC A GGACCUAGU	UC U A A
hsa-miR-3613-3p	0.77	-7.5	0.6468	CGAAAA AAAAAA	CUUCCCAACC CA

hsa-miR-524-5p	0.56	-18.4	0.6465	ACGA GAAACAUC	CUCUUUC AGG
hsa-miR-3613-3p	0.77	-13.1	0.6373	AAC CGAA AAAAACA	CUUCCC C AAA
hsa-miR-18b-5p	0.78	-22.2	0.6366	UUGACG GA ACGUGGAAU	GA U UCU
hsa-miR-625-3p	0.79	-17.7	0.6365	CC CUUUC AUAUCA	ACU CC AAG G
hsa-miR-4709-3p	0.68	-18.8	0.6312	UG CGUGGAG G AGAAGU	CGA UCU U
hsa-miR-324-3p	0.74	-26.8	0.6254	UCG C UGGACCCCGUCA	GG U G
hsa-miR-3919	0.8	-19.5	0.6205	UGACU CAG AAC AAGAGACG	GA
hsa-miR-524-5p	0.56	-19.4	0.6174	CUC UCA AAGG GAAACAU	UU CG C
hsa-miR-4432	0.59	-21.7	0.6172	UCCG GAA CUCAGAA	UA CGU A
hsa-miR-548y	0.78	-14.6	0.6142	CG UUUU UCAC UAAUGAA	C U G AA
hsa-miR-5003-3p	0.62	-17.9	0.6132	GG UU UUGG CUUUUCAU	GG G AU
hsa-miR-1244	0.77	-24.2	0.6127	UAGAGU UUUGG UGAUGA	UUGG AUG U A
hsa-miR-4696	0.77	-23.3	0.6107	CUA UGUCAUAGG AGAACG	U C C U
hsa-miR-548av-5p	0.71	-16.5	0.6085	AG CGU CAUGAAA	UUU G U A
hsa-miR-548av-5p	0.71	-10.7	0.6066	UUUAGG G AUGAAAA	C UUC
hsa-miR-520h	0.74	-14.8	0.6043	GAGAUUU C UUC GUGAAA	U C C CA
hsa-miR-520d-5p	0.56	-18.1	0.6042	UCC CGA GAAACAUC	CUU AGG
hsa-miR-520h	0.74	-26	0.6037	GAGAU UUCCC UCGUGAAAC	U U A
hsa-miR-3133	0.75	-9.5	0.6028	AAGAAAU	UAACCCAAAAUUCUC
hsa-miR-4474-5p	0.61	-17.3	0.6028	UAGU ACUCUGAU	ACACAGAC U
hsa-miR-4432	0.59	-14.6	0.5991	CCG AAC UC UCAGAA	U UAG G A
hsa-miR-548y	0.78	-19.8	0.5988	CCGU UUU GUCACU AAUGAAAA	U
hsa-miR-4659b-5p	0.71	-27.4	0.5987	AGAA UCUGUACCGUU	A GAA
hsa-miR-4696	0.77	-25.9	0.5964	UCUAC UC AGG CAGAACG	UG AU U
hsa-miR-3119	0.8	-16.1	0.5916	GUAG CA UUUUCGG	CG UUU A U
hsa-miR-550a-3p	0.75	-21.8	0.5878	AC CGGACU CCC U CAUUCUGU	U A
hsa-miR-130b-5p	0.8	-10.3	0.5867	UUUCUC	CAUCACGUUGUCCC A
hsa-miR-3613-3p	0.77	-8.2	0.5861	AAAAAC	CUUCCCAACCCGAAAAA A
hsa-miR-595	0.62	-22.1	0.5855	GUG GGUG GUGUGAAG	UCU U CC
hsa-miR-2355-3p	0.66	-24.8	0.5852	AGGUUUGU CGUUCCUGUU	UAG A
hsa-miR-3973	0.72	-17.2	0.5829	UUCC UACGAC UGAAAC	GA GAU A A
hsa-miR-548aq-5p	0.68	-17	0.5713	CCGU UUU GUCGUU AAUGAAAG	U
hsa-miR-4531	0.76	-21.2	0.5698	AGU CU UCGG AAGAGGUA	
hsa-miR-3681-3p	0.74	-19.2	0.567	AUC ACC ACU UCG UGACAC	UC U A
hsa-miR-3119	0.8	-15.5	0.5571	CGG AG CA UUUCGGU	U UUU AU
hsa-miR-548am-5p	0.78	-16.3	0.5555	CCGU UUUGG CGUU AAUGAAAA	U
hsa-miR-105-5p	0.69	-20.8	0.5549	UGG UCCU AC CGUAAAC	UG CAG U U
hsa-miR-628-5p	0.61	-23.4	0.5542	GGAGAUC UUUA CAGUCGUA	A UA
hsa-miR-449c-3p	0.78	-14.6	0.5536	ACGU UGAUCG	UGUCUCUCCUC UU
hsa-miR-4301	0.67	-26.9	0.5479	AGU UUCACUUCA UCACCCU	G
hsa-miR-4668-3p	0.71	-8.8	0.5447	GAC U UG CUAAAA	CU UU UUUUUC G
hsa-miR-4729	0.63	-16.6	0.5437	UCGAA UGUC UAUUUAC	A GGGU U

hsa-miR-676-3p	0.68	-21.1	0.5426	GUU UUGGA AUCCUG	UUGA G UC
hsa-miR-802	0.8	-14.7	0.5406	UCCU UUAGA CAAUGA	UGU AC AA C
hsa-miR-4659b-5p	0.71	-15.8	0.5382	AAG UCU UACCGU	AAG AA G U
hsa-miR-548an	0.72	-18.3	0.538	UUGGU CGGAAA	GUUU GUUA A
hsa-miR-5582-3p	0.8	-16	0.5243	UCCGU UGAA UUCAAAA	GGA G U U
hsa-miR-3973	0.72	-18.3	0.5205	CG CGACA UGAAAC	GAUUC AUUA A
hsa-miR-1243	0.75	-18.1	0.5119	UG GAUA AC UAGGUCA	G AG UUA A
hsa-miR-548aq-5p	0.68	-17.5	0.5095	CCG UUUGU CG AUGAAA	UU UUA G
hsa-miR-365b-3p	0.78	-20.3	0.508	UCCUA AAU CCGUAAU	UAU AA CC
hsa-miR-4420	0.71	-17	0.5056	AGUC UGU CU UA GUCACU	G GA G G
hsa-miR-5582-3p	0.8	-13.2	0.5014	UCC GAAU UUCAAA	GGA GUGU AU

Table 4.7. Analysis of downregulatory miR binding seed sites in OGA 3+5'UTR regions

miRNA	Ratio	dG_hybrid	LogitProb	TargetMatch	MirMatch
hsa-miR-421	0.75	-24.4	0.8846	CGGGUUAA AC AGACAACU	CG UU A
hsa-miR-582-3p	0.71	-19.4	0.8837	AAGUUGGUCAAU	CCAAGUCAAC
hsa-miR-5696	0.78	-12	0.8239	AG GAU AUUUACU	CCGU UCU GA C
hsa-miR-199a-3p	0.58	-19.2	0.8114	UUGG ACG UGAUGAC	A UUAC UC A
hsa-miR-1305	0.67	-14.9	0.795	GGGU AUCU CAACUUUU	AGAGA A
hsa-miR-27a-3p	0.75	-22.6	0.7941	GCC UCG UGACACUU	C UUGAA G
hsa-miR-3973	0.69	-29.4	0.7652	UCCG UACGACAUGAAACA	GAU AU
hsa-miR-4423-5p	0.73	-17.2	0.7605	GUAC UUUUCCGUU	C CCUUGU GA
hsa-miR-4709-3p	0.77	-21.1	0.7532	AUGUCUC AGAAGUU	CG GUGGAGG
hsa-miR-4735-3p	0.73	-20.7	0.7466	CAGA CGUGGAA	UA UUAAACU A
hsa-miR-3613-3p	0.73	-21.1	0.7409	UUC ACCCGAA AAAAAC	C CCA AAA A
hsa-miR-548ai	0.76	-16.7	0.7372	GUUAAUGGAAA	CCCUUUUUGAC
hsa-miR-4432	0.57	-18.8	0.7358	GUAG GUCUCAGAAA	UCC AAC
hsa-miR-548ar-5p	0.69	-22.7	0.7355	UUUUU ACGUUAAUGAA	CG G AA
hsa-miR-548ar-5p	0.69	-16.1	0.7332	CGUUUUU AC U AAUGAAAA	G G U
hsa-miR-3613-3p	0.73	-24.2	0.7306	CCCAA CCC AA AAAAACA	CUU G AAA
hsa-miR-574-5p	0.77	-25.1	0.7299	UGAGUG GUG GUGUGAG	UGUG U U U
hsa-miR-548a-5p	0.67	-14.5	0.7136	CAUUUU CGUU AAUGAAAA	C GAG
hsa-miR-541-5p	0.8	-19.3	0.7019	UC AC UGG CUG UAGGAAA	CC UCGUCU
hsa-miR-548d-5p	0.68	-19.4	0.6986	UUUUU GUGUUAAUGAA	CCG G AA
hsa-miR-3973	0.69	-10.8	0.6855	UGAAAC	GAUUCCGAUUACGACA A
hsa-miR-4511	0.74	-21.1	0.6672	UCCCG ACG CAAGAAG	UUU UUGU
hsa-miR-130a-5p	0.74	-17.8	0.6659	UGU AUC GU UACACUU	CGUC C GU
hsa-miR-5087	0.74	-21.1	0.6659	UACG UCG UUUCG UGUUUGGG	G G A
hsa-miR-5003-3p	0.79	-20.1	0.6583	GGGUUG UUGGAU CUUUUCAU	G
hsa-miR-4432	0.57	-19.7	0.6563	UCCG C UCUCAGAA	UAGAA G A
hsa-miR-93-3p	0.79	-18.6	0.6557	GAUC AGUCGU	GCCCUUCAC G CA

hsa-miR-3613-3p	0.73	-7.5	0.6468	CGAAAA AAAAAA	CUUCCCAACC CA
hsa-miR-192-5p	0.61	-20.2	0.642	AGUUA AUCCAGUC	CCGAC AGU
hsa-miR-548k	0.8	-14	0.6383	UCGUUUU GC U AUGAAAA	AG G UC
hsa-miR-3613-3p	0.73	-13.1	0.6373	AAC CGAA AAAAACA	CUUCCC C AAA
hsa-miR-18b-5p	0.66	-22.2	0.6366	UUGACG GA ACGUGGAAU	GA U UCU
hsa-miR-625-3p	0.75	-17.7	0.6365	CC CUUUC AUAUCA	ACU CC AAG G
hsa-miR-4709-3p	0.77	-18.8	0.6312	UG CGUGGAG G AGAAGU	CGA UCU U
hsa-miR-548a-5p	0.67	-22.4	0.6297	CAUUUUGA GCGUUAAUGAA	C AA
hsa-miR-101-3p	0.8	-13.1	0.6289	AG AAUA G AUGACA	A UC GU UC U
hsa-miR-5087	0.74	-17.8	0.627	UACG UCG UUUCG UGUUUG	G G A GG
hsa-miR-324-3p	0.72	-26.8	0.6254	UCG C UGGACCCCGUCA	GG U G
hsa-miR-548ar-3p	0.74	-11.3	0.6238	GAC UCAAAAU	CGUUUUUAUU G
hsa-miR-4659a-5p	0.78	-29.2	0.6188	AGAA UCUGUACCGUC	CAAA GAA
hsa-miR-499a-5p	0.79	-15.2	0.6173	GUGAC UUCAGAA	UUUGUA G UU
hsa-miR-4432	0.57	-21.7	0.6172	UCCG GAA CUCAGAA	UA CGU A
hsa-miR-5003-3p	0.79	-17.9	0.6132	GG UU UUGG CUUUUCAU	GG G AU
hsa-miR-371b-5p	0.66	-20.2	0.6005	UUUC ACG C G AG AAAACUCA	G G U
hsa-miR-4432	0.57	-14.6	0.5991	CCG AAC UC UCAGAA	U UAG G A
hsa-miR-4659b-5p	0.71	-27.4	0.5987	AGAA UCUGUACCGUU	A GAA
hsa-miR-542-3p	0.7	-20.8	0.5912	UCA UAGU UAGACAGUG	AAAG A U
hsa-miR-93-3p	0.79	-19.1	0.5887	GAUC AGUCGU CA	GCCCUUCAC G
hsa-miR-3613-3p	0.73	-8.2	0.5861	AAAAAC	CUUCCCAACCCGAAAAA A
hsa-miR-3973	0.69	-17.2	0.5829	UUCC UACGAC UGAAAC	GA GAU A A
hsa-miR-548k	0.8	-17.1	0.5723	CG AG CGU CAUGAAA	U UUUU G U A
hsa-miR-4509	0.73	-19.3	0.5671	UGGAAGA AGGAAAU	UUU UAU CA
hsa-miR-548d-5p	0.68	-16.3	0.5555	CCGU UUUGGU U AAUGAAAA	U GU
hsa-miR-2114-5p	0.66	-25.8	0.5512	CUG AGU UCCU UCCCUGAU	GCGA
hsa-miR-4641	0.8	-21.6	0.5501	UCCG UUC GUACCCG	AC UU AUACC U
hsa-miR-484	0.68	-25.1	0.5499	CCCC UG CUCGGA	UAGCCCU A CU
hsa-miR-371b-5p	0.66	-15.5	0.5485	UUC C CGG AG AAAACU	U A GG U CA
hsa-miR-93-3p	0.79	-21.2	0.545	CCCU UC CG AUC AGUCGU	G A G CA
hsa-miR-676-3p	0.59	-21.1	0.5426	GUU UUGGA AUCCUG	UUGA G UC
hsa-miR-4777-5p	0.78	-16.9	0.5421	UAU UAGAG AGU AGAUCUU	A AUA
hsa-miR-125a-5p	0.75	-31.6	0.5412	A GUCCA UCCC GAGUCCCU	GU AUU A
hsa-miR-4659b-5p	0.71	-15.8	0.5382	AAG UCU UACCGU	AAG AA G U
hsa-miR-548an	0.75	-18.3	0.538	UUGGU CGGAAA	GUUU GUUA A
hsa-miR-4659a-5p	0.78	-15.7	0.5366	AAG UCU UACCGU	CAAAAG AA G C
hsa-miR-154-3p	0.8	-17.2	0.5221	UAUC GUUG ACAUACU	U CA GC AA
hsa-miR-3973	0.69	-18.3	0.5205	CG CGACA UGAAAC	GAUUC AUUA A
hsa-miR-199a-3p	0.58	-17	0.5161	GGU AC UCUGAUGA	AUU UAC G CA
hsa-miR-499a-5p	0.79	-15.1	0.5119	ACG UCAGAAUU	UUUGUAGUG U
hsa-miR-365a-3p	0.79	-20.3	0.508	UCCUA AAU CCGUAAU	UAU AA CC
hsa-miR-4420	0.77	-17	0.5056	AGUC UGU CU UA GUCACU	G GA G G

hsa-miR-4999-3p	0.72	-17.7	0.5045	UGAC AACA U CCAUCA	AU G CU

Table 4.8. Analysis of upregulatory miR binding seed sites in OGA 3' UTR regions

miRNA	Ratio	dG_hybrid	LogitProb	TargetMatch	MirMatch
hsa-miR-4778-3p	1.43	-20.5	0.8208	U ACUCUGC AAGAAG	A UGAGACG UUCUUC
hsa-miR-551b-3p	1.84	-21.5	0.8063	UGGGAUC GGGUCG	ACUUUGG CCCAGC
hsa-miR-2115-5p	1.5	-22.2	0.795	CAGG GUC UGGAAG	GUCC CAG ACCUUC
hsa-miR-513c-5p	1.44	-20	0.7474	GUA AUGAU UCU CUUGAGA	UAU UGCUG GGA GAACUCU
hsa-miR-4747-5p	1.38	-21.3	0.7466	G UAAG CCUUCCUU	C GUUC GGAAGGGA
hsa-miR-2115-5p	1.5	-22.7	0.7226	CAGG GUC UGGAAG CU	GUCC CAG ACCUUC GA
hsa-miR-4693-5p	1.41	-20.2	0.7199	UGA CAGU UCACAGU	ACU GUCA AGUGUCA
hsa-miR-520c-3p	2.05	-17.1	0.7155	UCUC GCACUU	GGAG CGUGAA
hsa-miR-148b-3p	1.54	-16.1	0.7023	GA UGCACUG	CU ACGUGAC
hsa-miR-130b-3p	1.64	-18.6	0.6931	AUGU U UCG UAU UGCACU	UACG A AGU GUA ACGUGA
hsa-miR-4747-5p	1.38	-18.1	0.6912	UAAGAUU UUU CCUUCC	AUUCUGG GGA GGAAGG
hsa-miR-2115-5p	1.5	-13.5	0.6822	UC UGGAAG	AG ACCUUC
hsa-miR-29b-2-5p	1.44	-14.2	0.677	UAGGUU UUAU AAACCA	AUUCGG GGUA UUUGGU
hsa-miR-4325	1.37	-16.7	0.6168	UCAC G AU AGUGCA	AGUG C UG UCACGU
hsa-miR-513c-5p	1.44	-17.5	0.5967	GAC CCUC CUUGAG	CUG GGAG GAACUC
hsa-miR-513c-5p	1.44	-15	0.5961	ACC CUUGAG	UGG GAACUC
hsa-miR-148a-3p	1.63	-16.5	0.5706	AUA GUUUUGU A UGCACU	UGU CAAGACA U ACGUGA
hsa-miR-4693-5p	1.41	-17	0.5704	GUGAU AAG CACAGU	CACUG UUU GUGUCA
hsa-miR-148b-3p	1.54	-16.4	0.5693	AUA GUUUUGU UGCACU	UGU CAAGACA ACGUGA
hsa-miR-765	1.77	-18.2	0.5673	UAC UU CUU UCCUCC	GUG AA GAA AGGAGG
hsa-miR-130b-3p	1.64	-20.3	0.5648	GCCU UA CG UGCACUG	CGGG GU GU ACGUGAC
hsa-miR-148a-3p	1.63	-18.7	0.5367	GAAG UCUGU AG UGCACUG	UUUC AGACA UC ACGUGAC
hsa-miR-4739	1.37	-27.2	0.5102	GGUCU G UCU UCUCCCUU	CCGGG C AGG GGAGGGAA

Table 4.9. Analysis of upregulatory miR binding seed sites in OGT 3+5' UTR regions

miRNA	Ratio	dG_hybrid	LogitProb	TargetMatch	MirMatch
hsa-miR-519c-3p	1.35	-18	0.8264	UCUC UGCACUU	GGAG ACGUGAA
hsa-miR-302a-3p	1.45	-19.2	0.759	UCGCUA AC GCACUUA	AGUGGU UG CGUGAAU
hsa-miR-449b-5p	1.37	-28.8	0.756	UCAGU UAGCGA UGCACUGCU	GGUCG AUUGUU AUGUGACGG
hsa-miR-302b-3p	1.95	-16.6	0.751	GCUA AC GCACUUA	UGAU UG CGUGAAU
hsa-miR-148b-3p	1.63	-16.1	0.7023	GA UGCACUG	CU ACGUGAC
hsa-miR-1306-3p	1.39	-19.4	0.6387	GCU CA AGCCAAC	UGG GU UCGGUUG
hsa-miR-1207-3p	1.45	-18.6	0.6232	UGAGG GU CAGCUGA	ACUCC CG GUCGACU
hsa-miR-513a-5p	1.36	-20.4	0.61	AUG C CCUC CUGUGA	UAC G GGAG GACACU
hsa-miR-5700	1.61	-17.4	0.6	UCAGUAA UUA GUGCAUUA	AGUUAUU AAU UACGUAAU

hsa-miR-148a-3p	1.48	-16.5	0.5706	AUA GUUUUGU A UGCACU	UGU CAAGACA U ACGUGA
hsa-miR-148b-3p	1.63	-16.4	0.5693	AUA GUUUUGU UGCACU	UGU CAAGACA ACGUGA
hsa-miR-765	1.75	-18.2	0.5673	UAC UU CUU UCCUCC	GUG AA GAA AGGAGG
hsa-miR-449b-5p	1.37	-24.9	0.5582	CCAGU AC U ACUGCC	GGUCG UG A UGACGG
hsa-miR-148a-3p	1.48	-18.7	0.5367	GAAG UCUGU AG UGCACUG	UUUC AGACA UC ACGUGAC
hsa-miR-4739	1.38	-27.2	0.5102	GGUCU G UCU UCUCCCUU	CCGGG C AGG GGAGGGAA
hsa-miR-519c-3p	1.35	-18.2	0.5056	CCUC UAG GA UGCACU	GGAG AUU CU ACGUGA
hsa-miR-30c-2-3p	1.44	-22.7	0.5045	GG UGGA GGUCU UCUCCC	UC AUUU UCGGA AGAGGG

Table 4.10. Analysis of upregulatory miR binding seed sites in OGT 3' UTR regions

miRNA	Ratio	Seed_Type	dG_hybrid	LogitProb	TargetMatch	MirMatch
hsa-miR-1185-1-3p	1.65	6mer	-18.2	0.6433	CA AGGGGGACAUAUA	UAUUCU G
hsa-miR-19a-5p	1.52	offset-6mer	-18.3	0.6296	CACGU GAUA CGUUUU	ACAU U GA
hsa-miR-19a-5p	1.52	offset-6mer	-17.9	0.7993	ACGUU U CGUUUUG	ACAUC GA A A
hsa-miR-3122	1.83	offset-6mer	-23.3	0.6884	UUCUGGC GG CAGGGU	A AGAA UG
hsa-miR-3925-5p	1.43	6mer	-17.3	0.5274	UC AGG AA AG AAGAGA	CG UG UC A
hsa-miR-4470	2.69	offset-6mer	-17.5	0.5439	GAG CC GAAGG CAAACGG	A UG U
hsa-miR-4717-3p	1.54	7mer-A1	-17.7	0.6197	GGU UCGGU GUACAC	UCC G GG A

Table 4.11. Analysis of upregulatory miR binding seed sites in OGT 3' UTR regions

miRNA	Ratio	Seed_Type	dG_hybrid	LogitProb	TargetMatch	MirMatch
hsa-miR-1322	1.49	6mer	-23.3	0.5075	GUC UAGUCGUC GUAGUA	G G
hsa-miR-302b-3p	1.63	offset-6mer	-15	0.5934	UUUGUA C UCGUGA	GAUGAU CU AU
hsa-miR-302c-3p	1.75	offset-6mer	-16.1	0.5737	GGU UUUGUA C UCGUGA	GAC CU AU
hsa-miR-431-5p	1.54	offset-6mer	-19.1	0.7168	ACGU CUG ACGUUCU	A CCGG GU
hsa-miR-4470	2.12	offset-6mer	-17.5	0.5439	GAG CC GAAGG CAAACGG	A UG U
hsa-miR-4496	1.5	6mer	-17	0.5204	GG AGA GUCGA G AAAGGAG	G A UC
hsa-miR-4496	1.5	6mer	-22.2	0.6062	GGGAGA CGAA C AAAGGAG	GU GU
hsa-miR-520e	1.76	offset-6mer	-20.1	0.5817	GGGAGUU UC UCGUGA	UU CU AA
hsa-miR-548ap-5p	1.61	7mer-m8	-13.6	0.7168	UCUGG AAUGAAAA	UU CGUU
hsa-miR-548ap-5p	1.61	offset-6mer	-18.1	0.686	UUUC GCGUUAAUGAA	UG AA
hsa-miR-548ap-5p	1.61	6mer	-15.4	0.5457	UCUG GCG AUGAAA	UU UUA A
hsa-miR-5683	1.72	7mer-m8	-19.1	0.5924	UCUC UUAG GUAGACA	CUUCAG AC U

4.12 REFERENCES

1. Bond, M. R.; Hanover, J. A., A little sugar goes a long way: the cell biology of O-GlcNAc. *J Cell Biol* **2015,** *208* (7), 869-80.
2. Jiang, M.; Xu, B.; Li, X.; Shang, Y.; Chu, Y.; Wang, W.; Chen, D.; Wu, N.; Hu, S.; Zhang, S.; Li, M.; Wu, K.; Yang, X.; Liang, J.; Nie, Y.; Fan, D., O-GlcNAcylation promotes colorectal cancer metastasis via the miR-101-O-GlcNAc/EZH2 regulatory feedback circuit. *Oncogene* **2019,** *38* (3), 301-316.
3. Ong, Q.; Han, W.; Yang, X., O-GlcNAc as an Integrator of Signaling Pathways. *Front Endocrinol (Lausanne)* **2018,** *9*, 599.
4. Yang, X.; Qian, K., Protein O-GlcNAcylation: emerging mechanisms and functions. *Nat Rev Mol Cell Biol* **2017,** *18* (7), 452-465.
5. Wu, D.; Cai, Y.; Jin, J., Potential coordination role between O-GlcNAcylation and epigenetics. *Protein Cell* **2017,** *8* (10), 713-723.
6. Wright, J. N.; Collins, H. E.; Wende, A. R.; Chatham, J. C., O-GlcNAcylation and cardiovascular disease. *Biochem Soc Trans* **2017,** *45* (2), 545-553.
7. Singh, J. P.; Zhang, K.; Wu, J.; Yang, X., O-GlcNAc signaling in cancer metabolism and epigenetics. *Cancer Lett* **2015,** *356* (2 Pt A), 244-50.
8. Zhu, Y.; Shan, X.; Yuzwa, S. A.; Vocadlo, D. J., The emerging link between O-GlcNAc and Alzheimer disease. *J Biol Chem* **2014,** *289* (50), 34472-81.
9. Yuzwa, S. A.; Vocadlo, D. J., O-GlcNAc and neurodegeneration: biochemical mechanisms and potential roles in Alzheimer's disease and beyond. *Chem Soc Rev* **2014,** *43* (19), 6839-58.
10. Yang, Y. R.; Suh, P. G., O-GlcNAcylation in cellular functions and human diseases. *Adv Biol Regul* **2014,** *54*, 68-73.
11. Li, Z.; Yi, W., Regulation of cancer metabolism by O-GlcNAcylation. *Glycoconj J* **2014,** *31* (3), 185-91.
12. Hart, G. W., Nutrient regulation of immunity: O-GlcNAcylation regulates stimulus-specific NF-kappaB-dependent transcription. *Sci Signal* **2013,** *6* (290), pe26.
13. Fardini, Y.; Dehennaut, V.; Lefebvre, T.; Issad, T., O-GlcNAcylation: A New Cancer Hallmark? *Front Endocrinol (Lausanne)* **2013,** *4*, 99.
14. Hart, G. W.; Slawson, C.; Ramirez-Correa, G.; Lagerlof, O., Cross talk between O-GlcNAcylation and phosphorylation: roles in signaling, transcription, and chronic disease. *Annu Rev Biochem* **2011,** *80*, 825-58.
15. Hanover, J. A.; Yu, S.; Lubas, W. B.; Shin, S. H.; Ragano-Caracciola, M.; Kochran, J.; Love, D. C., Mitochondrial and nucleocytoplasmic isoforms of O-linked GlcNAc transferase encoded by a single mammalian gene. *Arch Biochem Biophys* **2003,** *409* (2), 287-97.
16. Shafi, R.; Iyer, S. P.; Ellies, L. G.; O'Donnell, N.; Marek, K. W.; Chui, D.; Hart, G. W.; Marth, J. D., The O-GlcNAc transferase gene resides on the X chromosome and is essential for embryonic stem cell viability and mouse ontogeny. *Proc Natl Acad Sci U S A* **2000,** *97* (11), 5735-9.
17. Tan, Z. W.; Fei, G.; Paulo, J. A.; Bellaousov, S.; Martin, S. E. S.; Duveau, D. Y.; Thomas, C. J.; Gygi, S. P.; Boutz, P. L.; Walker, S., O-GlcNAc regulates gene expression by controlling detained intron splicing. *Nucleic Acids Res* **2020,** *48* (10), 5656-5669.

18. Keembiyehetty, C. N.; Krzeslak, A.; Love, D. C.; Hanover, J. A., A lipid-droplet-targeted O-GlcNAcase isoform is a key regulator of the proteasome. *J Cell Sci* **2011,** *124* (Pt 16), 2851-60.
19. Qian, K.; Wang, S.; Fu, M.; Zhou, J.; Singh, J. P.; Li, M. D.; Yang, Y.; Zhang, K.; Wu, J.; Nie, Y.; Ruan, H. B.; Yang, X., Transcriptional regulation of O-GlcNAc homeostasis is disrupted in pancreatic cancer. *J Biol Chem* **2018,** *293* (36), 13989-14000.
20. Han, D. L.; Wang, L. L.; Zhang, G. F.; Yang, W. F.; Chai, J.; Lin, H. M.; Fu, Z.; Yu, J. M., MiRNA-485-5p, inhibits esophageal cancer cells proliferation and invasion by down-regulating O-linked N-acetylglucosamine transferase. *Eur Rev Med Pharmacol Sci* **2019,** *23* (7), 2809-2816.
21. Yu, F. Y.; Zhou, C. Y.; Liu, Y. B.; Wang, B.; Mao, L.; Li, Y., miR-483 is down-regulated in gastric cancer and suppresses cell proliferation, invasion and protein O-GlcNAcylation by targeting OGT. *Neoplasma* **2018,** *65* (3), 406-414.
22. Lo, W. Y.; Yang, W. K.; Peng, C. T.; Pai, W. Y.; Wang, H. J., MicroRNA-200a/200b Modulate High Glucose-Induced Endothelial Inflammation by Targeting O-linked N-Acetylglucosamine Transferase Expression. *Front Physiol* **2018,** *9*, 355.
23. Chai, Y.; Du, Y.; Zhang, S.; Xiao, J.; Luo, Z.; He, F.; Huang, K., MicroRNA-485-5p reduces O-GlcNAcylation of Bmi-1 and inhibits colorectal cancer proliferation. *Exp Cell Res* **2018,** *368* (1), 111-118.
24. Liu, Y.; Huang, H.; Liu, M.; Wu, Q.; Li, W.; Zhang, J., MicroRNA-24-1 suppresses mouse hepatoma cell invasion and metastasis via directly targeting O-GlcNAc transferase. *Biomed Pharmacother* **2017,** *91*, 731-738.
25. Liu, Y.; Huang, H.; Cao, Y.; Wu, Q.; Li, W.; Zhang, J., Suppression of OGT by microRNA24 reduces FOXA1 stability and prevents breast cancer cells invasion. *Biochem Biophys Res Commun* **2017,** *487* (3), 755-762.
26. Vaiana, C. A.; Kurcon, T.; Mahal, L. K., MicroRNA-424 Predicts a Role for beta-1,4 Branched Glycosylation in Cell Cycle Progression. *J Biol Chem* **2016,** *291* (3), 1529-37.
27. Murashov, A. K.; Pak, E. S.; Koury, M.; Ajmera, A.; Jeyakumar, M.; Parker, M.; Williams, O.; Ding, J.; Walters, D.; Neufer, P. D., Paternal long-term exercise programs offspring for low energy expenditure and increased risk for obesity in mice. *FASEB J* **2016,** *30* (2), 775-84.
28. Luo, P.; He, T.; Jiang, R.; Li, G., MicroRNA-423-5p targets O-GlcNAc transferase to induce apoptosis in cardiomyocytes. *Mol Med Rep* **2015,** *12* (1), 1163-8.
29. Solary, E.; Bernard, O. A.; Tefferi, A.; Fuks, F.; Vainchenker, W., The Ten-Eleven Translocation-2 (TET2) gene in hematopoiesis and hematopoietic diseases. *Leukemia* **2014,** *28* (3), 485-96.
30. Babae, N.; Bourajjaj, M.; Liu, Y.; Van Beijnum, J. R.; Cerisoli, F.; Scaria, P. V.; Verheul, M.; Van Berkel, M. P.; Pieters, E. H.; Van Haastert, R. J.; Yousefi, A.; Mastrobattista, E.; Storm, G.; Berezikov, E.; Cuppen, E.; Woodle, M.; Schaapveld, R. Q.; Prevost, G. P.; Griffioen, A. W.; Van Noort, P. I.; Schiffelers, R. M., Systemic miRNA-7 delivery inhibits tumor angiogenesis and growth in murine xenograft glioblastoma. *Oncotarget* **2014,** *5* (16), 6687-700.
31. Muthusamy, S.; DeMartino, A. M.; Watson, L. J.; Brittian, K. R.; Zafir, A.; Dassanayaka, S.; Hong, K. U.; Jones, S. P., MicroRNA-539 is up-regulated in failing heart, and suppresses O-GlcNAcase expression. *J Biol Chem* **2014,** *289* (43), 29665-76.

32. Wang, D.; Hu, X.; Lee, S. H.; Chen, F.; Jiang, K.; Tu, Z.; Liu, Z.; Du, J.; Wang, L.; Yin, C.; Liao, Y.; Shang, H.; Martin, K. A.; Herzog, R. I.; Young, L. H.; Qian, L.; Hwa, J.; Xiang, Y., Diabetes Exacerbates Myocardial Ischemia/Reperfusion Injury by Down-Regulation of MicroRNA and Up-Regulation of O-GlcNAcylation. *JACC Basic Transl Sci* **2018,** *3* (3), 350-362.

33. Chatterjee, S.; Pal, J. K., Role of 5'- and 3'-untranslated regions of mRNAs in human diseases. *Biol Cell* **2009,** *101* (5), 251-62.

34. Jing, Q.; Huang, S.; Guth, S.; Zarubin, T.; Motoyama, A.; Chen, J.; Di Padova, F.; Lin, S. C.; Gram, H.; Han, J., Involvement of microRNA in AU-rich element-mediated mRNA instability. *Cell* **2005,** *120* (5), 623-34.

35. Otsuka, H.; Fukao, A.; Funakami, Y.; Duncan, K. E.; Fujiwara, T., Emerging Evidence of Translational Control by AU-Rich Element-Binding Proteins. *Front Genet* **2019,** *10*, 332.

36. Lytle, J. R.; Yario, T. A.; Steitz, J. A., Target mRNAs are repressed as efficiently by microRNA-binding sites in the 5' UTR as in the 3' UTR. *Proc Natl Acad Sci U S A* **2007,** *104* (23), 9667-72.

37. Orom, U. A.; Nielsen, F. C.; Lund, A. H., MicroRNA-10a binds the 5'UTR of ribosomal protein mRNAs and enhances their translation. *Mol Cell* **2008,** *30* (4), 460-71.

38. Panda, A. C.; Sahu, I.; Kulkarni, S. D.; Martindale, J. L.; Abdelmohsen, K.; Vindu, A.; Joseph, J.; Gorospe, M.; Seshadri, V., miR-196b-mediated translation regulation of mouse insulin2 via the 5'UTR. *PLoS One* **2014,** *9* (7), e101084.

39. Wu, Q.; Liu, H. O.; Liu, Y. D.; Liu, W. S.; Pan, D.; Zhang, W. J.; Yang, L.; Fu, Q.; Xu, J. J.; Gu, J. X., Decreased expression of hepatocyte nuclear factor 4alpha (Hnf4alpha)/microRNA-122 (miR-122) axis in hepatitis B virus-associated hepatocellular carcinoma enhances potential oncogenic GALNT10 protein activity. *J Biol Chem* **2015,** *290* (2), 1170-85.

40. Trapannone, R.; Mariappa, D.; Ferenbach, A. T.; van Aalten, D. M., Nucleocytoplasmic human O-GlcNAc transferase is sufficient for O-GlcNAcylation of mitochondrial proteins. *Biochem J* **2016,** *473* (12), 1693-702.

41. Thu, C. T.; Chung, J. Y.; Dhawan, D.; Vaiana, C. A.; Mahal, L. K., High-Throughput miRFluR Platform Identifies miRNA Regulating B3GLCT That Predict Peters' Plus Syndrome Phenotype, Supporting the miRNA Proxy Hypothesis. *ACS Chem Biol* **2021,** *16* (10), 1900-1907.

42. Wolter, J. M.; Kotagama, K.; Pierre-Bez, A. C.; Firago, M.; Mangone, M., 3'LIFE: a functional assay to detect miRNA targets in high-throughput. *Nucleic Acids Res* **2014,** *42* (17), e132.

43. Zhou, P.; Xu, W.; Peng, X.; Luo, Z.; Xing, Q.; Chen, X.; Hou, C.; Liang, W.; Zhou, J.; Wu, X.; Songyang, Z.; Jiang, S., Large-scale screens of miRNA-mRNA interactions unveiled that the 3'UTR of a gene is targeted by multiple miRNAs. *PLoS One* **2013,** *8* (7), e68204.

44. Agrawal, P.; Kurcon, T.; Pilobello, K. T.; Rakus, J. F.; Koppolu, S.; Liu, Z.; Batista, B. S.; Eng, W. S.; Hsu, K. L.; Liang, Y.; Mahal, L. K., Mapping posttranscriptional regulation of the human glycome uncovers microRNA defining the glycocode. *Proc Natl Acad Sci U S A* **2014,** *111* (11), 4338-43.

Bibliography

1. Piras, V.; Tomita, M.; Selvarajoo, K., Is central dogma a global property of cellular information flow? *Front Physiol* **2012,** *3*, 439.
2. Wymann, M. P.; Schneiter, R., Lipid signalling in disease. *Nat Rev Mol Cell Biol* **2008,** *9* (2), 162-76.
3. Sasisekharan, R.; Shriver, Z.; Venkataraman, G.; Narayanasami, U., Roles of heparan-sulphate glycosaminoglycans in cancer. *Nat Rev Cancer* **2002,** *2* (7), 521-8.
4. Heindel, D. W.; Koppolu, S.; Zhang, Y.; Kasper, B.; Meche, L.; Vaiana, C. A.; Bissel, S. J.; Carter, C. E.; Kelvin, A. A.; Elaish, M.; Lopez-Orozco, J.; Zhang, B.; Zhou, B.; Chou, T. W.; Lashua, L.; Hobman, T. C.; Ross, T. M.; Ghedin, E.; Mahal, L. K., Glycomic analysis of host response reveals high mannose as a key mediator of influenza severity. *Proc Natl Acad Sci U S A* **2020,** *117* (43), 26926-26935.
5. Amon, R.; Reuven, E. M.; Leviatan Ben-Arye, S.; Padler-Karavani, V., Glycans in immune recognition and response. *Carbohydr Res* **2014,** *389*, 115-22.
6. van den Berg, T. K.; Honing, H.; Franke, N.; van Remoortere, A.; Schiphorst, W. E.; Liu, F. T.; Deelder, A. M.; Cummings, R. D.; Hokke, C. H.; van Die, I., LacdiNAc-glycans constitute a parasite pattern for galectin-3-mediated immune recognition. *J Immunol* **2004,** *173* (3), 1902-7.
7. De Giorgi, F.; Fumagalli, M.; Scietti, L.; Forneris, F., Collagen hydroxylysine glycosylation: non-conventional substrates for atypical glycosyltransferase enzymes. *Biochem Soc Trans* **2021,** *49* (2), 855-866.
8. Joshi, H. J.; Hansen, L.; Narimatsu, Y.; Freeze, H. H.; Henrissat, B.; Bennett, E.; Wandall, H. H.; Clausen, H.; Schjoldager, K. T., Glycosyltransferase genes that cause monogenic congenital disorders of glycosylation are distinct from glycosyltransferase genes associated with complex diseases. *Glycobiology* **2018,** *28* (5), 284-294.
9. Neelamegham, S.; Mahal, L. K., Multi-level regulation of cellular glycosylation: from genes to transcript to enzyme to structure. *Curr Opin Struct Biol* **2016,** *40*, 145-152.
10. Anugraham, M.; Jacob, F.; Nixdorf, S.; Everest-Dass, A. V.; Heinzelmann-Schwarz, V.; Packer, N. H., Specific glycosylation of membrane proteins in epithelial ovarian cancer cell lines: glycan structures reflect gene expression and DNA methylation status. *Mol Cell Proteomics* **2014,** *13* (9), 2213-32.
11. Nairn, A. V.; York, W. S.; Harris, K.; Hall, E. M.; Pierce, J. M.; Moremen, K. W., Regulation of glycan structures in animal tissues: transcript profiling of glycan-related genes. *J Biol Chem* **2008,** *283* (25), 17298-313.
12. Liu, G.; Marathe, D. D.; Matta, K. L.; Neelamegham, S., Systems-level modeling of cellular glycosylation reaction networks: O-linked glycan formation on natural selectin ligands. *Bioinformatics* **2008,** *24* (23), 2740-7.
13. Kurcon, T.; Liu, Z.; Paradkar, A. V.; Vaiana, C. A.; Koppolu, S.; Agrawal, P.; Mahal, L. K., miRNA proxy approach reveals hidden functions of glycosylation. *Proc Natl Acad Sci U S A* **2015,** *112* (23), 7327-32.
14. Agrawal, P.; Kurcon, T.; Pilobello, K. T.; Rakus, J. F.; Koppolu, S.; Liu, Z.; Batista, B. S.; Eng, W. S.; Hsu, K. L.; Liang, Y.; Mahal, L. K., Mapping posttranscriptional regulation of the human glycome uncovers microRNA defining the glycocode. *Proc Natl Acad Sci U S A* **2014,** *111* (11), 4338-43.

15. Kasper, B. T.; Koppolu, S.; Mahal, L. K., Insights into miRNA regulation of the human glycome. *Biochem Biophys Res Commun* **2014,** *445* (4), 774-9.
16. Schmiedel, J. M.; Klemm, S. L.; Zheng, Y.; Sahay, A.; Bluthgen, N.; Marks, D. S.; van Oudenaarden, A., Gene expression. MicroRNA control of protein expression noise. *Science* **2015,** *348* (6230), 128-32.
17. Liu, B.; Li, J.; Cairns, M. J., Identifying miRNAs, targets and functions. *Brief Bioinform* **2014,** *15* (1), 1-19.
18. Chendrimada, T. P.; Gregory, R. I.; Kumaraswamy, E.; Norman, J.; Cooch, N.; Nishikura, K.; Shiekhattar, R., TRBP recruits the Dicer complex to Ago2 for microRNA processing and gene silencing. *Nature* **2005,** *436* (7051), 740-4.
19. Michlewski, G.; Caceres, J. F., Post-transcriptional control of miRNA biogenesis. *RNA* **2019,** *25* (1), 1-16.
20. Khvorova, A.; Reynolds, A.; Jayasena, S. D., Functional siRNAs and miRNAs exhibit strand bias. *Cell* **2003,** *115* (2), 209-16.
21. Agrawal, P.; Fontanals-Cirera, B.; Sokolova, E.; Jacob, S.; Vaiana, C. A.; Argibay, D.; Davalos, V.; McDermott, M.; Nayak, S.; Darvishian, F.; Castillo, M.; Ueberheide, B.; Osman, I.; Fenyo, D.; Mahal, L. K.; Hernando, E., A Systems Biology Approach Identifies FUT8 as a Driver of Melanoma Metastasis. *Cancer Cell* **2017,** *31* (6), 804-819 e7.
22. Cheng, L.; Gao, S.; Song, X.; Dong, W.; Zhou, H.; Zhao, L.; Jia, L., Comprehensive N-glycan profiles of hepatocellular carcinoma reveal association of fucosylation with tumor progression and regulation of FUT8 by microRNAs. *Oncotarget* **2016,** *7* (38), 61199-61214.
23. Bernardi, C.; Soffientini, U.; Piacente, F.; Tonetti, M. G., Effects of microRNAs on fucosyltransferase 8 (FUT8) expression in hepatocarcinoma cells. *PLoS One* **2013,** *8* (10), e76540.
24. Gaziel-Sovran, A.; Segura, M. F.; Di Micco, R.; Collins, M. K.; Hanniford, D.; Vega-Saenz de Miera, E.; Rakus, J. F.; Dankert, J. F.; Shang, S.; Kerbel, R. S.; Bhardwaj, N.; Shao, Y.; Darvishian, F.; Zavadil, J.; Erlebacher, A.; Mahal, L. K.; Osman, I.; Hernando, E., miR-30b/30d regulation of GalNAc transferases enhances invasion and immunosuppression during metastasis. *Cancer Cell* **2011,** *20* (1), 104-18.
25. Peng, R. Q.; Wan, H. Y.; Li, H. F.; Liu, M.; Li, X.; Tang, H., MicroRNA-214 suppresses growth and invasiveness of cervical cancer cells by targeting UDP-N-acetyl-alpha-D-galactosamine:polypeptide N-acetylgalactosaminyltransferase 7. *J Biol Chem* **2012,** *287* (17), 14301-9.
26. Shan, S. W.; Fang, L.; Shatseva, T.; Rutnam, Z. J.; Yang, X.; Du, W.; Lu, W. Y.; Xuan, J. W.; Deng, Z.; Yang, B. B., Mature miR-17-5p and passenger miR-17-3p induce hepatocellular carcinoma by targeting PTEN, GalNT7 and vimentin in different signal pathways. *J Cell Sci* **2013,** *126* (Pt 6), 1517-30.
27. Li, W.; Ma, H.; Sun, J., MicroRNA34a/c function as tumor suppressors in Hep2 laryngeal carcinoma cells and may reduce GALNT7 expression. *Mol Med Rep* **2014,** *9* (4), 1293-8.
28. Duan, H. F.; Li, X. Q.; Hu, H. Y.; Li, Y. C.; Cai, Z.; Mei, X. S.; Yu, P.; Nie, L. P.; Zhang, W.; Yu, Z. D.; Nie, G. H., Functional elucidation of miR-494 in the tumorigenesis of nasopharyngeal carcinoma. *Tumour Biol* **2015,** *36* (9), 6679-89.
29. Nie, G. H.; Luo, L.; Duan, H. F.; Li, X. Q.; Yin, M. J.; Li, Z.; Zhang, W., GALNT7, a target of miR-494, participates in the oncogenesis of nasopharyngeal carcinoma. *Tumour Biol* **2016,** *37* (4), 4559-67.

30. Li, Y.; Li, Y.; Chen, D.; Jin, L.; Su, Z.; Liu, J.; Duan, H.; Li, X.; Qi, Z.; Shi, M.; Ni, L.; Yang, S.; Gui, Y.; Mao, X.; Chen, Y.; Lai, Y., miR30a5p in the tumorigenesis of renal cell carcinoma: A tumor suppressive microRNA. *Mol Med Rep* **2016,** *13* (5), 4085-94.
31. Lu, Q.; Xu, L.; Li, C.; Yuan, Y.; Huang, S.; Chen, H., miR-214 inhibits invasion and migration via downregulating GALNT7 in esophageal squamous cell cancer. *Tumour Biol* **2016,** *37* (11), 14605-14614.
32. Niu, J. T.; Zhang, L. J.; Huang, Y. W.; Li, C.; Jiang, N.; Niu, Y. J., MiR-154 inhibits the growth of laryngeal squamous cell carcinoma by targeting GALNT7. *Biochem Cell Biol* **2018,** *96* (6), 752-760.
33. Kahai, S.; Lee, S. C.; Lee, D. Y.; Yang, J.; Li, M.; Wang, C. H.; Jiang, Z.; Zhang, Y.; Peng, C.; Yang, B. B., MicroRNA miR-378 regulates nephronectin expression modulating osteoblast differentiation by targeting GalNT-7. *PLoS One* **2009,** *4* (10), e7535.
34. Dyrskjot, L.; Ostenfeld, M. S.; Bramsen, J. B.; Silahtaroglu, A. N.; Lamy, P.; Ramanathan, R.; Fristrup, N.; Jensen, J. L.; Andersen, C. L.; Zieger, K.; Kauppinen, S.; Ulhoi, B. P.; Kjems, J.; Borre, M.; Orntoft, T. F., Genomic profiling of microRNAs in bladder cancer: miR-129 is associated with poor outcome and promotes cell death in vitro. *Cancer Res* **2009,** *69* (11), 4851-60.
35. Shan, Y.; Ma, J.; Pan, Y.; Hu, J.; Liu, B.; Jia, L., LncRNA SNHG7 sponges miR-216b to promote proliferation and liver metastasis of colorectal cancer through upregulating GALNT1. *Cell Death Dis* **2018,** *9* (7), 722.
36. Nakagawa, Y.; Nishikimi, T.; Kuwahara, K.; Fujishima, A.; Oka, S.; Tsutamoto, T.; Kinoshita, H.; Nakao, K.; Cho, K.; Inazumi, H.; Okamoto, H.; Nishida, M.; Kato, T.; Fukushima, H.; Yamashita, J. K.; Wijnen, W. J.; Creemers, E. E.; Kangawa, K.; Minamino, N.; Nakao, K.; Kimura, T., MiR30-GALNT1/2 Axis-Mediated Glycosylation Contributes to the Increased Secretion of Inactive Human Prohormone for Brain Natriuretic Peptide (proBNP) From Failing Hearts. *J Am Heart Assoc* **2017,** *6* (2).
37. Schjoldager, K. T.; Joshi, H. J.; Kong, Y.; Goth, C. K.; King, S. L.; Wandall, H. H.; Bennett, E. P.; Vakhrushev, S. Y.; Clausen, H., Deconstruction of O-glycosylation--GalNAc-T isoforms direct distinct subsets of the O-glycoproteome. *EMBO Rep* **2015,** *16* (12), 1713-22.
38. Hintze, J.; Ye, Z.; Narimatsu, Y.; Madsen, T. D.; Joshi, H. J.; Goth, C. K.; Linstedt, A.; Bachert, C.; Mandel, U.; Bennett, E. P.; Vakhrushev, S. Y.; Schjoldager, K. T., Probing the contribution of individual polypeptide GalNAc-transferase isoforms to the O-glycoproteome by inducible expression in isogenic cell lines. *J Biol Chem* **2018,** *293* (49), 19064-19077.
39. Zhang, L.; Hammell, M.; Kudlow, B. A.; Ambros, V.; Han, M., Systematic analysis of dynamic miRNA-target interactions during C. elegans development. *Development* **2009,** *136* (18), 3043-55.
40. Pilobello, K. T.; Krishnamoorthy, L.; Slawek, D.; Mahal, L. K., Development of a lectin microarray for the rapid analysis of protein glycopatterns. *Chembiochem* **2005,** *6* (6), 985-9.
41. Pilobello, K. T.; Slawek, D. E.; Mahal, L. K., A ratiometric lectin microarray approach to analysis of the dynamic mammalian glycome. *Proc Natl Acad Sci U S A* **2007,** *104* (28), 11534-9.
42. Hsu, S. D.; Lin, F. M.; Wu, W. Y.; Liang, C.; Huang, W. C.; Chan, W. L.; Tsai, W. T.; Chen, G. Z.; Lee, C. J.; Chiu, C. M.; Chien, C. H.; Wu, M. C.; Huang, C. Y.; Tsou, A. P.; Huang, H. D., miRTarBase: a database curates experimentally validated microRNA-target interactions. *Nucleic Acids Res* **2011,** *39* (Database issue), D163-9.

43. Lee, T.; Wang, N.; Houel, S.; Couts, K.; Old, W.; Ahn, N., Dosage and temporal thresholds in microRNA proteomics. *Mol Cell Proteomics* **2015,** *14* (2), 289-302.
44. Wolter, J. M.; Kotagama, K.; Pierre-Bez, A. C.; Firago, M.; Mangone, M., 3'LIFE: a functional assay to detect miRNA targets in high-throughput. *Nucleic Acids Res* **2014,** *42* (17), e132.
45. Zhou, P.; Xu, W.; Peng, X.; Luo, Z.; Xing, Q.; Chen, X.; Hou, C.; Liang, W.; Zhou, J.; Wu, X.; Songyang, Z.; Jiang, S., Large-scale screens of miRNA-mRNA interactions unveiled that the 3'UTR of a gene is targeted by multiple miRNAs. *PLoS One* **2013,** *8* (7), e68204.
46. Liu, W.; Wang, X., Prediction of functional microRNA targets by integrative modeling of microRNA binding and target expression data. *Genome Biol* **2019,** *20* (1), 18.
47. Ameres, S. L.; Horwich, M. D.; Hung, J. H.; Xu, J.; Ghildiyal, M.; Weng, Z.; Zamore, P. D., Target RNA-directed trimming and tailing of small silencing RNAs. *Science* **2010,** *328* (5985), 1534-9.
48. Ameres, S. L.; Hung, J. H.; Xu, J.; Weng, Z.; Zamore, P. D., Target RNA-directed tailing and trimming purifies the sorting of endo-siRNAs between the two Drosophila Argonaute proteins. *RNA* **2011,** *17* (1), 54-63.
49. Cazalla, D.; Yario, T.; Steitz, J. A., Down-regulation of a host microRNA by a Herpesvirus saimiri noncoding RNA. *Science* **2010,** *328* (5985), 1563-6.
50. Baccarini, A.; Chauhan, H.; Gardner, T. J.; Jayaprakash, A. D.; Sachidanandam, R.; Brown, B. D., Kinetic analysis reveals the fate of a microRNA following target regulation in mammalian cells. *Curr Biol* **2011,** *21* (5), 369-76.
51. Chipman, L. B.; Pasquinelli, A. E., miRNA Targeting: Growing beyond the Seed. *Trends Genet* **2019,** *35* (3), 215-222.
52. Vogel, C.; Marcotte, E. M., Insights into the regulation of protein abundance from proteomic and transcriptomic analyses. *Nat Rev Genet* **2012,** *13* (4), 227-32.
53. Kosti, I.; Jain, N.; Aran, D.; Butte, A. J.; Sirota, M., Cross-tissue Analysis of Gene and Protein Expression in Normal and Cancer Tissues. *Sci. Rep.* **2016,** *6*, 24799.
54. Buccitelli, C.; Selbach, M., mRNAs, proteins and the emerging principles of gene expression control. *Nat Rev Genet* **2020,** *21* (10), 630-644.
55. Pascal, L. E.; True, L. D.; Campbell, D. S.; Deutsch, E. W.; Risk, M.; Coleman, I. M.; Eichner, L. J.; Nelson, P. S.; Liu, A. Y., Correlation of mRNA and protein levels: cell type-specific gene expression of cluster designation antigens in the prostate. *BMC Genomics* **2008,** *9*, 246.
56. Maier, T.; Guell, M.; Serrano, L., Correlation of mRNA and protein in complex biological samples. *FEBS Lett* **2009,** *583* (24), 3966-73.
57. Koussounadis, A.; Langdon, S. P.; Um, I. H.; Harrison, D. J.; Smith, V. A., Relationship between differentially expressed mRNA and mRNA-protein correlations in a xenograft model system. *Sci Rep* **2015,** *5*, 10775.
58. Ostlund, G.; Sonnhammer, E. L., Quality criteria for finding genes with high mRNA-protein expression correlation and coexpression correlation. *Gene* **2012,** *497* (2), 228-36.
59. Eichhorn, S. W.; Guo, H.; McGeary, S. E.; Rodriguez-Mias, R. A.; Shin, C.; Baek, D.; Hsu, S. H.; Ghoshal, K.; Villen, J.; Bartel, D. P., mRNA destabilization is the dominant effect of mammalian microRNAs by the time substantial repression ensues. *Mol Cell* **2014,** *56* (1), 104-15.

60. Zhang, X.; Zuo, X.; Yang, B.; Li, Z.; Xue, Y.; Zhou, Y.; Huang, J.; Zhao, X.; Zhou, J.; Yan, Y.; Zhang, H.; Guo, P.; Sun, H.; Guo, L.; Zhang, Y.; Fu, X. D., MicroRNA directly enhances mitochondrial translation during muscle differentiation. *Cell* **2014,** *158* (3), 607-19.
61. Panda, A. C.; Sahu, I.; Kulkarni, S. D.; Martindale, J. L.; Abdelmohsen, K.; Vindu, A.; Joseph, J.; Gorospe, M.; Seshadri, V., miR-196b-mediated translation regulation of mouse insulin2 via the 5'UTR. *PLoS One* **2014,** *9* (7), e101084.
62. Gabius, H. J.; Andre, S.; Jimenez-Barbero, J.; Romero, A.; Solis, D., From lectin structure to functional glycomics: principles of the sugar code. *Trends Biochem Sci* **2011,** *36* (6), 298-313.
63. Chai, Y.; Du, Y.; Zhang, S.; Xiao, J.; Luo, Z.; He, F.; Huang, K., MicroRNA-485-5p reduces O-GlcNAcylation of Bmi-1 and inhibits colorectal cancer proliferation. *Exp Cell Res* **2018,** *368* (1), 111-118.
64. Han, D. L.; Wang, L. L.; Zhang, G. F.; Yang, W. F.; Chai, J.; Lin, H. M.; Fu, Z.; Yu, J. M., MiRNA-485-5p, inhibits esophageal cancer cells proliferation and invasion by down-regulating O-linked N-acetylglucosamine transferase. *Eur Rev Med Pharmacol Sci* **2019,** *23* (7), 2809-2816.
65. Jiang, M.; Xu, B.; Li, X.; Shang, Y.; Chu, Y.; Wang, W.; Chen, D.; Wu, N.; Hu, S.; Zhang, S.; Li, M.; Wu, K.; Yang, X.; Liang, J.; Nie, Y.; Fan, D., O-GlcNAcylation promotes colorectal cancer metastasis via the miR-101-O-GlcNAc/EZH2 regulatory feedback circuit. *Oncogene* **2019,** *38* (3), 301-316.
66. Yu, F. Y.; Zhou, C. Y.; Liu, Y. B.; Wang, B.; Mao, L.; Li, Y., miR-483 is down-regulated in gastric cancer and suppresses cell proliferation, invasion and protein O-GlcNAcylation by targeting OGT. *Neoplasma* **2018,** *65* (3), 406-414.
67. Lo, W. Y.; Yang, W. K.; Peng, C. T.; Pai, W. Y.; Wang, H. J., MicroRNA-200a/200b Modulate High Glucose-Induced Endothelial Inflammation by Targeting O-linked N-Acetylglucosamine Transferase Expression. *Front Physiol* **2018,** *9*, 355.
68. Liu, Y.; Huang, H.; Liu, M.; Wu, Q.; Li, W.; Zhang, J., MicroRNA-24-1 suppresses mouse hepatoma cell invasion and metastasis via directly targeting O-GlcNAc transferase. *Biomed Pharmacother* **2017,** *91*, 731-738.
69. Vaiana, C. A.; Kurcon, T.; Mahal, L. K., MicroRNA-424 Predicts a Role for beta-1,4 Branched Glycosylation in Cell Cycle Progression. *J Biol Chem* **2016,** *291* (3), 1529-37.
70. Luo, P.; He, T.; Jiang, R.; Li, G., MicroRNA-423-5p targets O-GlcNAc transferase to induce apoptosis in cardiomyocytes. *Mol Med Rep* **2015,** *12* (1), 1163-8.
71. Babae, N.; Bourajjaj, M.; Liu, Y.; Van Beijnum, J. R.; Cerisoli, F.; Scaria, P. V.; Verheul, M.; Van Berkel, M. P.; Pieters, E. H.; Van Haastert, R. J.; Yousefi, A.; Mastrobattista, E.; Storm, G.; Berezikov, E.; Cuppen, E.; Woodle, M.; Schaapveld, R. Q.; Prevost, G. P.; Griffioen, A. W.; Van Noort, P. I.; Schiffelers, R. M., Systemic miRNA-7 delivery inhibits tumor angiogenesis and growth in murine xenograft glioblastoma. *Oncotarget* **2014,** *5* (16), 6687-700.
72. Muthusamy, S.; DeMartino, A. M.; Watson, L. J.; Brittian, K. R.; Zafir, A.; Dassanayaka, S.; Hong, K. U.; Jones, S. P., MicroRNA-539 is up-regulated in failing heart, and suppresses O-GlcNAcase expression. *J Biol Chem* **2014,** *289* (43), 29665-76.
73. Ghahramani Seno, M. M.; Gwadry, F. G.; Hu, P.; Scherer, S. W., Neuregulin 1-alpha regulates phosphorylation, acetylation, and alternative splicing in lymphoblastoid cells. *Genome* **2013,** *56* (10), 619-25.

74. Chan, J. K.; Kiet, T. K.; Blansit, K.; Ramasubbaiah, R.; Hilton, J. F.; Kapp, D. S.; Matei, D., MiR-378 as a biomarker for response to anti-angiogenic treatment in ovarian cancer. *Gynecol Oncol* **2014,** *133* (3), 568-74.
75. Liu, B.; Ma, X.; Liu, Q.; Xiao, Y.; Pan, S.; Jia, L., Aberrant mannosylation profile and FTX/miR-342/ALG3-axis contribute to development of drug resistance in acute myeloid leukemia. *Cell Death Dis* **2018,** *9* (6), 688.
76. Tatura, R.; Buchholz, M.; Dickson, D. W.; van Swieten, J.; McLean, C.; Hoglinger, G.; Muller, U., microRNA profiling: increased expression of miR-147a and miR-518e in progressive supranuclear palsy (PSP). *Neurogenetics* **2016,** *17* (3), 165-71.
77. De Antonellis, P.; Carotenuto, M.; Vandenbussche, J.; De Vita, G.; Ferrucci, V.; Medaglia, C.; Boffa, I.; Galiero, A.; Di Somma, S.; Magliulo, D.; Aiese, N.; Alonzi, A.; Spano, D.; Liguori, L.; Chiarolla, C.; Verrico, A.; Schulte, J. H.; Mestdagh, P.; Vandesompele, J.; Gevaert, K.; Zollo, M., Early targets of miR-34a in neuroblastoma. *Mol Cell Proteomics* **2014,** *13* (8), 2114-31.
78. Li, Y.; Sun, Z.; Liu, B.; Shan, Y.; Zhao, L.; Jia, L., Tumor-suppressive miR-26a and miR-26b inhibit cell aggressiveness by regulating FUT4 in colorectal cancer. *Cell Death Dis* **2017,** *8* (6), e2892.
79. Wang, M.; Wang, J.; Kong, X.; Chen, H.; Wang, Y.; Qin, M.; Lin, Y.; Chen, H.; Xu, J.; Hong, J.; Chen, Y. X.; Zou, W.; Fang, J. Y., MiR-198 represses tumor growth and metastasis in colorectal cancer by targeting fucosyl transferase 8. *Sci Rep* **2014,** *4*, 6145.
80. Huang, H.; Liu, Y.; Yu, P.; Qu, J.; Guo, Y.; Li, W.; Wang, S.; Zhang, J., MiR-23a transcriptional activated by Runx2 increases metastatic potential of mouse hepatoma cell via directly targeting Mgat3. *Sci Rep* **2018,** *8* (1), 7366.
81. Guo, Y.; Li, S.; Qu, J.; Ye, L.; Wang, S.; Fan, J.; Wang, Q.; Zhang, J., Let-7c inhibits metastatic ability of mouse hepatocarcinoma cells via targeting mannoside acetylglucosaminyltransferase 4 isoenzyme A. *Int J Biochem Cell Biol* **2014,** *53*, 1-8.
82. Wang, Y. Q.; Ren, Y. F.; Song, Y. J.; Xue, Y. F.; Zhang, X. J.; Cao, S. T.; Deng, Z. J.; Wu, J.; Chen, L.; Li, G.; Shi, K. Q.; Chen, Y. P.; Ren, H.; Huang, A. L.; Tang, K. F., MicroRNA-581 promotes hepatitis B virus surface antigen expression by targeting Dicer and EDEM1. *Carcinogenesis* **2014,** *35* (9), 2127-33.
83. Li, G.; Luna, C.; Qiu, J.; Epstein, D. L.; Gonzalez, P., Role of miR-204 in the regulation of apoptosis, endoplasmic reticulum stress response, and inflammation in human trabecular meshwork cells. *Invest Ophthalmol Vis Sci* **2011,** *52* (6), 2999-3007.
84. Vitiello, M.; Tuccoli, A.; D'Aurizio, R.; Sarti, S.; Giannecchini, L.; Lubrano, S.; Marranci, A.; Evangelista, M.; Peppicelli, S.; Ippolito, C.; Barravecchia, I.; Guzzolino, E.; Montagnani, V.; Gowen, M.; Mercoledi, E.; Mercatanti, A.; Comelli, L.; Gurrieri, S.; Wu, L. W.; Ope, O.; Flaherty, K.; Boland, G. M.; Hammond, M. R.; Kwong, L.; Chiariello, M.; Stecca, B.; Zhang, G.; Salvetti, A.; Angeloni, D.; Pitto, L.; Calorini, L.; Chiorino, G.; Pellegrini, M.; Herlyn, M.; Osman, I.; Poliseno, L., Context-dependent miR-204 and miR-211 affect the biological properties of amelanotic and melanotic melanoma cells. *Oncotarget* **2017,** *8* (15), 25395-25417.
85. Lim, S. M.; Park, S. H.; Lee, J. H.; Kim, S. H.; Kim, J. Y.; Min, J. K.; Lee, G. M.; Kim, Y. G., Differential expression of microRNAs in recombinant Chinese hamster ovary cells treated with sodium butyrate using digital RNA counting. *J Biotechnol* **2018,** *283*, 37-42.

86. Pan, S.; Cheng, X.; Chen, H.; Castro, P. D.; Ittmann, M. M.; Hutson, A. W.; Zapata, S. K.; Sifers, R. N., ERManI is a target of miR-125b and promotes transformation phenotypes in hepatocellular carcinoma (HCC). *PLoS One* **2013,** *8* (8), e72829.
87. Adhikari, S.; Mandal, P., Integrated analysis of global gene and microRNA expression profiling associated with aplastic anaemia. *Life Sci* **2019,** *228*, 47-52.
88. Bhise, N. S.; Chauhan, L.; Shin, M.; Cao, X.; Pounds, S.; Lamba, V.; Lamba, J. K., MicroRNA-mRNA Pairs Associated with Outcome in AML: From In Vitro Cell-Based Studies to AML Patients. *Front Pharmacol* **2015,** *6*, 324.
89. Serino, G.; Sallustio, F.; Curci, C.; Cox, S. N.; Pesce, F.; De Palma, G.; Schena, F. P., Role of let-7b in the regulation of N-acetylgalactosaminyltransferase 2 in IgA nephropathy. *Nephrol Dial Transplant* **2015,** *30* (7), 1132-9.
90. Liu, B.; Pan, S.; Xiao, Y.; Liu, Q.; Xu, J.; Jia, L., LINC01296/miR-26a/GALNT3 axis contributes to colorectal cancer progression by regulating O-glycosylated MUC1 via PI3K/AKT pathway. *J Exp Clin Cancer Res* **2018,** *37* (1), 316.
91. Nakamura, S.; Horie, M.; Daidoji, T.; Honda, T.; Yasugi, M.; Kuno, A.; Komori, T.; Okuzaki, D.; Narimatsu, H.; Nakaya, T.; Tomonaga, K., Influenza A Virus-Induced Expression of a GalNAc Transferase, GALNT3, via MicroRNAs Is Required for Enhanced Viral Replication. *J Virol* **2016,** *90* (4), 1788-801.
92. Qu, J. J.; Qu, X. Y.; Zhou, D. Z., miR4262 inhibits colon cancer cell proliferation via targeting of GALNT4. *Mol Med Rep* **2017,** *16* (4), 3731-3736.
93. Liu, Y.; Liu, H.; Yang, L.; Wu, Q.; Liu, W.; Fu, Q.; Zhang, W.; Zhang, H.; Xu, J.; Gu, J., Loss of N-Acetylgalactosaminyltransferase-4 Orchestrates Oncogenic MicroRNA-9 in Hepatocellular Carcinoma. *J Biol Chem* **2017,** *292* (8), 3186-3200.
94. Zhang, J.; Zhang, Z.; Wang, Q.; Xing, X. J.; Zhao, Y., Overexpression of microRNA-365 inhibits breast cancer cell growth and chemo-resistance through GALNT4. *Eur Rev Med Pharmacol Sci* **2016,** *20* (22), 4710-4718.
95. Stiegelbauer, V.; Vychytilova-Faltejskova, P.; Karbiener, M.; Pehserl, A. M.; Reicher, A.; Resel, M.; Heitzer, E.; Ivan, C.; Bullock, M.; Ling, H.; Deutsch, A.; Wulf-Goldenberg, A.; Adiprasito, J. B.; Stoeger, H.; Haybaeck, J.; Svoboda, M.; Stotz, M.; Hoefler, G.; Slaby, O.; Calin, G. A.; Gerger, A.; Pichler, M., miR-196b-5p Regulates Colorectal Cancer Cell Migration and Metastases through Interaction with HOXB7 and GALNT5. *Clin Cancer Res* **2017,** *23* (17), 5255-5266.
96. Wu, Q.; Liu, H. O.; Liu, Y. D.; Liu, W. S.; Pan, D.; Zhang, W. J.; Yang, L.; Fu, Q.; Xu, J. J.; Gu, J. X., Decreased expression of hepatocyte nuclear factor 4alpha (Hnf4alpha)/microRNA-122 (miR-122) axis in hepatitis B virus-associated hepatocellular carcinoma enhances potential oncogenic GALNT10 protein activity. *J Biol Chem* **2015,** *290* (2), 1170-85.
97. Yang, J.; Li, G.; Zhang, K., MiR-125a regulates ovarian cancer proliferation and invasion by repressing GALNT14 expression. *Biomed Pharmacother* **2016,** *80*, 381-387.
98. Liu, X.; Chen, J.; Guan, T.; Yao, H.; Zhang, W.; Guan, Z.; Wang, Y., miRNAs and target genes in the blood as biomarkers for the early diagnosis of Parkinson's disease. *BMC Syst Biol* **2019,** *13* (1), 10.
99. Gao, Y.; Liu, T.; Huang, Y., MicroRNA-134 suppresses endometrial cancer stem cells by targeting POGLUT1 and Notch pathway proteins. *FEBS Lett* **2015,** *589* (2), 207-14.
100. Thapa, I.; Fox, H. S.; Bastola, D., Coexpression Network Analysis of miRNA-142 Overexpression in Neuronal Cells. *Biomed Res Int* **2015,** *2015*, 921517.

101. Metzler-Guillemain, C.; Victorero, G.; Lepoivre, C.; Bergon, A.; Yammine, M.; Perrin, J.; Sari-Minodier, I.; Boulanger, N.; Rihet, P.; Nguyen, C., Sperm mRNAs and microRNAs as candidate markers for the impact of toxicants on human spermatogenesis: an application to tobacco smoking. *Syst Biol Reprod Med* **2015,** *61* (3), 139-49.
102. Wang, R.; Fang, J.; Ma, H.; Feng, L.; Lian, M.; Yang, F.; Wang, H.; Wang, Q.; Chen, X., Effect of microRNA-203 on tumor growth in human hypopharyngeal squamous cell carcinoma. *Mol Cell Biochem* **2015,** *405* (1-2), 97-104.
103. Serino, G.; Sallustio, F.; Cox, S. N.; Pesce, F.; Schena, F. P., Abnormal miR-148b expression promotes aberrant glycosylation of IgA1 in IgA nephropathy. *J Am Soc Nephrol* **2012,** *23* (5), 814-24.
104. Li, C.; Shi, J.; Zhao, Y., MiR-320 promotes B cell proliferation and the production of aberrant glycosylated IgA1 in IgA nephropathy. *J Cell Biochem* **2018,** *119* (6), 4607-4614.
105. Yang, L.; Zhang, X.; Peng, W.; Wei, M.; Qin, W., MicroRNA-155-induced T lymphocyte subgroup drifting in IgA nephropathy. *Int Urol Nephrol* **2017,** *49* (2), 353-361.
106. Hu, S.; Bao, H.; Xu, X.; Zhou, X.; Qin, W.; Zeng, C.; Liu, Z., Increased miR-374b promotes cell proliferation and the production of aberrant glycosylated IgA1 in B cells of IgA nephropathy. *FEBS Lett* **2015,** *589* (24 Pt B), 4019-25.
107. Chao, C. C.; Wu, P. H.; Huang, H. C.; Chung, H. Y.; Chou, Y. C.; Cai, B. H.; Kannagi, R., Downregulation of miR-199a/b-5p is associated with GCNT2 induction upon epithelial-mesenchymal transition in colon cancer. *FEBS Lett* **2017,** *591* (13), 1902-1917.
108. Li, Q.; Ran, P.; Zhang, X.; Guo, X.; Yuan, Y.; Dong, T.; Zhu, B.; Zheng, S.; Xiao, C., Downregulation of N-Acetylglucosaminyltransferase GCNT3 by miR-302b-3p Decreases Non-Small Cell Lung Cancer (NSCLC) Cell Proliferation, Migration and Invasion. *Cell Physiol Biochem* **2018,** *50* (3), 987-1004.
109. Gonzalez-Vallinas, M.; Molina, S.; Vicente, G.; Zarza, V.; Martin-Hernandez, R.; Garcia-Risco, M. R.; Fornari, T.; Reglero, G.; Ramirez de Molina, A., Expression of microRNA-15b and the glycosyltransferase GCNT3 correlates with antitumor efficacy of Rosemary diterpenes in colon and pancreatic cancer. *PLoS One* **2014,** *9* (6), e98556.
110. He, X. J.; Xiao, Y.; Zhang, Q.; Ma, L. P.; Li, N.; Yang, J., Detection and functional annotation of misregulated microRNAs in the brain of the Ts65Dn mouse model of Down syndrome. *Chin Med J (Engl)* **2013,** *126* (1), 108-13.
111. Riley, M. F.; Bochter, M. S.; Wahi, K.; Nuovo, G. J.; Cole, S. E., Mir-125a-5p-mediated regulation of Lfng is essential for the avian segmentation clock. *Dev Cell* **2013,** *24* (5), 554-61.
112. Wahi, K.; Friesen, S.; Coppola, V.; Cole, S. E., Putative binding sites for mir-125 family miRNAs in the mouse Lfng 3'UTR affect transcript expression in the segmentation clock, but mir-125a-5p is dispensable for normal somitogenesis. *Dev Dyn* **2017,** *246* (10), 740-748.
113. Raimo, M.; Orso, F.; Grassi, E.; Cimino, D.; Penna, E.; De Pitta, C.; Stadler, M. B.; Primo, L.; Calautti, E.; Quaglino, P.; Provero, P.; Taverna, D., miR-146a Exerts Differential Effects on Melanoma Growth and Metastatization. *Mol Cancer Res* **2016,** *14* (6), 548-62.
114. Wang, L.; Wei, Z.; Wu, K.; Dai, W.; Zhang, C.; Peng, J.; He, Y., Long noncoding RNA B3GALT5-AS1 suppresses colon cancer liver metastasis via repressing microRNA-203. *Aging (Albany NY)* **2018,** *10* (12), 3662-3682.
115. Liu, Y. X.; Wang, L.; Liu, W. J.; Zhang, H. T.; Xue, J. H.; Zhang, Z. W.; Gao, C. J., MiR-124-3p/B4GALT1 axis plays an important role in SOCS3-regulated growth and chemo-sensitivity of CML. *J Hematol Oncol* **2016,** *9* (1), 69.

116. Teruel, R.; Martinez-Martinez, I.; Guerrero, J. A.; Gonzalez-Conejero, R.; de la Morena-Barrio, M. E.; Salloum-Asfar, S.; Arroyo, A. B.; Aguila, S.; Garcia-Barbera, N.; Minano, A.; Vicente, V.; Corral, J.; Martinez, C., Control of post-translational modifications in antithrombin during murine post-natal development by miR-200a. *J Biomed Sci* **2013,** *20*, 29.
117. Cai, H.; Zhou, H.; Miao, Y.; Li, N.; Zhao, L.; Jia, L., MiRNA expression profiles reveal the involvement of miR-26a, miR-548l and miR-34a in hepatocellular carcinoma progression through regulation of ST3GAL5. *Lab Invest* **2017,** *97* (5), 530-542.
118. Tonevitsky, A. G.; Maltseva, D. V.; Abbasi, A.; Samatov, T. R.; Sakharov, D. A.; Shkurnikov, M. U.; Lebedev, A. E.; Galatenko, V. V.; Grigoriev, A. I.; Northoff, H., Dynamically regulated miRNA-mRNA networks revealed by exercise. *BMC Physiol* **2013,** *13*, 9.
119. Sun, M.; Zhao, X.; Liang, L.; Pan, X.; Lv, H.; Zhao, Y., Sialyltransferase ST3GAL6 mediates the effect of microRNA-26a on cell growth, migration, and invasion in hepatocellular carcinoma through the protein kinase B/mammalian target of rapamycin pathway. *Cancer Sci* **2017,** *108* (2), 267-276.
120. Han, Y.; Liu, Y.; Fu, X.; Zhang, Q.; Huang, H.; Zhang, C.; Li, W.; Zhang, J., miR-9 inhibits the metastatic ability of hepatocellular carcinoma via targeting beta galactoside alpha-2,6-sialyltransferase 1. *J Physiol Biochem* **2018,** *74* (3), 491-501.
121. Gao, L.; He, R. Q.; Wu, H. Y.; Zhang, T. T.; Liang, H. W.; Ye, Z. H.; Li, Z. Y.; Xie, T. T.; Shi, Q.; Ma, J.; Hu, X. H.; Chen, G., Expression Signature and Role of miR-30d-5p in Non-Small Cell Lung Cancer: a Comprehensive Study Based on in Silico Analysis of Public Databases and in Vitro Experiments. *Cell Physiol Biochem* **2018,** *50* (5), 1964-1987.
122. Liu, B.; Liu, Y.; Zhao, L.; Pan, Y.; Shan, Y.; Li, Y.; Jia, L., Upregulation of microRNA-135b and microRNA-182 promotes chemoresistance of colorectal cancer by targeting ST6GALNAC2 via PI3K/AKT pathway. *Mol Carcinog* **2017,** *56* (12), 2669-2680.
123. Jia, L.; Luo, S.; Ren, X.; Li, Y.; Hu, J.; Liu, B.; Zhao, L.; Shan, Y.; Zhou, H., miR-182 and miR-135b Mediate the Tumorigenesis and Invasiveness of Colorectal Cancer Cells via Targeting ST6GALNAC2 and PI3K/AKT Pathway. *Dig Dis Sci* **2017,** *62* (12), 3447-3459.
124. Miao, X.; Jia, L.; Zhou, H.; Song, X.; Zhou, M.; Xu, J.; Zhao, L.; Feng, X.; Zhao, Y., miR-4299 mediates the invasive properties and tumorigenicity of human follicular thyroid carcinoma by targeting ST6GALNAC4. *IUBMB Life* **2016,** *68* (2), 136-44.
125. Shan, Y.; Liu, Y.; Zhao, L.; Liu, B.; Li, Y.; Jia, L., MicroRNA-33a and let-7e inhibit human colorectal cancer progression by targeting ST8SIA1. *Int J Biochem Cell Biol* **2017,** *90*, 48-58.
126. Liu, Q. Y.; Miao, Y.; Wang, X. H.; Wang, P.; Cheng, Z. C.; Qian, T. M., Increased levels of miR-3099 induced by peripheral nerve injury promote Schwann cell proliferation and migration. *Neural Regen Res* **2019,** *14* (3), 525-531.
127. Ma, X.; Dong, W.; Su, Z.; Zhao, L.; Miao, Y.; Li, N.; Zhou, H.; Jia, L., Functional roles of sialylation in breast cancer progression through miR-26a/26b targeting ST8SIA4. *Cell Death Dis* **2016,** *7* (12), e2561.
128. Zhao, L.; Li, Y.; Song, X.; Zhou, H.; Li, N.; Miao, Y.; Jia, L., Upregulation of miR-181c inhibits chemoresistance by targeting ST8SIA4 in chronic myelocytic leukemia. *Oncotarget* **2016,** *7* (37), 60074-60086.
129. Wang, Z.; Hu, J.; Pan, Y.; Shan, Y.; Jiang, L.; Qi, X.; Jia, L., miR-140-5p/miR-149 Affects Chondrocyte Proliferation, Apoptosis, and Autophagy by Targeting FUT1 in Osteoarthritis. *Inflammation* **2018,** *41* (3), 959-971.

130. Wang, Y.; Chen, J.; Chen, X.; Jiang, F.; Sun, Y.; Pan, Y.; Zhang, W.; Zhang, J., MiR-34a suppresses HNSCC growth through modulating cell cycle arrest and senescence. *Neoplasma* **2017,** *64* (4), 543-553.
131. Wu, C. S.; Yen, C. J.; Chou, R. H.; Chen, J. N.; Huang, W. C.; Wu, C. Y.; Yu, Y. L., Downregulation of microRNA-15b by hepatitis B virus X enhances hepatocellular carcinoma proliferation via fucosyltransferase 2-induced Globo H expression. *Int J Cancer* **2014,** *134* (7), 1638-47.
132. Hu, J.; Wang, Z.; Pan, Y.; Ma, J.; Miao, X.; Qi, X.; Zhou, H.; Jia, L., MiR-26a and miR-26b mediate osteoarthritis progression by targeting FUT4 via NF-kappaB signaling pathway. *Int J Biochem Cell Biol* **2018,** *94*, 79-88.
133. Zheng, Q.; Zhang, D.; Yang, Y. U.; Cui, X.; Sun, J.; Liang, C.; Qin, H.; Yang, X.; Liu, S.; Yan, Q., MicroRNA-200c impairs uterine receptivity formation by targeting FUT4 and alpha1,3-fucosylation. *Cell Death Differ* **2017,** *24* (12), 2161-2172.
134. Zhao, L.; Feng, X.; Song, X.; Zhou, H.; Zhao, Y.; Cheng, L.; Jia, L., miR-493-5p attenuates the invasiveness and tumorigenicity in human breast cancer by targeting FUT4. *Oncol Rep* **2016,** *36* (2), 1007-15.
135. Feng, X.; Zhao, L.; Gao, S.; Song, X.; Dong, W.; Zhao, Y.; Zhou, H.; Cheng, L.; Miao, X.; Jia, L., Increased fucosylation has a pivotal role in multidrug resistance of breast cancer cells through miR-224-3p targeting FUT4. *Gene* **2016,** *578* (2), 232-41.
136. Liang, L.; Gao, C.; Li, Y.; Sun, M.; Xu, J.; Li, H.; Jia, L.; Zhao, Y., miR-125a-3p/FUT5-FUT6 axis mediates colorectal cancer cell proliferation, migration, invasion and pathological angiogenesis via PI3K-Akt pathway. *Cell Death Dis* **2017,** *8* (8), e2968.
137. Li, N.; Liu, Y.; Miao, Y.; Zhao, L.; Zhou, H.; Jia, L., MicroRNA-106b targets FUT6 to promote cell migration, invasion, and proliferation in human breast cancer. *IUBMB Life* **2016,** *68* (9), 764-75.
138. Hu, B.; Xu, C.; Tian, Y.; Shi, C.; Zhang, Y.; Deng, L.; Zhou, H.; Cao, P.; Chen, H.; Yuan, W., Inflammatory microRNA-194 and -515 attenuate the biosynthesis of chondroitin sulfate during human intervertebral disc degeneration. *Oncotarget* **2017,** *8* (30), 49303-49317.
139. Prudnikova, T. Y.; Mostovich, L. A.; Kashuba, V. I.; Ernberg, I.; Zabarovsky, E. R.; Grigorieva, E. V., miRNA-218 contributes to the regulation of D-glucuronyl C5-epimerase expression in normal and tumor breast tissues. *Epigenetics* **2012,** *7* (10), 1109-14.
140. Song, Y. Q.; Karasugi, T.; Cheung, K. M.; Chiba, K.; Ho, D. W.; Miyake, A.; Kao, P. Y.; Sze, K. L.; Yee, A.; Takahashi, A.; Kawaguchi, Y.; Mikami, Y.; Matsumoto, M.; Togawa, D.; Kanayama, M.; Shi, D.; Dai, J.; Jiang, Q.; Wu, C.; Tian, W.; Wang, N.; Leong, J. C.; Luk, K. D.; Yip, S. P.; Cherny, S. S.; Wang, J.; Mundlos, S.; Kelempisioti, A.; Eskola, P. J.; Mannikko, M.; Makela, P.; Karppinen, J.; Jarvelin, M. R.; O'Reilly, P. F.; Kubo, M.; Kimura, T.; Kubo, T.; Toyama, Y.; Mizuta, H.; Cheah, K. S.; Tsunoda, T.; Sham, P. C.; Ikegawa, S.; Chan, D., Lumbar disc degeneration is linked to a carbohydrate sulfotransferase 3 variant. *J Clin Invest* **2013,** *123* (11), 4909-17.
141. Yang, G.; Gong, Y.; Wang, Q.; Wang, Y.; Zhang, X., The role of miR-100-mediated Notch pathway in apoptosis of gastric tumor cells. *Cell Signal* **2015,** *27* (6), 1087-101.
142. Liep, J.; Kilic, E.; Meyer, H. A.; Busch, J.; Jung, K.; Rabien, A., Cooperative Effect of miR-141-3p and miR-145-5p in the Regulation of Targets in Clear Cell Renal Cell Carcinoma. *PLoS One* **2016,** *11* (6), e0157801.

143. Shi, X.; Su, S.; Long, J.; Mei, B.; Chen, Y., MicroRNA-191 targets N-deacetylase/N-sulfotransferase 1 and promotes cell growth in human gastric carcinoma cell line MGC803. *Acta Biochim Biophys Sin (Shanghai)* **2011,** *43* (11), 849-56.
144. Bao, L.; Yan, Y.; Xu, C.; Ji, W.; Shen, S.; Xu, G.; Zeng, Y.; Sun, B.; Qian, H.; Chen, L.; Wu, M.; Su, C.; Chen, J., MicroRNA-21 suppresses PTEN and hSulf-1 expression and promotes hepatocellular carcinoma progression through AKT/ERK pathways. *Cancer Lett* **2013,** *337* (2), 226-36.
145. Yang, L.; Zhang, S.; Guo, K.; Huang, H.; Qi, S.; Yao, J.; Zhang, Z., miR-125a restrains cell migration and invasion by targeting STAT3 in gastric cancer cells. *Onco Targets Ther* **2019,** *12*, 205-215.
146. Wang, G.; Zhao, W.; Gao, X.; Zhang, D.; Li, Y.; Zhang, Y.; Li, W., HNF1AAS1 promotes growth and metastasis of esophageal squamous cell carcinoma by sponging miR214 to upregulate the expression of SOX-4. *Int J Oncol* **2017,** *51* (2), 657-667.
147. Midgley, A. C.; Morris, G.; Phillips, A. O.; Steadman, R., 17beta-estradiol ameliorates age-associated loss of fibroblast function by attenuating IFN-gamma/STAT1-dependent miR-7 upregulation. *Aging Cell* **2016,** *15* (3), 531-41.
148. Pan, B.; Toms, D.; Shen, W.; Li, J., MicroRNA-378 regulates oocyte maturation via the suppression of aromatase in porcine cumulus cells. *Am J Physiol Endocrinol Metab* **2015,** *308* (6), E525-34.
149. Rock, K.; Tigges, J.; Sass, S.; Schutze, A.; Florea, A. M.; Fender, A. C.; Theis, F. J.; Krutmann, J.; Boege, F.; Fritsche, E.; Reifenberger, G.; Fischer, J. W., miR-23a-3p causes cellular senescence by targeting hyaluronan synthase 2: possible implication for skin aging. *J Invest Dermatol* **2015,** *135* (2), 369-377.
150. Zhang, J.; Chang, J. J.; Xu, F.; Ma, X. J.; Wu, Y.; Li, W. C.; Wang, H. J.; Huang, G. Y.; Ma, D., MicroRNA deregulation in right ventricular outflow tract myocardium in nonsyndromic tetralogy of fallot. *Can J Cardiol* **2013,** *29* (12), 1695-703.
151. Lagendijk, A. K.; Goumans, M. J.; Burkhard, S. B.; Bakkers, J., MicroRNA-23 restricts cardiac valve formation by inhibiting Has2 and extracellular hyaluronic acid production. *Circ Res* **2011,** *109* (6), 649-57.
152. Pan, B.; Toms, D.; Li, J., MicroRNA-574 suppresses oocyte maturation via targeting hyaluronan synthase 2 in porcine cumulus cells. *Am J Physiol Cell Physiol* **2018,** *314* (3), C268-C277.
153. Li, H. M.; Xiao, Y. J.; Min, Z. S.; Tan, C., Identification and interaction analysis of key genes and microRNAs in atopic dermatitis by bioinformatics analysis. *Clin Exp Dermatol* **2019,** *44* (3), 257-264.
154. Bai, F.; Jiu, M.; You, Y.; Feng, Y.; Xin, R.; Liu, X.; Mo, L.; Nie, Y., miR29a3p represses proliferation and metastasis of gastric cancer cells via attenuating HAS3 levels. *Mol Med Rep* **2018,** *17* (6), 8145-8152.
155. Pashaei, E.; Guzel, E.; Ozgurses, M. E.; Demirel, G.; Aydin, N.; Ozen, M., A Meta-Analysis: Identification of Common Mir-145 Target Genes that have Similar Behavior in Different GEO Datasets. *PLoS One* **2016,** *11* (9), e0161491.
156. Barter, M. J.; Tselepi, M.; Gomez, R.; Woods, S.; Hui, W.; Smith, G. R.; Shanley, D. P.; Clark, I. M.; Young, D. A., Genome-Wide MicroRNA and Gene Analysis of Mesenchymal Stem Cell Chondrogenesis Identifies an Essential Role and Multiple Targets for miR-140-5p. *Stem Cells* **2015,** *33* (11), 3266-80.

157. Straniero, L.; Rimoldi, V.; Samarani, M.; Goldwurm, S.; Di Fonzo, A.; Kruger, R.; Deleidi, M.; Aureli, M.; Solda, G.; Duga, S.; Asselta, R., The GBAP1 pseudogene acts as a ceRNA for the glucocerebrosidase gene GBA by sponging miR-22-3p. *Sci Rep* **2017,** *7* (1), 12702.
158. Chang, S.; He, S.; Qiu, G.; Lu, J.; Wang, J.; Liu, J.; Fan, L.; Zhao, W.; Che, X., MicroRNA-125b promotes invasion and metastasis of gastric cancer by targeting STARD13 and NEU1. *Tumour Biol* **2016,** *37* (9), 12141-12151.
159. Tao, J.; Liu, W.; Shang, G.; Zheng, Y.; Huang, J.; Lin, R.; Chen, L., MiR-207/352 regulate lysosomal-associated membrane proteins and enzymes following ischemic stroke. *Neuroscience* **2015,** *305*, 1-14.
160. Yang, C.; Ren, J.; Li, B.; Zhang, D.; Ma, C.; Cheng, C.; Sun, Y.; Fu, L.; Shi, X., Identification of clinical tumor stages related mRNAs and miRNAs in cervical squamous cell carcinoma. *Pathol Res Pract* **2018,** *214* (10), 1638-1647.
161. Yamada, Y.; Arai, T.; Sugawara, S.; Okato, A.; Kato, M.; Kojima, S.; Yamazaki, K.; Naya, Y.; Ichikawa, T.; Seki, N., Impact of novel oncogenic pathways regulated by antitumor miR-451a in renal cell carcinoma. *Cancer Sci* **2018,** *109* (4), 1239-1253.
162. Sun, Y.; Liu, X.; Zhang, Q.; Mao, X.; Feng, L.; Su, P.; Chen, H.; Guo, Y.; Jin, F., Oncogenic potential of TSTA3 in breast cancer and its regulation by the tumor suppressors miR-125a-5p and miR-125b. *Tumour Biol* **2016,** *37* (4), 4963-72.
163. Kwon, D. N.; Chang, B. S.; Kim, J. H., MicroRNA dysregulation in liver and pancreas of CMP-Neu5Ac hydroxylase null mice disrupts insulin/PI3K-AKT signaling. *Biomed Res Int* **2014,** *2014*, 236385.
164. Gan, B. L.; Zhang, L. J.; Gao, L.; Ma, F. C.; He, R. Q.; Chen, G.; Ma, J.; Zhong, J. C.; Hu, X. H., Downregulation of miR2245p in prostate cancer and its relevant molecular mechanism via TCGA, GEO database and in silico analyses. *Oncol Rep* **2018,** *40* (6), 3171-3188.
165. Xu, Q. F.; Pan, Y. W.; Li, L. C.; Zhou, Z.; Huang, Q. L.; Pang, J. C.; Zhu, X. P.; Ren, Y.; Yang, H.; Ohgaki, H.; Lv, S. Q., MiR-22 is frequently downregulated in medulloblastomas and inhibits cell proliferation via the novel target PAPST1. *Brain Pathol* **2014,** *24* (6), 568-83.
166. Lim, C. H.; Jeong, W.; Lim, W.; Kim, J.; Song, G.; Bazer, F. W., Differential expression of select members of the SLC family of genes and regulation of expression by microRNAs in the chicken oviduct. *Biol Reprod* **2012,** *87* (6), 145.
167. Hao, G. J.; Ding, Y. H.; Wen, H.; Li, X. F.; Zhang, W.; Su, H. Y.; Liu, D. M.; Xie, N. L., Attenuation of deregulated miR-369-3p expression sensitizes non-small cell lung cancer cells to cisplatin via modulation of the nucleotide sugar transporter SLC35F5. *Biochem Biophys Res Commun* **2017,** *488* (3), 501-508.
168. Wijayakumara, D. D.; Mackenzie, P. I.; McKinnon, R. A.; Hu, D. G.; Meech, R., Regulation of UDP-Glucuronosyltransferase 2B15 by miR-331-5p in Prostate Cancer Cells Involves Canonical and Noncanonical Target Sites. *J Pharmacol Exp Ther* **2018,** *365* (1), 48-59.
169. Margaillan, G.; Levesque, E.; Guillemette, C., Epigenetic regulation of steroid inactivating UDP-glucuronosyltransferases by microRNAs in prostate cancer. *J Steroid Biochem Mol Biol* **2016,** *155* (Pt A), 85-93.
170. Wijayakumara, D. D.; Hu, D. G.; Meech, R.; McKinnon, R. A.; Mackenzie, P. I., Regulation of Human UGT2B15 and UGT2B17 by miR-376c in Prostate Cancer Cell Lines. *J Pharmacol Exp Ther* **2015,** *354* (3), 417-25.

171. Papageorgiou, I.; Court, M. H., Identification and validation of the microRNA response elements in the 3'-untranslated region of the UDP glucuronosyltransferase (UGT) 2B7 and 2B15 genes by a functional genomics approach. *Biochem Pharmacol* **2017,** *146*, 199-213.
172. Zhang, J. J.; Wang, L. N.; Feng, Y.; Zhi, H.; Ma, G. S.; Ye, X. Z.; Qian, S. S.; Wang, B., [Association study on the microRNA-1 target gene polymorphism and the risk of premature coronary artery disease]. *Zhonghua Xin Xue Guan Bing Za Zhi* **2012,** *40* (5), 386-91.
173. Fu, T.; Kemper, J. K., MicroRNA-34a and Impaired FGF19/21 Signaling in Obesity. *Vitam Horm* **2016,** *101*, 175-96.
174. Kang, W. L.; Xu, G. S., Atrasentan increased the expression of klotho by mediating miR-199b-5p and prevented renal tubular injury in diabetic nephropathy. *Sci Rep* **2016,** *6*, 19979.
175. He, X. J.; Ma, Y. Y.; Yu, S.; Jiang, X. T.; Lu, Y. D.; Tao, L.; Wang, H. P.; Hu, Z. M.; Tao, H. Q., Up-regulated miR-199a-5p in gastric cancer functions as an oncogene and targets klotho. *BMC Cancer* **2014,** *14*, 218.
176. Jiang, B.; Gu, Y.; Chen, Y., Identification of novel predictive markers for the prognosis of pancreatic ductal adenocarcinoma. *Cancer Invest* **2014,** *32* (6), 218-25.
177. Mehi, S. J.; Maltare, A.; Abraham, C. R.; King, G. D., MicroRNA-339 and microRNA-556 regulate Klotho expression in vitro. *Age (Dordr)* **2014,** *36* (1), 141-9.
178. Koshizuka, K.; Hanazawa, T.; Kikkawa, N.; Katada, K.; Okato, A.; Arai, T.; Idichi, T.; Osako, Y.; Okamoto, Y.; Seki, N., Antitumor miR-150-5p and miR-150-3p inhibit cancer cell aggressiveness by targeting SPOCK1 in head and neck squamous cell carcinoma. *Auris Nasus Larynx* **2018,** *45* (4), 854-865.
179. Osako, Y.; Seki, N.; Koshizuka, K.; Okato, A.; Idichi, T.; Arai, T.; Omoto, I.; Sasaki, K.; Uchikado, Y.; Kita, Y.; Kurahara, H.; Maemura, K.; Natsugoe, S., Regulation of SPOCK1 by dual strands of pre-miR-150 inhibit cancer cell migration and invasion in esophageal squamous cell carcinoma. *J Hum Genet* **2017,** *62* (11), 935-944.
180. Lee, S. J.; Kim, S. J.; Seo, H. H.; Shin, S. P.; Kim, D.; Park, C. S.; Kim, K. T.; Kim, Y. H.; Jeong, J. S.; Kim, I. H., Over-expression of miR-145 enhances the effectiveness of HSVtk gene therapy for malignant glioma. *Cancer Lett* **2012,** *320* (1), 72-80.
181. Paul, P.; Chakraborty, A.; Sarkar, D.; Langthasa, M.; Rahman, M.; Bari, M.; Singha, R. S.; Malakar, A. K.; Chakraborty, S., Interplay between miRNAs and human diseases. *J Cell Physiol* **2018,** *233* (3), 2007-2018.
182. Bartel, D. P., Metazoan MicroRNAs. *Cell* **2018,** *173* (1), 20-51.
183. Bracken, C. P.; Li, X.; Wright, J. A.; Lawrence, D. M.; Pillman, K. A.; Salmanidis, M.; Anderson, M. A.; Dredge, B. K.; Gregory, P. A.; Tsykin, A.; Neilsen, C.; Thomson, D. W.; Bert, A. G.; Leerberg, J. M.; Yap, A. S.; Jensen, K. B.; Khew-Goodall, Y.; Goodall, G. J., Genome-wide identification of miR-200 targets reveals a regulatory network controlling cell invasion. *EMBO J* **2014,** *33* (18), 2040-56.
184. Agarwal, V.; Bell, G. W.; Nam, J. W.; Bartel, D. P., Predicting effective microRNA target sites in mammalian mRNAs. *Elife* **2015,** *4*.
185. Betel, D.; Koppal, A.; Agius, P.; Sander, C.; Leslie, C., Comprehensive modeling of microRNA targets predicts functional non-conserved and non-canonical sites. *Genome Biol* **2010,** *11* (8), R90.
186. Gumienny, R.; Zavolan, M., Accurate transcriptome-wide prediction of microRNA targets and small interfering RNA off-targets with MIRZA-G. *Nucleic Acids Res* **2015,** *43* (18), 9095.

187. Reczko, M.; Maragkakis, M.; Alexiou, P.; Grosse, I.; Hatzigeorgiou, A. G., Functional microRNA targets in protein coding sequences. *Bioinformatics* **2012,** *28* (6), 771-6.
188. Wang, X., Improving microRNA target prediction by modeling with unambiguously identified microRNA-target pairs from CLIP-ligation studies. *Bioinformatics* **2016,** *32* (9), 1316-22.
189. Chi, S. W.; Zang, J. B.; Mele, A.; Darnell, R. B., Argonaute HITS-CLIP decodes microRNA-mRNA interaction maps. *Nature* **2009,** *460* (7254), 479-86.
190. Hafner, M.; Landthaler, M.; Burger, L.; Khorshid, M.; Hausser, J.; Berninger, P.; Rothballer, A.; Ascano, M., Jr.; Jungkamp, A. C.; Munschauer, M.; Ulrich, A.; Wardle, G. S.; Dewell, S.; Zavolan, M.; Tuschl, T., Transcriptome-wide identification of RNA-binding protein and microRNA target sites by PAR-CLIP. *Cell* **2010,** *141* (1), 129-41.
191. Mukherji, S.; Ebert, M. S.; Zheng, G. X.; Tsang, J. S.; Sharp, P. A.; van Oudenaarden, A., MicroRNAs can generate thresholds in target gene expression. *Nat Genet* **2011,** *43* (9), 854-9.
192. Lemus-Diaz, N.; Boker, K. O.; Rodriguez-Polo, I.; Mitter, M.; Preis, J.; Arlt, M.; Gruber, J., Dissecting miRNA gene repression on single cell level with an advanced fluorescent reporter system. *Sci Rep* **2017,** *7*, 45197.
193. Ziauddin, J.; Sabatini, D. M., Microarrays of cells expressing defined cDNAs. *Nature* **2001,** *411* (6833), 107-10.
194. Wheeler, D. B.; Carpenter, A. E.; Sabatini, D. M., Cell microarrays and RNA interference chip away at gene function. *Nat Genet* **2005,** *37 Suppl*, S25-30.
195. Kittler, R.; Pelletier, L.; Heninger, A. K.; Slabicki, M.; Theis, M.; Miroslaw, L.; Poser, I.; Lawo, S.; Grabner, H.; Kozak, K.; Wagner, J.; Surendranath, V.; Richter, C.; Bowen, W.; Jackson, A. L.; Habermann, B.; Hyman, A. A.; Buchholz, F., Genome-scale RNAi profiling of cell division in human tissue culture cells. *Nat Cell Biol* **2007,** *9* (12), 1401-12.
196. Genovesio, A.; Giardini, M. A.; Kwon, Y. J.; de Macedo Dossin, F.; Choi, S. Y.; Kim, N. Y.; Kim, H. C.; Jung, S. Y.; Schenkman, S.; Almeida, I. C.; Emans, N.; Freitas-Junior, L. H., Visual genome-wide RNAi screening to identify human host factors required for Trypanosoma cruzi infection. *PLoS One* **2011,** *6* (5), e19733.
197. Castel, D.; Pitaval, A.; Debily, M. A.; Gidrol, X., Cell microarrays in drug discovery. *Drug Discov Today* **2006,** *11* (13-14), 616-22.
198. Erfle, H.; Neumann, B.; Liebel, U.; Rogers, P.; Held, M.; Walter, T.; Ellenberg, J.; Pepperkok, R., Reverse transfection on cell arrays for high content screening microscopy. *Nat Protoc* **2007,** *2* (2), 392-9.
199. Sturzl, M.; Konrad, A.; Sander, G.; Wies, E.; Neipel, F.; Naschberger, E.; Reipschlager, S.; Gonin-Laurent, N.; Horch, R. E.; Kneser, U.; Hohenberger, W.; Erfle, H.; Thurau, M., High throughput screening of gene functions in mammalian cells using reversely transfected cell arrays: review and protocol. *Comb Chem High Throughput Screen* **2008,** *11* (2), 159-72.
200. Rantala, J. K.; Makela, R.; Aaltola, A. R.; Laasola, P.; Mpindi, J. P.; Nees, M.; Saviranta, P.; Kallioniemi, O., A cell spot microarray method for production of high density siRNA transfection microarrays. *BMC Genomics* **2011,** *12*, 162.
201. Kim, H. C.; Kim, G. H.; Cho, S. G.; Lee, E. J.; Kwon, Y. J., Development of a cell-defined siRNA microarray for analysis of gene function in human bone marrow stromal cells. *Stem Cell Res* **2016,** *16* (2), 365-76.

202. Bajar, B. T.; Wang, E. S.; Lam, A. J.; Kim, B. B.; Jacobs, C. L.; Howe, E. S.; Davidson, M. W.; Lin, M. Z.; Chu, J., Improving brightness and photostability of green and red fluorescent proteins for live cell imaging and FRET reporting. *Sci Rep* **2016,** *6*, 20889.
203. Kohen, N. T.; Little, L. E.; Healy, K. E., Characterization of Matrigel interfaces during defined human embryonic stem cell culture. *Biointerphases* **2009,** *4* (4), 69-79.
204. Thu, C. T.; Mahal, L. K., Sweet Control: MicroRNA Regulation of the Glycome. *Biochemistry* **2020,** *59* (34), 3098-3110.
205. Varki, A., Biological roles of glycans. *Glycobiology* **2017,** *27* (1), 3-49.
206. Vasudevan, D.; Takeuchi, H.; Johar, S. S.; Majerus, E.; Haltiwanger, R. S., Peters plus syndrome mutations disrupt a noncanonical ER quality-control mechanism. *Curr Biol* **2015,** *25* (3), 286-295.
207. Holdener, B. C.; Percival, C. J.; Grady, R. C.; Cameron, D. C.; Berardinelli, S. J.; Zhang, A.; Neupane, S.; Takeuchi, M.; Jimenez-Vega, J. C.; Uddin, S. M. Z.; Komatsu, D. E.; Honkanen, R.; Dubail, J.; Apte, S. S.; Sato, T.; Narimatsu, H.; McClain, S. A.; Haltiwanger, R. S., ADAMTS9 and ADAMTS20 are differentially affected by loss of B3GLCT in mouse model of Peters plus syndrome. *Hum Mol Genet* **2019,** *28* (24), 4053-4066.
208. Weh, E.; Reis, L. M.; Tyler, R. C.; Bick, D.; Rhead, W. J.; Wallace, S.; McGregor, T. L.; Dills, S. K.; Chao, M. C.; Murray, J. C.; Semina, E. V., Novel B3GALTL mutations in classic Peters plus syndrome and lack of mutations in a large cohort of patients with similar phenotypes. *Clin Genet* **2014,** *86* (2), 142-8.
209. Maillette de Buy Wenniger-Prick, L. J.; Hennekam, R. C., The Peters' plus syndrome: a review. *Ann Genet* **2002,** *45* (2), 97-103.
210. Hennekam, R. C.; Van Schooneveld, M. J.; Ardinger, H. H.; Van Den Boogaard, M. J.; Friedburg, D.; Rudnik-Schoneborn, S.; Seguin, J. H.; Weatherstone, K. B.; Wittebol-Post, D.; Meinecke, P., The Peters'-Plus syndrome: description of 16 patients and review of the literature. *Clin Dysmorphol* **1993,** *2* (4), 283-300.
211. Liu, J.; Li, Y.; Chen, X.; Xu, X.; Zhao, H.; Wang, S.; Hao, J.; He, B.; Liu, S.; Wang, J., Upregulation of miR-205 induces CHN1 expression, which is associated with the aggressive behaviour of cervical cancer cells and correlated with lymph node metastasis. *BMC Cancer* **2020,** *20* (1), 1029.
212. Wang, L.; Zhang, S.; Zhang, W.; Cheng, G.; Khan, R.; Junjvlieke, Z.; Li, S.; Zan, L., miR-424 Promotes Bovine Adipogenesis Through an Unconventional Post-Transcriptional Regulation of STK11. *Front Genet* **2020,** *11*, 145.
213. Vasudevan, S.; Tong, Y.; Steitz, J. A., Switching from repression to activation: microRNAs can up-regulate translation. *Science* **2007,** *318* (5858), 1931-4.
214. Valinezhad Orang, A.; Safaralizadeh, R.; Kazemzadeh-Bavili, M., Mechanisms of miRNA-Mediated Gene Regulation from Common Downregulation to mRNA-Specific Upregulation. *Int J Genomics* **2014,** *2014*, 970607.
215. Dweep, H.; Sticht, C.; Pandey, P.; Gretz, N., miRWalk--database: prediction of possible miRNA binding sites by "walking" the genes of three genomes. *J Biomed Inform* **2011,** *44* (5), 839-47.
216. Dweep, H.; Gretz, N.; Sticht, C., miRWalk database for miRNA-target interactions. *Methods Mol Biol* **2014,** *1182*, 289-305.
217. Sticht, C.; De La Torre, C.; Parveen, A.; Gretz, N., miRWalk: An online resource for prediction of microRNA binding sites. *PLoS One* **2018,** *13* (10), e0206239.

218. Baek, D.; Villen, J.; Shin, C.; Camargo, F. D.; Gygi, S. P.; Bartel, D. P., The impact of microRNAs on protein output. *Nature* **2008,** *455* (7209), 64-71.
219. Didiano, D.; Hobert, O., Perfect seed pairing is not a generally reliable predictor for miRNA-target interactions. *Nat Struct Mol Biol* **2006,** *13* (9), 849-51.
220. Lal, A.; Navarro, F.; Maher, C. A.; Maliszewski, L. E.; Yan, N.; O'Day, E.; Chowdhury, D.; Dykxhoorn, D. M.; Tsai, P.; Hofmann, O.; Becker, K. G.; Gorospe, M.; Hide, W.; Lieberman, J., miR-24 Inhibits cell proliferation by targeting E2F2, MYC, and other cell-cycle genes via binding to "seedless" 3'UTR microRNA recognition elements. *Mol Cell* **2009,** *35* (5), 610-25.
221. Fan, Y.; Siklenka, K.; Arora, S. K.; Ribeiro, P.; Kimmins, S.; Xia, J., miRNet - dissecting miRNA-target interactions and functional associations through network-based visual analysis. *Nucleic Acids Res* **2016,** *44* (W1), W135-41.
222. Chang, L.; Zhou, G.; Soufan, O.; Xia, J., miRNet 2.0: network-based visual analytics for miRNA functional analysis and systems biology. *Nucleic Acids Res* **2020,** *48* (W1), W244-W251.
223. Huang, H. Y.; Lin, Y. C.; Li, J.; Huang, K. Y.; Shrestha, S.; Hong, H. C.; Tang, Y.; Chen, Y. G.; Jin, C. N.; Yu, Y.; Xu, J. T.; Li, Y. M.; Cai, X. X.; Zhou, Z. Y.; Chen, X. H.; Pei, Y. Y.; Hu, L.; Su, J. J.; Cui, S. D.; Wang, F.; Xie, Y. Y.; Ding, S. Y.; Luo, M. F.; Chou, C. H.; Chang, N. W.; Chen, K. W.; Cheng, Y. H.; Wan, X. H.; Hsu, W. L.; Lee, T. Y.; Wei, F. X.; Huang, H. D., miRTarBase 2020: updates to the experimentally validated microRNA-target interaction database. *Nucleic Acids Res* **2020,** *48* (D1), D148-D154.
224. Pinero, J.; Ramirez-Anguita, J. M.; Sauch-Pitarch, J.; Ronzano, F.; Centeno, E.; Sanz, F.; Furlong, L. I., The DisGeNET knowledge platform for disease genomics: 2019 update. *Nucleic Acids Res* **2020,** *48* (D1), D845-D855.
225. Dweep, H.; Gretz, N., miRWalk2.0: a comprehensive atlas of microRNA-target interactions. *Nat Methods* **2015,** *12* (8), 697.
226. Bond, M. R.; Hanover, J. A., A little sugar goes a long way: the cell biology of O-GlcNAc. *J Cell Biol* **2015,** *208* (7), 869-80.
227. Ong, Q.; Han, W.; Yang, X., O-GlcNAc as an Integrator of Signaling Pathways. *Front Endocrinol (Lausanne)* **2018,** *9*, 599.
228. Yang, X.; Qian, K., Protein O-GlcNAcylation: emerging mechanisms and functions. *Nat Rev Mol Cell Biol* **2017,** *18* (7), 452-465.
229. Wu, D.; Cai, Y.; Jin, J., Potential coordination role between O-GlcNAcylation and epigenetics. *Protein Cell* **2017,** *8* (10), 713-723.
230. Wright, J. N.; Collins, H. E.; Wende, A. R.; Chatham, J. C., O-GlcNAcylation and cardiovascular disease. *Biochem Soc Trans* **2017,** *45* (2), 545-553.
231. Singh, J. P.; Zhang, K.; Wu, J.; Yang, X., O-GlcNAc signaling in cancer metabolism and epigenetics. *Cancer Lett* **2015,** *356* (2 Pt A), 244-50.
232. Zhu, Y.; Shan, X.; Yuzwa, S. A.; Vocadlo, D. J., The emerging link between O-GlcNAc and Alzheimer disease. *J Biol Chem* **2014,** *289* (50), 34472-81.
233. Yuzwa, S. A.; Vocadlo, D. J., O-GlcNAc and neurodegeneration: biochemical mechanisms and potential roles in Alzheimer's disease and beyond. *Chem Soc Rev* **2014,** *43* (19), 6839-58.
234. Yang, Y. R.; Suh, P. G., O-GlcNAcylation in cellular functions and human diseases. *Adv Biol Regul* **2014,** *54*, 68-73.

235. Li, Z.; Yi, W., Regulation of cancer metabolism by O-GlcNAcylation. *Glycoconj J* **2014,** *31* (3), 185-91.
236. Hart, G. W., Nutrient regulation of immunity: O-GlcNAcylation regulates stimulus-specific NF-kappaB-dependent transcription. *Sci Signal* **2013,** *6* (290), pe26.
237. Fardini, Y.; Dehennaut, V.; Lefebvre, T.; Issad, T., O-GlcNAcylation: A New Cancer Hallmark? *Front Endocrinol (Lausanne)* **2013,** *4*, 99.
238. Hart, G. W.; Slawson, C.; Ramirez-Correa, G.; Lagerlof, O., Cross talk between O-GlcNAcylation and phosphorylation: roles in signaling, transcription, and chronic disease. *Annu Rev Biochem* **2011,** *80*, 825-58.
239. Hanover, J. A.; Yu, S.; Lubas, W. B.; Shin, S. H.; Ragano-Caracciola, M.; Kochran, J.; Love, D. C., Mitochondrial and nucleocytoplasmic isoforms of O-linked GlcNAc transferase encoded by a single mammalian gene. *Arch Biochem Biophys* **2003,** *409* (2), 287-97.
240. Shafi, R.; Iyer, S. P.; Ellies, L. G.; O'Donnell, N.; Marek, K. W.; Chui, D.; Hart, G. W.; Marth, J. D., The O-GlcNAc transferase gene resides on the X chromosome and is essential for embryonic stem cell viability and mouse ontogeny. *Proc Natl Acad Sci U S A* **2000,** *97* (11), 5735-9.
241. Tan, Z. W.; Fei, G.; Paulo, J. A.; Bellaousov, S.; Martin, S. E. S.; Duveau, D. Y.; Thomas, C. J.; Gygi, S. P.; Boutz, P. L.; Walker, S., O-GlcNAc regulates gene expression by controlling detained intron splicing. *Nucleic Acids Res* **2020,** *48* (10), 5656-5669.
242. Keembiyehetty, C. N.; Krzeslak, A.; Love, D. C.; Hanover, J. A., A lipid-droplet-targeted O-GlcNAcase isoform is a key regulator of the proteasome. *J Cell Sci* **2011,** *124* (Pt 16), 2851-60.
243. Qian, K.; Wang, S.; Fu, M.; Zhou, J.; Singh, J. P.; Li, M. D.; Yang, Y.; Zhang, K.; Wu, J.; Nie, Y.; Ruan, H. B.; Yang, X., Transcriptional regulation of O-GlcNAc homeostasis is disrupted in pancreatic cancer. *J Biol Chem* **2018,** *293* (36), 13989-14000.
244. Liu, Y.; Huang, H.; Cao, Y.; Wu, Q.; Li, W.; Zhang, J., Suppression of OGT by microRNA24 reduces FOXA1 stability and prevents breast cancer cells invasion. *Biochem Biophys Res Commun* **2017,** *487* (3), 755-762.
245. Murashov, A. K.; Pak, E. S.; Koury, M.; Ajmera, A.; Jeyakumar, M.; Parker, M.; Williams, O.; Ding, J.; Walters, D.; Neufer, P. D., Paternal long-term exercise programs offspring for low energy expenditure and increased risk for obesity in mice. *FASEB J* **2016,** *30* (2), 775-84.
246. Solary, E.; Bernard, O. A.; Tefferi, A.; Fuks, F.; Vainchenker, W., The Ten-Eleven Translocation-2 (TET2) gene in hematopoiesis and hematopoietic diseases. *Leukemia* **2014,** *28* (3), 485-96.
247. Wang, D.; Hu, X.; Lee, S. H.; Chen, F.; Jiang, K.; Tu, Z.; Liu, Z.; Du, J.; Wang, L.; Yin, C.; Liao, Y.; Shang, H.; Martin, K. A.; Herzog, R. I.; Young, L. H.; Qian, L.; Hwa, J.; Xiang, Y., Diabetes Exacerbates Myocardial Ischemia/Reperfusion Injury by Down-Regulation of MicroRNA and Up-Regulation of O-GlcNAcylation. *JACC Basic Transl Sci* **2018,** *3* (3), 350-362.
248. Chatterjee, S.; Pal, J. K., Role of 5'- and 3'-untranslated regions of mRNAs in human diseases. *Biol Cell* **2009,** *101* (5), 251-62.
249. Jing, Q.; Huang, S.; Guth, S.; Zarubin, T.; Motoyama, A.; Chen, J.; Di Padova, F.; Lin, S. C.; Gram, H.; Han, J., Involvement of microRNA in AU-rich element-mediated mRNA instability. *Cell* **2005,** *120* (5), 623-34.

250. Otsuka, H.; Fukao, A.; Funakami, Y.; Duncan, K. E.; Fujiwara, T., Emerging Evidence of Translational Control by AU-Rich Element-Binding Proteins. *Front Genet* **2019,** *10*, 332.
251. Lytle, J. R.; Yario, T. A.; Steitz, J. A., Target mRNAs are repressed as efficiently by microRNA-binding sites in the 5' UTR as in the 3' UTR. *Proc Natl Acad Sci U S A* **2007,** *104* (23), 9667-72.
252. Orom, U. A.; Nielsen, F. C.; Lund, A. H., MicroRNA-10a binds the 5'UTR of ribosomal protein mRNAs and enhances their translation. *Mol Cell* **2008,** *30* (4), 460-71.
253. Trapannone, R.; Mariappa, D.; Ferenbach, A. T.; van Aalten, D. M., Nucleocytoplasmic human O-GlcNAc transferase is sufficient for O-GlcNAcylation of mitochondrial proteins. *Biochem J* **2016,** *473* (12), 1693-702.
254. Thu, C. T.; Chung, J. Y.; Dhawan, D.; Vaiana, C. A.; Mahal, L. K., High-Throughput miRFluR Platform Identifies miRNA Regulating B3GLCT That Predict Peters' Plus Syndrome Phenotype, Supporting the miRNA Proxy Hypothesis. *ACS Chem Biol* **2021,** *16* (10), 1900-1907.